

End-to-end interstellar communication system design for power efficiency

David G. Messerschmitt
Department of Electrical Engineering and Computer Sciences
University of California at Berkeley

Version: ArXiv Version 1
Date: Thursday 18th July, 2019
Time: 15:13

© 2013 David Messerschmitt. This work is licensed under a Creative Commons
Attribution-NonCommercial-ShareAlike 3.0 Unported License.
<http://creativecommons.org/licenses/by-nc-sa/3.0/>

Contents

Abstract	7
Preface	8
Executive Summary	10
1 Introduction	13
1.1 Transmitter-receiver coordination	13
1.1.1 Guidance from impairments and fundamental limits	13
1.1.2 Guidance from resource constraints	14
1.1.3 Guidance from average power and bandwidth	15
1.2 Power-efficient design	16
1.2.1 Why average power is important	16
1.2.2 Why bandwidth is less important	16
1.2.3 Information rate vs. average power tradeoff	17
1.2.4 Analog signals	19
1.2.5 Two ways to reduce average power	19
1.2.6 Channel coding	20
1.2.7 Guidance from the fundamental limit	21
1.2.8 Characteristics of power-efficient signals	22
1.2.9 Interstellar coherence hole	23
1.2.10 Countering scintillation	24
1.2.11 Simplicity of power-efficient design	24
1.2.12 Discovery of power-efficient signals	25
1.2.13 Information-free beacons	27
1.2.14 The role of low duty factor	28
1.3 Implications for SETI observation programs	29
1.4 History and further reading	30
1.4.1 Modeling the interstellar medium	31
1.4.2 Terrestrial wireless communication	31
1.4.3 Optical communication	31
1.4.4 Power-efficient design	32
1.4.5 Broadband interstellar communication	32

2	Power-efficient signal design	34
2.1	Efficiency measures for communication	35
2.1.1	Power efficiency	36
2.1.2	Spectral efficiency	36
2.1.3	Energy consumption	37
2.1.4	Heat dissipation	39
2.1.5	Multiple lines of sight	39
2.1.6	Peak power	39
2.2	Basic building block: Energy bundles	40
2.2.1	Matched filtering	40
2.2.2	Phase-incoherent detection	42
2.2.3	The interstellar coherence hole	42
2.3	Information-bearing signals	45
2.3.1	Magnitude-based modulation	45
2.3.2	Location-based modulation	46
2.3.3	Choosing an information rate and power	49
2.4	Power efficiency vs. spectral efficiency	51
2.4.1	Channel models	51
2.4.2	Energy contrast ratio	52
2.4.3	Tradeoff between power efficiency and spectral efficiency	53
2.4.4	Channel coding	57
2.4.5	Wake-up call from the fundamental limit	58
2.5	Five principles of power-efficient design	58
2.5.1	Use energy bundles	60
2.5.2	Avoid channel impairments	61
2.5.3	Convey information by location rather than amplitude	61
2.5.4	Make energy bundles sparse	62
2.5.5	Combat scintillation with time-diversity combining	63
2.6	Discovery	67
2.6.1	Effective energy	68
2.6.2	Design modularity	71
2.6.3	Beacons	72
2.6.4	Information-bearing signals	75
2.7	History and further reading	78
3	The interstellar coherence hole	80
3.1	Definition of the coherence hole	80
3.2	Model of a coherence hole	84
3.2.1	Scattering within a coherence hole	85
3.2.2	Noise within a coherence hole	91
3.3	Frequency offset due to acceleration	92
3.4	Time-bandwidth product and degrees of freedom	93
3.5	Some observations about the ICH	94

3.6	Summary	95
4	The fundamental limit	96
4.1	Role of large bandwidth	97
4.2	Approaching the fundamental limit: channel coding	98
4.3	A channel code that approaches the fundamental limit	99
4.3.1	Structure of the channel code	99
4.3.2	Parameters of the codebook	102
4.3.3	Receiver processing for time diversity	104
4.3.4	The result	105
4.3.5	Argument for uniqueness of this channel code	107
4.4	Fundamental limit for the interstellar channel	108
4.4.1	Lower bound on power efficiency	109
4.4.2	Effect of other impairments on power efficiency	111
4.5	History and further reading	112
4.6	Summary	112
5	Communication	114
5.1	Diversity strategy	114
5.1.1	Parameters and tradeoffs	115
5.1.2	Reliability	116
5.1.3	Total bandwidth	117
5.1.4	Total energy hypothesis	117
5.1.5	Power efficiency	118
5.1.6	Multicarrier modulation	120
5.2	Outage strategy	121
5.2.1	Choice of an outage threshold	123
5.2.2	Comparison of channel codes	124
5.2.3	Adjusting information rate and average power	126
5.2.4	Spectral efficiency	127
5.3	Choice of $h(t)$	129
5.4	History and further reading	130
5.5	Summary	130
6	Discovery	131
6.1	Background	131
6.1.1	Channel model for discovery	131
6.1.2	Signal structure	133
6.1.3	Stages of discovery	134
6.1.4	Discovery reliability	134
6.1.5	Power optimization for discovery	136
6.1.6	Role of duty factor	136
6.2	Periodic beacons	138
6.2.1	Beacon structure and parameters	138

6.2.2	Characteristics of beacon observation	138
6.2.3	Tradeoffs in detection reliability	140
6.2.4	Detection reliability for a periodic beacon	145
6.2.5	Reducing average power by manipulating the energy per bundle	145
6.2.6	Reducing average power by manipulating the duty factor	147
6.2.7	Optimization of energy contrast ratio and duty factor	148
6.2.8	Uncoordinated periodic beacon design	155
6.3	Discovery of information-bearing signals	157
6.4	Power-optimizing information-bearing signals for discovery	163
6.4.1	M-ary FSK	163
6.4.2	M-ary FSK with time diversity	165
6.5	Discovery search strategies	166
6.5.1	Energy detection in discovery	168
6.5.2	Pattern recognition in discovery	169
6.6	Summary	170
7	Detection	172
7.1	Matched filter	173
7.1.1	Continuous-time channel model	173
7.1.2	Sufficient statistic formulation	173
7.1.3	Least-squares formulation	175
7.1.4	Detection performance	176
7.1.5	Known noise power spectral density	178
7.2	Search for an energy bundle	178
7.3	Choice of $h(t)$	179
7.3.1	Radio-frequency interference	179
7.3.2	Implicit coordination	180
7.3.3	Example	181
7.4	Summary	182
8	Sources of incoherence	183
8.1	Types of incoherence	183
8.2	Plasma dispersion	184
8.3	Source/observer motion	188
8.3.1	Effect of time-varying distance and passband signals	188
8.3.2	Constant velocity	189
8.3.3	Diurnal rotation and orbital motion	190
8.3.4	Motion compensation	191
8.4	Scattering	192
8.4.1	Geometry of scattering	193
8.4.2	Scattering within a coherence hole	195
8.4.3	Coherent patches on the scattering screen	195
8.4.4	Focusing by the scattering screen	196
8.4.5	Frequency coherence of scattering	197

8.5	Fading and the time coherence of scintillation	199
8.6	Numerical example	200
8.7	Summary	202
9	Conclusions	203
	Acknowledgements	205
	APPENDICES	206
A	Interstellar link budget	206
A.0.1	Required average receive power	206
A.0.2	Required average transmit power	207
B	Matched filtering	208
B.1	Modulation and demodulation	208
B.2	The LS solution	209
C	Statistical model for a coherence hole	210
C.1	Scintillation without modulation	210
C.2	Scintillation and amplitude modulation	211
D	Derivation of fundamental limits	212
D.1	Probabilistic bounds	212
D.1.1	Union bound	212
D.1.2	Weak law of large numbers	212
D.1.3	Chernoff bound	213
D.2	Channel code based on M-ary FSK and time diversity	213
E	Coin tossing analogy	216
E.1	Discrete matched filter	216
E.2	Immunity to discrete interference	217
F	Communication reliability	218
F.1	Multilevel on-off keying (OOK)	218
F.2	Probability of error for OOK	219
F.2.1	Additive white Gaussian noise (AWGN)	219
F.2.2	AWGN and scintillation	219
F.3	Error probability for M-ary FSK and time diversity	220
F.4	Error probability for M-ary FSK	221
F.4.1	Error Probability for (M,N)-ary FSK	222
G	Discovery reliability	223
G.1	Detection probability for single observation	223
G.1.1	Rayleigh fading	223
G.1.2	Rician fading	224

G.2	Detection probability for multiple independent observations	225
G.2.1	False alarm probability	225
G.2.2	Detection probability	226
H	Plasma dispersion	228
H.1	Coherence bandwidth	228
H.2	Partial equalization	228
I	Coherence time with fading	230
J	Search granularity in dilation and frequency	231
J.1	Time dilation error	231
J.2	Carrier frequency offset	232
	Bibliography	233
	Author	237

Abstract

Interstellar radio communication accounting for known impairments due to radio propagation in the interstellar medium (attenuation, noise, dispersion, and scattering) and motion is studied. Large propagation losses and large transmitted powers motivate us to maximize the power efficiency, defined as the ratio of information rate to average signal power. The fundamental limit on power efficiency is determined. The power efficiency for narrow-bandwidth signals assumed in many current SETI searches has a penalty in power efficiency of four to five orders of magnitude. A set of five power-efficient design principles can asymptotically approach the fundamental limit, and in practice increase the power efficiency by three to four orders of magnitude. The most fundamental is to trade higher bandwidth for lower average power. In addition to improving the power efficiency, average power can be reduced by lowering the information rate. The resulting low-power signals have characteristics diametrically opposite to those currently sought, with wide bandwidth relative to the information rate and sparse distribution of energy in both time and frequency. The design of information-free beacons power-optimized for a given observation time is also undertaken. Such beacons need not have wide bandwidth, but at low powers their energy is sparsely distributed in time. The discovery of both beacons and information-bearing signals is analyzed, and shown to require a substantial number of observations (growing as power is reduced) to achieve a high probability of success. The "false alarms" in current searches are characteristic signatures of possible power-efficient and power-optimized signals. Although existing SETI searches will fail to discover these signals, they can be discovered using common algorithms with straightforward modification to current search methodologies.

Preface

This is a report on my original research into interstellar communication over the past few years. The ground covered by this report is extensive, including modeling of the interstellar channel, power-efficient communications, and power-optimized discovery of both information-bearing signals and beacons. These topics have a lot of overlap and are all influenced by a common set of considerations, which is why I keep them together rather than separate them into individual papers.

I have consciously tried to make this extensive subject matter more accessible by including three increasingly detailed summaries of the overall results, starting with an executive summary, continuing with the introductory Chapter 1, and following that with a more detailed and technical summary in Chapter 2. The remaining chapters cover each constituent topic in greater depth. A difficulty with these remaining chapters is the “missing the forest for the trees” phenomenon. Therefore, I recommend that you reread Chapter 1 after finishing Chapter 2, and a third time after absorbing the remaining chapters. This should contribute to your overall understanding and appreciation of the relationship among the various more detailed topics.

Another challenge in writing this report has been a target audience that includes two distinct groups, physicists and astronomers on the one hand, and communication engineers on the other. I think both groups will benefit from this report, and I want both groups to understand the material. To address this challenge, I have generally included more explanation than usual, and attempted to bolster intuition as well as convey detailed technical knowledge. In the following I address each group of readers directly.

Physicists and astronomers

It is fair to say that based on about six decades of research by thousands of engineers and applied mathematicians, we now have a pretty complete understanding of the fundamentals of communication as they apply to interstellar communication. In particular, we have a much more complete understanding and far more relevant experience than was the case back in 1970 during the last detailed look at interstellar communication undertaken in the Cyclops report [1]. While plenty of interesting things are happening at the frontiers of knowledge, it is fair to say that these present-day efforts have little relevance to interstellar communication.

The body of knowledge on communication engineering is quite extensive, and often pretty arcane. I recognize that this is a obstacle to a physicist or astronomer interesting in exploring the possibilities for interstellar communication. I have significantly narrowed the design scope by restricting attention to power efficiency, primarily because I believe this is the appropriate design philosophy for interstellar communication, but also because this style of design is so much simpler than what is required for the typical terrestrial applications. I have specifically assumed little prior knowledge in order to make the material more accessible. Nevertheless, if you have difficulty with any of my explanations, please let me know so that I can improve future versions of this report.

Communication engineers

It isn't often that communication engineers get to play with an entirely new application, one with distinct and interesting challenges. Interstellar communication is one such opportunity. I hope that you find this interesting and find yourself motivated to perform additional research on the interstellar channel. This is "wide-area communication" writ large.

Communications engineers reading this report will encounter different challenges from physicists and astronomers. If you are like me, you will have difficulty reorienting your thinking to power-efficient design. Almost all the research on this approach was conducted by just a few people back in the 1960's, and there is little awareness of this body of knowledge in the present-day community. To my knowledge power-efficient design is not addressed in any of the standard textbooks, save a single section in a later chapter of Gallager's 1968 book on information theory [2]. If you are like me, it will take some time and effort to detach your brain from our discipline's obsession with spectral efficiency and wrap it around the very different mode of thinking surrounding power efficiency. In my case this did not occur as a sudden epiphany, but rather developed gradually over the past several years of pondering interstellar communications. Sensitized to this challenge and opportunity, it should come more easily to you.

The modeling of the interstellar channel involves some results from astronomy and astrophysics that will likely be unfamiliar. Although the ultimate Rayleigh and Rician fading model will be familiar to engineers with experience in terrestrial radio communication, the physical mechanisms leading to this model are likely to be unfamiliar. Fortunately what we require of the channel model to deal with power-efficient design is less complete and detailed than what would be needed if spectral efficiency were the goal. Since the first principle of power efficient design is to eliminate as many impairments as possible through conscious design of the transmit signal, we actually don't need to undertake detailed channel modeling. All we need do is convince ourselves that avoiding these impairments is feasible. For this reason, the level of detail in modeling is far less ambitious than what appears in the astrophysics literature, and I trust you can readily understand it. But again if you have difficulty with any of the explanations please let me know so that I can improve them.

Executive Summary

The end-to-end design of an interstellar communication system accounting for all known impairments due to radio propagation in the interstellar medium (attenuation, noise, dispersion, and scattering) and source/observer motion at radio wavelengths is undertaken. Numerous authors have noted the motivation to minimize transmit power in interstellar communication due to large propagation loss, but the full implications have never been explored. Our system design thus revolves around minimizing the average signal power for a given information rate, which we call *power-efficient design*. In existing SETI observation programs, it is typically assumed that the received signal has narrow bandwidth and is continuously received. We find that power-efficient information-bearing signals will be diametrically opposite to this, trading a wider bandwidth for lower average power and transmitting intermittently to conserve energy through a reduction in information rate. We also explore information-free beacons that minimize average power for a given receiver observation time, which we call *power-optimized design*. Power-optimized beacons need not have wide bandwidth, but they should also transmit intermittently. In terms of ease of discovery beacons offer no advantage over power-efficient information-bearing signals, but both types of signals can be sought using a common strategy.

The fundamental limit to communication through the interstellar medium is determined, in the form of the maximum achievable power efficiency (information rate divided by average power) consistent with reliable recovery of information by the receiver. This fundamental limit constrains any civilization, no matter how technologically advanced, and methodologies for approaching the fundamental limit provide compatible guidance to the transmitter and receiver designers. There are two ways to reduce average power, through greater power efficiency and through a reduction in information rate. The fundamental limit demonstrates an unavoidable coupling between higher power efficiency and greater bandwidth. The average power of a narrowband signal (as in existing searches) has an efficiency penalty relative to the fundamental limit on the order of four to five orders of magnitude due to its restricted bandwidth, and an additional penalty due to its continuous transmission, with further average power reductions permitted by information rate reduction. A set of five straightforward power-efficient design principles that allow the fundamental limit to be approached asymptotically are demonstrated. The remainder of the report focuses on finding practical measures based on these design principles that can substantially reduce the average power through the design of the transmit signal with compatible detection strategies at the receiver. At a given information rate, average power reductions on the order of three to four orders of magnitude can be obtained at the expense of relatively wide signal bandwidth and

a sparse distribution of signal energy in frequency. An additional reduction in average power can be obtained by reducing the information rate, with a resulting sparse distribution of signal energy in time.

According to our power-efficient design principles, information is communicated by on-off patterns of bundles of energy. The energy in each bundle is conveyed by a time-limited and bandwidth-limited waveform that must avoid most of the impairments in interstellar propagation and due to motion. This is accomplished by conforming to the time- and frequency-coherence properties of the propagation and motion, so that the waveform arrives at the receiver relatively undistorted. We call this the "interstellar coherence hole". These coherence properties are estimated for all known impairments, and it is shown that the resulting time-bandwidth product is sufficient to support power-efficient design at all carrier frequencies of interest. Power-efficient design requires no processing related to most impairments in either transmitter or receiver; rather, they must be avoided by conscious design of the transmit signal. The two impairments that cannot be avoided in this fashion are noise (due to the temperature of the cosmos and receiver circuitry) and scintillation (a time variation in the signal flux at the receive antenna due to scattering in the interstellar medium). Scintillation does not numerically affect the fundamental limit on power efficiency, but does profoundly influence the strategy of power-efficient design.

A power-efficient signal consists of energy bundles sparsely located in frequency, with multiple bits of information conveyed by the frequency of a single bundle. This is energy conserving and allows the signal to simultaneously have wide bandwidth (which is fundamentally required for high power efficiency) and avoid impairment due to the frequency incoherence of the interstellar propagation. Each bundle must have sufficient energy to be detected reliably, both for extracting information and for discovery, and must have a relatively short time duration to conform to the time coherence properties of the coherence hole. As average power is reduced, due to their fixed energy and time duration, bundles must be located more and more sparsely in time. Finally, two approaches to countering scintillation are studied. One is time diversity, in which energy bundles are repeated redundantly at time intervals larger than the coherence time, and their respective energies are averaged at the receiver. Combining these measures, it is demonstrated that the fundamental limit on power efficiency is approached as the sparsity of energy bundles in time and frequency increases without bound. The second approach to scintillation is a much simpler outage strategy, which deliberately sacrifices information arriving during periods of low received signal flux. In practice either of these methods can achieve an effective power efficiency within an order of magnitude the fundamental limit. The outage strategy is attractive in interstellar communication because it is likely the communication is structured as a single message transmitted repetitively, allowing for any sacrificed information due to outages to be interpolated over longer observations.

The challenge of discovering information-bearing signals and beacons is also addressed. Because it conveys no information, a beacon may be narrowband, although its energy bundles will be sparse in time at low average powers. An information-bearing signal and beacon at the same average power can be discovered with essentially the same difficulty by detecting individual energy bundles and extending observations where such energy bundles are detected. In both cases, multiple observations are required at the receiver to account for time sparsity in combination with

scintillation. For a fixed number of observations at the receiver, both types of signals can be power-optimized, and in the case of information-bearing signals the information rate is determined by this optimization. For example, assuming a thousand receiver observations the average power of a beacon can be reduced by about three orders of magnitude relative to a continuously transmitted signal of the type that is currently the target of SETI searches.

Power-efficient and power-optimized design have profound implications for both METI and SETI. They significantly alter both transmitted signals and receiver discovery techniques. First, power-efficient signals intrinsically require multiple observations during discovery, even as they avoid any processing related to interstellar signal propagation and motion. Second, post-detection pattern recognition must account for sparsity and randomness in frequency as well as time. Although existing and past SETI observation programs will fail to discover power-efficient and power-optimized signals, they can be fairly easily modified to seek such signals. Observation at even a single location (line of sight and frequency) should be considered a long-term project, and a worldwide shared database capturing individual energy bundle detections (today dismissed as "false alarms") can guide future observations to the most promising locations.

Chapter 1

Introduction

A fundamental characteristic of the Milky Way is its capability to support the sharing of information using electromagnetic radiation among intelligent civilizations separated by interstellar distances. This capability is subject to various intrinsic physical impairments such as large propagation loss, natural sources of noise, dispersion and scattering of electromagnetic radiation in the interstellar medium (ISM) and time-varying effects due to relative source/observer motion. This report explores this information-carrying capability, both in terms of its fundamental limits and in practical terms. This is the first study that comprehensively takes into account impairments in the ISM and due to motion in an end-to-end design of an interstellar communication system, and does so employing the principles and experience of communication engineering.

1.1 Transmitter-receiver coordination

Prominent among the obstacles to establishing communication is the impossibility of prior coordination between the designers of a transmitter and a receiver [3]. The transmitter chooses a specific signal structure and parameterization, and to achieve high sensitivity a receiver discovering that signal (and subsequently extracting information) must also assume a specific signal structure and search over a large parameter space including spatial, frequency, and temporal variables. Yet prior to the establishment of communication there is no feasible way to directly coordinate these choices.

1.1.1 Guidance from impairments and fundamental limits

One common lament is the unlikely compatibility of technologies and techniques in use across civilizations widely separated in their degree of scientific and technological development. Recent examples include Fridman [4], who asserted that "In each epoch we can only use our current technical knowledge to predict what kind of signals an ETI could send". A variant on the same

argument is Horvat, Nakć, and Otočan [5], who asserted that there is a requirement for “technological synchronicity” between two civilizations. Coming from the perspective of communication engineering, we profoundly disagree with these laments. This is because there has been notable success in identifying mathematically provable and fundamental limits that constrain any civilization, no matter how advanced their technology may be. These limits depend on the nature of the impairments encountered in propagation of a signal from one civilization to the next, and fortuitously these impairments are both observable and remain unchanged over time periods dramatically longer than the joint epoch of a transmitting and receiving civilization (which is governed by the interstellar propagation delay). Together these two invariants are not technologically dependent and serve as a powerful form of implicit coordination, as we hope to demonstrate in this report. Furthermore, it will be demonstrated that our own civilization at its current state of technological development is relatively easily capable of approaching the fundamental limit with an appropriate set of design principles in place.

1.1.2 Guidance from resource constraints

A less fundamental but nevertheless promising basis for coordination is reasonable presumptions about costs and objectives. For example, both transmitter and receiver will recognize that a serious practical obstacle to communication is the “needle in a haystack” challenge in discovering a signal originating from an extraterrestrial source. At minimum the receiver has to search for a signal over starting time and carrier frequency. Expanding the dimensions of search requires additional processing and the energy consumption associated with that processing, and increased probability of false alarm (reducing sensitivity by necessitating a more strict criterion for detection). Another example is the large average transmitted power which is necessary to overcome the large propagation loss at interstellar distances, suggesting to both transmitter and receiver designers a motivation to minimize the average power of the transmitted signal and the resultant energy consumption in the transmitter.

Even though they impact both transmitter and receiver, both the energy consumption in the transmitter and the processing requirements in the receiver are largely dictated by the transmitted signal design, and this is a reason that the end-to-end perspective taken here can be valuable. If both transmitter and receiver designers undertake parallel end-to-end designs, and in particular appreciate the impact of their decisions on the other, the interest of implicit coordination between their designs is served. For example, in this report we presume that energy consumption in the transmitter (for generated radiated power) and receiver (for the signal processing required during signal discovery) are a significant source of operational cost, and the goal should therefore be to minimize these sources of energy consumption. However, we also consider the available tradeoffs between energy consumption in the transmitter and in the receiver, and how these tradeoffs should be managed in light of economic and other considerations. Whatever resource assumptions are made, minimizing those resources places substantial constraints on the design, and this is fortunate because it serves the best interest of implicit coordination.

1.1.3 Guidance from average power and bandwidth

For a given set of impairments in the interstellar medium and due to relative motion, there is a fundamental limit on the information rate (usually measured in bits per second) at which reliable communication can occur. Calculation of the fundamental limit usually assumes that two resources are constrained: the average power of the signal and the bandwidth of the signal, and asks what is the highest information rate that can be achieved under those circumstances. The feasible information rate must increase when the constraint on average power is relaxed, and also when the constraint on bandwidth is relaxed, since the transmitter always has the option to utilize less power or less bandwidth than permitted by the constraint. This implies that increasing average power is always beneficial, and increasing bandwidth is always beneficial.

The existence of a fundamental limit is of great import to interstellar communication, for a couple of reasons. It gives an absolute reference against which to compare any concrete design, and reveals precisely how much additional performance can be wrung out of the design. More significantly, circumventing the various impairment in interstellar propagation and due to motion with the goal of moving toward the fundamental limit drives the design in certain directions. In fact, the closer a design is able to achieving a performance that approaches the fundamental limit, the more constrained it becomes. Thus the fundamental limit serves as source of implicit coordination, because if the transmitter and receiver designers examine the end-to-end communication problem independently, they will arrive at compatible conclusions about design approaches for both transmitter and receiver. The closer the transmitter seeks to approach the fundamental limit, the greater the receiver's confidence in the characteristics of the transmitted signal.

There is one remaining element of uncertainty or dissidence that could interfere with the strategy of implicit coordination by fundamental limit, and that is the relative importance to attach to average power and to bandwidth. These two design parameters play a similar role in communications to position and momentum in the Heisenberg uncertainty principle of physics. Just as more accurate knowledge of position of a particle fundamentally implies less accurate knowledge of its momentum, constraining the bandwidth of a communication signal more tightly implies fundamentally that the signal must have a greater average power, and vice versa. Depending on whether we place our priority bandwidth or on average power, the design is driven in very different directions. In terrestrial radio communications, priority is virtually always placed on bandwidth because of the high economic value attached to the radio spectrum. In interstellar communication, in contrast, we argue that the priority should be placed on average signal power due to the large energy requirements placed on radiated power at the transmitter due to the large propagation losses. This assumption leads to the approach of power efficient design, which is described next, and a very different design approach from what is prevalent in terrestrial communication.

1.2 Power-efficient design

The idea behind power efficient design is to assume that average power is the only limiting resources, and that bandwidth does not need to be constrained. By eliminating any bandwidth constraint, the average signal power is minimized. In addition, by eliminating any bandwidth constraint the communication design problem is greatly simplified, which is of great benefit in the context of interstellar communication where explicit transmitter-receiver design coordination is not feasible.

1.2.1 Why average power is important

Authors addressing SETI have noted the importance of energy and power arising from the challenges of overcoming an extraordinarily large propagation loss at interstellar distances, as well as the relative unimportance of signal bandwidth due to the wide microwave window that is available. For example, H. Jones argued that bandwidth is a relatively free resource in interstellar communication due to the broad microwave window [6]. P. Fridman recently asserted that power is surely a bigger issue than bandwidth [4]. In spite of this seeming consensus among authors, the implications of a design approach to interstellar communication that seeks to minimize average power has never been explored. That is the main subject of this report.

There is an important distinction between average and peak transmitted power. Average transmit power is directly related to the transmitter's energy consumption, which is a major part of transmitter operational costs. As a concrete example, at a modest information rate of one bit per second and a distance of one thousand light years, the average transmitter radiated power for the type of bandwidth-constrained signals targeted by present SETI searches and assuming Arecibo-sized antennas is about twice that of the Large Hadron Collider at CERN. Average power also determines the thermal management challenges for high-power transmit electronics, and thus is more important than peak power in the construction cost of a transmitter [7]. If the transmitter is performing a targeted search, average transmit power may have a large multiplier due to concurrent transmission on multiple lines of sight, or alternatively a lower gain (more omnidirectional) transmit antenna may be used and that also necessitates a commensurately higher average power.

1.2.2 Why bandwidth is less important

As long as we deal with some frequency-dispersive effects successfully, bandwidth is hardly constrained by the long-distance propagation and impairments in the interstellar medium. Of course the available bandwidth is not unlimited, because there is a finite microwave window where the interstellar medium is highly transparent. But in this report we assume that the bandwidth is unconstrained. In practice this means that the bandwidth required will be relatively large relative to the information rate, but not infinite.

In interstellar communication, it is expected that the information rates will be low relative to what is typical in terrestrial communication due to the high energy consumption. Low information rates

imply that the reception time required for a given size of message is longer, but this also seems perfectly acceptable for interstellar communication where extreme patience is required on the part of both transmitter and receiver even in the best of circumstances. When the information rate is low, it follows that bandwidth will be commensurately low even without going to the trouble to explicitly constrain the bandwidth. Our own electronics and processing technologies are capable of supporting large bandwidths with relative ease, and this is likely true of other civilizations at least as technologically advanced as our own.

In the remainder of this discussion, assume that the bandwidth is unconstrained. We will simply let the bandwidth fall where it may, since our priority is on achieving the lowest feasible average power. Seeking to reduce the bandwidth by constraining it can only increase the average power that is required, and that is not the direction we wish to go. Of course if the required bandwidth turns out to be impractically large, this strategy can be modified.

1.2.3 Information rate vs. average power tradeoff

The average signal power depends directly on the information rate. This is illustrated in Figure 1.1, which illustrates the special case where the information rate and average power are proportional to one another. That this dependence is typically linear is not surprising. A typical scheme translates a group of information bits into some waveform that is transmitted, and adjusts the information rate by adjusting how often that waveform (with different information bits) is transmitted. Adjusting the rate of transmission (and hence the information rate) translates directly to a commensurate adjustment to the average power.

Also shown is a prohibited region where reliable communication is not feasible because the average power is not large enough to overcome the noise and other impairments and still achieve reliable extraction of the information at this rate. The lower boundary of this region is called the *fundamental limit*. This fundamental limit applies to any civilization, no matter how technologically advanced. The existence of such a prohibited region was established by the seminal work of Claude Shannon in the late 1940's [8]. A mathematical model for the end-to-end propagation of the signal from transmitter to receiver is called a communication *channel*. Shannon's fundamental limit is called the *channel capacity*, and its details depends on the specific combination of impairments encountered in the communication channel, so every case has to be considered separately. The fundamental limit is determined in this report for the specific impairments encountered on the interstellar channel with unconstrained bandwidth, and the not-too-surprising result is that this fundamental limit on information rate is also linear in average power, just like the rate-vs-power dependence of a typical concrete communication design.

Since the variation in information rate is linear in average power, for both the fundamental limit and for typical concrete designs, it is convenient to characterize the limit in terms of a single parameter, the slope of that line. That slope is called the *power efficiency*, and it is defined as

$$\text{Power efficiency} = \frac{\text{Information rate}}{\text{Average power}} .$$

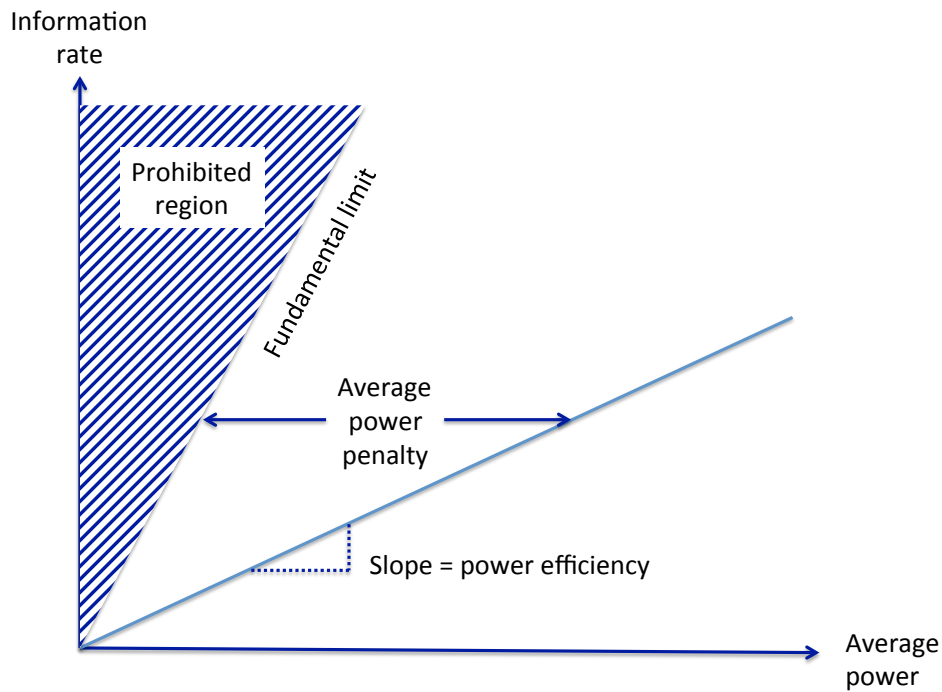


Figure 1.1: An illustration of the relationship between information rate and average power. There is a prohibited region where communication is not possible because the average power is insufficient to support the information rate. The lower boundary of that prohibited region is called the fundamental limit.

The power efficiency, which is a constant that does not depend on either average power or information rate (their ratio remains fixed even as they both vary), is a measure of how efficiently additional average power is converted into an increase in information rate. The higher power efficiency characteristic of the fundamental limit is a desirable objective because it permits a higher information rate for a given expenditure of average power. At a given information rate there is a penalty in average power for any concrete design relative to the fundamental limit directly attributable to the lower power efficiency achieved by the concrete design.

Figure 1.1 is intended to convey the concept of power efficiency, but is misleading as to scale. Over the range of signal designs considered in this report, the power efficiency can range over four to five orders of magnitude. Thus, the slope of the rate-vs-power curve may be dramatically smaller than the illustration. If power efficiency is considered an important metric of performance, the design methodology can make a major difference.

The main competitor to power efficiency is spectral efficiency, which is defined as

$$\text{Spectral efficiency} = \frac{\text{Information rate}}{\text{Signal bandwidth}}.$$

In communications the fundamental tradeoff between average power and bandwidth is easily reformulated as a tradeoff between power efficiency and spectral efficiency. Design techniques aimed at increasing one inevitably reduce the other. In this report power efficiency is emphasized, which implies that the spectral efficiency will be relatively poor.

1.2.4 Analog signals

Our description thus far assumes the information being conveyed from transmitter to receiver is digitally encoded. In fact, the analog interstellar transmission of a signal (such as music) has been experimented with [9]. Shannon dealt with this case, showing that analog signals can be digitally encoded, decoded, and recovered, and there is a fundamental limit to the fidelity with which this process occurs and a tradeoff between this fidelity and the digital information rate required. Thus, the fundamental limit on power efficiency dealt with here applies equally to analog signals, with an additional dependence between the fidelity with which the signal is recovered and the average signal power required for its transmission.

A major reason why digital representations of analog signals are preferred in practice is that the average power necessary to transmit such a signal digitally is dramatically lower than would be possible with the direct transmission of the analog representation. In practice this difference is due to compression (redundancy removal) possible during the conversion from analog to digital and also due to the wealth of techniques for increasing the power efficiency in the digital transmission. Thus digital representations of analog signals (like music) combined with digital transmission are overwhelmingly advantageous for interstellar communication, as they are for all forms of terrestrial communication.

1.2.5 Two ways to reduce average power

Our interest is in reducing the average power of the signal. There are a couple of ways to do this, one very simple and the other more sophisticated, as illustrated in Figure 1.2. The average power can always be reduced by a commensurate reduction in the information rate. The more interesting possibility is to hold the information rate constant while reducing the average power, and this is accomplished by *channel coding*, which is described shortly. Reducing the information rate does not change the power efficiency, while channel coding increases the power efficiency. Using both channel coding and information rate reduction simultaneously is attractive. Increasing the power efficiency with channel coding brings us closer to the fundamental limit, and following that by a reduction in information rate allows the average power to be reduced to whatever the transmitter can afford. Achieving the same average power without channel coding would reduce the information rate.

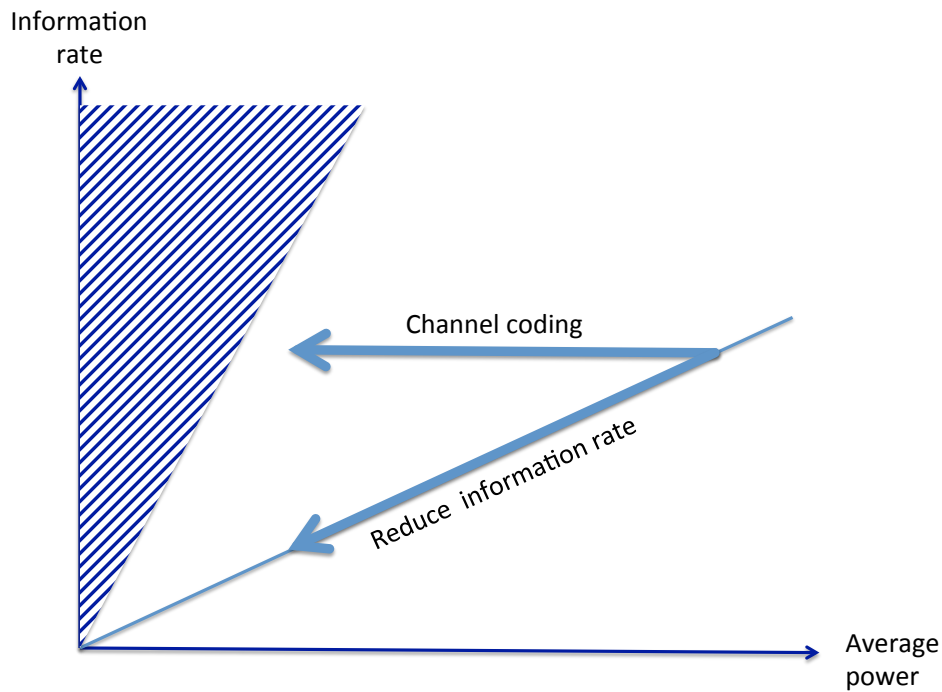


Figure 1.2: The motivation behind channel coding is to reduce the average power without having to reduce the information rate. A simpler but less effective approach is to reduce the average power by a commensurate reduction in information rate.

1.2.6 Channel coding

Shannon proved that it is feasible to approach the fundamental limit with channel coding. The simplest communication schemes we might conceive might map information bits into a waveform transmitted on the channel, and do so one bit at a time. For example, an approach called on-off keying (OOK) transmits a signal waveform to convey a "one" bit, and the absence of a signal waveform to convey a "zero" bit. Another example would be phase-shift keying (PSK), which transmits a sinusoid with zero phase or a sinusoid shifted in phase by 180 degrees. The idea behind channel coding is a straightforward but powerful generalization of this simple approach. While one bit represents two alternatives (like "on" or "off"), a group of M bits represents 2^M alternatives. So after dividing the information into groups of M bits, each group of M bits can be represented by transmitting one of 2^M waveforms, which are called *codewords*. The receiver reverses this process, deciding which of the 2^M waveforms is the most likely to have

been transmitted, and mapping the result into M bits. The essential characteristic of channel coding is that the receiver cannot discern individual bits by looking at the waveforms in a simpler way, but is forced to recover or extract all M bits together. A very simple example would be a variant on OOK, in which the transmitter starts with two bits, and transmits one of four OOK sequences, either $\{\text{ON}, \text{OFF}, \text{OFF}, \text{OFF}\}$ or $\{\text{OFF}, \text{ON}, \text{OFF}, \text{OFF}\}$ or $\{\text{OFF}, \text{OFF}, \text{ON}, \text{OFF}\}$ or $\{\text{OFF}, \text{OFF}, \text{OFF}, \text{ON}\}$.

Appropriate channel codes for improving power efficiency look very different from the approaches we are accustomed to in terrestrial communication. This is because terrestrial communication overwhelmingly seeks to minimize signal bandwidth as a priority over minimizing average power, due to the scarcity of spectral allocations and the resulting high monetary value attached to spectrum. The radiated power at the transmitter is usually small relative to the power consumed in the processing required in the receiver to deal with small signal bandwidth, so a penalty in radiated power is normally quite acceptable as the price paid for that reduced bandwidth. It is fair to say that previous authors addressing interstellar communication have been implicitly influenced by the approaches used in terrestrial communication, and thus have overlooked the opportunity to reduce the average transmitted power through the appropriate use of channel coding directed at achieving the highest power efficiency.

1.2.7 Guidance from the fundamental limit

This report establishes the fundamental limit on power efficiency for the interstellar channel, taking into account all known propagation and motion impairments. This establishes the maximum power efficiency that is theoretically consistent with reliable communication. The power efficiency that can be achieved with signal designs typically found in the literature on interstellar communication can then be compared to this fundamental limit. They must achieve lower power efficiency, and in fact we find that their penalty in power efficiency is substantial, on the order of four to five orders of magnitude, depending on the details of the signal chosen.

It is possible that an advanced civilization has developed extremely inexpensive energy sources, and would not be concerned about such a penalty in energy consumption. However, it seems more likely that the transmitter designer will have a keen interest in minimizing energy consumption, since that consumption can be large to start with. At minimum it seems appropriate to include power-efficient signals in the repertoire of signal types to be sought by a SETI observation program. A significantly more technologically advanced civilization is subject to the same fundamental limit on power efficiency as are we, and if they pursue the power-efficient (as opposed to spectrally efficient) design approach we would expect them to arrive at similar design principles. In any case we can be certain that even should they follow a different practical design approach, they can achieve no greater power efficiency than permitted by the fundamental limit.

It is not practically feasible to achieve the fundamental limit in practice, since that requires a channel code using waveforms that are infinitely wide in bandwidth and have an infinite time duration. Nevertheless a worthy goal is to approach as close to the limit as possible, approximating this limiting case with waveforms that are finite in bandwidth and time duration. It will be shown

that a set of five simple principles of power efficient channel-coding design can reduce the transmitted power significantly, without reducing the information rate. In fact, for any information rate and average power outside the forbidden region, it is shown that application of these principles in combination results in a channel code that can asymptotically achieve an error rate approaching zero. By asymptotically, we mean that certain parameters of the design grow without bound. Thus, to the extent that we are willing to let these parameters get large, we can get as close as we like to the fundamental limit at any desired error rate in the recovery of the data. On the other hand, staying in the realm of what might be considered practical choice of these parameters, there remains a penalty in power efficiency relative to the fundamental limit on the order of one order of magnitude.

In addition to energy consumption, use of these five principles of power efficient design can provide a powerful form of implicit transmitter-receiver coordination. The fundamental limit will presumably be known to both the transmitter and receiver, and a design that seeks to approach that limit will be a goal of any transmitter designer that considers average power and the resulting energy consumption to be a more limiting resource than bandwidth. The design of a channel code capable of approaching the limit is certainly not unique, but in our judgement the channel coding we demonstrate is the simplest way to achieve this goal. All five principles are themselves simple, each solves a significant challenge posed by impairments on the interstellar channel, and they are complementary to one another. In addition, we show that it is relatively straightforward to discover signals designed in accordance with these principles, whereas other most complicated approaches are likely to compromise discovery and render the reverse engineering of the details of the channel code more difficult for the receiver. Research into alternative approaches to power-efficient channel coding is nevertheless warranted.

1.2.8 Characteristics of power-efficient signals

The design principles we espouse result in a transmit signal with very specific characteristics. Again, we can't say with certainty that this is the only way to approach the fundamental limit, but in our judgement it is the simplest way.

A power-efficient signal can be expected to consist of on-off patterns of energy (which we call "energy bundles"). An energy bundle consists of a bandlimited and time-limited waveform which can be positioned in both time and frequency. The frequency is controlled by choice of the carrier frequency used to modulate the waveform. The receiver estimates the energy in bundles by calculating the magnitude-squared of the output of a matched filter, without seeking to recover any phase information. This energy estimate can be applied to a threshold to decide whether an energy bundle is present at a particular time and frequency, or not.

Each codeword in a power-efficient channel code consists of a specific pattern of energy bundles in time and frequency. The defining characteristic of these codewords is the high sparsity (or low density) of energy bundles in both time and frequency. Sparsity in frequency results in a large bandwidth relative to the information rate, which is a mandatory characteristic of any channel code capable of approaching the fundamental limit on power efficiency. The purpose of this fre-

quency sparsity is to convey *multiple bits* of information by the location of a *single* energy bundle, thereby conserving energy. For a fixed average power, sparsity in time enables each bundle to contain a larger amount of energy than would be possible if the transmitted signal were more continuously transmitted, and this larger energy allows the presence of the bundle to be more reliably detected in both communication and discovery. The purpose of sparsity in time is thus to improve the reliability with which an energy bundle can be distinguished from noise, and this is how the error rate can be driven asymptotically towards zero. A simple approach to discovery of the information signal is to searching for and detect individual energy bundles.

Typically the transmitter is designed to achieve a desired information rate and target error rate. For that given target error rate, the transmitter can reduce its average transmitted power by increasing the sparsity of energy bundles and simultaneously increasing the energy within each bundle. The fundamental limit on power efficiency dictates the lowest average power that is feasible, and that average power is approached as the sparsity of energy bundles in both time and frequency is increased without bound. In practice some finite values must be chosen, and this results in a residual penalty in average power.

Once the average power has been reduced by design of a power-efficient channel code, the average power can be reduced further if desired through a reduction in the information rate. This reduction increases the sparsity of energy bundles in time without reducing the bandwidth of the information-bearing signal. As the average power is reduced the energy bundles become more and more sparse in time, an observation that has profound consequences for the discovery strategy.

1.2.9 Interstellar coherence hole

Transmitted energy bundles are optimally detected at the receiver in the presence of noise by using a matched filter. The waveform that is chosen by the transmitter designer as a carrier for energy bundles can be specifically designed to avoid most of the interstellar impairments, specifically by restricting the waveform's time duration and bandwidth. The resulting waveform falls with the coherence time and the coherence frequency dictated by the interstellar propagation and transmitter-receiver motion. When as many impairments as possible are avoided in this fashion, the transmitted energy bundles are said to fall in an *interstellar coherence hole* (ICH).

There are two remaining impairments that cannot be avoided in this fashion: noise and scintillation. At radio frequencies noise is due to thermal effects such as the background radiation of the cosmos, star black-body radiation, and the finite temperature of the receiver's circuitry. Scintillation is due to scattering caused by the ionized nature of the interstellar medium, and inhomogeneities in ionization density, working in combination with the lateral motion of the receiver and turbulence in the interstellar clouds of ionized gas. Scintillation is manifested by a time variation in the average signal flux arriving at the receive antenna.

Making use of the ICH in the design of energy bundles does not compromise the available power efficiency. In fact, it is a necessary step to approaching the fundamental limit on power efficiency, or in other words violating the ICH and thereby introducing impairments in addition to noise

and scintillation will prevent the fundamental limit from being approached. The time duration and bandwidth of the resulting energy bundles are constrained as to parameterization based on physical quantities of the interstellar medium that can be observed and estimated by both transmitter and receiver designers, providing another form of implicit coordination. In fact, we should consider ourselves fortunate because the very existence of interstellar and motion impairments and our ability to observe and model them provides a wealth of information about the nature of channel codes and signal waveforms designed specifically to avoid those impairments.

1.2.10 Countering scintillation

The basic building block of an energy bundle confined to the ICH followed by a matched filter in the receiver is the optimum way to countering noise. It does nothing to deal with scintillation, however. The goal of a power-efficient channel code is to achieve reliable information recovery in spite of periods of low received signal flux characteristic of scintillation. Scintillation does not compromise the ability to approach the fundamental limit if *diversity combining* is employed. This strategy divides the total energy of a single energy bundle into a multiplicity of bundles which are at times or frequencies spaced far enough apart that they experience independent scintillation conditions. The receiver averages the energy estimates for individual bundles to obtain a more accurate estimate that is less affected by scintillation.

An alternative *outage strategy* abandons the goal of reliable recovery of all the information, but simply seeks reliable recovery of information during periods of higher-than-average received signal flux and ignores the received signal during periods of lower-than-average flux. With this simpler strategy, an additional burden is placed on a transmitter to encode the information in such a way that massive losses of data during outages can be recovered at the receiver, presumably through another layer of redundancy. In interstellar communication, the same message is likely transmitted repeatedly, since the transmitter has no idea when a receiver may be listening, and if so this redundancy provides a natural way to recover the information lost due to outages.

1.2.11 Simplicity of power-efficient design

One major benefit of power-efficient design (in addition to energy conservation) is its simplicity, which is quite beneficial when the transmitter and receiver designs are not explicitly coordinated. Removing the constraint on signal bandwidth simplifies design and it is relatively easy to identify simple and practical design principles that achieve high power efficiency. This can be seen in the types of channel coding schemes used in terrestrial communications, which can be said without exaggeration to be vastly more complex and opaque than what has been described for the power-efficient case.

One manifestation of this simplicity is due to the ICH. The approach of the ICH is to design the transmit signal to *avoid* as many interstellar impairments as possible, rather than trying to *compensate* for them in either transmitter or receiver as would typically be attempted in terrestrial

communication. This implies that there is no processing required in the receiver related to interstellar impairments, other than noise and scintillation, during either communication or discovery. Bandwidth is increased modestly with this approach, but this is of no concern when bandwidth is unconstrained.

A receiver should be able to readily "reverse engineer" a signal designed according to power efficiency principles to recover the "raw" information content. Of course inferring the "meaning" of that information entails a whole other level of difficulty that is not addressed in this report.

1.2.12 Discovery of power-efficient signals

It serves no useful purpose to transmit a signal with impressive power efficiency, but which is very difficult for the receiver to discover in the first place. It also serves little useful purpose to require another attention-attractive "pilot" or "beacon" signal to accompany the information-bearing signal, if that beacon requires a relatively high average power, undercutting the original goal. Thus, one significant design constraint in power efficient design is to insure that the signal can be discovered with a reasonable level of resources applied in the receiver. This issue is made more critical by the "needle in a haystack" problem of lack of prior knowledge as to the line of sight and frequency where a signal is to be found. Thus the challenges posited by the discovery of signals designed according to power-efficient principles is addressed in some detail in this report.

At first blush, one might expect that an information-bearing signal specifically designed to have low average power would be difficult to discover, precisely because of that low-power objective. Surely, I hear you say, a signal with lower average power will in general be more difficult to discover than a signal with higher average power. Generally that is true, but not in the way that one might expect. It all goes back to the structure of power-efficient signals, which have relatively low average power, but do *not* have relatively low peak power. In fact, they consist of energy bundles that are sparse in time and in frequency, but which have individually a sufficiently large energy to be readily detected. Thus at lower power levels the challenge is the increasing sparsity of the bundles, not their individual energies.

Power-efficient information-bearing signals are amenable to being discovered by an observation program that searches for individual energy bundles, but is not cognizant of any other details of the channel coding in use. Although there is a challenge for the receiver in guessing the waveform used to convey a single energy bundle, other than that they are relatively easy to detect because of their high energy content (in relation to the noise) and because they arrive with no appreciable impairments introduced by the interstellar propagation (such as "plasma dispersion" or "Doppler shift due to acceleration") that interfere with their detectability or require any related signal processing resources. After observing one or more individual energy bundles, the receiver should then monitor the "vicinity" (in both time *and* in frequency) for more individual energy bundles. Discovery is not a singular event, but rather emerges with a statistically significant number of detections of individual energy bundles, and becomes even more statistically significant as discernible and repeating patterns or energy bundles emerge.

The most significant challenge in discovery arises from the sparsity of energy bundles as well as the variation in received signal flux wrought by scintillation. Both these phenomena, individually and in conjunction with one another, imply that the most efficient use of receiver resources is to make relatively short observations looking for an energy bundle, but to repeat those observations multiple times in the same vicinity with intervening time intervals large relative to the coherence time of the scintillation. Thus, not only is discovery search a long-term project because of the large number of frequencies and lines of sight to be searched, but also because discovery at a single location is a long-term project consisting of numerous short observations spread over a significant period of time. Fortunately, individual energy bundles in a power-efficient signal will by design (in the interest of reliable information recovery) have sufficient energy to be detected at high reliability whenever an observation does overlap an energy bundle and scintillation conditions are simultaneously favorable.

In terms of the detection of individual energy bundles, there is no fundamental lower limit on average power like that for communication of information. This is because the receiver is extracting only a single bit of information (one or more energy bundles is present, or not) and has in principle an unlimited time (and hence an unlimited total available energy) to work with. Thus, as the receiver extends its total observation time in a given location, in principle perfect reliability in detection of one or more energy bundles is approached regardless of the average power of the signal and the strictness of the false alarm criterion. The practical limitation on detection reliability follows from the limited patience of a receiver to extend its observation time or its number of observations. Patience is required for several reasons. A transmitter may be transmitting only sporadically along our common line of sight as part a targeted scanning strategy. The transmitter can have no knowledge of the state of scintillation, and thus cannot “cherry pick” the right times to transmit. Thus during those periods when a transmitter is active, the signal may or may not encounter a favorable scintillation condition. Finally, when a transmission does encounter favorable scintillation, energy bundles are still sparse in both time and frequency. Fortunately sparsity in frequency is not an obstacle if the receiver employs multi-channel spectral estimation as is the case with current SETI searches.

In design of a transmit signal, therefore, the challenges of discovery suggest the inclusion of another objective in addition to power efficiency. The power efficiency criterion means that we are seeking the lowest average signal power consistent with a given information rate and a given objective for the reliability of information recovery at the receiver. In terms of discoverability, the transmitter has to assume that the receiver is making multiple observations, but also evidently a finite number of observations. The transmitter can make some assumption about the number of observations in place, or in other words make an assumption as to the minimum resources devoted to discovery by the receiver. Subject to that assumption, as well as an objective for the reliability of discovery, the transmitter seeks to minimize the average signal power. We call this strategy *power optimization* of the signal design. The compatibility of power efficiency in conveying information reliably and power optimization in enabling reliable discovery is studied.

Fortunately these two complementary design objectives do not clash with one another. The most significant observation is that there is a coupling between the number of observations necessary at the receiver and the information rate. Lower information rate results in lower average power and

fewer energy bundles per unit time, and hence a larger number of observations required of the receiver. Another conclusion is that time diversity does interfere with discoverability, since it lowers the amount of energy in each individual bundle, and this requires an appropriate modification (with a resultant penalty in average power) to the diversity strategy to maintain discoverability. This is an additional factor favoring the outage strategy to dealing with scintillation.

1.2.13 Information-free beacons

An alternative to an information-bearing signal is a *beacon*, or signal designed to be discovered but otherwise conveying no information. Reliability of information recovery and power efficiency are not relevant criteria for beacon design, so power optimization becomes the only relevant figure of merit. A *power-optimized* beacon design minimizes the average power of the beacon for a fixed total observation time at the receiver. Since it does not convey information, a beacon does not have to be sparse in frequency or have a wide bandwidth in order to achieve power optimization. At low average power, endowing individual energy bundles with a sufficient amount of energy to enable reliable detection of individual energy bundles during discovery does imply sparsity of energy bundles in time. This structure as well as scintillation imply that the receiver must make multiple observations in order to reliably detect a power-optimized beacon, unless it requires extraordinary high average power.

In 1970 the Cyclops report prescribed a type of narrowband beacon in which energy is transmitted continually, and this is the target of many current SETI searches [1]. A comparison between power-optimized beacons and a Cyclops beacon reveals that a substantial reduction in average power is available, but this does require that the receiver make multiple short observations. For example, assuming 1000 independent observations by the receiver, an average power reduction by a factor of about three orders of magnitude can be achieved at an equivalent reliability in the detection of individual energy bundles. In this example, an energy bundle is being transmitted and received about 3% of the time. As the number of receiver observations is increased, the necessary average power is further reduced, with no lower limit.

Such low-average-power beacons have very similar characteristics to information-bearing signals with low information rate, and in fact offer no particular advantage in terms of ease of discovery. The major difference is that an information-bearing signal will consist of energy bundles at multiple frequencies rather than just a single frequency, but multiple frequencies presents no special challenge if we assume that the receiver performs a multichannel spectral analysis. Minor modification to the design of an information-bearing signal entailing a small penalty in power efficiency may be required to enable efficient discovery. Both power-efficient information-bearing and power-optimized beacon signals can be discovered using a common search strategy and algorithms, because they both seek individual energy bundles. Although neither is likely to be discovered by existing SETI observational strategies, a roadmap is provided for how existing strategies can be initially enhanced, and later optimized to search for power-efficient and power-optimized signals.

1.2.14 The role of low duty factor

We have concluded that both information-bearing signals and beacons with low average power are characteristically composed of energy bundles that are sparse in time. In other words, an energy bundle is being transmitted only a fraction of the time, and the rest of the time the transmission is silent. The fraction of time for transmission is called the *duty factor*. There are many examples of low-duty-factor solutions to engineering challenges where average power is a consideration. A couple that have some similarity to interstellar communications are the photographer's flash unit and a pulsed radar. The flash unit is illuminating a target for the purpose of capturing an image, the radar is illuminating a target to monitor the reflection and estimate its position, and the communications transmitter is illuminating the target conditionally based on some information it wishes to convey. Examining the similarities and differences among these three applications offers some insight into the benefit of low duty factor design.

The first motivation for low duty factor in all three applications is energy conservation. In all three cases there is corruption by noise, and the intensity of the electromagnetic illumination has to be sufficiently high to overwhelm any noise that is present. Briefly creating the necessary intensity requires much less average energy consumption than would be necessary for continuous illumination at the same high intensity. This is important for the flash unit because it is battery powered, and reducing the energy required for each photograph allows more photographs within the total battery capacity. Radar and interstellar communication are similar to one another in that reducing average power reduces average energy consumption and eases the thermal management challenges in the transmitter electronics. The average power can be reduced by a reduction in the duty factor.

An astronomer might ask about the effect of "integration time", which is averaging over longer periods of time. This is an issue where the flash is significantly different from radar and communications. In the case of the flash, the illumination is essentially a thermal noise source, having the same characteristics and statistics as the thermal noise introduced in the sensor except (hopefully) with a higher noise temperature. The sensor measures the temperature of the illumination plus sensor noise. Averaging over longer periods of time reduces the spatial variation in the estimate of temperature, but does not eliminate the need for the temperature of the illumination to be high relative to the temperature of the sensor-introduced noise. Thus, the main requirement is for the illumination to be bright, with additional benefit from a longer duration of illumination (at the expense of total energy expended) in reducing the spatial statistical variation in the sensor's temperature estimate.

Integration time plays a very different role in radar and communications because of the matched filter. It would be possible to eschew the matched filter and operate like the photographic flash and camera sensor, but the fundamental limit on power efficiency could not be approached in this fashion. This is because the sensor would respond to all the noise within the bandwidth of the signal, whereas a matched filter responds only to that fraction of this in-band noise that is perfectly correlated with the deterministic signal waveform. However, in order to implement a

matched filter the receiver has to know (or guess) the waveform of the signal.¹ That waveform can be anything, such as a sinusoid or a noise-like signal, but the receiver has to know that exact waveform. When the output of the matched filter is sampled at the right time, the ratio of signal to noise depends only on the energy of the waveform, and not its time duration or bandwidth or any other property. This is a property of coherent detection, in contrast to the incoherent estimation in the camera sensor. With coherent detection, it is possible to increase the duration of the waveform arbitrarily while keeping its total energy fixed without penalty, beneficially reducing the peak power.²

Why then don't we fully exploit this integration time idea in radar and communications in order to transmit continuously rather than in bursts? The answer has to do with motion, specifically the motion of the source and target and (in the case of interstellar communication) motion of the turbulent clouds of gasses in the interstellar medium. This motion has the effect of modifying the waveform of the signal in an uncontrolled way, potentially interfering with the proper role of integration time in the operation of the matched filter. The effect we see at the matched filter output is a reduction in signal level (but no reduction in noise variance) due to the deleterious effects of motion. The time duration of the signal waveform has to be kept small enough to render this adverse effect of motion sufficiently small that it can be neglected, if we aspire to approaching the fundamental limit.

The low duty factor of low-power information-bearing signals or beacons is a critical property, one that profoundly influences the strategies for discovery of those signals. This low duty factor is an inevitable consequence of three considerations. First, the energy of individual bundles must be sufficiently large to overwhelm the noise. Second, the time duration of the energy bundles must be small enough to render the coherence-destroying property of motion negligible. Third, the only way to reduce the average signal power and stay true to the first two considerations is to maintain a fixed energy for each bundle while reducing the rate at which bundles are transmitted, or in other words reduce average power through a reduction in the duty factor. The peak power of the signal stays constant even as the average power is reduced.

1.3 Implications for SETI observation programs

The end-to-end approach taken in this report yields relevant insights into the design of both transmitter and receiver for interstellar communication. Near term the most profound implications apply to receiver design, which applies directly to the search for extraterrestrial intelligence (SETI). Most such searches at radio frequencies have assumed a continuously received signal, exploiting

¹ In principle a camera and its flash unit could use coherent detection, thereby allowing a lower total-energy illumination for each photograph. The reason it doesn't presumably has to do with the technological difficulties of doing this at optical wavelengths, where generating a non-monochromatic coherent waveform is difficult.

² Actually one form of incoherence creeps in, specifically phase incoherence. Even though the waveform may be known, there is an unknown phase factor due to scintillation and unknown carrier phase. The key property of this phase factor is that it is fixed for the duration of the waveform, so the matched filter can perform coherent integration in spite of this unknown phase. The output of the matched filter contains this unknown phase factor, which can be eliminated by calculating the magnitude. This is called phase-incoherent detection.

that assumption to reject false alarms through presumed signal persistence and adding a presumed extraterrestrial signatures such as Doppler-drift in frequency. This assumption of continuous transmission and reception implies a signal average power that is some orders of magnitude larger than necessary, should the transmitter designer seek to reduce its energy consumption and capital costs through a reduction in the duty factor of the signal.

Existing searches may in fact have detected individual energy bundles from a power-efficient information-bearing signal, or a power-optimized beacon, but also rejected these detected events as "false alarms". Such is the case for example for the most famous of these incidents, the so-called "Wow!" signal [10]. Fortunately these present-day search strategies can be fairly easily modified to search for power-efficient information-bearing signals and power-optimized beacons. The nature of the modification is mainly to eschew the concept of "false alarm" entirely, return to each location systematically over a long period of time, redefine the back-end pattern recognition pattern recognition algorithms, and maintain a worldwide shared database of all detected energy bundles (which are indistinguishable from "false alarm" events) to guide future observations to the most promising locations and to ultimately identify locations deserving of longer-term scrutiny. These searches should also be generalized to consider alternative waveforms carrying an energy bundle, such as noise-like waveforms which are advantageous in their immunity to local sources of radio-frequency interference [11].

A search for power-efficient and power-optimized signals most closely resembles Astropulse, which is a search for isolated radio-transient events [12]. The main difference is that Astropulse assumes signal waveforms that are short in time duration and have wide bandwidth, and thus are strongly affected by the frequency incoherence of the interstellar medium, principally plasma dispersion. As a result Astropulse requires a processing-intensive de-dispersion step to reverse this effect. Such a waveform is quite plausible for events of natural origin, but is not characteristic of explicitly designed power-efficient and power-optimized signals, which are necessarily and explicitly designed to avoid as many interstellar impairments as possible. A search for power-efficient signals fortunately requires no processing related to interstellar impairments other than noise (in particular this is the role of the matched filter). The parameters of the search, such as the presumed time duration and bandwidth of the waveform supporting an energy bundle, are constrained by interstellar impairments subject to observation and characterization by both transmitter and receiver.

1.4 History and further reading

Relevant past work can be found in the literature both from terrestrial communication and from the past research on SETI.

1.4.1 Modeling the interstellar medium

One principle of power-efficient design is to choose a transmit signal that avoids as many interstellar propagation impairments as possible. Given the current state of spacecraft and propulsion technology [13], there is no possibility of our own direct experimentation with interstellar communication except with the cooperation of intelligent civilizations elsewhere in our galaxy. Fortunately astrophysical models and astronomical observations (especially from pulsar astronomy [14]) provide relevant models that can be used as a basis of design and predictions of performance.

It is a well established principle in astrophysics that over relatively short periods of time the integrity of a monochromatic wave is preserved by the ISM, with the exceptions of a frequency shift (due to Doppler) and scintillation (time variations in phase and amplitude due to scattering in the interstellar medium) [15]. This concept is generalized here to waveforms with finite bandwidth, establishing the concept of an interstellar coherence hole (ICH), which turns out to be critically important to both power efficiency and ease of discovery. The time-bandwidth product of the ICH is a critical parameter, and estimates establish that it is large enough to support power-efficient communication at all carrier frequencies of interest. It is also large enough to support interesting spread-spectrum options in the choice of waveforms [11].

1.4.2 Terrestrial wireless communication

While the details and parameterization are different, both scattering and motion impairments have much in common with terrestrial wireless communication. Thus there is a wealth of theory, experience, and practice with terrestrial wireless impairments that can be tapped [16]. The major difference, as emphasized earlier, is the emphasis on power efficiency as opposed to minimizing bandwidth, which drives the design of channel codes in very different directions.

1.4.3 Optical communication

It is interesting that an especially relevant parallel to interstellar communication at *radio* wavelengths is terrestrial communication at *optical* wavelengths. Power-efficient techniques at the sacrifice of bandwidth are more commonplace in optical communication, which is rarely limited by bandwidth resources [?]. The search for power-efficient radio signals also has similarities to pulsed optical SETI [17], which interestingly also assumes unconstrained bandwidth and conservation of energy through pulsed signals. In addition, the scale of physical features for propagation through the ISM are very large relative to a wavelength, even at radio frequencies, and are thus best understood in terms of geometrical optics [18]. Thus, the literature of optical as well as radio communication is an aid to understanding interstellar radio communication.

1.4.4 Power-efficient design

After fundamental limits on power and spectral efficiency were first identified in 1948, the conceptually and practically simpler power efficiency case was the first one attacked. By 1969 the problem of power efficient design approaching fundamental limits on a channel with additive noise and Rayleigh fading (which is equivalent to interstellar scintillation in the presence of strong scattering) was fully understood. R. Kennedy in particular proposed a set of relatively simple principles for power-efficient design on this channel, and proved that the fundamental limit on power efficiency can be approached by a combination of those principles [19]. Here we apply Kennedy's principles to interstellar communication, with the added complication of numerous interstellar impairments that are not included in Kennedy's model. We show that all interstellar impairments save noise and scintillation can be avoided by appropriate design of the transmit signal, and this step is necessary to approach the fundamental limit.

Due to a lack of commercial applications, and also because the challenges and solutions were well understood, power-efficient communication has not seen much original research since Kennedy's results were published. Achieving similar objectives of approaching the fundamental limit with a severe bandwidth constraint on the Gaussian channel took several additional decades of research, culminating with success in the mid-1990's with the identification of turbo codes [20] and low-density parity check codes [21].

1.4.5 Broadband interstellar communication

Numerous authors have expressly considered interstellar communication, although none as comprehensively as here or emphasizing the methodology of communication engineering. Of particular interest is past work on using wider bandwidths in interstellar communication. Clancy was notable as the first author to suggest the combination of a broadband signal (in his case a narrow pulse) taking some account of the dispersion in the ISM [22]. This is a very different approach to expanding bandwidth than dictated by power-efficient principles because it unnecessarily triggers interstellar impairments.

A couple of authors have proposed, as we do here, transmit signals specifically tailored to circumvent effects introduced in interstellar radio propagation, including Cordes and Sullivan [23] and Shostak [24]. In particular, Shostak notes the significance of dispersion and scattering and suggests that it may be necessary to limit the per-carrier bandwidth, and suggested working around that limitation using multiple carriers, each modulated with a narrower bandwidth. This is called *multicarrier modulation* (MCM) [25]. MCM is a technique widely used in terrestrial wireless, with the same motivation, and is a meritorious way to achieve low bandwidth (although it cannot achieve high power efficiency). However, the common thread between Shostak's observations and this report is to divide the signal into narrower bandwidth slices to avoid interstellar dispersion. Shostak proposes doing that by transmitting independent information-bearing signals, whereas our power-efficient approach is to transmit energy bundles at different frequencies (not simultaneously!) as part of a channel coding scheme for a single information-bearing signal.

Harp et. al. propose a receiver autocorrelation technique supported by the transmit signal that can limit the effect of ISM impairments [26]. Morrison addresses the discovery of broadband signals by highlighting a specific example [27]. Other authors have suggested some benefits for using wider bandwidth. In addition to those previously mentioned [6, 22, 4], Cohen and Charlton advocated the use of wideband signals to overcome frequency-selective fading in improving the chances of discovery [28], as did Cordes and Sullivan [23]. In our own work, the ability of broadband signals to improve immunity to radio-frequency interference was advocated [11], and the spread-spectrum signals proposed there are fully compatible with the design of energy bundles for power-efficient design.

Chapter 2

Power-efficient signal design

Most past treatises dealing with the search for extraterrestrial intelligence (SETI) and interstellar communication at radio wavelengths have emphasized the importance of energy resources. This is because the energy consumption associated with transmission of the radio signal will be large relative to other communication applications, largely because of the large interstellar distances and consequently the large propagation loss. Energy consumption can be reduced by increasing the gain of the transmit and receive antennas, although this requires them to be physically larger (while no less dimensionally precise) and thus involve a higher capital expense [29, 30]. Another opportunity to reduce energy consumption is to increase the receiver sensitivity by using more sophisticated signal processing techniques, but that has been largely exhausted by using optimal or near-optimal signal detection techniques to counter the inevitable noise of thermal origin. Some future modest improvement in the noise temperature of receiver circuitry may well be possible.

There is a third possibility for reducing energy consumption, which is the design of the transmit signals with the specific goal of reducing their average power without affecting the reliability with which information can be recovered. Such changes in transmit signals must be accompanied by modified receiver signal processing algorithms at baseband to accommodate such signals. Surprisingly, this possibility has never been explored in the SETI community. This very challenge was addressed and essentially completely solved in the 1950's and 1960's by communication engineers, but it seems that work has not influenced interstellar communication or SETI. That decades-old work focused on minimizing the average signal power required for reliable exchange of information at a certain rate, and proved there exists a fundamental limit and identified signal design techniques that can approach that fundamental limit asymptotically. As shown here, there is a penalty of four to five orders of magnitude in average power (relative to the fundamental limit) required for the types of signals typically assumed in the SETI literature. The remainder of this chapter and report is devoted to finding ways to reduce that penalty substantially using relatively straightforward design techniques.

The models used assumed that the signal is affected by fading, which is a random fluctuation of signal amplitude, as well as thermal noise. Both of these phenomena are prominent in inter-

stellar communication. In astronomy the same phenomenon as fading is called scintillation, and noise of thermal origin is a universal feature of both the cosmos and receiver technology. In this report the fundamental limit on power requirements for interstellar communication at a certain information rate is derived, and it is shown that using a set of five simple signal-design principles accompanied by appropriate receiver signal-processing algorithms this fundamental limit can be approached. No civilization, present or future, can bypass this fundamental limit within the scope of the channel models we use, which themselves invoke the classical physics of radio propagation and noise.

In order to accomplish this in the context of interstellar communication, we must address a couple challenges that were not considered in the decades-earlier research by communication engineers. First, they did not directly deal with the specific impairments introduced in interstellar communication, although their models (which were motivated by terrestrial communication challenges) turn out in the end to be surprisingly relevant. Second, they assumed that transmitter and receiver designs are coordinated, and focused only on communication of information once the receiver has acquired the transmitter's signal. In interstellar communication, the initial discovery of the signal is more challenging than the communication of information once the signal is discovered, both because of the lack of coordination between transmitter and receiver designers and because of the "needle in a haystack" challenge of a large parameter space over which to search. The primary purpose of this report is to invoke the earlier theories relating to minimizing average power (and hence energy consumption), coupled to an in-depth study of these two additional challenges of interstellar impairments and signal discovery.

This chapter is an overview of our approach to power-efficient design. While the fundamental limit on average power is universal, concrete design approaches to reducing average power are less fundamental. There is nothing to rule out the possibility that there may be other viable design approaches. However, our approach does meet two important minimum requirements for power-efficient design. First, it is able to approach the fundamental limit asymptotically. Second, it is very straightforward, combining a set of five principles that individually address one of the challenges posed by the interstellar communication channel. Each of these is the simplest response we can think of to its particular challenge, and none of these five principles can be abandoned without compromising power efficiency. In our judgement, there could be no other simpler design approach that is able to approach the fundamental limit. Simplicity is important for interstellar communication because of the intrinsic lack of coordination. Nevertheless, further research seeking possible alternative approaches to achieving power efficiency should certainly be pursued.

2.1 Efficiency measures for communication

When designing an interstellar communication system there are different criteria of merit that could be used. In this report, the minimization of average signal power is the figure of merit that is emphasized. In this section it is argued that this is compelling from the perspective of the economics of interstellar communication and the nature of the physical impairments encountered

in interstellar radio propagation.

2.1.1 Power efficiency

The average power of a signal, which we denote here by \mathcal{P} , is obtained by accumulating the total energy of the signal over a very long time and dividing by the time interval. Average power alone would never suffice, because another relevant figure of merit is the information rate, which we denote here by \mathcal{R} . \mathcal{P} has the units of watts, and \mathcal{R} has the units of bits per second. As will be shown, if bandwidth is not constrained then for both practical realizations and at the fundamental limit these two quantities are proportional to one another, or $\mathcal{R} \propto \mathcal{P}$. Given this reality, it is the ratio of the two quantities that is of greatest interest. For an information-bearing signal, the *power efficiency* \mathfrak{P} is defined as the ratio of the information rate \mathcal{R} and the average received power \mathcal{P} ,

$$\mathfrak{P} = \frac{\mathcal{R}}{\mathcal{P}} \text{ bits per joule.} \quad (2.1)$$

It is often convenient to work with the reciprocal of \mathfrak{P} ,

$$\mathfrak{E}_b = \frac{1}{\mathfrak{P}} \text{ joules per bit.} \quad (2.2)$$

The energy per bit \mathfrak{E}_b is particularly easy to interpret, as it is the signal energy required to communicate exactly one bit of information. If a message consists of N bits, then the total energy required to convey that message is $N\mathfrak{E}_b$. If a sequence of bits is conveyed at information rate \mathcal{R} , the average power required is $\mathcal{P} = \mathcal{R}\mathfrak{E}_b$.

The energy per bit \mathfrak{E}_b is one important figure of merit, but there is also the issue of the reliability. Inevitably some bits will be incorrectly decoded by the receiver due to noise and other impairments introduced in the interstellar signal propagation. Such errors make a message more difficult to interpret, and thus we want these bit errors to occur infrequently. The reliability is measured by the bit error probability P_E . For example, if $P_E = 10^{-4}$ then as a long-term average one bit out of every 10,000 will be decoded incorrectly (a "0" is turned into a "1" or a "1" is turned into a "0"). The power efficiency \mathfrak{P} can only be stated in the context of a particular level of reliability. If the receiver designer is willing to accept a poorer reliability (larger P_E), then a higher \mathfrak{P} can result.

Higher power efficiency \mathfrak{P} is desirable, since it implies that a proportionally smaller energy is required to communicate a given message, which implies a proportionally smaller energy consumption at the transmitter. Assuming that the transmitter considers energy as a scarce resource, \mathfrak{P} has the property that "more is better", as something labeled as "efficiency" should.

2.1.2 Spectral efficiency

The major competitor for power-efficient design is spectrally efficient design, where the major design objective is to minimize the bandwidth or range of frequencies occupied by the transmit

Table 2.1: Energy use and annual energy cost for interstellar communication at a distance of 500 light years, a carrier frequency of 5 GHz, and using prototype Arecibo antennas and electronics with an assumed 50% antenna efficiency and a system noise temperature of 8 degrees kelvin. The assumed price of energy is \$0.10 per kilowatt-hour, and all figures are for communication along a single line of sight. The fundamental limit is compared to an on-off keying (OOK) information-bearing signal, which is typical of the types of signals that are targets of most current and past SETI searches.

Parameter	Fundamental limit	On-off keying
Transmit power consumption @ $\mathcal{R} = 1$ bps	4.6 kilowatts	175 megawatts
Annual cost of energy @ $\mathcal{R} = 1$ bps	\$4 thousand	\$153 million

signal. Let B_{total} be the total bandwidth required for an information-bearing signal. The ratio of \mathcal{R} to B_{total} is a good figure of merit describing the total bandwidth requirements. The *spectral efficiency* \mathfrak{S} is defined as

$$\mathfrak{S} = \frac{\mathcal{R}}{B_{\text{total}}} \text{ bits per second per Hz.} \quad (2.3)$$

The spectral efficiency is completely determined by the transmitter through its choice of the structure and parameterization of the signal that bears information. Assuming that the transmitter and receiver designers consider bandwidth to be a scarce resource, then spectral efficiency also has the property that "more is better".

Two different measures of efficiency have been defined, and a natural question is whether both types of efficiency can be achieved simultaneously. As will be developed in the remainder of this chapter, the answer is a definitive "no". There is a fundamental and unavoidable tradeoff, in that high power efficiency is associated with low spectral efficiency, and vice versa. Thus, the designer of an interstellar communication system has to choose sides. Is that designer going to emphasize power efficiency, or spectral efficiency? We believe that for interstellar communication the choice is obvious: power efficiency. This choice will now be justified by pointing out some implications of power efficiency to interstellar communication.

2.1.3 Energy consumption

The primary practical implication of average power is the energy consumption that it imposes on the transmitter. The average power required for a certain rate of information exchange is equivalent to the consumed energy required for exchange of a certain volume of information, and this is a metric of energy efficiency that may be of intense interest to the operator of a transmitter that has to pay the utility bills. Although a receiver can reliably extract information from a signal with very low average power, in the interstellar context the propagation losses are very large, and very large transmit average powers are required to achieve small received average power.

This situation is analyzed in Appendix A, where a link budget is developed for a typical interstellar communication scenario, and an example is displayed in Table 2.1. A fundamental lower limit on the energy per bit \mathfrak{E}_b for the interstellar channel is developed later in this chapter and in Chapter 4, and this lower limit on average power is compared to on-off keying (OOK), which

is described shortly and is typical of the types of signals being targeted in current and past SETI searches. A convenient unit of power consumption is the LHC, defined as the power consumption of the Large Hadron Collider (LHC) at the European Organization for Nuclear Research (CERN) for the collider alone. One LHC equals about 300 megawatts. The average transmit power \mathcal{P} required for reliable communication using OOK is about 38,000 times larger than the fundamental limit, at an information rate of $R = 1$ bit per second equals about 0.58 LHC.

As an example of a practical application, It has been suggested that a real-time representation of our music would be meritorious as a transmit signal [31]. Although it would not be necessary "stream" music in real time, consider the case where it is streamed.¹ At an information rate of 256 kilobits per second (a typical information rate for music purchased and downloaded), the transmitter's power consumption would be about 150,000 LHC. In practice it would be very difficult for the receiver to reverse engineer the complex compression algorithms required for this information rate, so a more realistic assumption might be the representation used for the older the compact audio disk, which requires an information rate of 1411 kilobits per second for a power consumption of 826,000 LHC. At the fundamental limit on power efficiency this drops to a "mere" 21.7 LHC. In general the conclusion is that at this distance, it may be too costly to stream music across such interstellar distances. So much for an intergalactic version of the iTunes store.

We do not know the price of energy for another civilization, but we do know that the price of electricity on Earth is roughly one U.S. dollars per ten kilowatt-hours, and at that price the annual energy cost of transmission at an information rate of one bit per second increases from \$4 thousand at the fundamental limit to \$153 million for OOK. This indicates that the cost of energy consumption, at least at Earth pricing, is very significant for OOK, which suggests great economic pressure to keep energy consumption at a level as close to the fundamental limit as feasible. Certainly this would be true if we were building a transmitter here on Earth, and it is a reasonable assumption that this would be true in other worlds as well.

There are several parameters that affect the energy consumption of Table 2.1 and should be kept in mind:

Reduce information rate. The average transmit power is proportional to the information rate $\mathcal{P} \propto \mathcal{R}$. Accepting a lower information rate will lower the power requirement. However, this approach may not be all it is cracked up to be. If we wish to convey a message of a certain fixed length, then reducing the information rate not only reduces the average power, but it also extends the time duration for transmission of the message and does nothing to reduce the total energy (or cost of energy) required to convey the message.

Increase carrier frequency. For fixed antennas, the average transmit power drops with an increase in carrier frequency f_c as $\mathcal{P} \propto f_c^{-2}$. This is because the gain of an antenna is related to its physical size in relation to the wavelength. However, larger f_c does impose more stringent requirements on the antenna.

¹ In [31] it is proposed to transmit an analog representation of music. The fundamental limit on power efficiency applies to analog sources as well as digital. In practical terms, approaching that fundamental limit requires a digital representation, including the maximum data compression to reduce the total information required to represent the music source to the minimum possible.

Reduce distance. The average transmit power increases with distance D as $\mathcal{P} \propto D^2$ in order to overcome the distance-related propagation loss. For example, if the distance in the example of Table 2.1 were doubled to 1000 light years, the average transmit power would have to increase by a factor of four.

All these parameters affect the fundamental limit and OOK equally, so they do nothing to reduce the average power penalty for OOK relative to the fundamental limit. As discussed in the remainder of this report, the transmit signal can be designed with the specific goal of reducing that penalty, obtaining a power efficiency that comes much closer to the fundamental limit as was illustrated in Figure 1.2. This is a far more attractive way to reduce the average power \mathcal{P} than reducing the information rate \mathcal{R} or distance D .

2.1.4 Heat dissipation

Any transmitter will fundamentally suffer some inefficiency in conversion from energy input to transmitted average power. There are two implications to this. First, the annual costs of energy consumption in Table 2.1 must be adjusted upward to account for this inefficiency. Second, the energy lost to inefficiency is converted to heat, which must be dissipated to (literally) prevent the transmitter electronics from melting. The amount of heat to dissipate will be proportional to the average transmit power, so OOK presents a drastically larger thermal management issue. Heat dissipation at these power levels will consume a major portion of the capital cost of building a transmitter. The comparable heat dissipation in the Large Hadron Collider is spread over an instrument that is 27 kilometers in circumference.

2.1.5 Multiple lines of sight

The transmitter requires the expenditure of a very large total energy in what may prove to be a hapless attempt to communicate with a receiver that never existed. The transmitter probably also has little idea of where its signal may be observed, and thus is likely to transmit signals along multiple lines of sight concurrently, just as the receiver is observing along different lines of sight. To have a reasonable expectation that a signal will be received, targeting thousands or tens of thousands of relatively nearby stars will be necessary. This multiple line-of-sight requirement magnifies by an equivalent factor the challenges relating to the cost of energy consumption and heat dissipation.

2.1.6 Peak power

The peak power $\mathcal{P}_{\text{peak}}$ is defined as the average energy measured over short time periods. Although the peak power does not relate directly to energy consumption or heat dissipation, there will nevertheless be a penalty in the capital cost of building a transmitter for larger peak power. It will be shown in the sequel that even as we reduce the average signal power there is little opportunity to simultaneously reduce the peak power. Peak power must always remain large enough

to overcome propagation losses and the noise floor at the receiver, while average power is most efficiently reduced by lowering the duty factor of the signal, transmitting a signal intermittently. The requirement on peak power is affected by the gains of the transmit and receiver antennas, so there is an opportunity to reduce both peak and average power by expending more resources on the antennas.

2.2 Basic building block: Energy bundles

Our approach to power-efficient design uses the *energy bundle* as a basic building block. We now describe the concept of an energy bundle, how it is transmitted, and how it is detected.

Our basic approach is to transmit a bundle of energy and at the receiver observe the bundle's excess energy over and above the noise. There are two defining characteristics of an energy bundle. First, at a given location (defined as carrier frequency and time) an energy bundle is either present or absent. Although this makes it appear like one bit of information is conveyed by this presence or absence of an energy bundle, in fact the essence of power efficient communication is to convey much more than one bit of information with a single energy bundle, as will be seen. Second, in its detection the receiver *estimates* the amount of energy in a bundle as the first step in *detecting* the presence or absence of an energy bundle, but is oblivious to any phase information. The distinction between estimation and detection is significant. Estimation seeks to answer the question "how much energy is present in a hypothetical bundle at this location", while detection seeks to answer the question "is there a bundle present or not at this location". Typically the detection question is answered by applying a threshold to an estimate of the energy.

In communications, a *channel* is the physical entity that conveys information from one physical location to another. Over a physical channel based on radio propagation through the interstellar medium, an energy bundle is associated with a waveform $\sqrt{\mathcal{E}_h} h(t)$, which represents the electric field of the electromagnetic wave. The waveform $h(t)$ is assumed to have unit energy, defined as

$$\int_0^T |h(t)|^2 dt = 1. \quad (2.4)$$

The amount of energy in the bundle is \mathcal{E}_h , which is quite significant because \mathcal{E}_h determines how reliably the energy bundle can be detected in the presence of noise. Two other important characteristics of the energy bundle are the time duration T and bandwidth B of waveform $h(t)$. We will see that these two quantities are constrained by the properties of the interstellar channel.

2.2.1 Matched filtering

Noise of thermal origin inevitably accompanies an energy bundle. In the presence of this noise, the best method for detecting the excess energy represented by $h(t)$ over and above the thermal noise is a filter matched to $h(t)$. This *matched filter* is illustrated in Figure 2.1 and discussed in greater detail in Chapters 3 and 7. Detection of an energy bundle by matched filtering is essential to



Figure 2.1: An illustration of an energy bundle and its detection using a matched filter. It consists of a waveform $h(t)$ shown on the left, which can be simple or complicated. The remainder of the figure illustrates how this bundle of energy can be detected using a matched filter, which consists of a convolution (represented by \otimes) with a time-reversed and conjugated version $h^*(-t)$ (illustrated in the middle), with the result equal to the autocorrelation of $h(t)$ (shown on the right). This autocorrelation can be sampled at zero lag, and the resulting value represents a filtered sample of the thermal noise. Various types of $h(t)$ can be used as the basis for an energy bundle, but arguably the most useful are the segment of a sinusoid (on top) and the segment of a noise-like signal (shown on the bottom).

power-efficient design, because any other detection method will be less reliable and thus requires a larger bundle energy \mathcal{E}_h . It is significant that in order to apply a matched filter the receiver must know (or be able to guess) the waveform $h(t)$ chosen by the transmitter. Alternatively, as part of a discovery search strategy the receiver (at the expense of additional computation) can trial more than one waveform $h(t)$.

When examining issues like the relative energy of an energy bundle and noise, it is important to settle on a common place to observe and measure such things. In radio communications it is conventional to do modeling and measurement of the signal in the receiver, and at baseband following demodulation. A slight complication is that a passband radio signal, which is associated with a physical quantity like the electric field of the radio wave, is intrinsically real-valued, but must be represented at baseband by *two* real-valued signals, called the in-phase and quadrature signal components. For mathematical convenience, as discussed further in Chapter 3, it is conventional to represent these two signals all at once by a single complex-valued signal, where the real-part represents the in-phase signal and the complex-part represents the quadrature signal. Thus, the baseband waveform $h(t)$ is actually assumed to be complex-valued, and is said to have a magnitude $|h(t)|$ and a phase $\arg h(t)$. The matched filter actually filters the reception by convolving it with an impulse response $h^*(-t)$, a conjugated and time-reversed replica of $h(t)$.

In this report, $h(t)$ is assumed to be non-zero over the timescale $t \in [0, T]$. The range of frequencies present in $h(t)$ depends on the frequency used in the demodulation stage, but for simplicity and symmetry with time it is assumed that the demodulation frequency is at the bottom of the band of passband signals. That arbitrary convention makes $H(f)$, the Fourier transform of $h(t)$, non-zero for the range of frequencies $f \in [0, B]$. A waveform with only positive-frequency content is necessarily complex-valued, but we already expected this.

2.2.2 Phase-incoherent detection

The phase stability of an interstellar communication channel will be very poor because of the great distances involved and also because of scattering and scintillation phenomena as discussed in Chapter 3. Changes on the order of a fraction of a wavelength at the carrier frequency matter to phase, and one wavelength is absolutely minuscule in comparison to the distances involved in interstellar communication. In addition, the phase of the carrier frequency generated at the transmitter is unknown. For both these reasons, the receiver cannot depend on any phase information in a single energy bundle, and must use phase-incoherent detection of the bundle. This implies that the magnitude of the matched filter output is calculated, and phase is discarded. The square of this magnitude is an estimate of the single real-valued parameter \mathcal{E}_h . We call it an *energy* bundle because all the receiver is able to measure is its energy.

In our approach to power efficient design, an energy bundle will have only two possible energies, either zero or \mathcal{E}_h . The reason for this will become clear shortly, when power efficiency is contrasted to spectral efficiency.

2.2.3 The interstellar coherence hole

Impairments introduced in the interstellar medium (ISM) and due to the relative motion of the transmitter and receiver can have a deleterious effect on the detection of energy bundles by modifying the transmitted $h(t)$ to something different before it appears in the baseband receiver processing. However, by placing an upper bound on both $T \leq T_c$ and $B \leq B_c$, most of these effects can be rendered negligible, as discussed in Chapter 8. The largest values T_c and B_c are called respectively the *coherence time* and *coherence bandwidth* of the interstellar channel, and a waveform that meets these constraints is said to fall in an *interstellar coherence hole* (ICH). The coherence time T_c represents the time scale over which the interstellar phenomenon can be approximated as time-invariant, or unchanging. The coherence bandwidth B_c is the bandwidth scale over which any frequency-selective or frequency distortion phenomena can be neglected.

One significance of the ICH is that as long as energy bundles conform to its constraints, no processing is necessary in the transmitter or receiver relative to the interstellar impairments. However, the question arises as to whether the ICH constraint causes some compromise in performance. This is addressed in Chapter 4, where it is shown that not only does limiting energy bundles to the ICH not compromise power efficiency, but this constraint is actually necessary to approach the fundamental limits on power efficiency.

Two forms of coherence time

There are actually two coherence times of significance. The coherence time T_c discussed thus far is the *phase* coherence time, and it measures the time interval over which the phase, while unknown, remains stable enough that its effect on the energy estimate at the matched filter output can be neglected. When observing two energy bundles at different times, there will also be a variation

in the observed energy contained within the bundles, even though each was transmitted with the same energy. This energy difference results from a scintillation-induced variation in the received flux (the magnitude-squared of field intensity) impinging on the receiver's antenna. A longer *flux* coherence time T_f is the time over which the flux, and hence energy observed in each bundle, is stable. Generally speaking $T_f \gg T_c$.

Time-bandwidth product

The number of *degrees of freedom* of $h(t)$ is defined as

$$K = B T. \quad (2.5)$$

The degrees of freedom K is an important characteristic of $h(t)$, and is discussed further in Chapters 3 and 8. Chapter 8 estimates that for typical values of the physical parameters of interstellar communication and motion, $B_c T_c \gg 1$. This is a physical property of the Milky Way of immense significance to communication, because if it were not true then the interstellar propagation would be too unstable for reliable interstellar communication. Nature has been kind to us and other civilizations that seek mutual contact. In practical terms, it means that choosing an $h(t)$ that meets the constraint of the ICH is feasible, and the assumption of simultaneous bandlimiting and time limiting of $h(t)$ is a reasonable one when $K \gg 1$.²

Peak power

Together \mathcal{E}_h and T determine the peak power,

$$\mathcal{P}_{\text{peak}} = \frac{\mathcal{E}_h}{T}. \quad (2.6)$$

Since a smaller $\mathcal{P}_{\text{peak}}$ is generally advantageous, this suggests choosing T as large as possible, or $T \approx T_c$. Radio astronomers call T the "integration time", and seek to maximize it in order to gather more energy from a source.

Impairments remaining in a coherence hole

The impairments cannot *all* be eliminated by sufficiently reducing T and B . There are two impairments that persist no matter how small these parameters are chosen, and the transmitter and receiver must deal with these two impairments. These are additive noise (of thermal origin) and multiplicative noise (called *scintillation*). They are analyzed in Chapter 3, where a resulting model for the interstellar channel is developed that can be employed in communication system design.

² There is an uncertainty relation for the Fourier transform which asserts that $h(t)$ cannot be strictly speaking simultaneously bandlimited and time-limited. However, this assumption is a useful approximation for larger values of time-bandwidth product K , but we can say for sure that $K \geq 1$.

The matched filter is the receiver's way of dealing with noise optimally. When matched filter detection is used for this purpose, scintillation manifests itself as a variation in phase and magnitude of the sampled output of the matched filter from one energy bundle to another. The phase difference does not affect a receiver that estimates only the magnitude or energy in the bundle. Any difference in magnitude, however, is significant and a major consideration in the design of both communications and discovery strategies. Scintillation is an astronomical term, and the same phenomenon is called *fading* in the communications engineering literature. Fading is a usual affliction for radio communication in the presence of relative motion between transmitter, receiver, and the physical environment.

Choice of $h(t)$

The modeling of noise in the presence of matched filter estimation and detection yields an important insight. In terms of performance, the detailed shape of the waveform $h(t)$ does not matter, as long as it conforms to the constraints $T \leq T_c$ and $B \leq B_c$. The performance, as measured by detection reliability, is influenced only by the energy \mathcal{E}_h , and not the choice of waveform $h(t)$.

This lack of guidance from a performance standpoint makes the choice of $h(t)$ a potentially controversial issue. Two cases of particular interest are illustrated in Figure 2.1. The first is a time segment of a sinusoid, for which B is on the order of $B \approx 1/T$, and thus $K \approx 1$.³ The other interesting case is a segment of a noise-like waveform, where $B \gg 1/T$ and $K \gg 1$. The characteristic of a noise-like waveform that makes it particularly suitable is that it can be designed to spread its energy more or less uniformly over the entire range of times $t \in [0, T]$ and frequencies $f \in [0, B]$. The considerations that enter the choice of $h(t)$ are discussed further in Chapter 7. The immunity to noise is not impacted by $h(t)$, but the immunity to radio-frequency interference (RFI) that may be present at the receiver is the major argument for choosing a noise-like waveform. In particular, the sinusoid (although conceptually simple) is highly susceptible to interference, whereas a properly designed noise-like waveform is maximally immune to interference [11]. Another conceptually simple choice is a narrow pulse, and this option has also been pursued in SETI searches [32, 32]. However, the narrow pulse violates the coherence bandwidth constraint $B \leq B_c$ and thus is not of interest for power-efficient design.

When $h(t)$ is chosen to match the constraints of an ICH, almost all impairments introduced by radio propagation through the interstellar medium and by the relative motion of transmitter and receiver are avoided. The reason that an energy bundle should be designed to avoid these impairments is that introducing impairments results in a reduction in the energy as it is observed at the matched filter output, and this reduces the sensitivity of the detection because it increases the energy necessary in each bundle to achieve reliable detection. This in turn reduces the power efficiency.

³ For a complex-valued waveform, each degree of freedom is actually a complex-valued quantity, so this one degree of freedom encompasses both a magnitude and a phase.

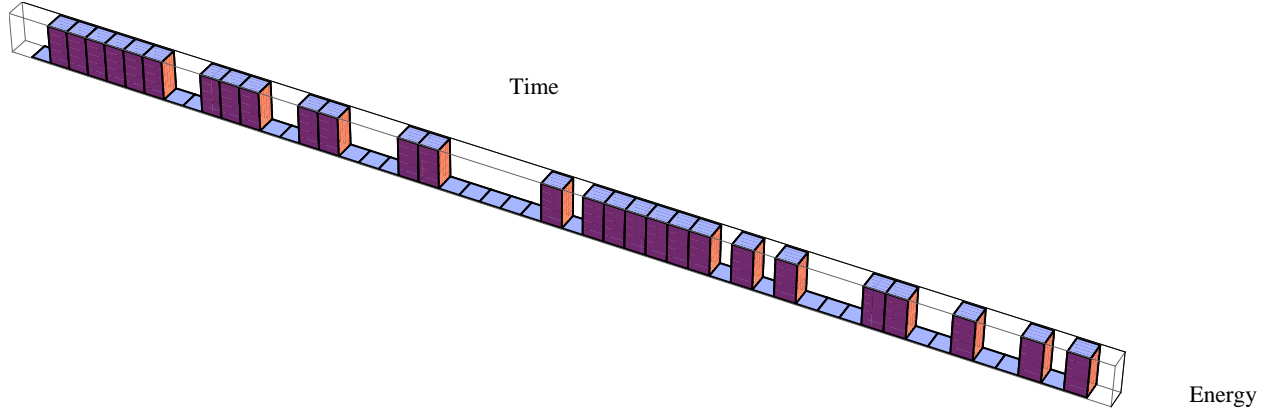


Figure 2.2: In on-off keying (OOK), in each time slot the presence or absence of a bundle of energy represents a single bit of information.

2.3 Information-bearing signals

The average power \mathcal{P} of a signal is defined as the long-term average of the energy per unit time, and has the units of watts. For an information-bearing signal communicating at an information rate \mathcal{R} , power-efficient design seeks to minimize power \mathcal{P} for a signal representing rate \mathcal{R} . If the information bearing signal has bandwidth B_{total} , then the goal of spectrally efficient design is to minimize B_{total} for a given \mathcal{R} . This section illustrates by example the major difference between power-efficient and spectrally efficient design. The significance of this difference is that terrestrial communication emphasizes spectral efficiency, and this makes power-efficient design significantly distinctive and unfamiliar.

2.3.1 Magnitude-based modulation

When the desire is to achieve high spectral efficiency without concern for average power, a good approach is to encode the information in the magnitude of an energy bundle. This is efficient because increasing the number of possible magnitudes increases the information content but has no impact on the bandwidth.

On-off keying

A simple baseline case, which is neither power-efficient nor spectrally efficient, is the on-off keying (OOK) as illustrated in Figure 2.2. In OOK the presence or absence of a bundle of energy is used to represent one bit of information. In the k th time slot of width T , the signal is $A_k \cdot \sqrt{\mathcal{E}_h} h(t - kT)$ where $A_k = 0$ or $A_k = 1$ depending on the information bit. Although current and past SETI searches generally assume a beacon rather than information-bearing signal, the signal they are searching for strongly resembles OOK for $A_k \equiv 1$.

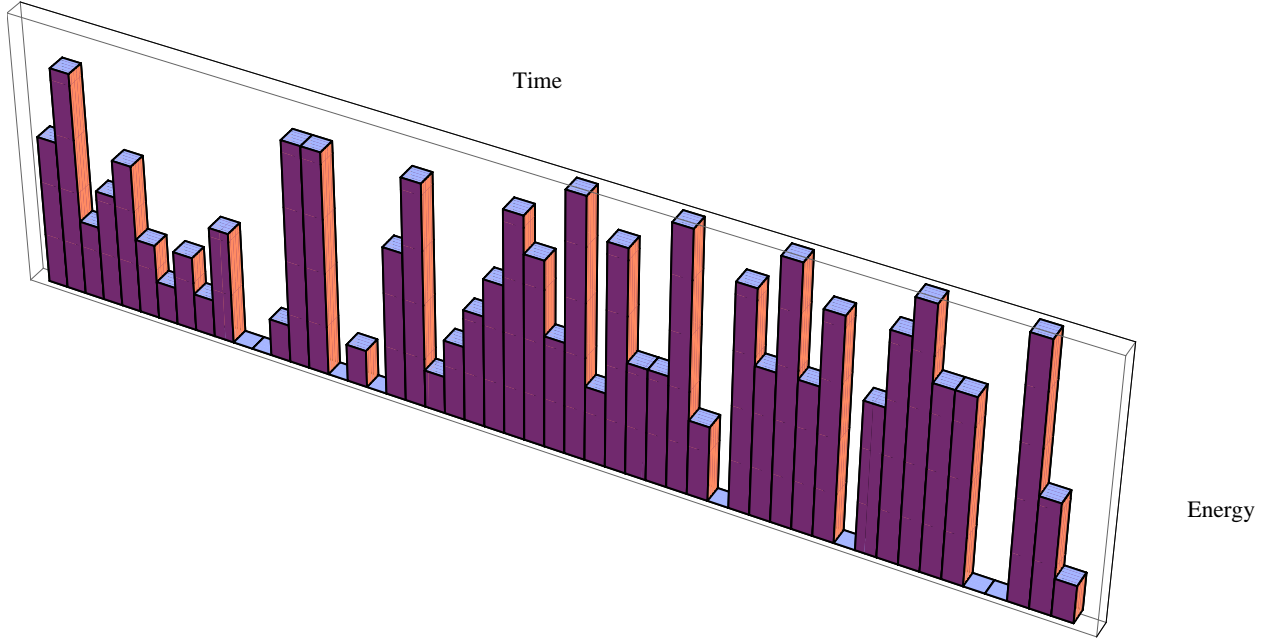


Figure 2.3: Spectrally efficient design is illustrated by multilevel keying. At each time slot, a bundle of energy assumes one of $M = 8$ values (including zero), and thus represents $\log_2 M = 3$ bits of information.

Multilevel keying

OOK is easily improved upon with respect to spectral efficiency by using multilevel keying, as illustrated in Figure 2.3. Rather than one information bit per energy bundle, $\log_2 M$ bits of information can be conveyed by transmitting one of M different levels of energy. (The case shown is $M = 8$, corresponding to $\log_2 8 = 3$ bits of information per bundle.) This represents an improvement in spectral efficiency because each bundle of energy consumes the same time and bandwidth as OOK, but conveys more information bits.

Multilevel keying is inefficient in its use of power, and thus represents a backward step in power efficiency. In order to maintain fixed immunity to the noise that accompanies each energy bundle, the average energy in each bundle is increased by a factor proportional to M^2 . The number of bits communicated increases more slowly, by only a factor of $\log_2 M$, and thus the energy required to communicate each bit of information is minimized for $M = 2$. Suitably generalized, this is a reason that two values for the energy per bundle, zero and \mathcal{E}_h , is advantageous for power-efficient design.

2.3.2 Location-based modulation

If the desire is to improve power efficiency without concern about bandwidth, a general approach is to convey information by the *location* of an energy bundle in frequency or time. This way a single bundle with energy equal to \mathcal{E}_h can communicate multiple bits of information. This poten-

tially offers greater power efficiency than OOK because the number of locations (and hence bits of information) can be increased with less impact on the average power.⁴

Suppose a single energy bundle is located at one of M places. These places should not overlap in time or frequency, but can be located at either different times or different frequencies or both. If the receiver is able to successfully ascertain the correct location of the single energy bundle, $\log_2 M$ bits of information has been conveyed from transmitter to receiver.

M-ary frequency-shift keying

In M-ary frequency-shift keying (FSK), a single energy bundle is located at one of M frequencies, thereby conveying $\log_2 M$ bits of information. It is illustrated in Figure 2.4 (the case shown is $M = 64$, corresponding to $\log_2 64 = 8$ bits of information). The transmitted signal takes the form $\sqrt{\mathcal{E}_h} h(t) e^{i2\pi A_k f_0 t}$, where $A_k \in \{0, 1, \dots, M-1\}$ and f_0 is the frequency spacing, typically equal to $f_0 = B$ so that the energy bundle locations do not overlap in frequency. Compared to multilevel keying, this requires M times as much bandwidth, so it is spectrally less efficient. However, it is more power-efficient than either OOK or multilevel keying because the energy transmitted in each time slot is \mathcal{E}_h but each time slot communicates $\log_2 M$ times as much information for that fixed expenditure of energy.

It is extremely significant for interstellar communication that in location-based modulation the bandwidth B of each energy bundle can remain fixed, even as M and the total signal bandwidth B_{total} increases. Increasing B_{total} in this manner is totally consistent with confining each energy bundle to an ICH, and thus maintaining the advantages of minimal impairment due to interstellar propagation. In this manner, increasing the total bandwidth B_{total} need not invoke interstellar impairments that we would normally associate with violation of the coherence bandwidth constraint. This is because the signal has been broken down into smaller energy bundles that individually do not trigger interstellar impairments other than noise and scintillation. If those energy bundles do not overlap one another in time or frequency as transmitted, the same is true as observed at the receiver because time-dispersive and frequency-dispersive impairments introduced by the interstellar medium and motion have been rendered sufficiently small that they can be ignored.

M-ary pulse-position modulation

While M-ary FSK represents information by the the location of energy bundles in frequency, an alternative is M-ary *pulse-position modulation* (PPM), as illustrated in Figure 2.5. In PPM information is conveyed by the position of an energy bundle in time. The transmitted signal is of the form $\sqrt{\mathcal{E}_h} h(t - A_k/MT)$, where $A_k \in \{0, 1, \dots, M-1\}$.

Because of the presence of frequency-dependent dispersion in the interstellar channel, FSK is a more natural choice than PPM. As we attempt to increase the power efficiency in PPM, each bun-

⁴ Some increase in \mathcal{E}_h is necessary to maintain fixed noise immunity because of the greater opportunity to make errors, but it is modest. This tradeoff is investigated in Chapters 4 and 5.

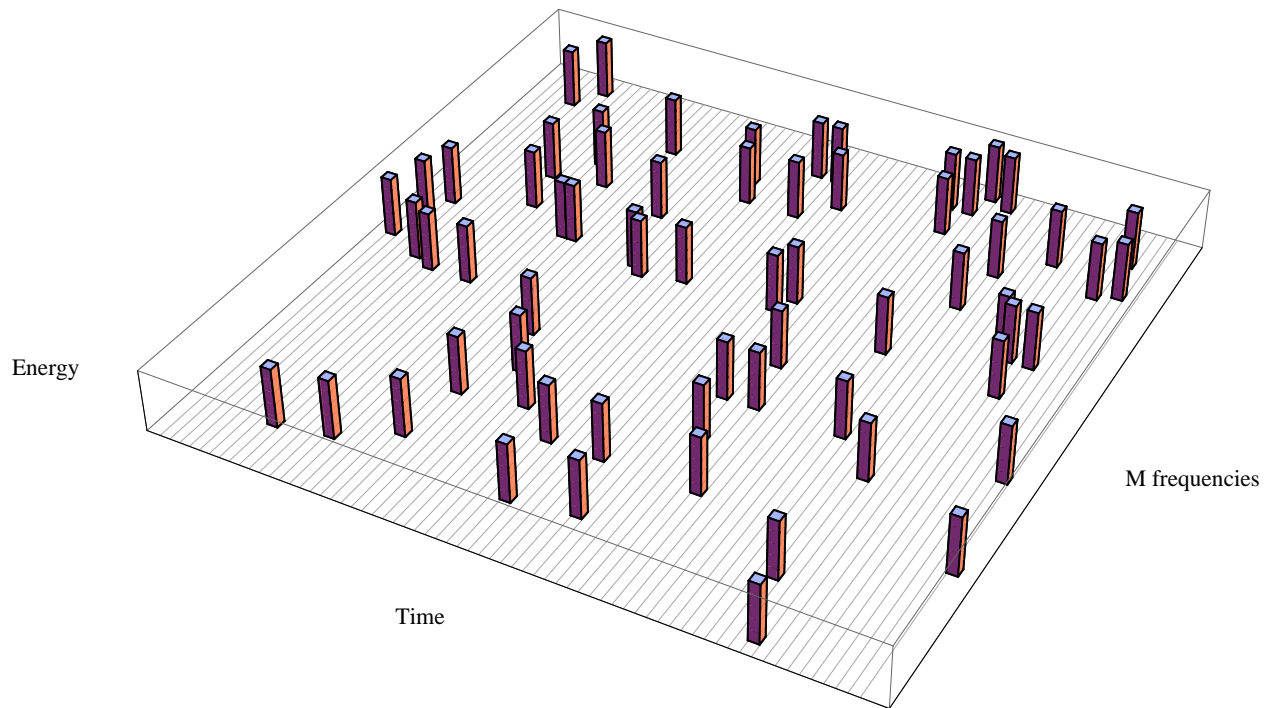


Figure 2.4: Power-efficient design is illustrated by M-ary FSK. In each time slot, a bundle of energy assumes one of $M = 64$ different frequencies, representing $\log_2 M = 8$ bits of information.

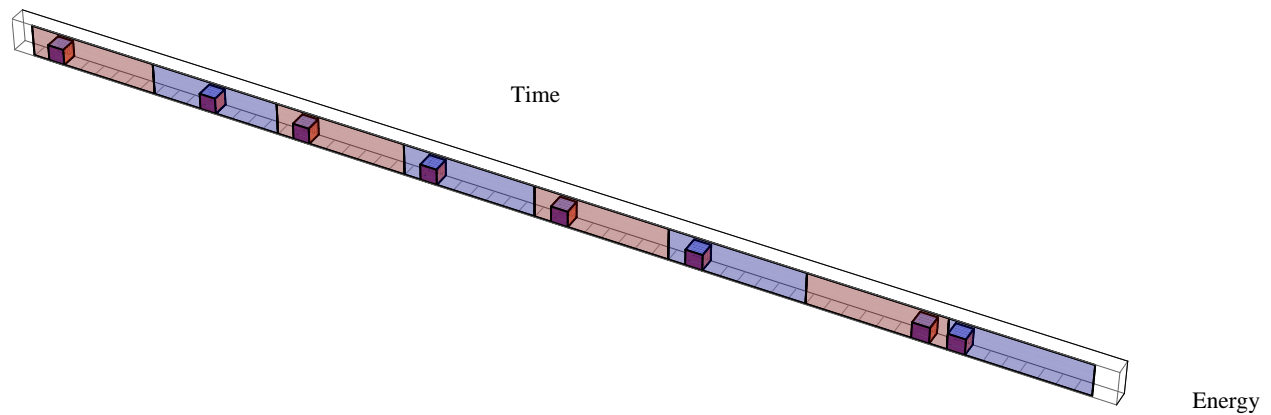


Figure 2.5: Power-efficient design is also illustrated by pulse-position modulation (PPM). Time is divided into codewords with $M = 8$ positions each, and $\log_2 M = 3$ bits of information are conveyed by the location of a single pulse within each codeword.

dle assumes a shorter and shorter time duration and this expands its bandwidth. Eventually that bandwidth will exceed the frequency coherence of the propagation, and the energy bundles will suffer significant distortion. In FSK, in contrast, power efficiency improves as bundles are transmitted on more frequencies, but the parameterization of each individual bundle remains unchanged. For this reason, M-ary FSK is adopted in our design approach, and PPM will receive no further consideration.

2.3.3 Choosing an information rate and power

In M-ary FSK $\log_2 M$ bits of information are conveyed by a single energy bundle. This grouping of M possible energy bundle locations and the associated $\log_2 M$ bits of information is called a *codeword*. This terminology comes from channel coding, which will be described shortly. The information rate \mathcal{R} is easily adjusted by changing the rate at which these codewords are transmitted, and this choice also affects the average power \mathcal{P} . Suppose that codewords are transmitted at rate F codewords per second. The \mathcal{R} and \mathcal{P} then scale as

$$\mathcal{R} = F \cdot \log_2 M \quad (2.7)$$

$$\mathcal{P} = F \cdot \mathcal{E}_h. \quad (2.8)$$

Assuming that M and \mathcal{E}_h are held fixed,⁵ both \mathcal{R} and \mathcal{P} can be manipulated by the choice of F , with a energy per bit

$$\mathfrak{E}_b = \frac{\mathcal{P}}{\mathcal{R}} = \frac{\mathcal{E}_h}{\log_2 M}. \quad (2.9)$$

For fixed M and \mathcal{E}_h , the relationship $\mathcal{R} \propto \mathcal{P}$ is maintained as F is varied. The rate F is simply a way to dial in any rate \mathcal{R} and average power \mathcal{P} desired, with the constraint that $\mathcal{P} \propto \mathcal{R}$.

There is an upper limit on the codeword rate F dictated by the coherence bandwidth B_c in conjunction with the uncertainty principle $BT \geq 1$. Together these two constraints imply that

$$T \geq \frac{1}{B} \geq \frac{1}{B_c}. \quad (2.10)$$

The time duration T of each energy bundle is constrained by the coherence properties of the interstellar channel at the carrier frequency in use, and this places an upper limit on the codeword rate $F \leq B_c$. This limit on F does not, however, constrain the information rate \mathcal{R} in (2.7) since M can be arbitrarily large as long as the total bandwidth B_{total} is not constrained.

Duty factor

⁵ The value of \mathcal{E}_h is determined by how much energy in the signal is necessary to overcome the noise. Thus, the minimum value of \mathcal{E}_h is determined by the reliability with which the $\log_2 M$ information bits are to be extracted from the signal. This required value of \mathcal{E}_h actually depends on M , as follows from more detailed modeling in Chapters 4 and 5.

Cyclops and phase-coherent detection

The last four decades of SETI observations have been largely based on the original prescription of the Cyclops report of 1970 [1]. This inspirational effort comprehensively studied various aspects of interstellar communication and discovery. However, largely because it is more than four decades old, some of its conclusions are dated. Recognizing its wide and lasting influence, it is useful to contrast the conclusions of Cyclops with those of this report, which are in some respects starkly different.

The pulsar was discovered in 1967, and by 1970 had barely begun to inform our understanding of the impairments of the interstellar medium. Thus, in its calculations of feasible information rate \mathcal{R} , Cyclops focused on phase-coherent detection of binary phase-shift keying. We now know that at greater interstellar distances scattering will create a propagation that is deeply unstable in phase, and will not support this sort of phase coherent detection. Even differential phase-shift keying, which relies not on absolute phase but differences in phase between adjacent energy bundles, appears impractical.^a This is particularly true at a lower information rate, which is characterized by a slower rate of transmission of codewords, and therefore a greater temporal separation of those codewords and a greater opportunity for the phase instability to be influential.

The energy bundle is associated with phase-incoherent detection, which is tolerant of the phase instability due to scattering, motion, etc. Somewhat surprisingly, as shown in Chapter 4, phase-incoherent detection does not compromise our ability to approach the fundamental limit on power efficiency.

^a On the other hand, positioning two or more energy bundles within a single coherence hole would allow for differential phase detection.

For any value of codeword rate F , the *duty factor* is defined as

$$\delta = F T. \quad (2.11)$$

Since any $F \geq 0$ is suitable, the only constraint on δ is $\delta \geq 0$. The rate \mathcal{R} and average power \mathcal{P} can be expressed in terms of duty factor as

$$\mathcal{R} = \delta \cdot \frac{\log_2 M}{T} \quad (2.12)$$

$$\mathcal{P} = \delta \cdot \frac{\mathcal{E}_h}{T} = \delta \cdot \mathcal{P}_{\text{peak}}. \quad (2.13)$$

The concept of duty factor is most useful when $0 \leq \delta \leq 1$. In this case δ has the interpretation as the fraction of the time that is occupied by an active energy bundle, with the remaining fraction of time $(1 - \delta)$ consisting of blank intervals during which no energy bundle is being transmitted. When $\delta = 1$ (or equivalently $F = 1/T$) an energy bundle is being transmitted at all times. Adjusting the duty factor is an equivalent way to control the rate \mathcal{R} and average power \mathcal{P} . An M-ary FSK signal with a duty factor of $\delta = 1/4$ is illustrated in Figure 2.6.

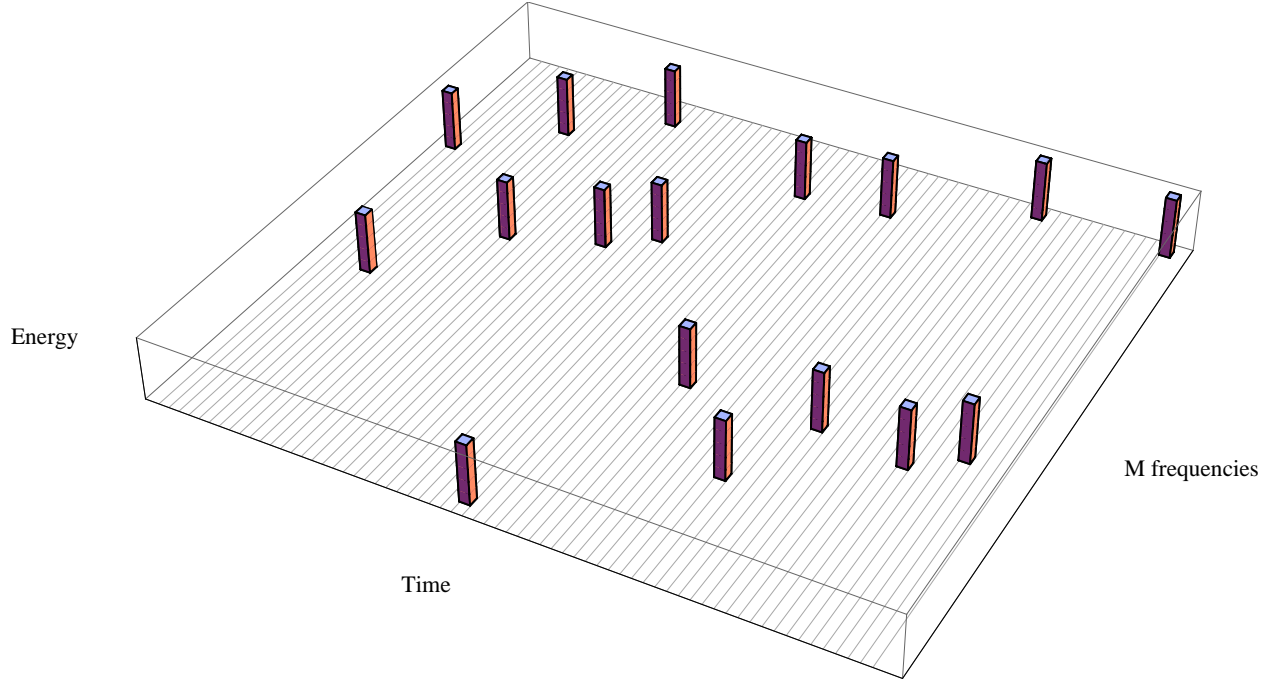


Figure 2.6: Figure 2.4 is repeated with a duty factor $\delta = 1/4$. Both the average power \mathcal{P} and information rate \mathcal{R} are reduced by δ .

2.4 Power efficiency vs. spectral efficiency

In the last section we saw an interesting divide. There seemed to be two distinct sets of techniques, one (using multilevel modulation) conserving bandwidth but wasting power, and the other (using M-ary FSK) conserving power but wasting bandwidth. Is this just an accident, or clever choice of examples, or is something more fundamental going on? The answer is that it is fundamental, at least at the fundamental limit. Recall the definitions of power efficiency and spectral efficiency in Section 2.1. We will now show that at the fundamental limit higher power efficiency inevitably results in poorer spectral efficiency, and vice versa. One consequence is that there is a global maximum power efficiency $\mathfrak{P} \leq \mathfrak{P}_{\max}$ for interstellar communications that cannot be exceeded. Since \mathfrak{P}_{\max} is a constant independent of \mathcal{P} and \mathcal{R} , it follows that at the fundamental limit the relationship $\mathcal{R} \propto \mathcal{P}$ that characterizes the rate-power tradeoff for practical communication techniques is a feature of the fundamental limit on power efficiency as well.

2.4.1 Channel models

There is no single fundamental limit on communications, but rather it depends on the nature of impairments encountered by the signal as it passes from transmitter to receiver, a model of which is called a communications channel. It is helpful to use the simplest model that captures the essential impairments, those impairments that place limits on the ability to communicate reliably. The impairments relevant to interstellar communication are covered in some detail in Chapter

8, but it is also shown there that most of them can be rendered negligible by appropriate design of the transmit signal. The impairments that cannot be avoided are modeled in Chapter 4 and the fundamental limit on power efficiency that follows from this model is determined in Chapter 4.

To get us started, and to capture the flavor of the fundamental limit, a simpler case of additive noise in isolation is considered here. This is modeled as

$$Y(t) = X(t) + N(t), \quad (2.14)$$

where $Y(t)$ is the received signal corrupted by noise, $X(t)$ is the portion of $Y(t)$ attributable to the transmitted signal, and $N(t)$ is *additive white Gaussian noise* (AWGN). AWGN is modeled as a real-valued zero-mean random process $N(t)$ with a Gaussian amplitude distribution, and is wide-sense stationarity with a constant power spectral density N_0 . Since the power spectral density is flat, not a function of frequency, the noise is said to be *white*.

The significance of the whiteness property is that any two samples $N(t_1)$ and $N(t_2)$ are statistically independent for $t_1 \neq t_2$. N_0 has the interpretation of the average power of the noise within a one Hz bandwidth, and it has the units of watts per Hz, or equivalently joules. As a consequence of the unit energy in $h(t)$ of (2.4), it turns out that the variance of the noise at sampled output of the matched filter is also N_0 . This can get a little confusing, because N_0 plays two roles, one as the power spectral density of the white noise at the input to the matched filter, and another as the variance (or energy) of the noise component of one sample at the output of the matched filter.

Scintillation is another property introduced by scattering phenomena in the interstellar medium. The model of this (not included in (2.14)) is a complex-valued Gaussian random variable that multiplies the signal with a single parameter, its variance σ_s^2 . As discussed in Chapter 3, due to the physics of scattering it is always the case that $\sigma_s^2 = 1$. However, for generality, and to highlight the role that scintillation plays, we always carry the σ_s^2 parameter without substituting its numerical value.

2.4.2 Energy contrast ratio

The matched filter output sampled at correct point in time (aligned with an input energy bundle) is characterized by three parameters $\{\mathcal{E}_h, \sigma_s^2, N_0\}$. The signal component, ignoring any unknown phase shift, is the product of $\sqrt{\mathcal{E}_h}$ and a scintillation multiplicative noise, with has zero mean and variance σ_s^2 . Of course, in the absence of any energy bundle, the signal component is identically zero. In addition, there is an additive noise sample which is Gaussian distributed with zero mean and variance N_0 .

The interpretation of a given energy \mathcal{E}_h at the output of the matched filter depends on the size of the scintillation and the level of the noise N_0 . In particular, when we characterize the reliability of algorithms for detecting an energy bundle, it turns out that it is the ratio of \mathcal{E}_h and N_0 that matters, rather than the values of each parameter alone. When the noise variance gets larger, the signal

energy must get larger in proportion to maintain the same reliability. For that reason, we define the *energy contrast ratio* as

$$\zeta = \frac{\text{Signal energy}}{\text{Average noise energy}} \quad (2.15)$$

in a single sample at the output of the matched filter.⁶ For the simplest case where scintillation is absent, at the matched filter output the size of the signal is $\sqrt{\mathcal{E}_h}$ so that the numerator in (2.15) equals the square of the signal, while the denominator equals the variance of the noise term.

A couple of different definitions of "signal energy" in the numerator will prove useful. When scintillation is present the signal term is actually random, so ζ is defined with the signal-squared in the numerator replaced by the variance of the signal,

$$\zeta_s = \frac{\mathcal{E}_h \sigma_s^2}{N_0}. \quad (2.16)$$

For some purposes, the signal energy \mathcal{E}_h needs to be replaced by the signal energy per bit \mathfrak{E}_b , resulting in an alternative definition of energy contrast ratio,

$$\zeta_b = \frac{\mathfrak{E}_b \sigma_s^2}{N_0}. \quad (2.17)$$

2.4.3 Tradeoff between power efficiency and spectral efficiency

The Shannon limit takes the form of a quantity called the *channel capacity* \mathcal{C} that can be quantified for any given channel model [8]. The significance of \mathcal{C} is that whenever the information \mathcal{R} is less than or equal to capacity $\mathcal{R} \leq \mathcal{C}$ it is mathematically possible to communicate with perfect reliability through the channel. Conversely, whenever $\mathcal{R} > \mathcal{C}$ it is mathematically impossible to communicate reliably. Perfect reliability is an asymptotic result, applying in the limit of unbounded complexity and time delay.

One of the easiest channel models for determining capacity is the AWGN model of (2.14). The impact of scintillation on the achievable power efficiency is considered in Chapter 4 and was accounted for in the example of Table 2.1, but in the interest of simplicity let us neglect scintillation and the other impairments on the interstellar channel for now. Shannon showed that the capacity of an AWGN channel is given by

$$\mathcal{R} \leq \mathcal{C} = B_{\text{total}} \cdot \log_2 (1 + \text{SNR}_{\text{in}}) \text{ bits/sec} \quad (2.18)$$

$$\text{SNR}_{\text{in}} = \frac{\mathcal{P}}{N_0 B_{\text{total}}}. \quad (2.19)$$

⁶ The terminology "energy contrast ratio" is adopted from [33]. There is a resemblance to the concept of signal-to-noise ratio (SNR), except that SNR is always defined as a ratio of powers rather than energies. The use of SNR can be confusing since its numerical value depends on several assumptions, like the bandwidth in use and the point in the system that it is measured. The energy contrast ratio does not depend on factors like integration time or bandwidth, and is measured in one standard place, in one sample at the matched filter output.

Existence of fundamental limits was a revelation

This idea that communication is subject to fundamental physical limits was a revelation when Shannon introduced it in 1948 [8]. Prior to that time, it was expected that more and more complicated and sophisticated techniques could achieve higher and higher information rates. As it turns out there is a hard limit on the information rate that can be achieved. Also, it was assumed that completely reliable communication would be impossible at any rate due to the deleterious effect of noise. In fact, it is theoretically possible to achieve arbitrarily high reliability for any information rate, as long as that rate is less than capacity. It was also found in the late 1940's that practical communication systems at the time performed poorly relative to this fundamental limit, and the research that followed seeking to reduce that penalty has remarkably improved the performance of communication systems.

Similarly, the existence of a fundamental limit is a great asset for interstellar communication. This limit alerts us to the fact that relative to the types of signals typically considered for interstellar communication to date, a substantial improvement in power efficiency is feasible. The fundamental limit also constrains what any civilization can achieve, no matter how advanced. If we can achieve a practical design that approaches the fundamental limit, we know that no other civilization can do significantly better. We also find that a design that approaches the fundamental limit becomes strongly constrained, reducing design freedom and providing specific guidance on signal structure to both transmitter and receiver. Thus, the fundamental limit proves valuable as a form of implicit coordination between transmitter and receiver [3].

This famous formula applies to the case where the average signal power is constrained to be \mathcal{P} , and the total bandwidth of the signal is constrained to be B_{total} . In this case SNR_{in} is the signal-to-noise ratio at the *input* to the receiver, since $N_0 B_{\text{total}}$ is the total noise power within the signal bandwidth and it is advantageous for the front end of the receiver to remove all noise outside the signal bandwidth before doing anything else.

Although it isn't immediately obvious, (2.18) harbors within it a fundamental tradeoff between power efficiency and spectral efficiency. Specifically, the bound of (2.18) is easily algebraically manipulated to create an equivalent bound on power efficiency \mathfrak{P} expressed in terms of spectral efficiency \mathfrak{S} ,

$$\mathfrak{P} \leq \mathfrak{P}_{\text{max}} \cdot g(\mathfrak{S}) \quad (2.20)$$

where the two factors are

$$\mathfrak{P}_{\text{max}} = \frac{1}{N_0 \log 2} \quad \text{and} \quad g(x) = \frac{x \log 2}{2^x - 1}. \quad (2.21)$$

In this bound, $\mathfrak{P}_{\text{max}}$ is the maximum possible power efficiency \mathfrak{P} that can be achieved for the AWGN channel, and the factor $g(\mathfrak{S})$ represents a reduction in power efficiency \mathfrak{P} that must be sacrificed to achieve a given spectral efficiency \mathfrak{S} . The region represented by (2.20) is illustrated in Figure 2.7 by plotting the function $g(\mathfrak{S})$.

Figure 2.7 harbors several important insights. Substantial increases in power efficiency \mathfrak{P} are feasible only by forcing spectral efficiency \mathfrak{S} to get small, or equivalently for a given information \mathcal{R} reducing power \mathcal{P} to its lowest levels dictates increasing bandwidth B_{total} . There is, however,

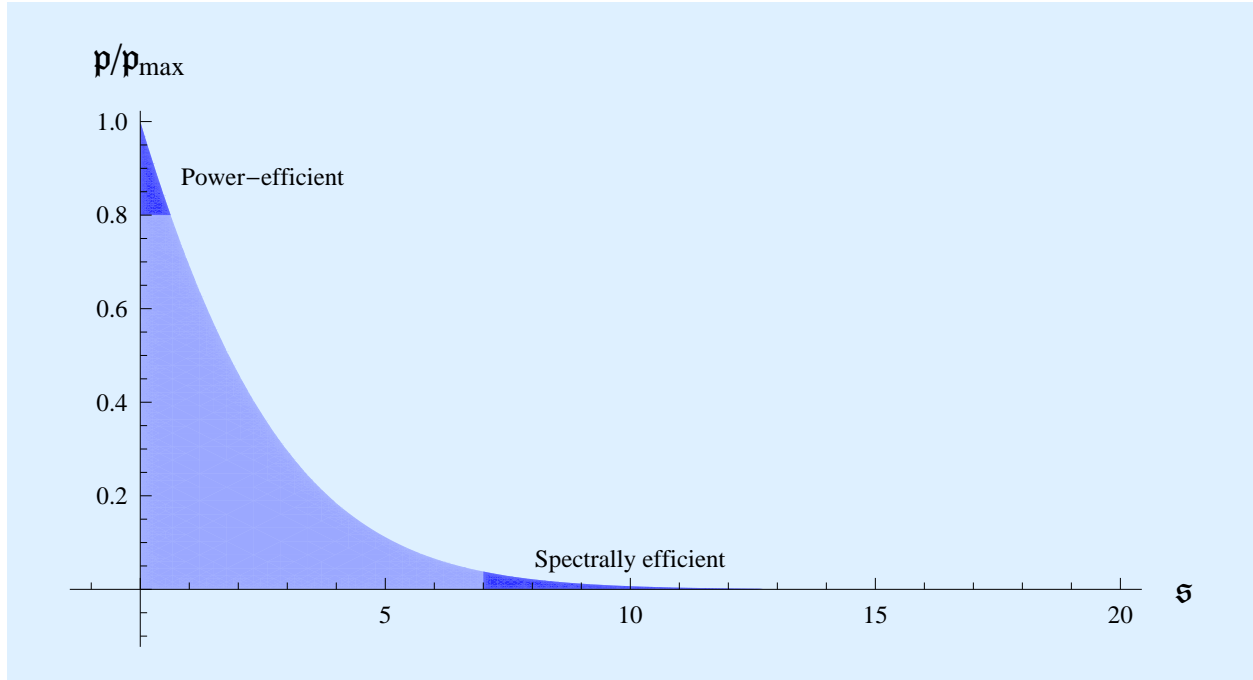


Figure 2.7: In the presence of white Gaussian noise (characteristic of natural sources of thermal noise), Shannon proved that reliable communication is possible within the shaded region of $\{\mathfrak{P}/\mathfrak{P}_{\max}, \mathfrak{S}\}$ and not possible outside that region. The horizontal axis is the spectral efficiency \mathfrak{S} and the vertical axis the power efficiency \mathfrak{P} normalized by the global maximum possible power efficiency \mathfrak{P}_{\max} . Commercial terrestrial wireless systems invariably operate in the spectrally efficient regime where \mathfrak{S} is favored at the expense of \mathfrak{P} . Interstellar communication should operate in the power-efficient regime where \mathfrak{P} is favored at the expense of \mathfrak{S} . As a result, we would expect an interstellar communication system to use a relatively wide bandwidth relative to the information rate. The global maximum power efficiency \mathfrak{P}_{\max} can only be achieved as $\mathfrak{S} \rightarrow 0$, or equivalently the total signal bandwidth B_{total} is unbounded.

a global maximum \mathfrak{P}_{\max} that can be achieved, no matter how small \mathfrak{S} . Another insight is that spectral efficiency \mathfrak{S} can be increased without limit – there is no global maximum – but only at the expense of reducing \mathfrak{P} . High spectral efficiency pays a price in terms of the required \mathcal{P} .

As shown this tradeoff between the two types of efficiency only applies to a channel model that includes AWGN, but not scintillation. In Chapter 4 the issue of scintillation is addressed. While scintillation has a material effect on the channel capacity \mathcal{C} in general, it is shown there that scintillation has no effect on the global maximum power efficiency \mathfrak{P}_{\max} . Thus scintillation does not reduce (or increase) the achievable power efficiency \mathfrak{P} .

Terrestrial vs interstellar communication

Terrestrial communication usually emphasizes high spectral efficiency \mathfrak{S} due to the high commercial value attached to spectrum allocations. Each government allocates a specific band of frequencies for specific purposes, and that band is typically bought and sold by different companies

as they seek commercial gain from offering wireless services based on that bandwidth. Further, there is considerable pressure to match information rates between these wireless services and pre-existing copper wire-based networking, such as ethernet, which places a premium on high information rate \mathcal{R} . Thus, there is an ever-increasing economic value placed on the spectrum, and increasing pressure to reduce the bandwidth B_{total} by using more and more sophisticated and processing-intensive signal processing that improves the spectral efficiency. In addition, in terrestrial services, particularly over relatively short range, the average transmit powers are typically not an issue from the perspective of energy costs. There is pressure to increase battery life in mobile terminals, but the power devoted to radio transmission is typically small relative to the power consumed by the aforementioned signal processing. Thus, an acceptable tradeoff is to increase power \mathcal{P} and reduce power efficiency \mathfrak{P} in the interest of less bandwidth B_{total} and higher spectral efficiency \mathfrak{S} . Putting these considerations together, the motivation to operate in the “spectrally efficient” region shown in Figure 2.7 is overwhelming. In contrast, as argued earlier in this chapter there is strong pressure to operate in the “power efficient” region in interstellar communication.

Fundamental limit on power efficiency

From (2.21) there is a fundamental global limit on the power efficiency \mathfrak{P} that can be achieved, regardless of the amount of bandwidth B_{total} consumed,

$$\mathfrak{P} \leq \mathfrak{P}_{\text{max}} = \frac{1}{N_0 \log 2}. \quad (2.22)$$

Keep in mind that \mathcal{P} is the average power (not peak power) measured in the receiver at the same point the total noise N_0 is measured, typically in the receiver baseband processing. While \mathcal{P} is directly related to the transmit average power and energy consumption, it is also influenced by the propagation distance, transmit antenna directivity or gain, and receive antenna collection area. Expressed in terms of the energy contrast ratio per bit defined in (2.17), (2.22) becomes

$$\zeta_b \geq \log 2 = 0.693 \text{ } (-1.59 \text{ dB}). \quad (2.23)$$

This is a remarkably simple and universal result, which will be shown in Chapter 4 to apply to the interstellar channel, even with its numerous propagation and motion impairments including scintillation. It simply asserts that each bit of information has to be accompanied by a certain energy delivered to the receiver, that energy being proportional to the size of the noise N_0 power density. Surely this is one of the important and fundamental properties of our Milky way, as it governs the minimum energy that must be delivered to the receiver for each bit of information when the goal is reliable communication among civilizations separated at interstellar distances.

In summary, there are numerous reasons in interstellar communication to put power efficiency at the front of the line, making it a higher priority than spectral efficiency. This places operation in the “power efficient” regime in Figure 2.7, rather than the “spectrally efficient” regime. This makes interstellar communication a very different animal from terrestrial communication, as will be seen. It also implies that one expects a signal for interstellar communication to have relatively

Power-efficient design is conceptually simple

One of the strongest arguments for using power-efficiency (as opposed to spectral efficiency) as the primary design goal is the conceptual simplicity of power-efficient design. The reason is that both power and spectral efficiency place a constraint on power and energy, but spectral efficiency places an additional bandwidth constraint. This additional constraint in the design makes it conceptually and practically much harder. The penalty in average power for practical techniques relative to the fundamental limit on power efficiency was essentially closed by 1967. A similar accomplishment in approaching the limit on spectral efficiency did not occur until 1994. There is a vast difference in conceptual and practical complexity of the techniques in the two cases.

The practical significance of this to interstellar communication follows from the lack of coordination between transmit and receive designers. In interstellar communication, it can be argued convincingly that the design techniques must be conceptually simple to have hope of transmitter and receiver landing in a compatible zone. This places a practical obstacle in the way of achieving high spectral efficiency, but less of an obstacle for high power efficiency. The relatively low processing requirements for power-efficient designs are also a considerable advantage during discovery, where our experience in SETI observation programs has been that the speed of search is practically limited by the technology, budgetary, and energy consumption requirements of the receive signal processing.

poor spectral efficiency, or consume relatively wide bandwidths relative to its information rate. On the face of it this would seem to contradict the need to avoid interstellar impairments, but in fact it does not. Typically in power-efficient design (as illustrated by M-ary FSK) the bandwidth of an energy bundle B is much less than the total bandwidth of the signal B_{total} , and these parameters can be chosen independently. It is B that is governed by the ICH, and it is B_{total} that determines the spectral efficiency \mathfrak{S} .

2.4.4 Channel coding

In proving his famous theorem, Shannon introduced channel coding. In general channel coding takes a group of $\log_2 M$ bits and associates a different waveform with each of the M alternatives represented by those bits. For the particular case where the channel code is structured around energy bundles, that waveform consists of a collection of one or more energy bundles at different times and translated by different frequencies. M-ary FSK is a simple example. Given a “base” waveform $h(t)$, the waveform actually transmitted over time duration T is equal to $h(t)$ shifted by one of M uniformly spaced frequencies. The frequency offset is determined by all $\log_2 M$ bits, and observing the frequency transmitted tells you the entire set of M bits. There is no way to infer one bit without inferring them all. As $\log_2 M$ grows, the mapping becomes exponentially more complicated.

2.4.5 Wake-up call from the fundamental limit

To gain some perspective on the significance of (2.22), it is useful to relate it to a simple but concrete modulation scheme, OOK as illustrated in Figure 2.2. Recall that OOK is a simple but “middle of the road” option, one that is neither particularly spectrally efficient nor power efficient. It is characteristic of the type of signals that have been the primary target for SETI discovery searches over the past five decades.

OOK is analyzed in Appendix F.2, where its probability of error P_E in the presence of AWGN with or without scintillation is determined as a function of the energy contrast ratio ζ_b , and the result is plotted in Figure 2.8. The AWGN-only case is included even though it is not directly relevant to the interstellar channel because it allows us to quantify how much of the penalty in power efficiency is due to noise, and how much is due to scintillation. As expected, P_E decreases rapidly as the signal energy \mathcal{E}_b increases in relation to the noise energy N_0 . Also shown, as a vertical line, is the fundamental limit on ζ_b at minus 1.59 dB, as given by (2.23). This plot reveals a substantial penalty for OOK relative to the fundamental limit. That penalty depends on the reliability that we demand, but at a moderate reliability of $P_E = 10^{-4}$ it is 15.5 dB for AWGN and 46.1 dB for AWGN in combination with scintillation, corresponding to linear factors of 35.9 and 40,740. Recall that the average power required is proportional to the information rate, or $\mathcal{P} = \mathcal{R}$. The conclusion of Figure 2.8, is that the constant of proportionality is about 40 thousand times larger for OOK than the fundamental limit. A substantial improvement in power efficiency relative to OOK is possible, especially in the presence of scintillation. This makes a substantial impact on the energy consumption and costs as illustrated by the example of Table 2.1, where this penalty is assumed in comparing the OOK to the fundamental limit.

In Chapter 4 a simple channel code is demonstrated that can approach the fundamental limit of (2.23) asymptotically as the bandwidth is increased. In Chapter 5 it is shown that a constrained-complexity version of that channel code can substantially increase the power efficiency, although never eliminate the penalty entirely. This channel code combines five principles of power-efficient design principles that will now be described. A simpler outage strategy is also analyzed in Chapter 5, and shown to also be effective in dealing with scintillation as long as it is acceptable to suffer a loss of recovered information during long periods of low received signal flux.

2.5 Five principles of power-efficient design

The bound on energy contrast ratio of (2.23) is a provable mathematical result. If this bound is satisfied, reliable communication is possible, and if it is not satisfied then reliable communication is not possible. As shown in Chapter 4, this limit applies to the interstellar channel with all its impairments, including but not limited to noise and scintillation. This provides a measure of how well we are doing relative to an absolute standard, the same standard that will constrain any other civilization, no matter how advanced. The techniques for approaching the fundamental limit not only improve the power efficiency, which we have argued is a compelling objective for

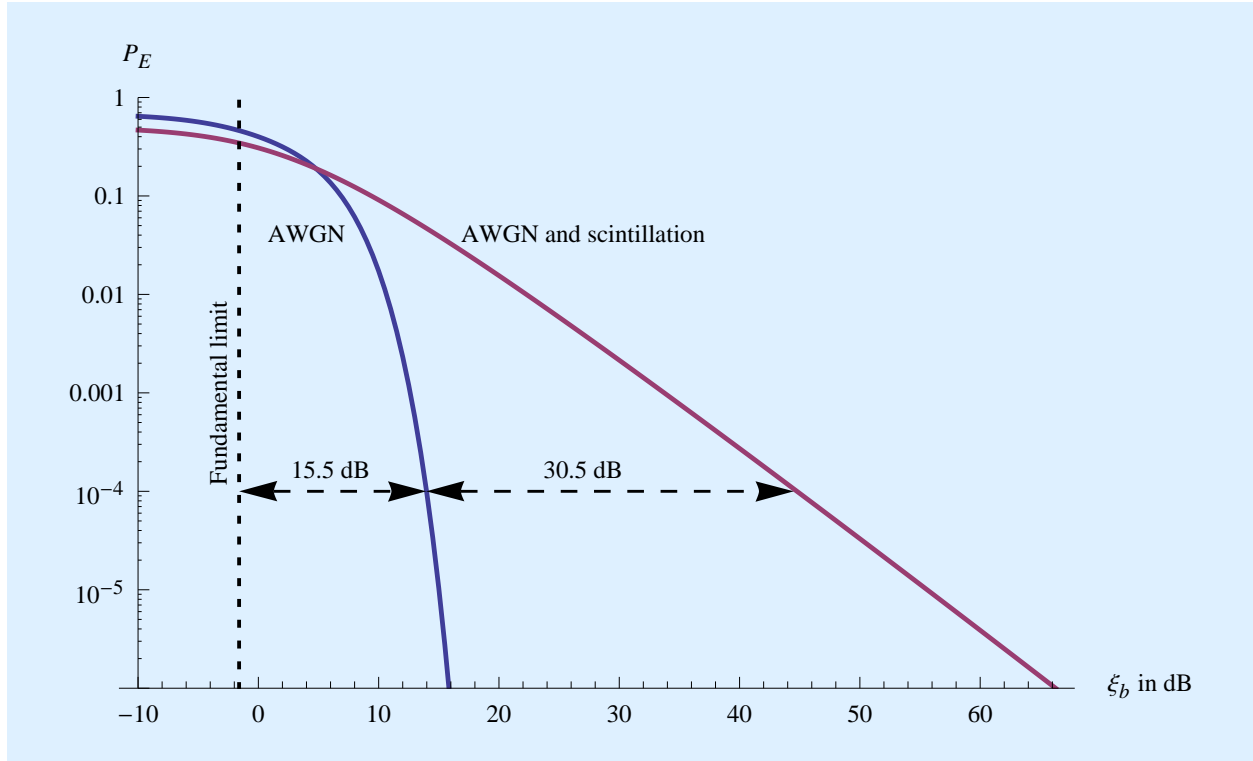


Figure 2.8: A log plot of the error probability P_E vs the energy contrast ratio pr bit ξ_b for the baseline on-off keying (OOK) modulation of Figure 2.2. Two cases are considered, average white Gaussian noise (AWGN) alone and AWGN combined with scintillation. The fundamental limit is $\xi_b = -1.6$ dB, and is shown as the vertical line on the left. The penalty for the two cases relative to the fundamental limit is arbitrarily defined at a bit error probability of $P_E = 10^{-4}$ (an average of one bit out of every 10,000 in error) although it gets larger for smaller P_E and gets smaller for larger P_E . With scintillation, the penalty in average power is 46.1 dB, or a linear factor of 40,740. For AWGN alone, the penalty is 15.4 dB, or a linear factor of 35.9. Scintillation adds a penalty of 30.5 dB, or a linear factor of 1135.

interstellar communication, but they also act as a form of implicit coordination between transmit and receive designs.

In this section, five design principles that collectively approach the fundamental limit are listed and described, referring back to earlier examples for illustration. It is demonstrated in Chapter 4 that by combining these principles in a concrete channel code the fundamental limit can be approached asymptotically. Four of these are drawn from R.S. Kennedy's research in the 1960's into power-efficient design for the fading noisy channel [19]. Kennedy's work of course did not address the specific impairments of the interstellar channel, so we have added a fifth principle, which is to restrict the energy bundles to fall within the parameters of the interstellar coherence hole (ICH). It is shown in Chapter 4 that this added principle does not affect the fundamental limit, and in fact is necessary to approach the fundamental limit. Fortuitously, it converts the interstellar channel into something similar to that analyzed by Kennedy.

Any set of practical techniques for improving power efficiency \mathfrak{P} and for approaching the funda-

mental limit are not as fundamental as the limit itself. It is possible that a designer somewhere else in the Milky Way could come up with a different collection of design techniques that works as well. What gives us confidence that these five principles do have universal appeal is that they are each very straightforward, and each has a compelling and complementary purpose in increasing power efficiency and approaching closer to the fundamental limit. They are simple enough to be practical for the uncoordinated interstellar channel. Our own judgement is that it would not be possible to approach the fundamental limit in any simpler way. Further, the existence of a fundamental limit provides an absolute and universal standard against which to evaluate the utility of these principles. Recognizing, however, that there is nothing absolute and universal about these five design principles, it is certainly appropriate to put further thought and research into alternative ways of approaching the fundamental limit on power efficiency.

The five principles will now be described in order. Section 2.3 and Chapters 5 and 6 illustrate the application of these principles to concrete designs. In particular, the implication of constraining the complexity of the channel code is addressed in Chapters 5, where the resulting penalty relative to the fundamental limit is quantified.

2.5.1 Use energy bundles

The presence of a signal of technological origin along a given line of sight can be detected by bundles of excess energy conveyed by some carrier waveform $h(t)$. The transmitter should use only two values for the energy of an energy bundle, zero and \mathcal{E}_h , because to use any more values while maintaining detection reliability increases the power requirement more than it increases the information rate. The receiver, knowing or guessing $h(t)$, can determine the portion of the energy in the reception that is aligned with $h(t)$ by applying a matched filter to the reception followed by sampling and taking the magnitude squared. Due to phase instability in the interstellar channel combined with motion of transmitter and receiver, no phase information can be trusted, and this is why the receiver should estimate magnitude (total energy) only. That total energy aligned with $h(t)$ includes both signal energy of technological origin (if present) and inevitably noise energy as well. When the total energy aligned with $h(t)$ is significantly larger than what would be expected of noise alone, then it can be inferred with confidence (high probability) that excess signal energy of technological origin carried by $h(t)$ is present.

If the power spectral density of the noise is unknown or uncertain, the receiver may not have full visibility into how much noise energy is typically aligned with $h(t)$. This may occur, for example, when there are astronomical sources of thermal noise along and near the line of sight. In that case, the energy aligned with $h(t)$ can be compared to the total energy of the signal within the time duration T and bandwidth B occupied by $h(t)$. Regardless of the noise level, when a larger fraction of the total energy is aligned with $h(t)$ this is indicative of a signal of technological origin carried by $h(t)$. This simple approach is described and analyzed in Chapter 7 and shown to be very effective, especially as the number of degrees of freedom $K = BT$ in $h(t)$ grows.

The ability to distinguish energy of technological origin from thermal noise of natural origin depends on the amount of the bundle energy \mathcal{E}_h arriving in the baseband circuitry of the receiver.

Other parameters of $h(t)$, including bandwidth B , time duration T , and its detailed waveform do not influence the receiver's ability to distinguish $h(t)$ from noise. This signal energy depends on the total transmitted energy in the bundle, the propagation loss (which depends on distance), and the transmit and receive antenna gains (which depends on the size and precision of the antennas). Since this baseband bundle energy has to be larger than the noise energy, there is little opportunity to reduce the average signal power by the specific means of reducing the amount of energy in individual energy bundles. This reality is established by modeling the discovery process in Chapter 6 and the post-discovery communication process in Chapter 5. This implies that the requirements on peak transmitted power and antenna gains in conjunction with propagation loss cannot be relaxed without harming the reliability of communication. Reductions in average receive and transmit power must be obtained by reducing the duty factor rather than reducing the amount of energy in each bundle.

2.5.2 Avoid channel impairments

A variety of impairments introduced by radio propagation through the interstellar medium, as well as by the relative motion of transmitter, receiver, and interstellar medium, are listed, described, and modeled in Chapter 8. One approach to dealing with these impairments would be to compensate for them in the receiver. This is the normal approach in spectrally efficient design, but is inappropriate for power-efficient design because such processing would inevitably carry a penalty in enhancement of noise, and thereby reduce the receiver sensitivity and necessitate an increase in signal power to compensate. The alternative is to avoid the impairments in the first place by the appropriate choice of the transmit signal $h(t)$ serving as a carrier of energy, at a modest penalty in bandwidth. It is shown in Chapter 8 that by restricting the time duration $T \leq T_c$ and bandwidth $B \leq B_c$ of a transmitted waveform $h(t)$, the impairments reflected in the energy estimate at a receive matched filter output can be rendered negligible. The parameters $\{T_c, B_c\}$ define the interstellar coherence hole (ICH), and depend on parameters of the interstellar propagation, parameters of motion, and carrier frequency.

There are two exceptions, noise and scintillation, which cannot be circumvented by restrictions on T and B . The integrity of individual energy bundles are not affected by scintillation (because T is chosen to be short relative to the coherence time T_c of the scintillation), but scintillation will result in a variation and uncertainty in the energy of individual energy bundles arriving at the receiver. These remaining impairments are an important feature of the resulting model of the interstellar channel, and they are described and modeled in Chapter 3.

2.5.3 Convey information by location rather than amplitude

In communication engineering, there are three common ways to convey one or more bits of information to a receiver: by adjusting the amplitudes and/or phases of a carrier waveform $h(t)$, by adjusting the location of $h(t)$ in time and/or frequency, and by transmitting one from among a set of waveforms $\{h_n(t), 1 \leq n \leq N\}$. Amplitude/phase modulation is commonly used in spectrally

efficient design, because increasing the number of alternative amplitudes and/or phases does not increase the required bandwidth. However, it is inefficient in its use of energy, because for fixed noise immunity the required energy per bit \mathcal{E}_b increases monotonically with the number of bits conveyed by modulating the amplitude or phase of a single waveform.

For power-efficient design, the second and third techniques are available, because multiple bits of information can be conveyed with the energy of a single waveform. This is illustrated by M-ary FSK, which is also an example of the third technique for the special case where $N = M$ and $\{h_n, 1 \leq n \leq N\}$ are orthogonal waveforms, called orthogonal modulation. M-ary FSK is also an example of a channel code, where the location of a single energy bundle is determined not by an individual bit, but by a collection of $\log_2 M$ bits.

2.5.4 Make energy bundles sparse

Delivering an energy per bundle large enough to overwhelm the noise at the receiver allows individual energy bundles to be reliably detected. This is useful for reliable information recovery, and also for discovery of the signal in the first place. With this constraint, the only way to reduce the average signal power is to have fewer energy bundles per unit time. The time duration of each energy bundle is also bounded by the coherence time of the interstellar channel, $T \leq T_c$. This implies that at low average power levels energy bundles will be sparse in time, by which we mean that periods of transmitted power are interspersed with large blank intervals with no transmitted signal. Combining that with location-based information recovery, which results in energy bundles that are sparse in frequency, the conclusion is that bundles are sparse in both time and frequency.

In this report, the same basic technique of bundle sparsity is encountered consistently, including the following contexts:

Reduce information rate \mathcal{R} . As discussed in Section 2.3.3, to maintain the reliability of energy recovery, \mathcal{R} should be reduced by reducing the duty factor δ . Low duty factor is synonymous with energy bundles that are sparse in time.

Increasing power efficiency \mathfrak{P} . Suppose we wish to minimize the average power \mathcal{P} required for a given fixed information rate \mathcal{R} , or in other words approach the fundamental limit in power efficiency. As shown in Chapter 4, this can be accomplished by using M-ary FSK as $M \rightarrow \infty$, which encodes more and more bits of information using the location of a single energy bundle, implying increasing sparsity of energy bundles in frequency. For fixed \mathcal{R} , $M \rightarrow \infty$ implies that duty factor $\delta \rightarrow 0$, implying increasing the sparsity of energy bundles in time as well.

Minimizing number of observations in discovery. If the transmitter wishes to reduce its energy consumption by reducing average power \mathcal{P} , then during discovery of that signal the receiver must increase the number of observations required to reliably detect that signal. It is shown in Chapter 6 that the best tradeoff between transmitter energy consumption and receiver

observations is achieved when the transmitter reduces its power by reducing the duty factor δ , implying that the energy bundles are increasingly sparse in time.

One surprising result from Chapter 4 is that the fundamental limit for the interstellar channel is not affected by scintillation. This does not mean that scintillation can be ignored in practice, but merely that the presence of scintillation does not increase or reduce the power efficiency that can be obtained. The sparsity of energy bundles is the reason for this. As the fundamental limit is approached, the density of energy bundles in time and frequency approaches zero. As a result the error probability becomes dominated by the receiver's ability to accurately detect the *absence* of energy bundles, or in other words the primary source of unreliability is false alarms in the detection of individual energy bundles. These false alarms are a noise-only phenomenon, and are not influenced by scintillation.

2.5.5 Combat scintillation with time-diversity combining

While a channel code like M-ary FSK can approach the fundamental limit for power efficiency on the AWGN channel without scintillation, it does nothing to counter scintillation. Scintillation causes a relatively slow variation in the signal magnitude, as well as relatively rapid variations in phase. For a signal consisting of intermittent energy bundles, like M-ary FSK, scintillation causes a variation in observed energy per bundle with time. As it turns out, scintillation (discussed in Chapter 3) does not affect the *average* energy per bundle, and it also does not affect the fundamental limit on power efficiency (see Chapter 4). It does cause the *received* energy per bundle to sometimes be greater than average and at other times less than average. If no other measures are taken, this will cause the reliability of information extraction to vary with time. In particular, there will be periods during which essentially no information is extracted, and the result of that is poor the overall reliability.

The transmitter can counter scintillation by introducing *time diversity*, which then allows the receiver to do *diversity combining*. The idea is simple, and widely used in terrestrial wireless systems. Instead of transmitting a single bundle with energy \mathcal{E}_h to represent M bits, the energy is divided among J bundles with energy \mathcal{E}_h spaced out in time at intervals, so the total energy becomes $J\mathcal{E}_h$. Crucially, these energy bundles are spaced at time intervals large relative to the coherence time. Statistically, some of those bundles will be attenuated by scintillation, and some will be amplified, but these effects will be statistically independent. In diversity combining, the receiver combines these bundles by averaging the per-bundle received energy estimates, that averaging being a much more reliable estimate of the transmitter's intention because it averages out the statistical variations in bundle energy due to scintillation. Because of this averaging, the energy in each bundle \mathcal{E}_h can be reduced, perhaps by as much as a factor of J .

An example of a time-diversity channel code is the "time-diversity FSK" that is illustrated in Figure 2.9. It uses the M-ary FSK code described in Section 2.3.2 as a starting point by defining M frequencies where a single energy bundle may be present, communicating $\log_2 M$ bits of information with a single energy bundle. For time diversity, within each codeword the energy bundle is repeated J times. The J exact replicas are spaced at intervals larger than the flux coherence time

Cyclops and power efficiency

One of the more profound and influential conclusions of the Cyclops report is embodied in the quote [1, p.39]:

...the ultimate detectability of a signal depends on the ratio of the received energy \mathcal{E}_h to the spectral density N_0 of the noise background. The energy of the signal \mathcal{E}_h can be increased, of course, by increasing the radiated power, but once a practical limit of power has been reached, further increase is only possible by increasing the signal duration T . This narrows the signal spectrum B . In the limit, therefore, *we would expect interstellar contact signals to be highly monochromatic.*

In order to relate this quote to our results, we have taken the liberty of inserting our own notation $\{\mathcal{E}_h, N_0, \mathcal{P}, T, B\}$, which was not included in the original. The italics are from the original.

When viewed with the benefit of hindsight in the year 2013, this statement has several shortcomings:

- First, it is critical to recognize that the “radiated power” referred to is the peak transmitted power, rather than the average transmitted power \mathcal{P} . For a given received energy \mathcal{E}_h (which determines the “detectability”, or what we call here the reliability of detection), the peak power can be reduced by increasing the duration T of an energy bundle.
- The issue of average power and energy consumption is not addressed, and thus the merits of intermittent or low-duty factor as the best way to reduce the average power \mathcal{P} is not considered. Unfortunately, search strategies based on the Cyclops prescription will fail to discover signals designed according to power-efficient principles.
- The statement that increasing T inevitably reduces B is incorrect. We now understand that the noise-like signals of spread spectrum allow T and B to be chosen independently [11]. Thus, the italicized conclusion that an interstellar contact signal must be highly monochromatic is incorrect. It can be, especially for beacons as opposed to information-bearing signals, but it doesn’t have to be.
- It is critical to recognize that the “signal spectrum” refers to the bandwidth B of individual energy bundles, rather than the bandwidth B_{total} of the signal as a whole. For a channel code such as M-ary FSK, $B_{\text{total}} \gg B$, so the implication of highly monochromatic is incorrect.
- The report does not recognize the distinction between power-efficient and spectrally efficient design.
- Since it predates most of the science of the interstellar medium, Cyclops does not acknowledge the critical role of scintillation in addition to noise.

Ironically, at the time the Cyclops report was written, power-efficient design for channels with noise and scintillation was already fully understood, including both fundamental limits and specific design principles to approach those limits. The authors of Cyclops were understandably not aware of this research which (like the discovery of pulsars) predates the report by only a few years. The overwhelming attention to spectrally efficient design in terrestrial commercial wireless communication has also heavily influenced the SETI community, as manifested by its exclusive attention to design principles that seek spectral efficiency.

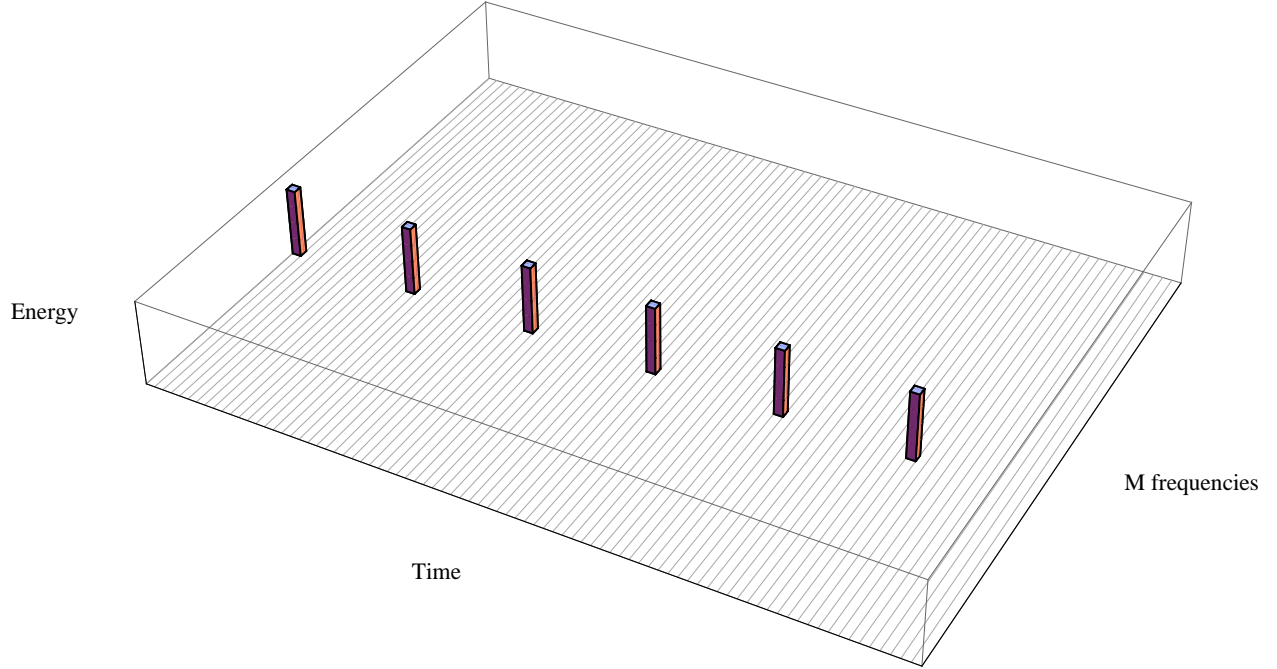


Figure 2.9: Example of one codeword from a time-diversity channel code for the interstellar channel with noise and scintillation. This code uses M-ary FSK ($M = 64$ is illustrated) to communicate $\log_2 M$ bits of information ($\log_2 64 = 8$ is illustrated). In this case, the frequency chosen is 25 (out of 64 possibilities). Each energy bundle at one FSK frequency is repeated J times ($J = 6$ is illustrated) for time diversity, with a spacing between repetitions equal to $12 \times T$ in this case. This spacing between repetitions should be larger than the flux coherence time T_f of the channel (which is likely to be much larger than shown in this example). There are various ways to position codewords relative to one another, as discussed further in Chapter 5).

T_f , so that they each experience a different state of scintillation. We would like this spacing to be large enough that the J values of scintillation are statistically independent. The receiver can estimate the energy at each individual time and frequency, but accumulate that energy over the J replica locations to average out the variation in flux \mathcal{F} due to scintillation. This averaging is called *phase-incoherent time diversity combining*.

The utility of a combination of M-ary FSK and time diversity to reduce the penalty relative to the fundamental limit is illustrated in Figure 2.10, drawing on results from Chapter 5. Increasing M from $M = 2$ to $M = 2^{20}$ (to combat AWGN) and increasing J from $J = 1$ to $J = 49$ (to combat scintillation) reduces that penalty by 37.2 dB, which corresponds to a reduction in average power by a linear factor of 5,300. This reduction in power is obtained at the expense of increasing the total bandwidth B_{total} by a factor of $2^{20} \approx 10^6$. For example, if the bandwidth of each energy bundle is one Hz, then B_{total} is approximately one MHz. This is consistent with what was seen in Figure 2.8, in that without the benefits of M-ary FSK and time diversity a very large average signal power is necessary to overcome scintillation and still achieve a consistently low error probability P_E . In Chapter 4 it is shown that a channel code like Figure 2.9 can approach the fundamental limit on power efficiency for the interstellar channel asymptotically, in the sense that for any power

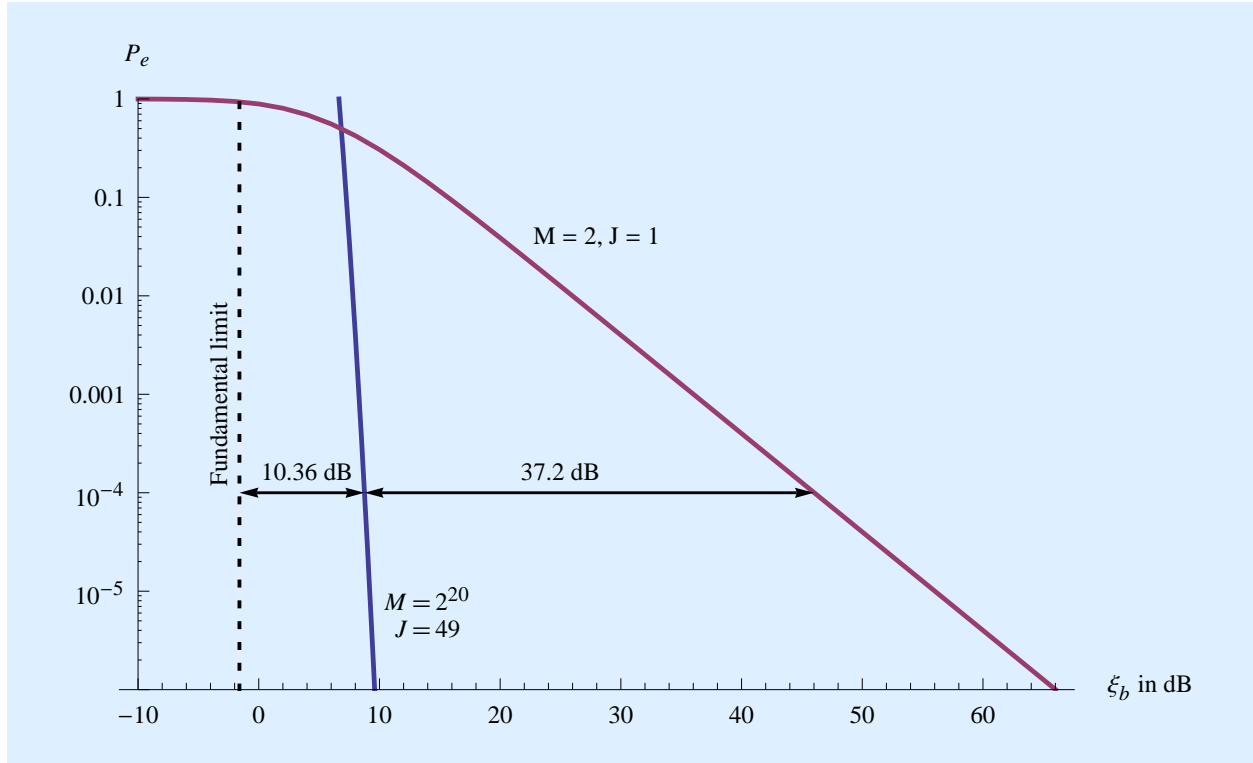


Figure 2.10: A comparison of M-ary FSK with time diversity and binary FSK without time diversity, made by plotting the bit error probability P_E against the energy contrast ratio per bit ξ_b . When $M = 2^{20} \approx 10^6$, the degree of time diversity $J = 49$ is chosen to minimize ξ_b as will be shown in Chapter 5. By increasing M from $M = 2$ to $M = 2^{20}$ and increasing J from $J = 1$ to $J = 49$, the average power required to achieve an error probability $P_E = 10^{-4}$ is reduced by 37.2 dB, or a linear factor of 5,300. Nonetheless there remains a penalty relative to the fundamental limit of $\xi_b = -1.6$ dB of 10.36 dB, or a linear factor of 10.9 in average power.

efficiency below the fundamental limit the error probability can be driven to zero $P_E \rightarrow 0$ as $J \rightarrow \infty$ and $M \rightarrow \infty$. Figure 2.10 illustrates what portion of that job can be accomplished with finite J and M , but also emphasizes that a penalty remains due to using finite values.⁷ That penalty is 10.4 dB, or a linear factor of 10.9 in average power.

In Chapter 5 a simpler strategy is also explored, based on the observation that M-ary FSK alone can approach to within 3 dB the fundamental limit on the AWGN channel without scintillation (that 3 dB is due to phase-incoherent detection of energy bundles). If the designers abandon the objective of obtaining *consistently* small P_E , then a simpler approach is feasible. The receiver can monitor the state of the scintillation, and declare periods of *outage* whenever the received flux is below average. During outages no attempt is made to recover information from the received signal, so the error rate overall is very high. However, knowing explicitly what information has

⁷ Some other factors than finite J and M contribute to this penalty. The method used for detection of energy bundles is modified to be insensitive to the bundle energy and noise power, at some expense in power efficiency. Phase-incoherent detection of energy bundles also contributes.

been discarded is easier to deal with than random errors in unknown locations. By deliberately throwing away some information, the information \mathcal{R} is effectively reduced, which reduces the effective power efficiency.

2.6 Discovery

The preceding has emphasized the reliable recovery of information from a signal. However, this extraction of information from an information-bearing signal is only possible once the presence of that signal has been established. That is the role of *discovery*, which is addressed in Chapter 6. Discovery involves a different set of challenges from communication, even when dealing with the same information-bearing signal. Discovery is made difficult due to the “needle in a haystack” challenge of searching a large parameter space consisting of spatial, frequency, and time variables. Also it lacks prior knowledge of signal characteristics and parameterization, such as power level, repetition time, channel coding structure, duty factor, etc.

If the signal is assumed to consist of energy bundles arranged in time and in frequency, as strongly suggested by power-efficient design principles, then the challenge becomes simpler. The initial stage of discovery can focus on detecting individual energy bundles, a challenge addressed in Chapter 7. Whereas in communication the receiver knows fairly precisely where and when to look for energy bundles, during discovery there is no prior guidance based on prior observations. However, there is substantial guidance based on fundamental limits and the design principles that they suggest. For power-efficient signals energy bundles are sparse, meaning most observations will not overlap an energy bundle. For the case of power-efficient information-bearing signals, that sparsity is in frequency as well as time. When the power and rate of the signal are reduced by lowering the duty factor, this becomes even more extreme. Scintillation is another factor that affects all signals, power efficient or not, and results in periods when the per-bundle energy is attenuated.

As a result of signal intermittency by design and due to scintillation, a search for individual energy bundles cannot hope to be successful with a single observation at each frequency. Multiple observations in the same location (line of sight and carrier frequency) are necessary to have a reasonable chance of an observation interval overlapping an actual energy bundle with sufficiently large power to detect reliably. To take account of scintillation, multiple observations are most efficient when they are spaced at intervals larger than the coherence time of the ISM. This critical role of multiple observations in combating scintillation was pointed out by Cordes, Lazio, and Sagan in 1993 [34, 35], but their work substantially underestimates the number of observations necessary, especially when discovering power-efficient signals with low duty factor.

After one energy bundle is detected, discovery can shift to a pattern recognition mode, in which additional energy bundles are sought at the same carrier frequency or nearby frequencies, and likely to be separated by “blank” intervals. This is another area where the discovery of power-efficient signals differs from present and past practice in SETI observation programs, which have assumed that energy is continuously transmitted, and confined to a single frequency or a fre-

quency that is varying linearly with time due to the effects of acceleration.

2.6.1 Effective energy

Power efficiency is not relevant as a metric of performance in the discovery stage, because there is no concept of information rate \mathcal{R} to maximize. Rather we use another metric called *effective energy* that captures the operational resources devoted at transmitter and receiver, and the possible tradeoffs between those resources. There are two primary operational costs in discovery. For the transmitter, the primary operational cost is energy consumption, which relates directly to the average transmitted signal power. As a proxy for this transmit power, we use the average receive power \mathcal{P} , which is proportional to transmit power if the transmit and receive antenna gains and the propagation distance are held fixed. At the receiver, the primary operational cost during discovery is the signal processing devoted to multiple observations, and the energy consumed by this processing. The total processing devoted to a single line of sight is proportional to $L T_o$, where L is the number of observations and T_o is the time interval devoted to each individual observation. The total effective energy of those energy bundles that overlap the receiver's observations is the product of the average power and the observation time, or

$$\mathcal{E}_{\text{eff}} = \mathcal{P} L T_o. \quad (2.24)$$

Power optimization for discovery

The design of the transmitted signal has a profound impact on the effective energy required for discovery of that signal at a given level of reliability. That reliability is measured by the false alarm probability P_{FA} and the detection probability P_{D} . In Chapter 6 a "detection event" is defined as a decision that one or more energy bundles is present during the total observation period. Thus, P_{FA} is defined as the probability of a detection event when in fact the reception consists of noise alone, and P_{D} is the probability of a detection event when the reception contains a signal of technological origin corrupted by scintillation and noise. The design of a signal has been *power-optimized for discovery* when at a given reliability $\{P_{\text{FA}}, P_{\text{D}}\}$ the value of effective energy \mathcal{E}_{eff} is minimized. This is equivalent to minimizing the total resources devoted by transmitter and receiver.

Total effective energy hypothesis

It is not surprising that, as shown in Chapter 6, if the signal design has been power-optimized for discovery, then at a given level of detection reliability the effective energy \mathcal{E}_{eff} stays almost constant as \mathcal{P} , L , and T_o are varied (subject to some constraints on T_o discussed shortly). This *total effective energy hypothesis* quantifies an important tradeoff between transmitter and receiver resources. According to our principles of power-efficient design, the average power is reduced by decreasing the duty factor δ , and not by reducing the energy per bundle. Thus individual energy bundles can be detected reliably, but only when the receiver's observations overlap an energy bundle. With these assumptions, the necessary total observation time $L T_o \propto 1/\mathcal{P}$. This

suggests (and it is in fact true) that a signal with arbitrarily small \mathcal{P} can be detected at any level of reliability if the receiver is willing to increase its observation time sufficiently. In practical terms, the receiver may not be able or motivated to extend observations at a given location (line of sight and frequency) indefinitely, and any such practical limitation will place a lower bound on the average received power \mathcal{P} of a signal that can be detected reliably.

As the transmitter reduces its average transmit power, the receiver can make up for this by increasing the total observation time $L T_o$, thus transferring cost from transmitter (in the form of energy consumption for transmission) to receiver (in the form of energy consumption for processing). Of course a similar transfer in the opposite direction, from receiver to transmitter, is also possible. Several economic arguments point in different directions:

1. The *value* of discovery accrues to the receiver alone, at least in the timeframe of the generation conducting the observations. This would suggest a high expectation on the part of the transmitter designer that the receiver should make a disproportionate investment, allowing the transmitter to reduce its energy consumption.
2. The receiver processing power is disproportionately large because of the "needle in a haystack" issue of having to search a large parameter space consisting of different frequencies and different lines of sight, and the transmitter should be sympathetic to this and reduce the receiver's energy consumption required for observations in a single location by increasing the transmitter's own energy consumption.
3. It is likely that the transmitter will have multiple targets in different lines of sight. This raises the energy costs for the transmitter, and suggests transferring those costs to the receiver.

Overall it seems as if considerations 2. and 3. tend to neutralize one another, leaving 1. as the dominant consideration. If so, this favors using low-power signals at the transmitter, and accompanying this by a relatively large number of observations L at the receiver.

There is another tradeoff internal to the receiver between the number of observations and the duration of each observation. In particular, for a given average receive power \mathcal{P} the number of observations $L \propto 1/T_o$. Thus, the number of observations can be reduced if each observation has proportionally greater duration. However, this exact tradeoff holds only when duration of each observation T_o contains no more than one energy bundle. The reason is that two or more bundles occurring during a single observation have a statistical correlation in the amount of energy they carry if (as it turns out is likely) these energy bundles are spaced at an interval that is small relative to the coherence time of the scintillation. In the presence of scintillation, it is more efficient to space observations far enough apart that the energy of any energy bundles that overlaps those observations is statistically independent, and to keep the observation duration T_o small enough that there is no more than one energy bundle overlapping a single observation. This places an upper bound on T_o . On the other end, in order to capture the total effective energy \mathcal{E}_{eff} within a bundle, the observation time T_o must be greater than the duration T of a single energy bundle. This places a lower bound on T_o .

The pervasive use of low duty factor to reduce energy consumption

It seems as if current and past SETI discovery search strategies are strongly influenced by receiver design issues, but have not paid sufficient attention to transmitter design, and in particular the issues of energy consumption. Not only is the propagation loss that has to be overcome very great, but a transmitter is likely to transmit along multiple lines of sight, magnifying the total energy consumption. Many engineering applications have used low duty factor as a tool for reducing energy consumption while retaining high peak powers for functional purposes. In view of this engineering history, the conclusions here are hardly surprising.

A premier example is radar, where high energy is necessary due to low target reflectivity. Radars invariably transmit short bursts of energy. This has nothing to do with delay and distance estimation (transmitting white noise and cross-correlating transmission and reception would work well), but is done to reduce energy consumption. Other examples abound. Lighthouses concentrate the light in one direction in order to be reliably detected (seen), and then rotate the whole assembly for 360 degree coverage without the energy consumption that would be required for isotropic illumination at similar powers. Mobile photography employs light flashes rather than continuous illumination to increase battery life. Pneumatic drills use high-energy impacts to fracture rock, but space those impacts over time to reduce energy consumption.

Bundle energy hypothesis

The total effective energy hypothesis comes with an important caveat. It is valid only if the design of the signal by the transmitter has been power-optimized for discovery. This hypothesis in and of itself does not say anything about how to perform this power optimization. For a signal that is structured as a repeated transmission of energy bundles, such as the power-efficient information-bearing signals considered earlier, the design question becomes a simple one. For a total average received power \mathcal{P} , what should be the rate at which energy bundles are transmitted and received, and what amount of energy \mathcal{E}_h should be contained within each energy bundle? For a given average power \mathcal{P} , the designer of the transmit signal has a choice between a larger amount of energy per bundle and a lower average rate of transmission of bundles, or the reverse.

A second *bundle energy hypothesis* is verified in Chapter 6. This hypothesis asserts that as average power \mathcal{P} is varied, and the noise power spectral density N_0 is held fixed, the energy per bundle \mathcal{E}_h (or equivalently the energy contrast ratio ζ_s) should remain approximately constant. The logic behind this hypothesis simply notes that when an energy bundle overlaps a single observation in the receiver, the detection probability is determined by the energy contrast ratio ζ_s . Thus the bundle energy hypothesis is equivalent to hypothesizing that the detection probability for this individual energy bundle should remain fixed, even as the rate of transmitted bundles and the average power \mathcal{P} is varied. It turns out that a detection probability of 57% is about optimum, corresponding to $\zeta_s \approx 14$ to 15 dB. The practical basis of this hypothesis is that if the designer attempts to reduce \mathcal{E}_h in the interest of reducing \mathcal{P} , then the detection probability falls fast and dramatically. Making up for this by increasing the number of observations L is possible, but this

Table 2.2: From the perspective of discovery, two hypotheses separate the design parameters into two sets. The first set captures those concerns that affect the amount of energy per bundle at the receiver baseband. The second set captures those concerns that affect the tradeoff between average receive power and the number of observations performed by the receiver in each location (line of sight and frequency band). These concerns do not overlap one another, and thus can be addressed independently. The hypotheses are verified in Chapter 6.

Hypothesis	Design invariant	Contributing design parameters
Bundle energy	\mathcal{E}_h = received energy per bundle	Transmit energy per energy bundle Peak transmitted power Transmit antenna gain Receive antenna collection area
Total effective energy	\mathcal{E}_{eff} = total effective received energy overlapping all observations	Average transmit power \mathcal{P} = average received power L = number of independent observations T_o = duration of each observation

is an inefficient tradeoff because it results in an \mathcal{E}_{eff} much larger than necessary.

2.6.2 Design modularity

As illustrated in Table 2.2, the two energy hypotheses create a desirable modularity in the design. By this, we mean that there are two distinct sets of design parameters, one associated with the total effective energy hypothesis, and the other associated with the bundle energy hypothesis. Within each of these two sets, the design parameters can be traded off against one another while remaining faithful to the respective hypothesis. However, as each set of design parameters is manipulated, this does not interact with the parameters associated with the other set. Engineers appreciate modularity because it creates a separation of concerns, which in turn reduces the complexity of the design process. This separation of concerns is particularly significant in the context of interstellar communication, in view of the lack of explicit coordination of the transmitter and receiver designs.

We have argued that a major consideration in interstellar communication is energy consumption. In the transmitter most energy consumption is related to the average transmit power \mathcal{P} , and in the receiver to the baseband signal processing, which is related to the total observation time $L T_o$ in each location. The bundle energy hypothesis is consequential, because it tells us that the average power should be reduced not by reducing the amount of received energy \mathcal{E}_h in each bundle, but rather by reducing the rate at which energy bundles are transmitted. This implies that reaching low average powers is achieved primarily by reducing the duty factor δ of the signal, making it more and more intermittent in character. While reducing δ necessitates increasing the number of independent observations L or the duration of each observation T_o , this increase in observation time is far smaller than would be necessary to compensate for the alternative strategy of reducing \mathcal{P} by reducing \mathcal{E}_h .

Energy consumption applies to the operational cost, but also to that portion of the capital costs related to heat dissipation due to inefficiencies in energy conversion to radio frequencies. Other capital costs are influenced by the peak transmit power, the size of the transmit and receive antenna, and the signal processing hardware at baseband. To a degree the peak transmit power can be reduced by extending the duration T of each energy bundle, but this opportunity is limited by the coherence time T_c of the interstellar channel. In Chapter 8 it is shown that the coherence time is dominated by uncompensated acceleration due to orbital dynamics, although this source of incoherence can be compensated by the transmitter and receiver in which case the dominant source of time incoherence becomes scintillation. The strategy of reducing average transmitted power by reducing duty factor will cause the peak transmitted power to be larger than the average transmitted power. Within the constraint of a fixed energy per bundle \mathcal{E}_h , tradeoffs can be made among peak transmit power, transmit antenna directivity or gain, and receive antenna collection area. However, reductions in average transmit power in the interest of reducing the transmitter's operational costs will not yield an overall benefit in these other sources of capital expense.

2.6.3 Beacons

Many SETI observation programs have drawn on the Cyclops study published in 1970 [1]. Cyclops did not emphasize information-bearing signals, but rather proposed a search for beacons. An interstellar beacon is designed to attract attention, but not embed within it any other information. The primary argument for beacons is simplicity, since there is no need to guess or make assumptions about the structure of an information-bearing signal. The type of beacon proposed by Cyclops is simply an unmodulated carrier, which can be detected by multichannel spectral analysis. Cyclops also assumed that relative acceleration of source and observer would cause the observed frequency of the unmodulated carrier to vary linearly with time.

The relative simplicity of the beacon makes it a good place to begin in addressing discovery issues. A simple generalization of this Cyclops beacon is a *periodic beacon* consisting of the regular transmission of energy bundles. This approach is motivated by the bundle energy hypothesis, which addresses how to perform power-optimization of a beacon for discovery. If the transmitter wishes to reduce the average receive power \mathcal{P} (and hence the average transmit power) while minimizing the impact of this power reduction on the resources allocated by the receiver, then it will do so by keeping the energy of each bundle \mathcal{E}_h fixed and reducing the duty factor. Adhering to this hypothesis, suppose the energy bundles are spaced at intervals of T_p , so that the period of the beacon is T_p . If each energy bundle has duration T , then the duty factor of the beacon is

$$\delta_p = \frac{T}{T_p}. \quad (2.25)$$

A periodic beacon is illustrated in Figure 2.11 for the case of a 12.5% duty factor.

The Cyclops beacon can be considered a special case of a periodic beacon with a particular choice

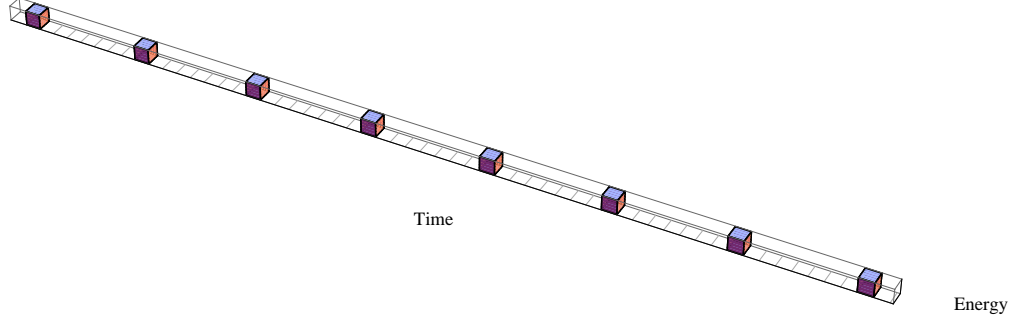


Figure 2.11: Illustration of a periodic beacon consisting of periodic energy bundles. The duty factor of this example is $\delta_p = 1/8$ (12.5%).

Beacons can be narrowband or broadband

The tradeoff between power efficiency and spectral efficiency of Figure 2.7 applies to information-bearing signals, predicting that interstellar information-bearing signals will have a relatively large bandwidth B_{total} relative to their information rate. This is not because energy bundles are necessarily broadband (they can have bandwidth B between $1/T$ and the coherence bandwidth B_c), but because information is conveyed by the position of energy bundles in time and frequency, which consumes extra bandwidth. Since a beacon is an information-bearing signal in the limit of zero information rate \mathcal{R} , this conclusion does not have much to say about the bandwidth of a beacon. In fact, a beacon can be low power and at the same time be narrowband. For example, the bandwidth of a periodic beacon is equal to the bandwidth $1/T < B \leq B_c$ of its constituent energy bundles. A periodic beacon can have the same bandwidth as a Cyclops beacon with the choice $B \approx 1/T$, even as its average power is much lower due to its low duty factor. Alternatively, a periodic beacon can be relatively broadband if $B \approx B_c$ as permitted by the coherence bandwidth of the interstellar channel (which is highly dependent on the carrier frequency). As its average power \mathcal{P} is changed, the bandwidth B_{total} of a beacon does not need to change.

of waveform and with 100% duty factor,

$$h(t) = \frac{1}{\sqrt{T}}, \quad 0 \leq t < T \quad (2.26)$$

$$T_p = T \quad \text{or} \quad \delta_p = 1. \quad (2.27)$$

Within the class of periodic beacons, the Cyclops beacon design maximizes the operational cost to the transmitter by maximizing the average power \mathcal{P} and thus its energy consumption, and minimizes the cost to the receiver by minimizing the number of observations L . In fact, if \mathcal{E}_h is large enough to overcome scintillation, even $L = 1$ observations will be adequate for reliable detection. On the other hand, if we assume that the transmitter designer is interested in reducing its energy consumption, it is unlikely to transmit a 100% duty factor Cyclops beacon. If the transmitter does reduce \mathcal{P} by choosing a lower duty factor, then the search strategies pursued over the past four

decades generally fail to discover the beacon.

A more detailed analysis of a periodic beacon design is performed in Chapter 6, and in particular the considerations that go into the choice of duty factor. Only a fraction δ_p of observations overlap a given observation, assuming that the duration of each observation is $T_o = 2T$. The number of observations L required to achieve a given reliability of discovery has to be increased to compensate for this lower probability of overlap. By the bundle energy hypothesis, however, the alternative of reducing \mathcal{P} by reducing the bundle energy \mathcal{E}_h would have a much more dramatic effect on L . The value of δ_p can be optimized for each value of \mathcal{P} , and this confirms the bundle energy hypothesis to good approximation. In particular, the regime $1 \leq L \leq 10^3$ is explored. At the \mathcal{P} for which the extreme value $L = 10^3$ is optimized for reliable detection, for example, it is found that the optimum duty factor is $\delta_p \approx 3\%$, and a Cyclops beacon ($\delta_p = 1$) would require $L \approx 10^{15}$ to achieve the same reliability. That is about twelve orders of magnitude greater, demonstrating that the Cyclops beacon is clearly impractical at an average power this low.

In practice there cannot be a joint optimization of \mathcal{P} and L due to the lack of coordination. Without coordination, the transmitter chooses a value for δ_p and the receiver must choose values for L and T_o . Once the value of δ_p is chosen and fixed by the transmitter, any variation in average received power \mathcal{P} is due to a change in the amount of energy per bundle \mathcal{E}_h , which in turn is due to uncertainty or change in transmitted energy per bundle, transmit antenna gain, propagation distance, and receive antenna collection area. Choosing a smaller δ_p benefits the transmitter designer by reducing the energy consumption if \mathcal{E}_h is kept fixed, or alternatively allows a larger transmitted energy per bundle if energy consumption is kept fixed. Generally the transmitter will want to conservatively choose a sufficiently large energy per bundle so that \mathcal{E}_h is sufficiently large to account for the expected worst-case conditions (distance, receive antenna collection area, and noise level). From this anchor point, the transmitter designer can adjust δ_p to trade off energy consumption against its expectations about the total observation time at the receiver.

The receiver designer can render the receiver more sensitive, meaning able to reliably detect the beacon at lower average power levels, by increasing the receive antenna collection area, the number of observations L , and the duration of each observation T_o . The collection area is based on an assumption as to the transmitted energy per bundle, the transmit antenna gain, and the propagation distance. L and T_o are based on an assumption as to the minimum duty factor δ_p of the beacon, or in other words the energy consumption the transmitter is willing to allocate. For a given choice of L and T_o , the detection will become unreliable if δ_p is too small and the probability of overlap between an energy bundle and the observation shrinks.

The transmit and receiver designs are both based on worst-case assumptions. If any of those assumptions are violated, the reliability of detection will suffer. If any of the parameters are larger than the worst-case assumption, then the choices made are not resource-optimizing but nevertheless the reliability of detection is not harmed. In fact, it is enhanced. For example, Figure 2.12 shows how the reliability of detection (as represented by the miss probability $(1 - P_D)$) varies with average received power \mathcal{P} for two sets of design choices made by the transmitter and receiver. For fixed δ_p the power is varied by a change in energy per bundle \mathcal{E}_h , which will occur with a variation in propagation distance or transmitter and receiver antenna gains. Two cases are compared, a Cy-

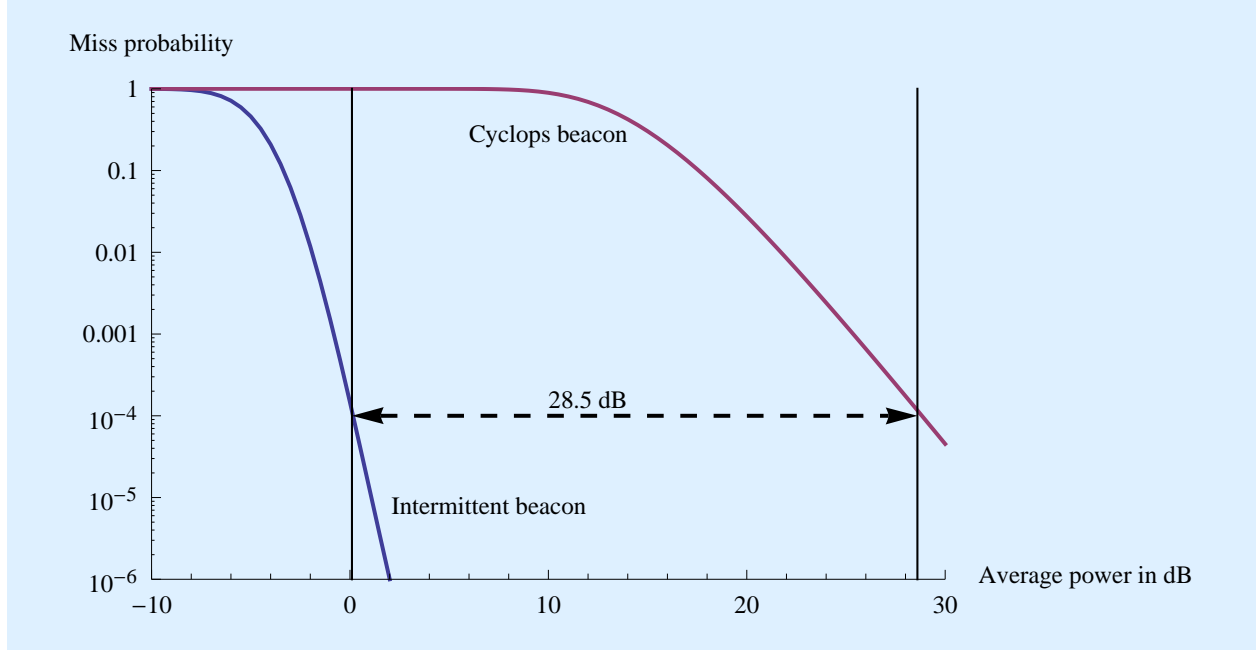


Figure 2.12: A log plot of the miss probability ($1 - P_D$) as a function of the average received power in dB in the presence of AWGN and scintillation. The absolute power scale is not specified, and is irrelevant to the comparison. The two cases shown correspond to a Cyclops beacon ($\delta_p = 1$ and $L = 3$) and an intermittent periodic beacon ($\delta_p = 3\%$ and $L = 1000$). These design choices remain fixed as the average received power (and average transmit power) are varied. See Chapter 6 for a more detailed comparison of beacon designs.

clops beacon with a small number of observations ($\delta_p = 1$ and $L = 3$) and an intermittent beacon with low-duty-factor and a large number of observations ($\delta_p = 3\%$ and $L = 1000$).⁸ The intermittent beacon can achieve high reliability of discovery at a considerably lower average power. For example, at a miss probability of $1 - P_D = 10^{-4}$ the average power of the intermittent beacon is 28 dB lower, corresponding to a reduction in average power \mathcal{P} by a linear factor of 708. Of course smaller L enables smaller reductions in power, while larger L can accommodate smaller average power \mathcal{P} , without limit. As predicted by the total effective energy hypothesis, the relationship is $\mathcal{P} \propto 1/L$ for approximately fixed detection reliability.

2.6.4 Information-bearing signals

A difference between a beacon and an information-bearing signal as described thus far is that the former is designed for reliable discovery, and the latter for reliable recovery of information. In spite of difference in objectives, the design objectives for the beacon and for the information-bearing signal are well aligned. The periodic beacon is structured around energy bundles, as is the information-bearing signal. The impact on the receiver when lowering the average received power of a beacon is minimized by keeping the energy per bundle \mathcal{E}_h fixed and reducing the

⁸ The values of δ_p and L were power-optimized at $\xi = 1$ (0 dB) corresponding to the vertical line on the left to achieve a miss probability of $1 - P_D = 10^{-4}$.

Why transmit a beacon?

One basic question that SETI researchers have always faced is whether to expect to find a beacon rather than an information-bearing signal. Generally this question has been resolved by searching for a beacon, the logic being that beacons are simpler and thus easier to discover. This logic has some validity in the regime of spectrally efficient signals, because achieving high spectral efficiency requires very complex channel coding techniques. At minimum this makes such information-bearing signals difficult to reverse engineer to extract the embedded information, but it may also interfere with their discovery. In any case, all this complexity does not contribute to discoverability in any constructive way, and discovery is the foremost objective.

Within the regime of power-efficient design, in contrast, there is no big distinction between a beacon and an information-bearing signal. Both have the same basic structure consisting of a sparse assembly of energy bundles, the only difference being a greater randomness in the location of the bundles for the information-bearing signal. The way to achieve lower average power is the same: Keep the amount of energy in each energy bundle \mathcal{E}_h constant while making them more sparse by reducing the duty factor δ . Thus, both can be discovered in the same way, by first detecting an energy bundle and then continuing the observations looking for more energy bundles in the near vicinity in time and frequency. Essentially the distinction between the two types of signals disappears, and it seems unlikely that a civilization going to all the trouble of transmitting a signal would neglect to embed information within that signal at a rate \mathcal{R} consistent with the average power \mathcal{P} that it can afford. Embedding that information does not help discovery, but does not harm it either. Further, once that information has been successfully decoded the statistical argument for technological and intelligent origin of that signal is vastly improved, and the receiving civilization is informed by any information content that is successfully decoded.

While the transmitter has to make a choice between a beacon and an information-bearing signal, fortunately the receiver can hedge its bets by searching for both simultaneously. The search for an information-bearing signal follows the same prescription as a beacon, but has to be a bit more flexible at the post-detection pattern-recognition phase. In particular, it has to hold open the possibility of detecting energy bundles at nearby frequencies. That is all.

duty factor δ . The same design principle applies to an information-bearing signal: To keep the reliability of information extraction fixed, as the information rate \mathcal{R} (and thus average power \mathcal{P}) is reduced the energy per bundle \mathcal{E}_h and energy per bit \mathcal{E}_b are kept fixed, and the duty factor δ is reduced.

An information-bearing signal also has to be discovered, and thus its design has to consider the dual purpose of reliable information extraction and reliable discovery. Addressing for a moment the discovery challenge, the only difference between a periodic beacon and an information-bearing signal following the power-efficiency design rules is that the information-bearing signal has some additional randomness in the location of energy bundles in time and frequency.

In the power-optimized and power-efficient regime, discovery of a beacon and an information-bearing signal are essentially the same. Both concentrate on the detection of an individual energy bundle by making a relatively large number of observations in the same location. Following the detection of one or more energy bundles, those observations should be extended at that location,

including nearby frequencies. A pattern-recognition algorithm operating over an extended period of time can then distinguish a false alarm from an actual signal of non-natural or technological origin, and also discern from the pattern of locations of energy bundles the structure and objective of the signal. For example, an M-ary FSK signal consists of periodic energy bundles, typically with less than 100% duty factor, just like the beacon. The difference is that these bundles are randomly situated at M uniformly spaced frequencies, rather than all appearing at the same frequency. In the context of multi-channel spectral analysis combined with matched filtering, the detection of individual energy bundles is anticipated, but the receiver must be prepared for additional randomness in the time-frequency locations where those detections occur.

Since during discovery the receiver has no idea whether a non-natural signal is present or not, the timing of its observations have no relationship to the actual location of energy bundles. Thus, any additional randomness in location will not affect the detection process. In a typical discovery search scenario the receiver is performing a multichannel spectral analysis, so it will observe energy bundles that occur at nearby frequencies as easily as bundles that occur at a single frequency. The existence of these multiple frequencies increases the number of locations that must be processed in looking for energy bundles, and this greater number of locations increases the false alarm probability P_{FA} . However, this increase is a consequence of the multichannel spectral analysis and not the randomness of the information-bearing signal, and the same increase in P_{FA} will occur with either a beacon or an information-bearing signal. The conclusion is that if a beacon and an information-bearing signal possess the same average rate of energy bundle transmission, and those energy bundles have the same energy \mathcal{E}_h , then there is essentially no difference in the reliability with which a beacon and an information-bearing signal can be detected.

A transmitter designer choosing a beacon rather than an information-bearing signal is likely to be motivated by achieving a low average power \mathcal{P} using a low duty factor δ_p . If the transmitter designer chooses instead to transmit an information-bearing signal, there is an additional benefit in increasing \mathcal{P} and δ_p , which is a higher information rate \mathcal{R} . If that is the choice, then the information-bearing signal can be discovered while employing less resources (in the form of observation time) at the receiver than can the beacon. This is because the rate at which energy bundles are arriving is greater for the information-bearing signal, and thus fewer observations are required for reliable detection. This conclusion is valid, however, only if the energy per bundle \mathcal{E}_h is comparable for the beacon and the information-bearing signal. This question is investigated in Chapter 6, where it is found that the value of \mathcal{E}_h is approximately the same between a beacon designed in accordance with the bundle energy hypothesis and an information-bearing signal with sufficiently large \mathcal{E}_h to enable reliable extraction of information. This is not surprising, since in both cases \mathcal{E}_h is chosen to enable a reliable decision between the presence or absence of an energy bundle in a given location. Thus, a beacon and an information-bearing signal of the same average power \mathcal{P} can be detected with the same reliability, and that information-bearing signal will also have sufficiently high \mathcal{P} to reliably extract information from it.

The foregoing applies to an information-bearing signal such as M-ary FSK without time diversity. When time diversity is introduced, the discovery issue is complicated by the lower energy per bundle \mathcal{E}_h . This makes the signal intrinsically harder to discover, although an adjustment to the signal design to account for discovery is needed, as pursued in Chapter 6.

2.7 History and further reading

The origin of power-efficient communication is the insight of Shannon into fundamental limits to communication [8]. First applied to the AWGN, this theory clearly demonstrated the tradeoff between power efficiency and spectral efficiency. Further, this theory highlighted the fact that substantial progress was possible in both regimes because of a substantial penalty for the best practices at the time relative to the fundamental limits. While the proof of Shannon's theorem is not constructive and gave no specific prescription, it provided a general direction by showing that channel coding is necessary to close that penalty.

Early and rapid progress in the power-efficient regime came relatively early because it is conceptually and practically simpler. It was shown in 1961 that orthogonal coding could achieve capacity asymptotically on the AWGN channel [36]. M-ary FSK and PPM are examples of the more general class of orthogonal codes, all of which exhibit identical P_E performance. Also directly relevant to interstellar communication and discussed in Chapter 3, the capacity of a Rayleigh fading channel (equivalent to scintillation in the ISM) was established to be the same as the AWGN by R.S. Kennedy during the 1960's [19]. The proof was constructive, based on demonstrating a combination of techniques that asymptotically achieved the AWGN capacity.

This flurry of activity in power-efficient design was primarily of theoretical interest driven by the the relative conceptual simplicity of the challenge. It is always better to solve the easier problem before moving on to the harder problem. Little research on power-efficient design has appeared in the literature since 1970, as the problem was essentially solved by then. Rather, attention has focused on the much more conceptually challenging (and commercially important) spectrally efficient domain, which is also more technically challenging. Most practical applications demanded spectral efficiency because of the limited overall capacity of the radio spectrum for a growing set of applications and growing traffic. As a reflection of the much greater difficulty, channel coding in the spectrally efficient regime required many decades of research and incremental improvement before the *turbo codes* that were demonstrated in 1993 finally closed the penalty relative to channel capacity [20] on the AWGN. On the other hand, power-efficient design has been used in optical communications, usually in the form of PPM [37], because spectral efficiency is hardly a consideration. Optical communication thus serves as a better practical validation of power-efficient design than terrestrial wireless communication.

The famous Shannon capacity formula for the AWGN channel appears in several papers on SETI, most notably in the work of S. Shostak in which the Shannon formula was applied to characterize the fundamental limit on the interstellar channel [38]. Shostak's results differ from those here in a couple of significant respects. For one, the Shannon limit is characterized in terms of the transmitted power density rather than the total average power \mathcal{P} . This obscures the tradeoffs between spectral efficiency and power efficiency that are highlighted here. Second, scintillation was not considered. Third, channel coding techniques that can actually approach the fundamental limit were not considered.

Due to the emergence of battery-operated mobile terminals, there has been much recent attention to "energy-efficient" wireless communication [39]. In this case energy efficiency refers to extend-

ing the battery life. Because the radio communications demands spectral efficiency, battery life is dominated by the extensive processing required in the terminals for signal processing and protocol implementation, and the power devoted to radio-frequency transmission is small by comparison. Thus, this recent work focuses mostly on protocol design for lower power consumption in the receiver computation, and has little relevance to interstellar communication, where discovery rather than communication is the major contributor to the receiver's processing burden and energy consumption.

Chapter 3

The interstellar coherence hole

In Chapter 2 a fundamental limit was established on the power efficiency obtainable on the additive white Gaussian noise (AWGN) channel. However, in interstellar communication noise is only one of a number of impairments due to the ISM and due to relative motion between source and observer. These impairments are listed in Table 3.1. It is, however, possible to choose a transmitted signal that avoids many of them. Avoiding impairments by signal design is one of the principles of power-efficient design, since compensating for them at the receiver, even if that is possible, typically invokes a noise penalty. The interstellar coherence hole (ICH) is a constraint on the bandwidth and time duration of a signal such that it suffers the minimum possible impairment in propagation through the interstellar medium (ISM) and after being influenced by the relative motion of the source and observer.

The appropriate channel model for energy bundles includes only impairments encountered by a signal falling within an ICH. From Table 3.1 these include noise and scintillation, which are further characterized in this chapter. In addition, the model must include the possibility of a frequency offset between two ICH signals, although this frequency offset can be avoided if both the source and observer compensate for their relative acceleration due to their respective planetary motion. The remaining impairments can be neglected in the channel model, but due to their significance as a determinant of the size of the ICH (time duration and bandwidth) they are characterized in Chapter 8 in terms of underlying physical parameters.

3.1 Definition of the coherence hole

The concept of an ICH is illustrated in Figure 3.1. A complex-valued baseband signal $h(t)$ was defined in Section 2.2, including unit energy, Fourier transform confined to $f \in [0, B]$, time confined to $t \in [0, T]$, and degrees of freedom $K = BT$. After modulation to carrier frequency f_c , the real part $\Re\{h(t)\}$ becomes the in-phase signal, and the imaginary part $\Im\{h(t)\}$ becomes the quadrature signal. After experiencing the ISM impairments at passband and demodulation back to baseband in the receiver, the matched filter with impulse response $h^*(-t)$ is applied. (See

Table 3.1: A list of the impairments affecting interstellar communication. They are divided into three categories: Intra-ICH impairments apply to signals falling within the interstellar coherence hole (ICH). Inter-ICH impairments apply to two signals that each fall within the ICH but are fairly widely separated in time. Extra-ICH impairments can apply to signals with bandwidth and time duration too large to fall in the ICH.

Source	Impairment	Symptom and cause
Intra-ICH	Noise	Additive white Gaussian noise (AWGN) of thermal origin from background radiation, emission, and the receiver temperature (Section 3.2.2)
	Scintillation	Variation in signal flux at the observer due to the constructive and destructive interference of different paths through the scattering medium that varies with time due to the component of relative velocity of source and observer perpendicular to the line of sight (Section 3.2.1) as well as slower variations due to turbulence in the interstellar gas clouds
Inter-ICH	Frequency offset	Signals separated in time may be observed with a relative frequency offset due to the component of relative acceleration in the direction of the line of sight (Section 3.3)
Extra-ICH	Delay spread	A relative variation in delay for different signal components due to wavelength-dependent group delay for paths passing through a scattering medium (Section 8.2), and also due to the different propagation delays of separate paths through the scattering medium (Section 8.4)
	Carrier phase shift	A variation of carrier phase with time due to the relative acceleration of source and observer (Section 8.3)

Appendix B.1 for an analysis of the modulation and demodulation and Chapter 7 for a detailed analysis of the matched filter.) The matched filter does not account for any impairments other than additive white Gaussian noise (AWGN), so the question is how other impairments affect the matched filter output $z(t)$. Our goal is to establish the simple model for $z(0)$ shown whenever $h(t)$ falls within an ICH. This model adds scintillation, but no other impairments, and is justified in Chapter 8.

Having defined a receiver structure appropriate for noise-only, it is appropriate to return to Figure 3.1 and ask what happens when other impairments are introduced, including propagation impairments in the ISM and effects due to the relative motion of source/observer. There is a good understanding of the ISM and its effects on radio propagation arising from natural phenomena such as pulsars [42]. In particular, the ISM is populated by clouds of low-density plasma consisting principally of hydrogen ions and free electrons, and thus it is a conductive medium that affects radio propagation. Based on these observations, together with theoretical modeling based on an understanding of the underlying physics of plasmas and Doppler effects, good models are available for this propagation. The models in the astrophysics literature are commonly monochromatic, and tell us that the effect of ISM propagation on a monochromatic signal is group delay, propagation loss, and scintillation. Group delay is primarily due to the speed-of-light propagation over large distances. Propagation loss is due to the spherical spreading of energy during propagation,

A word about terminology and nomenclature

This paper deals with both physical models and communications. Generally we use a nomenclature consistent with the astrophysics literature when dealing with physical models, and a notation consistent with the communications engineering literature when dealing with communications. For example, the dispersion measure is DM, but the K -factor for a Rician fading model is κ . A similar division is used for terminology, for example in dealing with scintillation and fading (which are similar phenomena with different names in astrophysics and communications).

Generally deterministic signals are denoted by a lower-case letter and random signals by upper case (like $z(t)$ vs $Z(t)$). Physical constants are usually denoted by a Greek letter, unless the convention in the physics or communications literature is different (for example the dispersion measure DM or noise power spectral density N_0). The probability of an event A is denoted by $\Pr\{A\}$. For a random variable X , the $f_X(x)$ is the probability density function and $F_X(x)$ is the cumulative distribution function, so the two are related by

$$F_X(x) = \Pr\{X \leq x\} = \int_{-\infty}^x f_X(u) du \quad \text{and} \quad f_X(x) = \frac{d}{dx} F_X(x).$$

The averaging or expectation operator is denoted as $\mathbb{E}[\cdot]$ (whereas in the physics literature the alternative notation $\langle \cdot \rangle \equiv \mathbb{E}[\cdot]$ is often used). For example

$$\mathbb{E}[X^2] = \int x^2 f_X(x) dx.$$

The variance of a random variable X is denoted as $\text{Var}[X] = \mathbb{E}[X^2] - (\mathbb{E}[X])^2$, and the standard deviation of X is $\sqrt{\text{Var}[X]}$.

Simultaneous bandlimiting and time-limiting

Strictly speaking a waveform cannot be simultaneously bandlimited and time limited. However, a classical uncertainty principle of Fourier transforms [40, 41] states that if $K = BT \gg 1$ then waveforms exist with most of their energy concentrated in $f \in [0, B]$ and $t \in [0, T]$, and “most” approaches “all” as $K \rightarrow \infty$. This should not be surprising in light of the sampling theory, which says that an $h(t)$ precisely confined to $f \in [0, B]$ can be sampled at rate $1/B$ without losing any information. If only K consecutive samples are non-zero (the remaining infinity of samples are all zero) then the waveform is approximately (although not precisely) confined to time interval $T = K/B$.

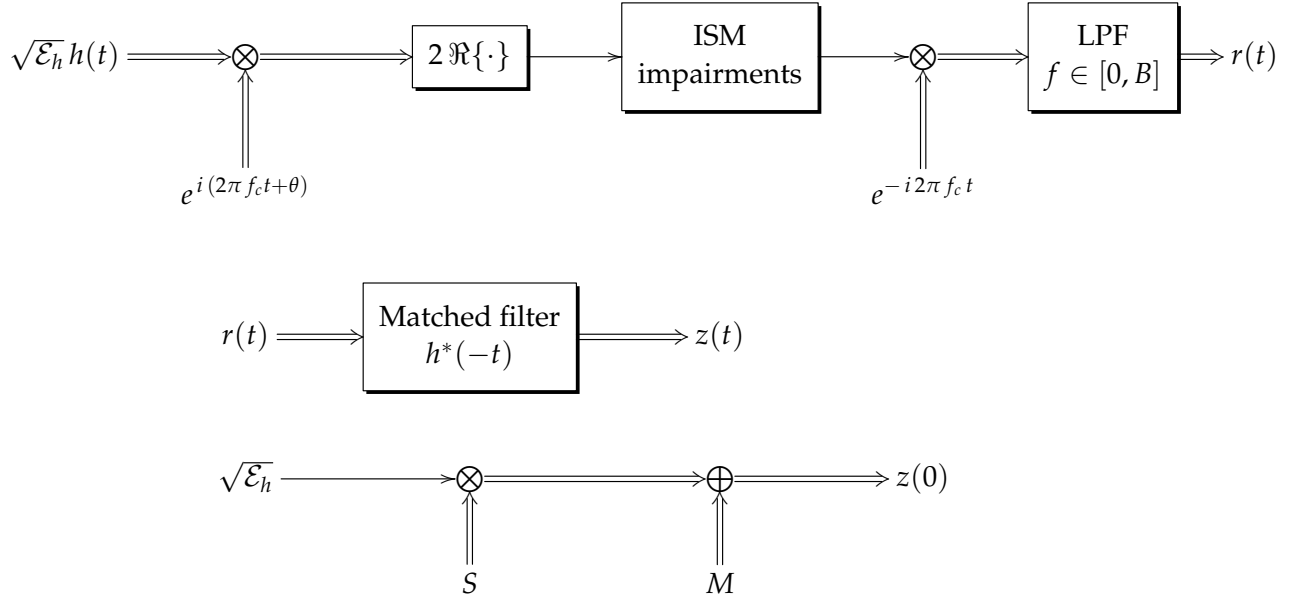


Figure 3.1: The three diagrams from top to bottom represent (a) the radio channel from input $\sqrt{\mathcal{E}_h} h(t)$ to output $r(t)$ including modulation and demodulation, (b) the optimum baseband receiver processing assuming the ISM propagation is not present, and (c) the simplified end-to-end model taking account of all ISM impairments and source/observer motion, but assuming that the bandwidth and time duration of $h(t)$ are sufficiently small to fall within an interstellar coherence hole (ICH). The scintillation is represented by a multiplicative noise S , which like additive noise M is complex-valued. For the special case of strong scattering, S is Gaussian with identically distributed and statistically independent real and imaginary parts. All signals represented by a single arrow (\rightarrow) are real-valued, and all signals represented by a double arrow (\Rightarrow) are complex-valued.

with only a tiny portion of that energy captured by the receiving antenna. Scintillation will be addressed shortly.

A waveform $h(t)$ is affected in similar ways to a sinusoid, but with additional complications due to its non-zero bandwidth. However, if the bandwidth B of $h(t)$ is restricted, it would not be surprising if we reached a point at which the distortion of $h(t)$ due to these complicated effects simplified to be similar to those experienced by a monochromatic signal. Further, if we shrink the time duration T of $h(t)$, it would not be surprising if the time-varying effects like Doppler became insignificant. These effects are still manifested, but for sufficiently small T their time-varying nature can be neglected. Like a sinusoid, the remaining impairments of a fixed delay, a propagation loss, additive noise and scintillation remain, and these are characteristics of the ICH. These intra-ICH impairments will now be further characterized. The significant physical parameters for interstellar communication are listed in Table 3.2, including values that will be used for numerical examples. The nature and significance of these parameters will be explained as we proceed.

Table 3.2: All the significant physical parameters determining the strength of impairments in interstellar communication, together with numerical values used in examples. Generally the values are chosen to be worst-case, in the sense that they minimize the ICH size.

Source	Parameter	Description
ISM	DM	The dispersion measure equals the total column density of free electrons along the line of sight (Section 8.2). DM = 1000 is approximately the largest DM observed in pulsar astronomy; DM will be much smaller for most lines of sight. Pre-equalization in either transmitter or receiver can reduce the effective value to the uncertainty ΔDM (Appendix H.2).
	D	A distance-of-propagation measure. In Figure 3.2, D is the distance from screen to observer, and more generally it is defined by (8.21). The coherence bandwidth of scattering decreases with D and the scattering becomes stronger, so we use a relatively large value of $D = 250$ light years (this corresponds to $D_1 = D_2 = 500$ light years)
	r_{diff}	The diffraction scale characterizes the turbulent clouds of interstellar plasma, and equals the range of x at the scattering screen over which the phase introduced by the screen is approximately constant. It is wavelength-dependent, with $r_{\text{diff}} \propto f_c^{6/5}$, with a typical value of $r_{\text{diff}} = 10^7$ meters at $f_c = 0.3$ GHz [18].
Motion	P	Period of circular motion, either diurnal rotation about axis or orbital motion around star. $P = 1$ day (8.6×10^4 sec) for the diurnal rotation of the Earth.
	R	Radius of circular motion, either diurnal rotation about axis or orbital motion around star. $R = 6.38 \times 10^6$ meters for the diurnal rotation of the Earth.
	v_{\perp}	The velocity of the observer transverse to the line of sight. Although [34] estimates a typical value $v_{\perp} = 10$ km per sec, we conservatively adopt $v_{\perp} = 50$ km per sec.

3.2 Model of a coherence hole

If a signal $h(t)$ falls within an ICH, then the model of its propagation through the ISM simplifies to that shown in Figure 3.1 and is captured by the equation

$$Z = \sqrt{\mathcal{E}_h} e^{i\Theta} S + M. \quad (3.1)$$

where S is the multiplicative scintillation noise and M is the additive noise. The unknown carrier phase Θ can be omitted, since S also has a completely random phase. The scintillation multiplier can be written in terms of magnitude and phase as

$$S = \sqrt{\mathcal{F}} e^{i\Phi} \quad (3.2)$$

where \mathcal{F} is the received signal flux (normalized so that the flux would be $\mathcal{F} = 1$ in the absence of scintillation) and Φ is a random phase that is uniformly distributed on $[0, 2\pi]$. This model omits propagation loss and group delay, which can be considered separately.

While Φ does not add any new uncertainty to the phase, since the carrier phase is unknown anyway, it does capture the rapid phase fluctuation between two ICH's that are non-overlapping in time. The scintillation flux \mathcal{F} is the significant new element of the model. The magnitude of the signal is affected by both \mathcal{E}_h and \mathcal{F} . These are both energy measures, so their contribution to the signal magnitude is the square root. The received signal energy is multiplied by \mathcal{F} , becoming $\mathcal{E}_h \cdot \mathcal{F}$, and it is possible to have $\mathcal{F} > 1$ or $\mathcal{F} < 1$ implying that scintillation results in either an increase or a decrease in signal level. The presence of the random phase term $e^{i\Phi}$ in the signal renders the phase of Z basically useless, but the magnitude $|Z|^2$ contains useful information about the presence of a signal ($\mathcal{E}_h > 0$) or the absence of a signal ($\mathcal{E}_h = 0$).

In the model of (3.1), by definition $\mathbb{E}[\mathcal{F}] = \sigma_s^2$ and $\mathbb{E}[|M|^2] = N_0$. The energy contrast ratio ξ_s which was defined earlier in (2.16) can be expressed directly in terms of the flux parameters as

$$\xi_s = \frac{\mathcal{E}_h \cdot \mathbb{E}[\mathcal{F}]}{N_0}. \quad (3.3)$$

Another useful parameter of the scintillation is the *modulation index*, defined as

$$m_{\mathcal{F}} = \frac{\sqrt{\text{Var}[\mathcal{F}]}}{\mathbb{E}[\mathcal{F}]}. \quad (3.4)$$

This index is a measure of the typical variation in the flux \mathcal{F} (as measured by standard deviation) in relation to its mean-value. Thus when $m_{\mathcal{F}} \approx 0$ there is a very small variation in signal level due to scintillation (at least in relation to the average signal level) and when $m_{\mathcal{F}} \approx 1$ the standard deviation is equal to the mean value.

This simple model of (3.1) is now related to the physics of scattering [18] followed by noise of thermal origin.

3.2.1 Scattering within a coherence hole

Scattering is due to variations in electron density within the turbulent interstellar clouds. Because the distance scales are so large, even at radio frequencies the phenomenon can be modeled by geometrical optics using a ray approximation to the radio propagation. This is illustrated by a simple one-dimensional model in Figure 3.2. Although the conductive medium in turbulent clouds is actually spread through three dimensions, this simplified model captures the essential features. A thin one-dimensional *scattering screen* is placed in the path of a plane wave, and an observer views the resulting intensity at distance D . The essential feature that causes scattering is the non-homogeneity of the screen which has a group delay $\tau(x)$ that depends on the position x on the screen. The resulting diffractive and refractive effects at the observer result from constructive or destructive interference among rays passing through different x that influence the signal level.

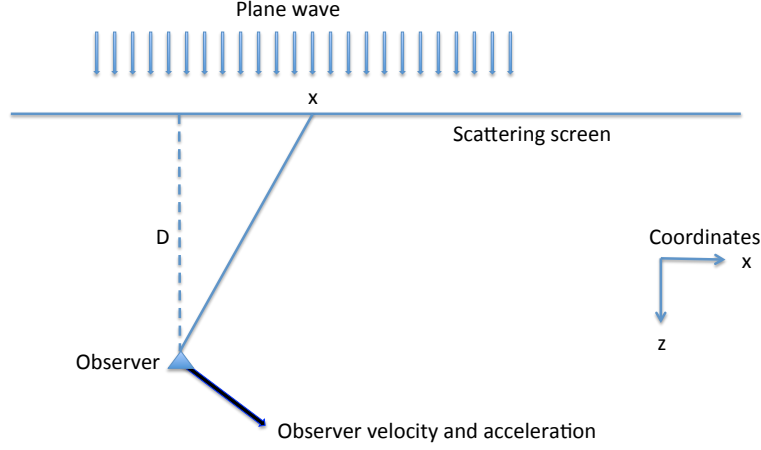


Figure 3.2: Illustration of the geometry of scattering using a simplified one-dimensional scattering screen. Rays pass through the screen (located at distance D from the observer) at different lateral distances x and encounter different group delays and phase shifts due to small variations in electron density.

The phase shift encountered by a given ray is affected by (a) the phase shift encountered at the screen, (b) the phase shift due to propagation from point x on the screen to the observer, and (c) changes in the latter phase shift with time due to the observer's motion. Although (b) and (c) are deterministic and easily modeled, (a) is unknown and subject only to statistical analysis based on a model of turbulent motion of interstellar clouds. An essential characteristic of this model is the *diffraction scale* r_{diff} , which measures the range of x over which the phase is statistically likely to remain fairly constant. It is these "coherent patches" of stationary phase that contribute most strongly to the energy that arrives at the observer. Other areas on the screen without coherent phase tend not to contribute much net energy, since they result in a jumble of phases that destructively interfere.

A second important geometric feature of the scattering is the *Fresnel scale* r_F , given by

$$r_F = \sqrt{\lambda_c D} = \sqrt{\frac{c D}{f_c}} \quad (3.5)$$

where λ_c is the wavelength and f_c is the frequency of the carrier, c is the speed of light. The Fresnel scale r_F is the distance over which the phase shift due to the variation in distance with x is small, and has no relationship to the phase shift of the scattering screen. The phase shifts as a

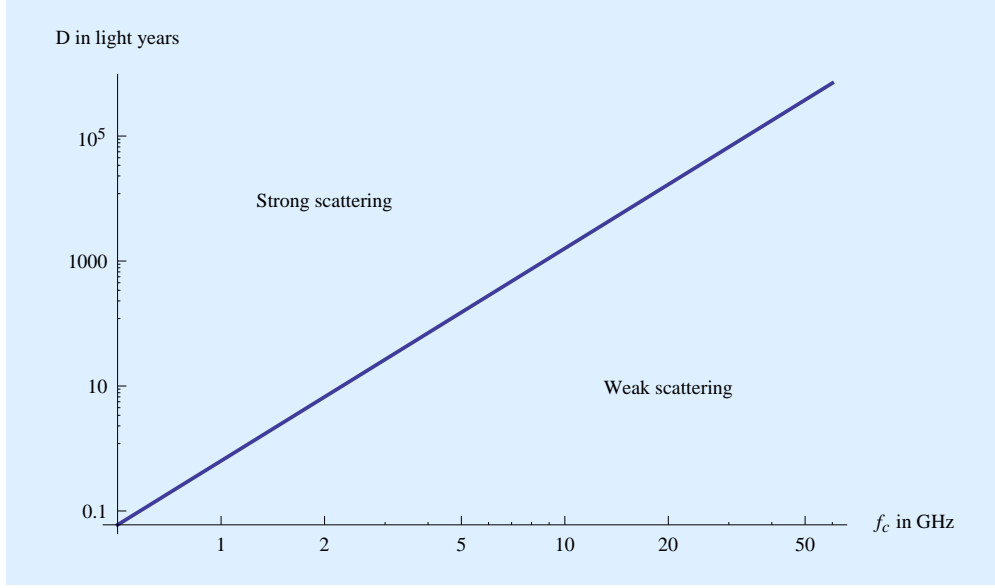


Figure 3.3: A log-log plot showing the boundary between weak and strong scattering for variation of the distance D in light years (according to the definition of (8.21)) and the carrier frequency f_c . The numerical value of r_{diff} given in Table 3.2 is assumed.

function of x are small over a scale $|x| \leq r_F$ (called the first Fresnel zone) because over this scale the variation in propagation distance is smaller than one wavelength. Along with coherence of phase introduced by the screen, coherence of phase due to the geometry is another necessary condition for the constructive interference of rays and hence a significant contribution to the energy arriving at the observer.

There is an important interplay between r_{diff} and r_F that determines the character of the resulting signal impairment. The regime where $r_{\text{diff}} \gg r_F$ is called *weak scattering*, and $r_{\text{diff}} \ll r_F$ is called *strong scattering*. Interstellar communication can encounter both types of scattering as determined primarily by the interaction between the parameters D and f_c . The scales follow $r_{\text{diff}} \propto f_c^{6/5}$ and $r_F \propto f_c^{-1/2}$, and hence $r_{\text{diff}}/r_F \propto f_c^{17/10}$, and in addition $r_{\text{diff}}/r_F \propto D^{-1/2}$ [18]. Adopting these models, the boundary between these regimes is illustrated in Figure 3.3 for a typical value for r_{diff} . Strong scattering dominates for lower carrier frequency f_c and larger distance D .

The character of scintillation is different for strong and weak scattering, so they are now considered separately.

Strong scattering regime

See Figure 3.4 for an illustration of the distinctive geometries that separate strong vs. weak scattering. In the strong scattering regime of Figure 3.4a, $r_{\text{diff}} \ll r_F$, and thus the typical coherent patch of stationary phase is at a scale much shorter than r_F . Within the first Fresnel zone the geometric variation in phase is not much of a factor, but even coherent patches occurring outside the first

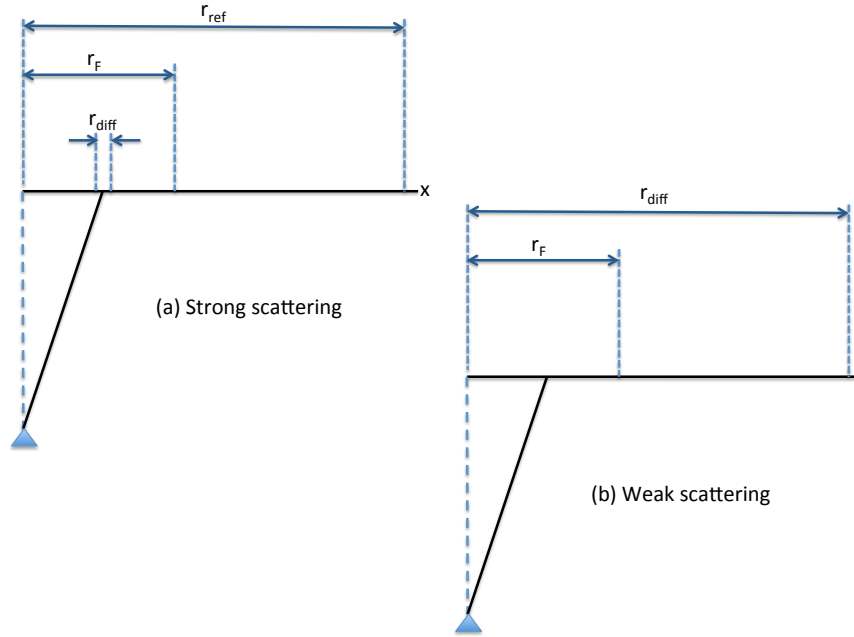


Figure 3.4: An illustration of the difference in geometries between (a) strong scattering and (b) weak scattering. The x scale is exaggerated relative to the z scale to magnify the distinction.

Fresnel zone are significant contributors to the received flux, albeit at a reduced energy, because the geometric contribution to phase variation can still be small over the smaller $r_{\text{diff}} \ll r_F$ scale. In fact, there is a longer *refraction scale* $r_{\text{ref}} > r_F$ over which coherence patches make a significant contribution (it happens that $r_{\text{ref}} = r_F^2 / r_{\text{diff}}$). Within the refraction scale there are multiple distinct coherent patches, each contributing energy with a propagation delay that increases with x . The maximum delay that is a significant contributor roughly corresponds to $x = r_{\text{ref}}$. In strong scattering there is *multipath distortion* due to the multiple pathways that arrive at the observer, each corresponding to a distinct coherent patch, and each having a distinct group delay.

Thus far the discussion has assumed a monochromatic (sinusoidal) signal is propagating through the scattering screen. To model the ICH, the question is what the effect of this multipath distortion is on a finite bandwidth waveform $h(t)$. This question is considered in more depth in Chapter 8, but the results can be summarized as follows. Assume that there are N paths corresponding to distinct coherent patches, where the n th path is characterized by an amplitude r_k and a phase shift ϕ_n . Although $h(t)$ will also be distorted by plasma dispersion (see Section 8.2), within an ICH this effect can be neglected. Although there is some smearing of energy over time due to the geometric variation of propagation delay within a single coherent path, within the ICH due to the choice of a maximum bandwidth for $h(t)$ this effect can be neglected to lump all this energy into a single discrete delay τ_n . Although the exact amplitudes are unknown, it is the phases that are very

random. Phase is very sensitive to slight perturbations of conditions over such long distances and those perturbations can easily be large relative to one wavelength.

In our simple model, the observation consists of a superposition of these paths,

$$r(t) = \sqrt{\mathcal{E}_h} \cdot \sum_{n=1}^N r_n e^{i\Phi_n} h(t - \tau_n). \quad (3.6)$$

This basic model is very familiar in terrestrial wireless communication, where the multipath distortion is due to radio waves bouncing over various obstacles like buildings and hills [16]. There are two distinct effects to consider: the delays $\{\tau_n\}$ and the phases $\{\phi_n\}$.

Consider first the delays $\{\tau_n\}$. As seen from geometric reasoning, all $\tau_n < \infty$ since as x increases (and equivalently propagation delay increases) eventually a point is reached where the geometric variation in phase across a coherent patch yields an insignificant observed net flux. Thus, define the *delay spread* τ_s of the scattering as the maximum of the $\{\tau_n, 1 \leq \tau \leq N\}$. Recall that in the model of the ICH of Figure 3.1 it is the response of a matched filter to the reception $r(t)$ that matters. The response of the matched filter to a single term $h(t - \tau_n)$ is

$$\int_0^T h(t - \tau_n) h^*(t) dt = \int_0^B |H(f)|^2 e^{-i2\pi f \tau_n} df. \quad (3.7)$$

The effect of delay τ_n is reflected in the frequency-domain by the phase term $e^{-i2\pi f \tau_n}$. This term can be ignored (and hence τ_n can be neglected) if the total phase shift variation across $f \in [0, B]$ is less than $\alpha\pi$, or

$$2B\tau_s \ll \alpha, \quad (3.8)$$

where $0 \leq \alpha \leq 1$ is a parameter chosen to adjust the strictness of the criterion. Intuitively, the "width" or rate of change of $h(t)$ is limited by B ; the larger B , the faster can be the variations in $h(t)$. As long as τ_s is less than $\alpha/2B$, the effect on $h(t)$ is hardly noticeable because the waveform of $h(t)$ is changing too slowly to see the effects of that delay.

This establishes delay spread as a frequency coherence issue, in that its effects are mitigated and eventually can be neglected as bandwidth B is decreased. Thus, within an ICH it can be assumed that (3.8) is satisfied and (3.6) simplifies to

$$Z(0) = r(t) \otimes h^*(-t)|_{t=0} = \sqrt{\mathcal{E}_h} \cdot \sum_{n=1}^N r_n e^{i\Phi_n}, \quad (3.9)$$

which is consistent with (3.1) without the noise. In (3.9) the magnitude and phase of the scintillation are,

$$\sqrt{\mathcal{F}} e^{i\Phi} = S = \sum_{n=1}^N r_n e^{i\Phi_n}. \quad (3.10)$$

A new complex-valued random variable S has been introduced, capturing both the magnitude and phase of the scintillation.

The flux \mathcal{F} is the average observed energy associated with unit-energy waveform $h(t)$ after it is intercepted by the screen. No reduction in B and/or T can rid us of \mathcal{F} , and thus scintillation

is a characteristic of the ICH model. It affects even the limiting case of a monochromatic signal ($B \rightarrow 0$) [35, 34, 15]. The phase shifts of different paths are a very sensitive function of the physical parameters, including plasma density and path length. For example, differences in the $\{\tau_n\}$ too small to cause frequency incoherence will still have a big effect on the $\{\Phi_n\}$. On the other hand, the $\{r_n\}$ can be expected to vary reasonably slowly with time, since they are dependent on the large-scale geometry of multiple paths of propagation through the ISM. Thus, in (3.9) the liberty has been taken to make the $\{r_n\}$ constants and the $\{\Phi_n\}$ random variables.

Working back from these assumed statistics of the $\{\Phi_n\}$ it is straightforward to show (Appendix C.1) that S has zero mean ($\mathbb{E}[S] = 0$), and by a Central Limit Theorem argument it is a Gaussian random variable with second order statistics

$$\mathbb{E}[S^2] = 0 \quad \text{and} \quad \sigma_s^2 = \mathbb{E}[|S|^2] = \sum_{n=1}^N r_n^2. \quad (3.11)$$

The condition $\mathbb{E}[S^2] = 0$ implies that the real and imaginary parts $\Re\{S\}$ and $\Im\{S\}$ are statistically independent and each have variance $\sigma_s^2/2$. In different ICH's that do not overlap in time or in frequency, the values of S may have some statistical dependency, more so in magnitude than in phase because the $\{r_n\}$ are determined primarily by turbulence in the interstellar clouds and the motion of the receiver. The effect of motion is considered in more detail in Section 8.5, where it is shown that it results in time incoherence that can be neglected for sufficiently small T .

From the Gaussian distribution of S and (3.11), it follows that $\mathbb{E}[\mathcal{F}] = \sigma_s^2$ and $\text{Var}[\mathcal{F}] = \sigma_s^4$, and thus from (3.4) the modulation index is $m_{\mathcal{F}} = 1$. Thus, the standard deviation of flux equals its mean, independent of σ_s^2 . However, a deeper examination of the physics reveals that [18]

$$\mathbb{E}[\mathcal{F}] = \sigma_s^2 = 1. \quad (3.12)$$

This is valid for both weak and strong scattering, and thus neither weak nor strong scattering affects the numerical value of the energy contrast ratio ξ_s that was defined in (2.16). There is a simple physical argument behind (3.12). Scattering is a lossless phenomenon, redistributing energy at the plane of the observer but not affecting the total energy. Thus, while the motion of the observer within this plane causes a variation in observed signal flux, a long-term average of that flux is no different from the constant flux in the absence of scattering.

For strong scattering $\sqrt{\mathcal{F}}$ has a Rayleigh distribution, and thus this type of scintillation is called *Rayleigh fading* in the communications engineering literature. There is a wealth of relevant experience in designing wireless mobile communication systems that encounter Rayleigh fading.

Weak scattering regime

Returning to Figure 3.4b, in weak scattering (where $r_{\text{diff}} \gg r_F$) the scale of coherent patches is large relative to the Fresnel scale. This implies that geometric effects are dominant in the sense that the delay spread and received flux are determined by the geometry more than the coherence patches, although the latter remain very significant in determining whether the flux is high (a coherence patch overlaps the observer's first Fresnel zone) or low (the observer's first Fresnel zone falls in a

region of chaotic phase or transition). For weak scattering, the modulation index is less than unity [18],

$$m_{\mathcal{F}} = \left(\frac{r_{\text{F}}}{r_{\text{diff}}} \right)^{5/6} < 1, \quad (3.13)$$

or the variations in flux \mathcal{F} are smaller than the mean. Since $m_{\mathcal{F}} = 1$ for a completely random scintillation, this implies that \mathcal{F} has a deterministic component that contributes to $\mathbb{E}[\mathcal{F}]$ but does not contribute to $\sqrt{\text{Var}[\mathcal{F}]}$. In communications engineering this is called a *specular* component, and the case $m_{\mathcal{F}} < 1$ is called *Rician fading*, because $\sqrt{\mathcal{F}}$ has a Rician distribution. The model used in communications engineering for Rician flux is [16]

$$\sqrt{\mathcal{F}} e^{i\Phi} = \sqrt{\gamma} \sigma_s e^{i\Psi} + \sqrt{1-\gamma} \sigma_s S \quad (3.14)$$

$$\gamma = \frac{\kappa}{1+\kappa}, \quad (3.15)$$

where S has the same statistics as in Rayleigh fading. Comparing with (3.10), there is the addition of a specular term which has a constant magnitude and a random phase Ψ uniformly distributed on $[0, 2\pi]$ and independent of S . A parameter $0 \leq \kappa < \infty$ called the *K-factor* controls how much of the energy is in the constant-magnitude term vs the random term, all the while maintaining a constant average flux $\mathbb{E}[\mathcal{F}] = \sigma_s^2$. The modulation index

$$m_{\mathcal{F}} = \frac{\sqrt{1+2\kappa}}{1+\kappa}, \quad (3.16)$$

is plotted in Figure 3.5. The Rayleigh fading case (strong scattering) corresponds to $\kappa = 0$, while $m_{\mathcal{F}}$ decreases as κ increases. Rayleigh fading is therefore “worst case” in the sense of “largest modulation index”.

Rician fading is characteristic of wireless propagation when there is an unobstructed specular path from source to observer that contributes a constant flux (albeit with random phase Ψ), accompanied by multiple random paths that contribute to a variation in flux. In order to get proper articulation between weak and strong scattering at the transition ($r_{\text{diff}} = r_{\text{F}}$), we must have $\sigma_s^2 = 1$ in (3.14). For a given value of $m_{\mathcal{F}}$ from (3.13), the appropriate κ can be read off of Figure 3.5 or calculated from (3.16).

3.2.2 Noise within a coherence hole

Suppose that the ISM introduces AWGN $N(t)$ with power spectral density N_0 into $r(t)$. Then the noise at the matched filter output in Figure 3.1 is

$$M = \int_0^T e^{-i2\pi f_c t} h^*(t) N(t) dt. \quad (3.17)$$

This random variable is (Appendix C) zero-mean Gaussian with variance $E|M|^2 = N_0$, and further $\mathbb{E}[M^2] = 0$ and thus $\Re\{M\}$ and $\Im\{M\}$ are independent and have the same variance $N_0/2$.

It is significant that neither B nor T affects the statistics of M . Thus, the statistics of the noise at the matched filter output do not change as B and T decrease, and thus noise remains an important

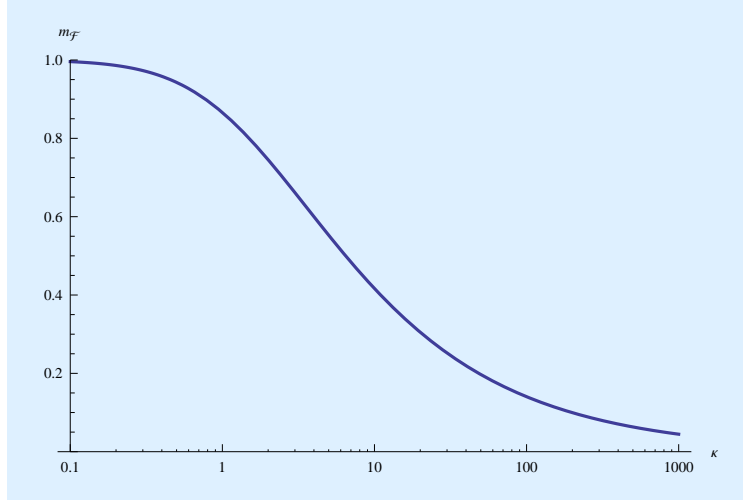


Figure 3.5: The modulation index m_F of Rician fading as a function of the K -factor κ .

impairment within an ICH. The intuitive explanation for this is that within bandwidth B the total noise power is $N_0 B$, and thus the total noise energy within time T is $N_0 B T = N_0 K$. Although this *total* noise energy increases with K , the matched filter extracts the noise in only one degree of freedom and rejects the noise in the remaining $K - 1$ degrees of freedom, leaving a total noise energy aligned with $h(t)$ equal to N_0 and independent of K .

3.3 Frequency offset due to acceleration

When multiple energy bundles are transmitted, each bundle may experience a different scintillation phase Φ and flux \mathcal{F} . In addition, the carrier frequency is offset according to any uncorrected acceleration between source and observer along the line of sight. This phenomenon is modeled in Chapter 8. The significant sources of acceleration are the diurnal rotation of a planet or moon about its axes and the orbital motion of a planet about its host star or a moon about its host planet. A transmitter and a receiver can readily correct the signal to remove the effects of this acceleration based on their knowledge of the local orbital mechanics. However, if either fails to make this correction, acceleration becomes more important than scintillation in determining the coherence time T_c . In addition, uncorrected acceleration results in a carrier frequency offset between two energy bundles separated in time. If the receiver suspects or assumes the presence of acceleration, this will affect the energy bundle pattern recognition algorithms in discovery, and even more significantly the extraction of information from the signal. However, correction for acceleration is simple and does not require much processing, so it would be surprising if the transmitter failed to make this correction.

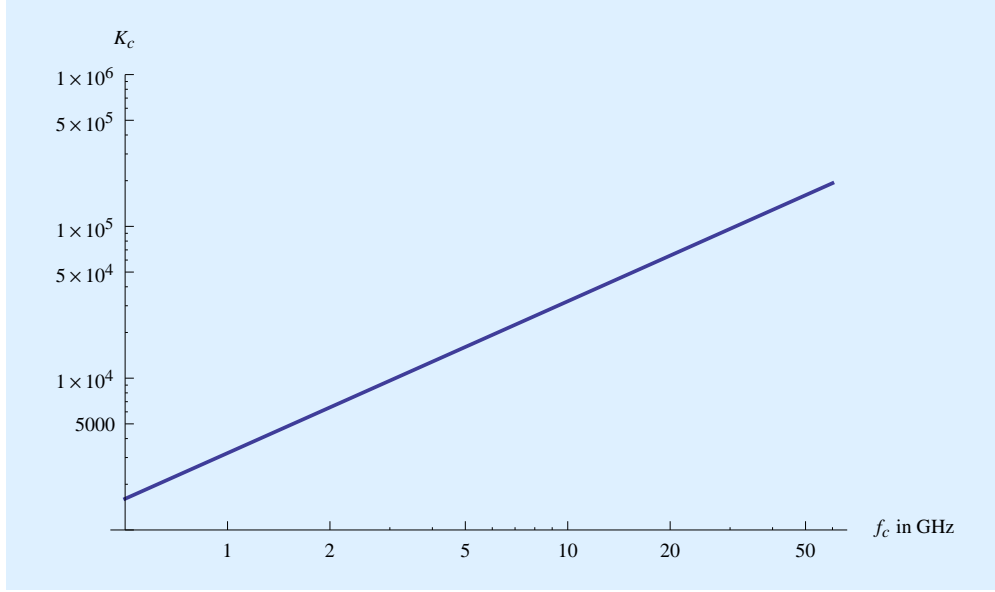


Figure 3.6: A log-log plot of $K_c = B_c T_c$, the degrees of freedom for an ICH, vs the carrier frequency f_c for the numerical values of Table 3.2. A safety factor of $\alpha = 0.1$ is assumed, except for acceleration where the safety factor is $\alpha = 0.01$. The components B_c and T_c are shown in Figure 8.9.

3.4 Time-bandwidth product and degrees of freedom

An important secondary parameter of the ICH is its time-bandwidth product $K_c = B_c T_c$, which is called the *degrees of freedom* (DOF). K_c is the number of complex-valued numbers that are required to fully specify any waveform $h(t)$ that falls in an ICH. K_c depends on the specific line of sight (LOS) and the carrier frequency f_c . If $K_c \leq 1$, then interstellar communication becomes very difficult because for all practical purposes the ICH does not exist, or putting it another way the inherent incoherence of interstellar propagation between a source and observer in relative motion severely distorts virtually any waveform $h(t)$ that we attempt to transmit. This would be particularly problematic for discovery, since there is no opportunity to estimate $h(t)$ in advance nor even observe the current ISM “weather” conditions to infer some of its likely properties. If on the other hand, if $K_c \gg 1$, then interstellar communication becomes relatively straightforward, because the transmit signal can be chosen to circumvent all impairments save noise and scintillation. In Chapter 8, K_c is estimated using the numerical values of Table 3.2 and the result is shown in Figure 3.6. This estimate varies over a range $K_c \approx 1000$ to 10^5 for the range $0.5 \leq f_c \leq 60$ GHz. In addition, if both the transmitter and receiver correct for their respective accelerations in the direction of the line of sight, then T_c (and hence K_c) increases substantially.

The choice of $h(t)$ is of considerable importance from two perspectives. First, the choice should be a waveform that the receiver can guess in order to apply a matched filter, because there is no possibility of conveying the precise $h(t)$ to the receiver prior to discovery. Second, while the choice of $h(t)$ has no relevance to the power efficiency of the system, it does have considerable significance to the RFI immunity of the signal, which argues for choosing as large a K as possible

[11]. Of course, the largest value is $K = K_c$ consistent with the ICH.

3.5 Some observations about the ICH

We can consider ourselves fortunate that the ISM and source/observer motion introduce impairments from the perspective of implicit coordination of transmitter and receiver [3]. The source and observer can independently estimate $\{T_c, B_c\}$ and the resulting K_c based on common observable physical characteristics of line of sight, and they should arrive at similar (although not identical) estimates. This provides source and observer a common reference in choosing some free parameters in the transmit signal $h(t)$, and reduces the ambiguity and the size of a discovery search at the receiver. In addition to RFI immunity, this is another argument for choosing $K = K_c$, as this choice minimizes the ambiguity in K between transmitter and receiver. At the same time as ambiguity is reduced, ISM and motion impairments (with the exceptions of noise and scintillation) do not adversely affect the feasible power efficiency, our ability to reliably communicate, or introduce any added processing requirements in either transmitter or receiver.

The estimate of $\{T_c, B_c\}$ depends on several circumstances:

Definition of coherence. Coherence improves gradually as $\{T, B\}$ are decreased, but perfection is not attainable. How much coherence is enough depends to some extent on the usage; for example, some information-representation schemes are more sensitive to incoherence (and to particular types of incoherence) than others. Thus the transmitter and receiver will adjust their definitions of coherence somewhat (fortunately in compatible ways) based on other aspects of the system design.

The line of sight and observer motion. Dispersion and scattering and source/observer motion depend on the line of sight. In particular, the relevant parameters of the line of sight from Table 3.2 are the dispersion measure DM, the diffraction scale r_{diff} , and the distance D . Astronomical observations yield considerable information [42], but with some residual uncertainty. A lot is also known about the motion impairments, which depend on the radial acceleration a_{\parallel} and the transverse velocity v_{\perp} . This is particularly true of a_{\parallel} because acceleration can be inferred from an accelerometer or equivalently from modeling of the dominant sources of acceleration, which are the orbit of a planet about its star as well as the revolution about its axis.

Carrier frequency. All impairments depend on the wavelength (carrier frequency) in use.

Inevitably there will be some discrepancy between the source and observer estimates, particularly in reference to the density of electrons along their line of sight and the nature of their inhomogeneity. Information about this is presumably due primarily to pulsar observations, and the source and observer must base their estimates on pulsars that typically have a different orientation relative to the line of sight.

There are also two forms of compensation that can be performed at the transmitter and that have the effect of increasing the size of the ICH: one is for acceleration and the other equalizes for

the best-case dispersion along the line of sight (Chapter 8). The receiver designer must therefore account for the possibility that the transmitter may have compensated for one or both of these effects, or not.

3.6 Summary

While the interstellar medium and relative motion of source and observer introduce impairments to signals that can be severe, most of these can be avoided by reducing the time duration and bandwidth of the waveform $h(t)$ that is used as the basis of an energy bundle. The resulting interstellar coherence hole (ICH) serves as the foundation of a power-efficient design for an interstellar communication system. Two impairments that cannot be avoided in this way are additive white Gaussian noise (AWGN) and scintillation. AWGN is due to cosmological and stellar sources, as well as the non-zero temperature of the receiver circuitry. Scintillation is due to the constructive and destructive interference of multiple paths through the interstellar medium due to the presence of inhomogeneous clouds of ionized gasses. The ICH is characterized by a coherence time and a coherence bandwidth for the interstellar channel, both of which can be estimated for typical physical parameters as shown in Chapter 8.

Chapter 4

The fundamental limit

In Section 2.4 the fundamental limit on power efficiency through the channel model with additive white Gaussian noise (AWGN) and assuming an average power constraint was displayed, and used to demonstrate that there is a tradeoff between power efficiency and spectral efficiency. However, as shown in Chapter 3 and 8, although AWGN is one of the impairments on the interstellar channel, there are others. This chapter develops a fundamental limit for the interstellar channel based on the results of Chapters 3 and 8. Generally, it considers only the case of the power efficiency limit, in the absence of any constraint on the total signal bandwidth B_{total} , because this unconstrained bandwidth case is far easier. That is, this chapter explores the fundamental limit applying to power-efficient design, rather than spectrally efficient design.

The results of this chapter can be summarized in the single equation

$$\zeta_b = \frac{\mathfrak{E}_b \sigma_s^2}{N_0} > \log 2, \quad (4.1)$$

where ζ_b is the energy contrast ratio per bit defined in (2.17). This is the fundamental limit on power efficiency that can be obtained on the interstellar channel. In particular it establishes a minimum energy that the transmitter must deliver to the receiver for each bit of information that is conveyed reliably, meaning with arbitrarily small probability of error. This chapter establishes this relationship, and Chapter 5 describes concrete and practical designs for channel coding on the interstellar channel and compares the power efficiency that they achieve to the fundamental limit of (4.1).

The most significant result of this chapter is a concrete channel code that can approach the fundamental limit asymptotically. By that we mean that as long as \mathfrak{E}_b satisfies (4.1) for this channel code, then the probability of error P_E can be driven arbitrarily close to zero as some parameters of the channel code become unbounded. This channel code combines the five principles of power-efficient design outlined in Section 2.5. Both the channel code and its proof of asymptotic optimality provides considerable insight into what is necessary to approach the fundamental limit. It also provides practical guidance for the concrete designs in Chapter 5.

4.1 Role of large bandwidth

The Shannon *channel capacity*, published in 1948, is a mathematically provable upper bound on the information rate \mathcal{R} that can be achieved reliably for a given channel model [8]. More modern developments of Shannon's results are found in [43, 44]. Although channel capacity is a general concept, for the AWGN channel of (2.14) the result is particularly simple to derive. Unless the average power of $X(t)$ is constrained, the capacity becomes infinite, so it is assumed that $\mathbb{E}[X^2(t)] \leq \mathcal{P}$. It is important to note that the average signal power \mathcal{P} is referenced to the same point as the noise in (2.14), which is usually chosen to be at the receive antenna output and before baseband signal processing. To understand the implications of this to the average transmit power, we have to work backwards, taking into account the transmit and receive antenna gains and the propagation loss.

The Shannon capacity for the AWGN channel was given in (2.18), and from that result the fundamental limit on power efficiency \mathfrak{P} was inferred. That limit, when expressed in terms of the energy contrast ratio per bit ξ_b is given by (4.1). At this fundamental limit, $\mathcal{R} \propto \mathcal{P}$, or every increase in \mathcal{R} demands a proportional increase in \mathcal{P} . This is exactly the same tradeoff that was seen in practical designs like M-ary FSK in Section 2.3, although the constant of proportionality is certain to be smaller reflecting a penalty that must be incurred by practical outcomes.

Perhaps the most significant observation was the tradeoff between spectral efficiency and power efficiency, and in particular the observation that high power efficiency implies poor spectral efficiency, or equivalently a large total bandwidth B_{total} relative to the information rate \mathcal{R} . It is important to understand the critical role of large bandwidth, and that is a theme of the remainder of this chapter. A different but insightful interpretation follows from the observation that the input signal-to-noise ratio SNR_{in} of (2.19) is very small in the regime where B_{total} is allowed to be large. When $\text{SNR}_{\text{in}} \approx 0$, (2.18) can be expanded in a Taylor series as

$$\mathcal{R} \leq \frac{\mathcal{P}}{N_0 \log 2} \cdot \left(1 - \frac{\text{SNR}_{\text{in}}}{2} + \frac{\text{SNR}_{\text{in}}^2}{3} - \dots \right) \xrightarrow{\text{SNR}_{\text{in}} \rightarrow 0} \frac{\mathcal{P}}{N_0 \log 2}. \quad (4.2)$$

Thus, another characteristic of power-efficient communication is a very small SNR_{in} because of a large B_{total} , and in this special case (2.18) simplifies to (4.2), in which $\mathcal{R} \propto \mathcal{P}$ at the limit.

To approach the fundamental limit on power efficiency \mathfrak{P} the bandwidth B_{total} must be *unconstrained*. It is important to note that unconstrained bandwidth is different than *unlimited* bandwidth, because the bandwidth actually utilized in any practical design (such as those in Section 2.3 or Chapter 5) will always be finite. Unconstrained bandwidth merely assumes that bandwidth is not a consideration in the transmitter's signal design, which focuses exclusively on achieving high power efficiency. However, one implication of (4.2) is that any approach that can asymptotically approach the fundamental limit must consume a total bandwidth B_{total} that approaches infinity. Putting it another way, any practical approach (such as those discussed in Chapter 5) must use a finite bandwidth, and this reality alone inevitably creates a penalty in power efficiency

How does large bandwidth square with interstellar impairments?

One possible source of misunderstanding arises from the seeming contradiction between two observations. In this chapter, it is shown in several ways that large total signal bandwidth B_{total} is necessary to asymptotically approach the fundamental limit on power efficiency. In Chapter 8 it is shown that a large bandwidth is problematic in that some interstellar impairments become increasingly significant with increasing bandwidth. By restricting the bandwidth B of an energy bundle to $B \leq B_c$, where B_c is the coherence bandwidth, a decrease in receiver sensitivity due to these impairments is avoided. Thus, a large bandwidth and a restricted bandwidth are simultaneously necessary to approach the fundamental limit. Are these two observations incompatible with one another?

No, they are completely compatible! In this chapter, it is shown that a channel code composed of energy bundles can approach the fundamental limit asymptotically. Basing this channel code on energy bundles makes it impervious to all interstellar impairments other than noise and scintillation, as long as the constraint $B \leq B_c$ is adhered to (as well as a similar constraint on time duration). By spreading these energy bundles out in frequency as well as time, the bandwidth of each codeword B_{total} is increased accordingly. Any channel code that approaches the fundamental limit must asymptotically have codewords that obey the condition $B_{\text{total}} \rightarrow \infty$, even as each energy bundle constituent of the codewords must obey the constraint $B \leq B_c$.

relative to the fundamental limit.

4.2 Approaching the fundamental limit: channel coding

Channel coding is the most general way to think of transmitting a sequence of information bits over a physical channel. Shannon's channel capacity is based on this general model, deriving conditions under which channel coding can or cannot achieve reliable communication of information.

Channel coding can be described in a general way as follows. Supposing the information rate is \mathcal{R} , then the number of bits to be communicated during a time period with duration t_0 is $t_0\mathcal{R}$, and if the average power is constrained to \mathcal{P} then the total energy available during this period is $t_0\mathcal{P}$. This can be accomplished by defining a *codebook* of $2^{t_0\mathcal{R}}$ distinct waveforms on this interval, where each *codeword* in this codebook meets the energy constraint.¹ Depending on the actual $t_0\mathcal{R}$ information bits presented to the transmitter, the appropriate codeword is transmitted. Shannon's channel capacity theorem states that if $\mathcal{R} \leq \mathcal{C}$ then there exists a codebook for each t_0 with the property that as $t_0 \rightarrow \infty$ the probability of the receiver choosing the wrong codeword (due to noise or other impairments) approaches zero. Conversely, if $\mathcal{R} > \mathcal{C}$ then the probability of choosing the wrong codeword is bounded away from zero.

The proof of Shannon's theorem demonstrates that a sequence of codebooks exists such that as $t_0 \rightarrow \infty$ the error probability goes to zero. However, the theorem is not constructive and doesn't

¹ More accurately, individual codewords can violate the energy constraint as long as the average over all codewords does not.

say how to design actual codebooks. Construction of a codebook is usually challenging, in part because its membership is growing exponentially with t_0 . In the spectrally efficient regime, the additional constraint on the bandwidth of each codeword is challenging. But the unconstrained bandwidth case is much simpler. Although the existence of a fundamental limit inspired immediate and substantial progress, it took less than two decades of research by applied mathematicians to find codebooks that approach capacity in the easier power-efficient case, and about three *additional* decades for the spectrally efficient case.

The M-ary FSK of Section 2.3 is a simple examples of channel coding. The characteristic that makes them a channel code is that it maps M information bits onto a signal, rather than doing that mapping one bit at a time. The resulting signal is a function of all M bits, and there is no feasible way to determine a single bit without determining all M of them.

4.3 A channel code that approaches the fundamental limit

M-ary FSK is a very useful weapon in the power-efficient design arsenal, and for this reason is included among the five design principles of Section 2.5. In fact, the first case attacked and solved was the AWGN channel with unconstrained bandwidth $B_{\text{total}} \rightarrow \infty$, and M-ary FSK was shown to fit the bill in this case, achieving an error probability that approaches zero as $M \rightarrow \infty$. This applies directly only to the case of phase-coherent detection on an AWGN channel without scintillation.

When scintillation is added to AWGN, as well as the numerous other impairments due to interstellar propagation and motion of the source and observer, we have to work harder. This is attributable to the necessity of phase-incoherent detection, and also due to the statistical variation in the received energy per bundle. We now demonstrate a concrete channel code that overcomes both of these challenges and approaches the fundamental limit of (4.1) for the AWGN channel both with and without scintillation, and in the scintillation case in the absence of any side information about the scintillation in the receiver. This will be a key step in the primary result of this chapter, which is to show that (4.1) is the fundamental limit for the interstellar channel, implying that the impairments on the interstellar channel other than noise do not influence the fundamental limit on power efficiency. This also gives us valuable guidance on how to improve the power efficiency for the interstellar channel in practice, which is pursued in Chapter 5.

4.3.1 Structure of the channel code

We now demonstrate a concrete channel code that can asymptotically approach the fundamental limit on the interstellar channel. This channel code is conceptually simple, and thus provides considerable guidance on how to efficiently communicate through the interstellar channel in practice. Further, this channel code is unbeatable. More advanced civilizations might be able to come up with a different channel code, but they could never improve on its power efficiency. To design the code, the five principles of power-efficient design listed in Section 2.5 are combined.

Use energy bundles

The channel code is based on transmitting energy bundles, and constraining those bundles to conform to the coherence bandwidth $B \leq B_c$ and the coherence time $T \leq T_c$. Each codeword will communicate $\log_2 M$ bits of information, or in other words the codebook counts 2^M member codewords. The transmitter chooses one of those 2^M codewords, and the receiver detects which codeword was transmitted. We will show that as long as (4.1) is satisfied, the probability of error P_E in the detection of a single bit approaches $P_E \rightarrow 0$ as $M \rightarrow \infty$. Of course for any finite value of M a more stringent criterion than (4.1) will have to be satisfied to achieve $P_E \approx 0$, and the resulting penalty relative to the fundamental limit is explored in Chapter 5.

Use M-ary FSK

The $\log_2 M$ bits of information are conveyed by the location of energy bundles at one of M different frequencies. These frequencies are chosen to be sufficiently far apart that there is no frequency-overlap among the M possible locations for energy bundles. An arbitrarily large amount of information can be communicated by each codeword simply by choosing a large M .

It is interesting that we do not need to resort to multicarrier modulation (MCM) to achieve any \mathcal{R} we desire. In fact, we *cannot* approach the fundamental limit using MCM. In practice, of course, a finite M (number of frequencies in FSK) and J (number of repetitions of an energy bundle in the time diversity) must be chosen with a resulting penalty relative to the fundamental limit, and in that case MCM is a valuable practical technique for increasing the information \mathcal{R} without resorting to impractically large values of M .

Use time diversity

Each actual energy bundle is redundantly repeated J times with an intervening interval larger than the coherence time of the scintillation and time diversity combining is utilized by the receiver to counter the effects of scintillation. An example of a channel code that combines M-ary FSK with time diversity was illustrated in Figure 2.9. A similar illustration of a single codeword (showing the locations of energy bundles in time and frequency) is given in Figure 4.1. The basic idea is that the total energy is divided between the J replicas, which experience the scintillation independently. Averaging the J estimates gives a more reliable indication of the transmitter intention. The J energy bundles are located at one frequency out of M possibilities, conveying $\log_2 M$ bits of information.

Interestingly, if M is sufficiently large each codeword will encounter significant variation in the received signal flux at different frequencies. Fortunately this is not an issue because each codeword uses only a single frequency to transmit its J energy bundles. Those J bundles beneficially experience the statistical variation of energy per bundle with time. The details of the received signal flux at other frequencies may be different, but no energy bundles are being transmitted at those frequencies so that variation is not observed by the receiver.

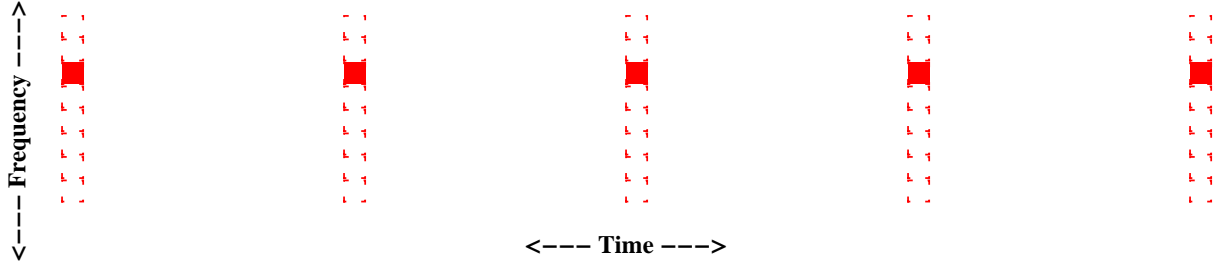


Figure 4.1: A two-dimensional representation of a single codeword for M-ary FSK ($M = 8$ is illustrated) combined with time diversity using J identical repetitions of each FSK symbol ($J = 6$ is illustrated). Each energy bundle has time duration T , and the spacing between repetitions is $11 \times T$. Although the parameterization is different, this is similar to the codeword illustrated in Figure 2.9.

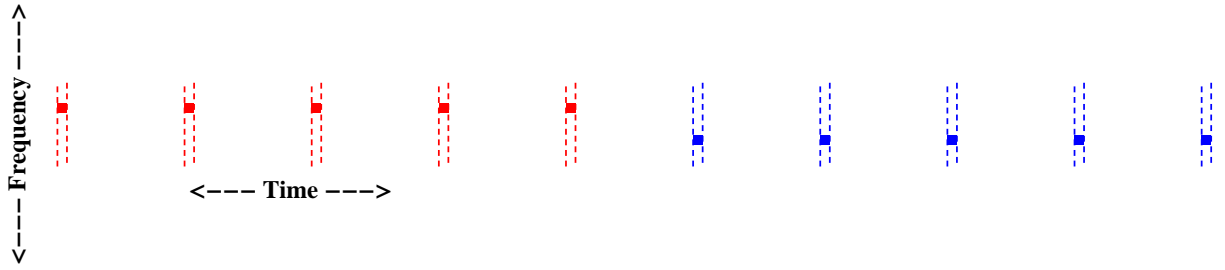


Figure 4.2: An illustration of how the individual codewords of Figure 4.1 can be transmitted sequentially to communicate a stream of information. Shown are two codewords communicating a total of 6 bits of information in twice the time as would be required for a single codeword. The duty cycle of this scheme is $\delta = 1/12$, because transmission occurs during T seconds out of every $12 \times T$ seconds.

Figure 4.1 shows only a single codeword out of a codebook containing M codewords. An issue which turns out to be important is how a multiplicity of these codewords are positioned in time to convey a sequence of information bits. One possibility, illustrated in Figure 4.2, is to transmit codewords sequentially. Another possibility, illustrated in Figure 4.3, is to interleave the codewords in time. Anywhere between two (the example shown) and J codewords can be interleaved in this fashion.

It will turn out that the fundamental limit is approached as $J \rightarrow \infty$. This allows the law of large numbers to kick in and give the receiver an increasingly accurate estimate of the transmitted energy per bundle even in the face of the statistical variations in the energy of each bundle due to scintillation. Together, the two conditions $M \rightarrow \infty$ and $J \rightarrow \infty$ have profound implications. A single code word grows in both bandwidth and in time duration, in both cases without bound. The number of information bits communicated by a single codeword also grows, so for a fixed total information rate it follows that individual codewords are transmitted at a lower and lower rate. In summary, as we approach the fundamental limit, more and more information is crammed in a single codeword, and each codeword grows in size in both time and frequency with a correspondingly lower rate of transmitting codewords.

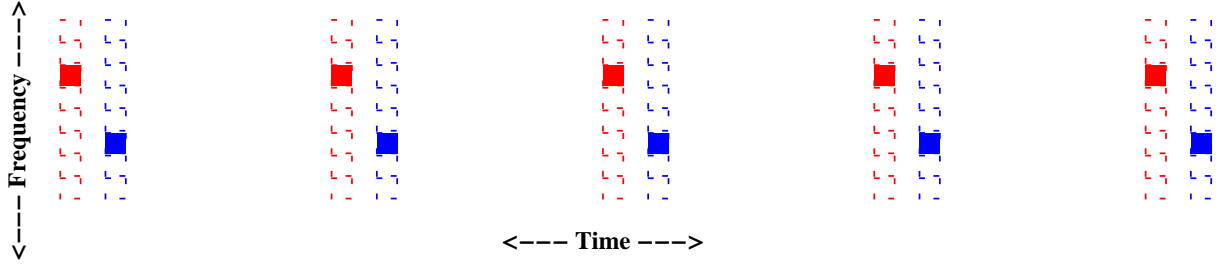


Figure 4.3: An illustration of how the individual codewords of Figure 4.1 can be interleaved in time to communicate a stream of information. This interleaving would be combined with sequential transmission (which was illustrated in Figure 4.2). Shown are two codewords communicating a total of 6 bits of information in slightly more time than would be required for a single codeword. The duty cycle of this scheme is $\delta = 1/6$, because transmission occurs during $2 \times T$ seconds out of every $12 \times T$ seconds. This duty cycle is double that of Figure 4.2 because twice as many codewords are packed in the same overall time.

Use low duty cycle

For any fixed information rate \mathcal{R} and average power \mathcal{P} that we choose as design goals, there is a tradeoff between using a larger M and lower duty cycle δ , or a smaller M and larger duty cycle. It will turn out that the fundamental limit is only approached as $M \rightarrow \infty$, or equivalently $\delta \rightarrow 0$. It will also turn out that the reason for this is that as $\delta \rightarrow 0$ the energy in each bundle \mathcal{E}_h grows, and this is necessary to achieve a vanishing error probability $P_E \rightarrow 0$. Thus a reduction in duty cycle is used as a way to “punch through” the scintillation, since it is also true that for a constant information rate \mathcal{R} and average power \mathcal{P} the energy in each bundle \mathcal{E}_h increases as the duty cycle δ is reduced.

Together these characteristics imply that each codeword becomes increasingly sparse as the fundamental limit is approached. Each codeword has $M \cdot J$ possible locations for energy bundles, but only J of these locations are used. Out of the M frequencies in total, only one is used. Similarly, the duty cycle δ is small, and only a fraction δ of the time is there an energy bundle currently being transmitted at *any* frequency. For a fixed average power \mathcal{P} , this sparsity allows the energy of each bundle that is transmitted to be as large as necessary to insure reliable detection of energy bundles.

4.3.2 Parameters of the codebook

The parameters of the codebook as we have defined it are $\{\mathcal{R}, \mathcal{P}, T, M, J, \mathcal{E}_h, \delta\}$. The two primary parameters $\{\mathcal{R}, \mathcal{P}\}$ are fixed as a design objective, and our challenge is to adjust the secondary parameters $\{T, M, J, \mathcal{E}_h, \delta\}$ in a way that reduces the error probability P_E . In the following, it is extremely important to keep the mindset that $\{\mathcal{R}, \mathcal{P}\}$ are fixed and unassailable. The question then is under what conditions on $\{\mathcal{R}, \mathcal{P}\}$ it is possible to drive $P_E \rightarrow 0$. The answer will be that this is possible if $\{\mathcal{R}, \mathcal{P}\}$ satisfy

$$\frac{\mathcal{R}}{\mathcal{P}} < \frac{\sigma_s^2}{N_0 \log 2}, \quad (4.3)$$

which is equivalent to the fundamental limit of (4.1).

The other question is how the secondary parameters $\{T, M, J, \mathcal{E}_h \delta\}$ should be adjusted, under the condition that $\{\mathcal{R}, \mathcal{P}\}$ are fixed, to achieve $P_E \rightarrow 0$ when (4.3) is satisfied. The parameter T , the duration of each energy bundle, is relatively simple to deal with since it is constrained by the coherence time $T \leq T_c$. Generally it is advantageous to choose T as large as possible, since that reduces the transmitted peak power. Otherwise T is not particularly significant. Regarding the remaining parameters, we must allow $J \rightarrow \infty$ and $\delta \rightarrow 0$, which implies also that $M \rightarrow \infty$. Roughly speaking choosing a large M counters the additive noise while a large J counters the scintillation. The purpose of choosing a small δ is to increase \mathcal{E}_h , which allows more reliable decisions on the presence or absence of an energy bundle to be made.

Information rate

In terms of the other parameters, the net information rate is

$$\mathcal{R} = \delta \cdot \frac{\log_2 M}{JT}. \quad (4.4)$$

This is because $\log_2 M$ bits of information are conveyed by each codeword, each of which consumes a total transmission time of JT . For fixed M and J , the highest information rate occurs with a 100% duty cycle, meaning an energy bundle is being transmitted at some frequency at all times. This can be achieved, for example, by interleaving codewords to avoid any "blank" intervals, and then transmitting the resulting fully-interleaved codewords sequentially with time. More generally, when $\delta < 1$ the result is a reduction in \mathcal{R} .

Remember however that \mathcal{R} is actually fixed, and also assume that T has been chosen according to time coherence criteria. In that case (4.4) reveals a tradeoff between the parameters $\{M, J, \delta\}$. Generally as J is increased and δ is reduced, which is necessary to approach the fundamental limit, then M has to be increased to compensate. Increasing J is consuming more transmission time, so achieving the desired rate \mathcal{R} requires that more information be conveyed during that transmission time by increasing M . Similarly, reducing δ reduces the transmission time, requiring that the remaining transmission time be used more efficiently by increasing the "information density" of the transmission time actually in use, again by increasing M .

The duty cycle is determined by how successive codewords are positioned in time. For example, δ is different in Figures 4.2 and 4.3. The only significant parameter of a scheme for transmitting codewords sequentially or interleaving them, or some combination, is δ , which affects the information rate \mathcal{R} by the factor δ in (4.4). Driving δ to zero can be accomplished, for example, by adding a "blank" interval of arbitrary length between transmitted codewords.

Average power

In terms of the parameters of the channel code, the average power is

$$\mathcal{P} = \delta \cdot \frac{\mathcal{E}_h}{T}. \quad (4.5)$$

When the energy of each constituent bundle is \mathcal{E}_h , each codeword requires a total energy of $J \mathcal{E}_h$. Since the cumulative transmission time is $J T$, the power during the codeword transmission is $J \mathcal{E}_h$ divided by $J T$. This would equal the average power if codewords were being transmitted with a 100% duty cycle. The actual average power is reduced by a factor of δ .

The energy per bit \mathfrak{E}_b of this channel code is

$$\mathfrak{E}_b = \frac{J \mathcal{E}_h}{\log_2 M} = \frac{\delta \mathcal{E}_h}{\mathcal{R} T} \quad \text{or} \quad \zeta_b = \frac{\delta}{\mathcal{R} T} \cdot \zeta_s, \quad (4.6)$$

where ζ_b is the energy contrast ratio per bit defined in (2.17) and ζ_s is the energy contrast ratio per energy bundle defined in (2.16).

Now we can understand the reason that $\delta \rightarrow 0$ is necessary to approach the fundamental limit. When operating near the fundamental limit, $\zeta_b \approx \log 2$ is approximately fixed. Holding ζ_b , \mathcal{R} , and T fixed, from (4.6) we have that $\zeta_s \propto 1/\delta$. The duty cycle δ is a means of controlling ζ_s , and thus controlling the reliability of the decision on the presence or absence of each individual energy bundle. A minimum value of ζ_s is required to make a reliable decision on the presence or absence of an energy bundle at each candidate location. By choosing δ appropriately, we can insure that ζ_s is sufficiently large. In fact, as $\delta \rightarrow 0$ it happens that $\mathcal{E}_h \rightarrow \infty$, which is precisely how the code achieves an error probability $P_E \rightarrow 0$. Putting it another way, at a constant power \mathcal{P} , reducing the duty cycle δ allows the energy in each bundle to increase, and the channel code is able to do this while holding the information rate \mathcal{R} fixed by increasing M . Thus, the code has effectively traded increased M (and bandwidth B_{total}) for increased ζ_s so as to overwhelm the noise and scintillation with a very large amount of energy in each energy bundle. As M increases and δ decreases, energy bundles become more and more sparse in both frequency and in time, and hence each bundle can have a larger energy \mathcal{E}_h while maintaining constant average power \mathcal{P} .

In effect a lower duty cycle δ is used to “punch through” the scintillation by jacking up the energy in each bundle, even as the number of bundles is reduced to compensate for this and keep the average power fixed. This is an important lesson to remember in designing practical channel codes for the interstellar channel, as is undertaken in Chapter 5. Increasing the energy per bundle by reducing the duty cycle is also a technique that makes signals easier to discover, as discussed in Chapter 6.

4.3.3 Receiver processing for time diversity

The receiver makes productive use of time diversity by averaging the received energy over time, thus averaging the variations in scintillation and yielding a more reliable indication of whether

an energy bundle is present or not. In particular, assume that there are $M \cdot J$ matched filters, one matched to each candidate location. Let the complex-valued sampled outputs of these filters be $\{Z_{k,m}, 1 \leq k \leq J, 1 \leq m \leq M\}$, where the k index refers to different times and the m index refers to different frequencies. If the actual energy bundle is located at frequency $m = n$,

$$Z_{k,m} = \begin{cases} \sqrt{\mathcal{E}_h} S_{k,n} + M_{k,n}, & m = n \\ M_{k,m}, & 1 \leq m \leq M-1, m \neq n. \end{cases} \quad (4.7)$$

where $S_{k,m}$ is a complex-valued random scintillation and $M_{k,m}$ is a complex-valued additive noise. By assumption, the $\{S_{k,m}, 1 \leq k \leq J, 1 \leq m \leq M\}$ and $\{M_{k,m}, 1 \leq k \leq J, 1 \leq m \leq M\}$ are Gaussian and mutually independent. The receiver can average over the J energy estimates formed by the matched filter outputs at each index m , forming M decision variables

$$Q_m = \frac{1}{J} \sum_{k=1}^J |Z_{k,m}|^2, \quad 1 \leq m \leq M. \quad (4.8)$$

The decision algorithm processes $\{Q_m, 1 \leq m \leq M\}$ to choose a value of m as the location of the single energy bundle.

4.3.4 The result

It is shown in Appendix D.2 that when (4.3) is satisfied (and hence (4.1) is satisfied), the bit error probability $P_E \rightarrow 0$ as $J \rightarrow \infty$ and $\delta \rightarrow 0$. The proof assumes that the receiver has precise knowledge of the noise power spectral density N_0 , the energy per bundle \mathcal{E}_h , and the scintillation variance σ_s^2 , and uses a threshold λ applied to the $\{Q_m, 1 \leq m \leq M\}$ to choose a value of m . On the other hand, the receiver needs no knowledge of the scintillation S_k (including the current flux $\mathcal{F}_k = |S_k|^2$) or noise M_k .

The proof in Appendix D.2 applies equally to the AWGN channel with scintillation and the AWGN channel without scintillation. This implies that the channel code defined here will work equally well for weak scattering (Ricean statistics) and strong scattering (Rayleigh statistics). Communication engineers will undoubtedly find this observation surprising, because we would not normally consider using time diversity in the absence of scintillation, and because phase-coherent detection is an option in the absence of scintillation and this would presumably improve the performance. The reason for this goes back to the observation that $\mathcal{E}_h \rightarrow \infty$, which swamps out the noise in the interest of driving $P_E \rightarrow 0$ and makes the form of detection irrelevant in the limit.

A related observations that is surprising is that scintillation does not affect the fundamental limit. The reason for this becomes evident in the proof of Appendix D.2. The M-ary FSK plus time diversity channel code circumvents scintillation by making energy bundles sparse in both frequency and time. Thus it neatly avoids scintillation almost all of the time, by transmitting nothing. The error probability P_E then becomes dominated by the probability of a false alarm in detection of an energy bundle where none exists, and that probability is not affected by scintillation.

It is also significant that the fundamental limit on power efficiency is *not* affected by the size of the ICH represented by parameters $\{B_c, T_c, K_c\}$, assuming of course that $K_c \gg 1$. Intuitively this is

Characteristics of power-efficient information-bearing signals

By displaying a channel code that asymptotically approaches the fundamental limit on the interstellar channel, some characteristics of such signals are revealed. First of all, the critical and complementary role of each of the five principles of power efficient design of Section (2.5) is revealed.

Stepping back and examining the coding scheme, the most defining characteristic is the sparsity of energy bundles, in both time and frequency. The channel code achieves power efficiency by conserving on the number of energy bundles that are transmitted, beneficially increasing the amount of energy in each bundle. This becomes evident in both the frequency and time dimensions:

- Asymptotically, the bandwidth of each individual codeword becomes unlimited, because $M \rightarrow \infty$. This unlimited bandwidth is characteristic of any channel code that approaches the fundamental limit, because the spectral efficiency must asymptotically approach zero.
- At any given time there is either zero or one energy bundle being transmitted, and taken together with the large bandwidth the density of energy bundles becomes sparse in the frequency dimension.
- The total time duration of each codeword becomes very large as the time diversity grows, or $J \rightarrow \infty$. This growing and unlimited time duration is also characteristic of any channel code that approaches the fundamental limit.
- Asymptotically the fraction of the time that an energy bundle is being transmitted, which is the duty cycle, shrinks as $\delta \rightarrow 0$. Thus, energy bundles become very sparse in the time dimension as well.
- Asymptotically the amount of energy in each bundle grows, also without bound. This is critical to achieving $P_E \rightarrow 0$.

These are only asymptotic properties. Any practical and concrete code will use fixed values of $M < \infty$, $J < \infty$, and $\delta > 0$ and as a result the energy per bundle will also be finite. As a result of these practical choices, there must be a penalty in power efficiency (represented by the energy contrast ratio per bit ξ_b that is actually achieved) relative to the fundamental limit of (4.1). Choosing J larger helps to close that penalty because the law of large numbers, and choosing δ smaller helps to close the penalty because it increases the energy per bundle. In either case the consequence is a larger M and total bandwidth B_{total} . Practical approaches to improving the power efficiency and the consequences are considered in Chapter 5.

because the only impact of the ICH size is the duration of energy bundles T and their bandwidth, neither of which influences the fundamental limit on power efficiency.

Remarkably, a simple channel code has been found that approaches the fundamental limit asymptotically as its complexity (as measured by the $M \cdot J$ locations in each codeword) grows without bound. A constrained-complexity version of this same channel code (with finite M and J) is a good candidate for practical application to the interstellar channel, and this is explored further in Chapter 5.

4.3.5 Argument for uniqueness of this channel code

Basing a practical channel code on one that is capable of approaching the fundamental limit on power efficiency is attractive. Not only can high power efficiency be achieved this way, but it potentially also provides an indirect window into the thought processes of a transmitter designer who follows this same approach. An important question, however, is the uniqueness of such a channel code. There is no mathematical basis for claiming uniqueness. As an example of this, we need look no farther than spectrally efficient design, where there are two distinct (and very different) classes of codes that have been shown to approach the Shannon limit, turbo codes [20] and low-density parity check codes [21].

The relative simplicity of power-efficient design is a significant help here. That we are able to so directly and easily find a code with the desired properties, based on simple intuition no less, is encouraging. While we could never make a mathematical argument for the uniqueness of this solution, we can make a logical argument. The reader will have to judge how compelling this argument is, and of course the challenge goes out to readers to identify a different but equally simple channel code that also possesses the asymptotic property. We have tried and failed.

First, our code is structured around the energy bundle. All known digital communication systems use a transmitted signal that is similarly structured about the “modulation” of some continuous-time analog waveform $h(t)$. The first specific characteristic of the energy bundle idea, as opposed to the most general use of modulation, is that there is no attempt to embed information in the phase, only the magnitude. This is necessary because of the intrinsically unstable phase due to scintillation, where natural phenomena and motion need modify the effective distance by a mere wavelength (out of multiple light years) before the phase becomes randomized. The second specific characteristic is the on-off nature of the magnitude. A couple of arguments can be made for this. One is Occam’s razor, since two levels is surely the simplest choice, and it is sufficient to achieve the asymptotic property. The other argument is the inherent power inefficiency in using more than two levels. At least if those levels are uniformly spaced for fixed noise immunity, the energy increases more rapidly than the increase in information conveyed. The additional ICH constraints on time duration and bandwidth for an energy bundle are necessary to achieve the maximum power efficiency as shown later in Section 4.4.2.

It is notable that the crucial discovery phase can be based on the detection of individual energy bundles. Thus from the perspective of discovery the only characteristic of the channel code that matters is its reliance on energy bundles, and an assumption that each bundle has sufficient energy to overwhelm the noise during favorable scintillation conditions. Other features of the channel code can be inferred following discovery from observation of the time-frequency pattern of detected energy bundles.

Second, our code is structured around the idea of using the location of an energy bundle in time or frequency to encode multiple bits of information. An arbitrary amount of information (specifically $\log_2 M$ bits) can be embedded in using one of M alternative locations. We know that there could be more energy-efficient mechanism for encoding information (this one can approach the fundamental limit, after all), and finding a functionally simpler approach seems out of the ques-

tion. For example, if we transmit $L > 1$ energy bundles in M locations, then it is easy to show that the power efficiency is monotonically decreasing in L .

Third, our code specifically uses frequency as the locator (frequency-shift keying). Here there is clearly a viable competitor, which is using M locations in time (this is pulse-position modulation). By using frequency as a locator, there is no need to change the time duration or bandwidth of each energy bundle as the fundamental limit is approached, or in other words the limited frequency coherence property of the ICH need never be violated. Consuming bandwidth is a necessary element of power efficiency, war using time as the locator would necessarily increase the total bandwidth B_{total} by requiring the bandwidth $B = B_{\text{total}}$ of individual bundles to expand, but this is incompatible with other impairments on the interstellar channel since these bundles would eventually violate the limits on ICH frequency coherence.

Countering the effects of scintillation is a challenge where there is greater flexibility. At the expense of consuming even more bandwidth there is the option to use frequency diversity rather than time diversity. There may also be some utility in using more than one level for the redundant energy bundles, and in fact we will see an example of that in Chapter 6 in the interest of improving discovery reliability. There is also the option explored in Chapter 5 of relaxing our reliability objective and adopting a simpler outage strategy to deal with scintillation. This approach trades simplicity for periods of information loss during periods of low received signal flux.

4.4 Fundamental limit for the interstellar channel

To summarize the results thus far, (4.1) quantifies the greatest power efficiency that can be obtained on the AWGN channel without scintillation, and absent a bandwidth constraint. This is a straightforward consequence of Shannon's channel capacity formula for that channel, as shown in Section 2.4.3. In addition, a concrete channel code based on M-ary FSK and time diversity was shown in Section 4.3 to asymptotically approach the fundamental limit of (4.1). This was established in the absence of any side information available to the receiver as to the state of the received signal flux. This channel code was based on energy bundles falling in the ICH, and therefore is compatible with the interstellar channel.

Together, these results suggest (but do not prove) that the fundamental limit on the power efficiency that can be obtained on the interstellar channel is given by (4.1). Why are we not quite there yet? All that has been shown thus far is that scintillation and the lack of knowledge of the scintillation state in the receiver do not *decrease* the attainable power efficiency. But is it possible that scintillation could *increase* the available power efficiency. The same question applies to all those other impairments described in Chapter 8. They cannot decrease the available power efficiency, since a channel code based on the ICH is able to asymptotically approach (4.1), but is it possible that they could relax the fundamental limit on power efficiency?

The answer is that (4.1) is the fundamental limit on power efficiency for the interstellar channel. To establish this, we now tie up these two loose ends. Readers interested primarily in interstellar communication can safely skip to Chapter 5, as the following does not offer significant new

insights on how to communicate more reliably.

4.4.1 Lower bound on power efficiency

To show that power efficiency cannot be improved by scintillation, it suffices to find a lower bound on power efficiency, and show that this lower bound equals the fundamental limit of (4.1). The lower bound we use is based on the strong assumption that the receiver has complete knowledge of the current state of the scintillation. This added knowledge can only relax the fundamental limit, allowing reliable communication at equal or higher power efficiencies, since the receiver always has the option of ignoring this side information.

To derive this result, a discrete-time channel model that characterizes a communication system constrained to transmit a sequence of energy bundles conforming to the ICH is defined. Then a fundamental limit for this channel assuming receiver knowledge of the state of the scintillation is determined, and shown to equal (4.1).

Discrete-time channel model

The basic idea behind structuring the signal around the ICH is to transmit a sequence of energy bundles, the only constraint being that these bundles do not overlap in time or frequency. Since the total bandwidth B_{total} is considered to be unconstrained, we don't have to worry about the details of where these bundles are placed. These locations have no impact on the power efficiency \mathfrak{P} that can be achieved nor on the derivation of the results to follow.

A channel model appropriate for studying fundamental limits requires a generalization of the input-output model of Figure 3.1. That model is linear in $\sqrt{\mathcal{E}_h}$, so that the sequence of root-energies can be replaced by a general discrete-time complex-valued input signal X_k , resulting in a relationship between input sequence $\{X_k\}$ and sampled matched filter output sequence $\{Z_k\}$,

$$Z_k = S_k \cdot X_k + M_k. \quad (4.9)$$

For the channel code considered in Section 4.3, $\{X_k\}$ is always chosen to be drawn from the alphabet $X_k \in \{\sqrt{\mathcal{E}_h}, 0\}$, but for purposes of determining fundamental limits it is important not to constrain the values of $\{X_k\}$ in any other manner than average power. The index k does not necessarily represent time only, as energy bundles may be transmitted at different frequencies as well as times.

The total rate at which energy bundles are transmitted and received is assumed to be $F \text{ sec}^{-1}$. Since the bandwidth B_{total} is unconstrained, the value of F can be chosen freely. The average power constraint will be met if

$$F \cdot \sigma_X^2 \leq \mathcal{P}, \quad (4.10)$$

where $\sigma_X^2 = \mathbb{E}[|X_k|^2]$. Note that there is a tradeoff between F and σ_X , and in particular as $F \rightarrow \infty$ we must have $\sigma_X \rightarrow 0$.

Side information

For the channel model of (4.9), in order to obtain a lower bound assume that the receiver knows the scintillation sequence $\{S_k\}$. This strong assumption can only maintain or improve the attainable power efficiency since the receiver has the option of ignoring this knowledge. The first action the receiver should perform is to equalize the phase of the scintillation multiplier by forming the sequence

$$Z_k \cdot \frac{S_k^*}{|S_k|} = \sqrt{\mathcal{F}_k} \cdot X_k + M_k \cdot \frac{S_k^*}{|S_k|}. \quad (4.11)$$

This processing is reversible, and thus cannot affect the fundamental limit. The channel model can thus be replaced by

$$\tilde{Z}_k = \sqrt{\mathcal{F}_k} \cdot X_k + \tilde{M}_k, \quad (4.12)$$

where $\{\tilde{Z}_k\}$ and $\{\tilde{M}_k\}$ are phase-shifted versions of $\{Z_k\}$ and $\{M_k\}$. In particular, the distribution of noise $\{\tilde{M}_k\}$ is identical to the original noise $\{M_k\}$. Of course the flux $\mathcal{F}_k = |S_k|^2$ is a real-valued quantity, and is assumed to be known to the receiver but not the transmitter.

Ergotic capacity

Suppose for a moment that $\mathcal{F}_k = \mathcal{F}$ is constant. Then the capacity of a discrete-time channel with additive complex-valued zero-mean Gaussian noise is well known [45, Section 4.2.3],

$$\mathcal{R} \leq \mathcal{C} = F \cdot \log_2 \left(1 + \frac{\mathcal{F} \sigma_X^2}{N_0} \right). \quad (4.13)$$

This is a discrete-time version of the AWGN channel capacity (2.18). The ergotic capacity merely averages the capacity over the flux,

$$\mathcal{R} \leq \mathcal{C} = \mathbb{E} \left[F \cdot \log_2 \left(1 + \frac{\mathcal{F} \sigma_X^2}{N_0} \right) \right] \quad (4.14)$$

where the expectation is over the random ensemble for \mathcal{F} .

The assumptions behind the ergotic capacity can be summarized as follows [16, Sec. 5.4.5]. For any fixed value of flux \mathcal{F} , (4.13) applies. This "instantaneous" capacity is increased relative to the noise-only case if $\mathcal{F} > 1$ or decreased if $\mathcal{F} < 1$. As the actual flux \mathcal{F}_k changes with time, this "instantaneous" capacity also changes, and (4.14) is the average of these instantaneous capacities.² The transmitter cannot tailor the channel code at different times according to the instantaneous conditions. The transmitter can, however, use a codebook that spans a time duration that is very large relative to the known time scale of the fluctuations in \mathcal{F} , and also tailor the code to the known distribution of the scintillation. In this case each code word statistically experiences the full range of \mathcal{F}_k for which it is designed. Thus, predicated on the assumption that the receiver knows $\{S_k\}$, the ergotic capacity is the fundamental limit on the rate \mathcal{R} that can be achieved.

² The term "ergotic" refers to an equality between a time average and ensemble average. This definition of capacity assumes that the time-average capacity is equal to the ensemble-average capacity, which will be valid for a wide range of conditions.

Power efficiency with side information

Expressing the ergodic capacity of (4.14) in terms of the average power \mathcal{P} from (4.10),

$$\mathcal{R} \leq \mathcal{C} = \mathbb{E} \left[F \cdot \log_2 \left(1 + \frac{\mathcal{F} \mathcal{P}}{F N_0} \right) \right]. \quad (4.15)$$

The argument of $\mathbb{E}[\cdot]$ is monotonically increasing in rate F (for every value of \mathcal{F}), so by taking advantage of unconstrained bandwidth and letting $F \rightarrow \infty$ (the unconstrained bandwidth case) the maximum information rate is achieved. This maximum rate is

$$\mathcal{R} \leq \mathcal{C} \xrightarrow{F \rightarrow \infty} \mathbb{E} \left[\frac{\mathcal{F} \mathcal{P}}{N_0 \log 2} \right] = \frac{\mathcal{P} \sigma_s^2}{N_0 \log 2}. \quad (4.16)$$

This is equivalent to (4.1), establishing that knowledge of the scintillation by the receiver does not increase the achievable power efficiency or, in other words, relax the fundamental limit.

4.4.2 Effect of other impairments on power efficiency

In fact, this result is stronger than it appears because any transmitter design that violates ICH integrity introduces additional ISM and motion impairments into the received signal, and we would expect that dealing with these would reduce (and could not increase) the power efficiency. A reasonable hypothesis is that a design based on the ICH structure can achieve greater power efficiency than any design that deliberately violates the integrity of the ICH.

To investigate this further, assume that the transmitter uses a unit-energy waveform $h(t)$ as a carrier for an energy bundle and the receiver implements a filter matched to $h(t)$, but the actual received waveform has been changed to $S \cdot g(t)$ by the effects of interstellar impairments including a scintillation multiplier S . Then the magnitude of the sampled matched filter output Z can be bounded by the Schwartz inequality,

$$|Z|^2 = \left| \int_0^T S \cdot g(t) \cdot h^*(t) dt \right|^2 \leq \int_0^T |S \cdot g(t)|^2 dt = \mathcal{F} \cdot \int_0^T |g(t)|^2 dt, \quad (4.17)$$

with equality if and only if $g(t) = z \cdot h(t)$ for some complex-valued constant $z \neq 0$. On the other hand, if there is no interstellar impairment other than scintillation, or in other words $h(t)$ falls in the ICH, then the same output is $|Z|^2 = \mathcal{F}$. Thus, the only way that non-scintillation impairments could increase the signal level, and hence improve on the receiver sensitivity, is if they increase the signal energy, or

$$1 < \int_0^T |g(t)|^2 dt. \quad (4.18)$$

While we know that scintillation can increase signal energy temporarily (although not on average), an examination of the other impairments in Chapter 8 reveals none that are capable of increasing the signal energy. For example, plasma dispersion is an all-pass (phase-only) filtering function, and thus neither reduces nor increases the total signal energy.

As a proof of the fundamental limit on power efficiency for the interstellar channel, this argument does have one shortcoming. We have shown that when communication is based on the energy bundle, giving us the option of avoiding all interstellar impairments save noise and scintillation, then it has been shown that the best power efficiency results when the energy bundle adheres to the ICH. This does not rule out the possibility that deliberately violating the ICH constraints would allow even higher power efficiency than the fundamental limit of (4.1) by using some other approach than the energy bundle. Since none of the ICH-excluded impairments would permit more energy to arrive at the receiver, it is our judgment that this could not be the case. Under these conditions generally impairments result in reduced (rather than increased) power efficiency due to the enhancement of noise and increase in false alarm probability resulting from processing to encounter impairments. This possibility should, however, be explored with greater mathematical rigor before ruling it out permanently.

4.5 History and further reading

The publication of Shannon's channel capacity theorem in 1948 resulted in a flurry of activity pursuing concrete channel codes that could approach the fundamental limit. The easier unconstrained bandwidth case was addressed first. Fano showed in 1961 that M-ary FSK and PPM both approach fundamental limits on power efficiency on the AWGN channel as $M \rightarrow \infty$ and using phase-coherent detection [36]. These are special cases of a more general class of *orthogonal codes* that all have this nice property. For spectrally efficient design, where B_{total} is constrained, fundamental limits were approached by very complex turbo codes in 1993 [20]. Later it was shown that low-density parity check codes (first described by Gallager in 1960) can also approach the fundamental limit [21].

Because scintillation (fading) is an important impairment in terrestrial radio communications, there is an extensive literature. There is no single definition of capacity, because it is dependent on the assumptions about knowledge of the current scintillation conditions at the transmitter and at the receiver [46]. For an intuitive explanation of these alternative sets of assumptions and their consequences, [16, Sec. 5.4] is recommended.

With the exception of the use of the ICH and the role of interstellar impairments more generally, most of the results of this chapter can be traced to the work of R.S. Kennedy in 1969 [19], who determined the fundamental limit on power efficiency for a continuous-time Rayleigh fading channel in the absence of any such knowledge in the receiver. For a more readily available and concise derivation see [47, Section II], and Kennedy's results are also summarized in Gallager's 1968 textbook on information theory [2, Section 8.6].

4.6 Summary

The fundamental limit on power efficiency for the interstellar channel has been determined for unconstrained bandwidth and in the absence of any side information about the state of the scin-

tillation in the receiver. A concrete channel coding based on M-ary FSK combined with time diversity has been shown capable of approaching the fundamental limit asymptotically, and will serve as the basis for a practical constrained-complexity design in Chapter 5. That channel coding makes use of all five of the principles of power-efficient design described in Section 2.5, and concretely illustrates the necessary and complementary role of each of those principles in achieving high power efficiency. The fundamental limit is not relaxed if the receiver possesses side information about the scintillation. To obtain the maximum possible power efficiency, bandwidth must be unconstrained and allowed to increase arbitrarily, so very poor spectral efficiency is a necessary feature of any interstellar communication system operating near the power efficiency limit.

The fundamental limit depends on the two physical parameters $\{N_0, \sigma_s^2\}$ alone, and is not affected by the ICH parameters $\{T_c, B_c\}$ or the carrier frequency f_c . Its numerical value is not affected by the presence or absence of scintillation, since under all conditions of scattering (both weak and strong) the phenomenon is lossless and thus $\sigma_s^2 = 1$. It is also shown that a signal design structured about the interstellar coherence hole (ICH) developed in Chapter 3 possesses the same fundamental limit, implying that nothing need be lost in power efficiency by constraining the design in this way. Indeed any design using signals violating the time duration and bandwidth constraints of the ICH will necessarily sacrifice some signal level at the matched filter output, and thus operate at a reduced power efficiency for equivalent reliability.

Perhaps the most significant outcome of this chapter is a fundamental limit that constrains all civilizations, no matter how experienced or advanced they may be. In demonstrating a channel coding that asymptotically approaches this limit, a great deal of insight into how both we and other civilizations might approach the fundamental limit is developed. This should help us anticipate the types of signals to expect, and thereby aid in the discovery of such signals in an uncoordinated environment.

Chapter 5

Communication

Having established the fundamental limit on power efficiency in Chapter 4, the question is how close this limit can be approached with by a concrete design. We have seen that actually approaching the limit requires a channel code with codewords that grow with time duration and expand in bandwidth, and an energy per bundle that grows, all without bounds. In contrast any concrete channel code must necessarily have a finite duration and finite bandwidth, a finite energy in each bundle, and a probability of error $P_E > 0$. Putting in this “complexity” constraint will limit the available power efficiency to something less than permitted by the fundamental limit. The one aspect of the channel code of Chapter 4 that carries over without modification is the restriction of energy bundles to the interstellar coherence hole (ICH).

The question addressed in this chapter is how close to the fundamental limit we can reach with such a parameterization while staying in the realm of what might be considered practical. This is considered for the M-ary FSK channel code with time diversity considered in Chapter 4, but restricting M and J to be fixed and finite values rather than allowing them to grow without bound. A simpler approach based on M-ary FSK (to counter noise) combined with an outage approach (in which information is lost during periods of low received signal flux) is then considered and compared. The outage approach looks attractive for the interstellar channel.

According to the classification of Figure 5.1 proposed in [3], this design only addresses the signal layer, omitting the reliability and message layers. The signal layer is intrinsically unreliable (due to $P_E > 0$) due to noise and scintillation, and thus the design of the reliability and message layers will be affected by the results described here. In particular, the outage strategy changes the reliability layer requirements profoundly.

5.1 Diversity strategy

Diversity combining is one of the principles of power-efficient design of Section 2.5. The idea behind time diversity is to transmit each energy bundle multiple times with a time spacing large relative to the coherence time of the channel, or a frequency spacing large relative to the coherence

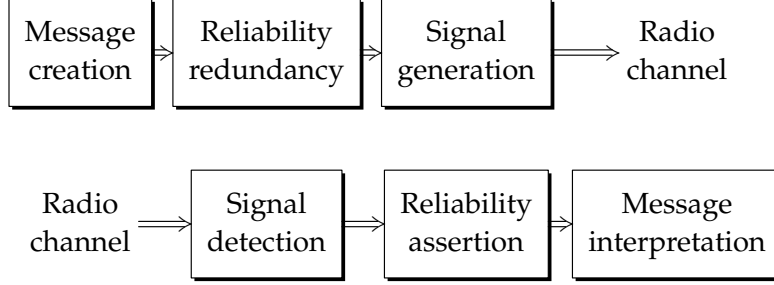


Figure 5.1: Three distinct layers of functionality in the interstellar communication of messages [3]. These are the signal layer (including generation and detection), the reliability layer (including redundancy and assertion), and the message layer (including creation and interpretation). Our concrete design in this chapter considers only the signal layer, but demonstrates that the reliability layer must deal with not only random dispersed errors but also, in the case of an outage strategy, substantial periods with no recovered data due to low received signal flux.

bandwidth of the channel. At the receiver, diversity combining averages the signal energy from these redundant versions of the bundle to form an estimate that asymptotically averages out the received flux and thus allows reliable extraction of the information in spite of scintillation. To make it practical, finite values for M and J are used, creating a penalty in the achieved energy contrast ratio per bit ζ_b relative to the fundamental limit. Our primary interest is in the quantifying this penalty, which also depends on the objective for error probability P_E .

5.1.1 Parameters and tradeoffs

The channel code of Section 4.3.1 can asymptotically approach the fundamental limit on power efficiency on the interstellar channel, so our concrete design uses a constrained-complexity version of this code. As illustrated in Figure 4.1, one codeword consists of an energy bundle at one frequency out of M and is repeated J times to counter the time-varying effects of scintillation. To convey a stream of information, codewords are merged by some combination of interleaving (as illustrated in Figure 4.2) or sequential transmission (Figure 4.3).

The parameters of the channel code are listed in Table 5.1, using the same notation as Section 4.3.1. The duty factor δ is now a secondary parameter, determined by the choice of $\{\mathcal{R}, T, J, M\}$. However, not all combinations of these parameters are feasible, corresponding to the constraint $0 < \delta \leq 1$. Although any \mathcal{R} can be accommodated in principle by making M sufficiently large, for given values of $\{\mathcal{R}, T, M\}$, the available time diversity is limited by

$$J \leq \frac{\log_2 M}{\mathcal{R} T}. \quad (5.1)$$

This bound arises because there is limited transmission time available for redundant energy bundles. Choosing a larger M has the beneficial effect of increasing the available transmission time, thus allowing a larger J .

Table 5.1: A list of parameters of a constrained-complexity channel code based on FSK and time diversity. The design parameters describe all relevant choices. The secondary parameters describe the consequences of those choices in determining the information rate and power efficiency.

Category	Parameter	Description
Design parameters	J	Number of time repetitions of each energy bundle
	M	Number of frequency offsets for energy bundles Each codeword conveys $\log_2 M$ bits of information The minimum is $M \geq 2^{J\mathcal{R}}$
	$\mathcal{R} T$	Normalized information rate $\mathcal{R} T = 1$ equals the rate of 100% duty factor on-off keying (OOK)
	\mathcal{E}_h	Received energy in each bundle
Physical parameters	N_0	Power spectral density of noise
	σ_s^2	Average of the received signal flux \mathcal{F} $\sigma_s^2 = 1$ based on the physics of scattering
Secondary parameter	δ	Duty factor Faction of time an energy bundle is transmitted
Reliability	P_E	Probability of error in each decoded bit

On-off keying (OOK) with 100% duty factor has rate $\mathcal{R} = 1/T$, so $\mathcal{R} T = 1$ corresponds to this baseline OOK case. When $\mathcal{R} T < 1$, this is equivalent in information rate to OOK with less than 100% duty factor, and $\mathcal{R} T > 1$ has a higher information rate than can be achieved by single-carrier OOK (this is possible because M can be as large as we choose). It appears that a smaller information rate \mathcal{R} is generally helpful, because from (5.1) this allows a larger J for a given M . However, it will be now be shown that choosing a larger J is not always beneficial.

5.1.2 Reliability

In Section 4.3.1 it was established that the bit error probability $P_E \rightarrow 0$ is possible using this channel code at power efficiency \mathfrak{P} less than the fundamental limit (energy per bit \mathfrak{E}_b above the fundamental limit). A threshold detection algorithm in the context of M-ary FSK in combination with time diversity was used (and is necessary) to prove this result. The threshold algorithm required precise knowledge of the parameters $\{\mathcal{E}_h, N_0\}$. For practical application, however, a *maximum energy* detection algorithm is more desirable. This algorithm chooses the value of m meeting the criterion

$$\max_{1 \leq m \leq M} Q_m \quad (5.2)$$

as the location of an energy bundle, where Q_m is the decision variable given by (4.8). A desirable characteristic of this maximum algorithm, which is actually a feature of M-ary FSK as a channel coding technique, is that knowledge of $\{\mathcal{E}_h, N_0\}$ is not needed. We know that an energy bundle is present at exactly one frequency, and the only issue is to decide which one. The maximum energy algorithm simply chooses the location where the estimated energy is highest, assuming that this "excess" energy is due to the presence of an energy bundle.

When M and J are finite we must have $P_E > 0$. A tight upper bound on the error probability P_E for the maximum algorithm is determined in Appendix F.3,

$$P_E \leq \frac{M}{2} \cdot \left(\frac{4(1 + \xi_s)}{(2 + \xi_s)^2} \right)^J. \quad (5.3)$$

Note that P_E depends only on the energy contrast ratio ξ_s , and not on the individual parameters $\{\mathcal{E}_h, N_0\}$. The maximum algorithm adjusts automatically to wherever ξ_s may be, always yielding the most reliable detection (lowest P_E) dictated by whatever conditions it encounters.

In Figure 2.10 the tradeoff between the energy contrast ratio per bit ξ_b and P_E was illustrated by plotting (5.3) for two cases, $M = 2$ and $M = 2^{20} \approx 10^6$. For the second case $J = 49$ is chosen because that choice minimizes ξ_b , as will be shown shortly. This figure illustrates that there is no single value for the penalty in average power relative to the fundamental limit, but rather this penalty depends on our objective for P_E . In numerical examples we choose $P_E = 10^{-4}$, or an average of one error out of every 10,000 bits.

5.1.3 Total bandwidth

In the following numerical comparisons, the value $M = 2^{20} \approx 10^6$ is assumed. This corresponds to a total bandwidth $B_{\text{total}} = 1$ MHz if the energy bundle bandwidth is $B = 1$ Hz, or correspondingly greater B_{total} for larger values of B . For comparison purposes, an M and B_{total} three orders of magnitude smaller and larger are also calculated.

One issue that should be kept in mind is the frequency stability of the received transmission. If there is any frequency drift due to acceleration, then this will interfere with the accurate recovery of the information. Thus, this small B and large B_{total} assumes that both transmitter and receiver have corrected for their respective acceleration as discussed in Section 3.3.

5.1.4 Total energy hypothesis

One question is how the energy per bundle \mathcal{E}_h is affected by the transmission of J bundles in time diversity. This question is best addressed by fixing the error probability P_E and then varying J for a fixed value of M . A *total energy hypothesis* states that the reliability as measured by P_E is approximately fixed if the total energy $J \mathcal{E}_h$ (or equivalently $J \xi_s$) is held fixed as J increases. As shown in Figure 5.2, ξ_s does decrease steadily as time diversity J increases, but the total energy

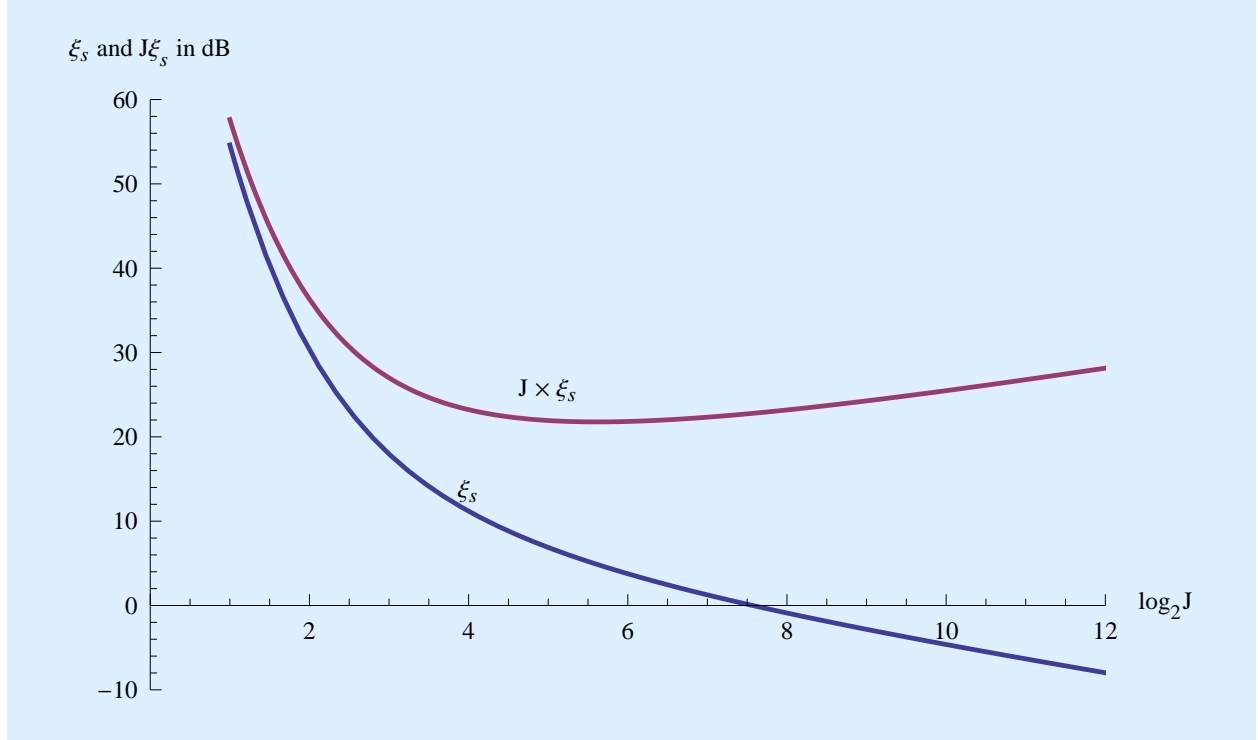


Figure 5.2: A plot of the energy contrast ratio ξ_s in dB for each energy bundle required to achieve a reliability $P_E = 10^{-4}$ vs. the time diversity J . The number of frequencies is kept fixed at $M = 2^{20}$. There is a steady decrease in the required ξ_s as a benefit of the law of large numbers. The total energy $J\xi_s$ in all bundles remains fairly constant, confirming the total energy hypothesis.

$J\xi_s$ does remain relatively fixed.¹ There is a minimum value of total energy at $J \approx 2^5$, and beyond that there is a slow increase in the total energy. Subsequent calculations will reveal that J should not be chosen too large, so most we expect to operate near this minimum.

Based on the total energy hypothesis, $\xi_s \approx 1/J$ maintains approximately fixed error probability P_E as J increases. Time diversity allows the energy per individual bundle to decrease, and it also desirably decreases the peak transmitted power by spreading the total energy of each codeword over a greater total transmission time JT . On the other hand, as discussed in Chapter 6, it also makes discovery more difficult because the detection of each individual energy bundle less reliable. It is shown there that a small adjustment to the channel code can mitigate this adverse effect at a small penalty in power efficiency.

5.1.5 Power efficiency

To see how the power efficiency \mathfrak{P} is affected by a change in the parameterization of the channel code, it is convenient to work instead with the energy per bit $\mathfrak{E}_b = 1/\mathfrak{P}$ or equivalently the

¹ This is in contrast to the asymptotic results of Section 4.3.1, where $\xi_s \rightarrow \infty$ as the fundamental limit is approached. The difference is that there $M \rightarrow \infty$, and here M is held fixed.

energy contrast ratio per bit ζ_b . This quantity is plotted in Figure 5.3 for three different values of M and as a function of J . The values of M illustrated are $\{2^{10} \approx 10^3, 2^{20} \approx 10^6, 2^{30} \approx 10^9\}$. The total bandwidth B_{total} for these cases depend on the bandwidth B of each energy bundle and the frequency spacing of the bundle locations, which is at least B . The three choices correspond to about one kHz, one MHz, and one GHz for $B = 1$ Hz.

This figure illustrates three different observations:

- Consistent with (5.1), for any value of $\{\mathcal{R}, M\}$ there is a maximum feasible value of J . This maximum value is proportional to $\log_2 M$, or $J \propto \log_2 M$.
- The energy contrast ratio ζ_b does not decrease monotonically with J . There is an optimum value of J that gets us the closest to the fundamental limit, and fortunately (from an implementation perspective) that optimum value is modest in size. The reason for this behavior is a tradeoff between two competing effects. On the one hand, as J increases the receiver's estimate of bundle energy becomes more accurate, and that is reflected in the J exponent in (5.3). On the other hand, as J increases, for fixed M the energy contrast ratio decreases as $\zeta_s \propto 1/J$ for fixed \mathcal{E}_b . This is because there are J energy bundles contributing to the total received energy, and if J is larger there is less energy to allocate to each of those J energy bundles.
- If the optimum value of J is chosen, increasing M is beneficial in getting us closer to the fundamental limit on ζ_b for the optimum choice of J .

The direct coupling between M and J (the latter at the optimum point) is helpful to implicit coordination between transmitter and receiver, because it indicates that for a transmitter intent on reducing its transmitted power one of these variables is dependent on the other. Reflecting that, in the subsequent comparisons we can eliminate the parameter J by substituting its optimum value. That optimum value is shown in Figure 5.4 for a fixed information rate, demonstrating a linear relationship.

Assuming that the transmitter always chooses a value for J that maximizes the power efficiency, the relationship of the achieved energy contrast ratio per bit ζ_b to $\log_2 M$ is illustrated in Figure 5.5 for several information rates \mathcal{R} . The channel code performs well for all rates less than OOK with 100% duty factor ($\mathcal{R} T < 1$) because there is sufficient room for the optimum degree of time diversity J at larger values of $\log_2 M$. However, at information rates higher than OOK, the channel code performs poorly because the constraint on J given by (5.1) is too small to allow the optimum choice of J to be used. There is simply too little transmission time available to achieve the needed time diversity (which consumes transmission time since energy bundles are repeated J times) at higher rates, where we want to transmit codewords more frequently.

The M-ary FSK with time diversity channel code, after the optimizing choice of J , suffers a material penalty relative to the fundamental limit due to the choice of finite values for M and J . At $M = 2^{20}$ the penalty is 10.4 dB (a linear factor in average power of 10.9). The penalty decreases slowly with M , becoming 9.8 dB (a linear factor of 9.5) at $M = 2^{30}$. We expect that the penalty will not approach zero as $M \rightarrow \infty$ for two reasons. One is the use of phase-incoherent detection, and the other is the use of the maximum algorithm of (5.2) as a concession to practical concerns about knowledge of

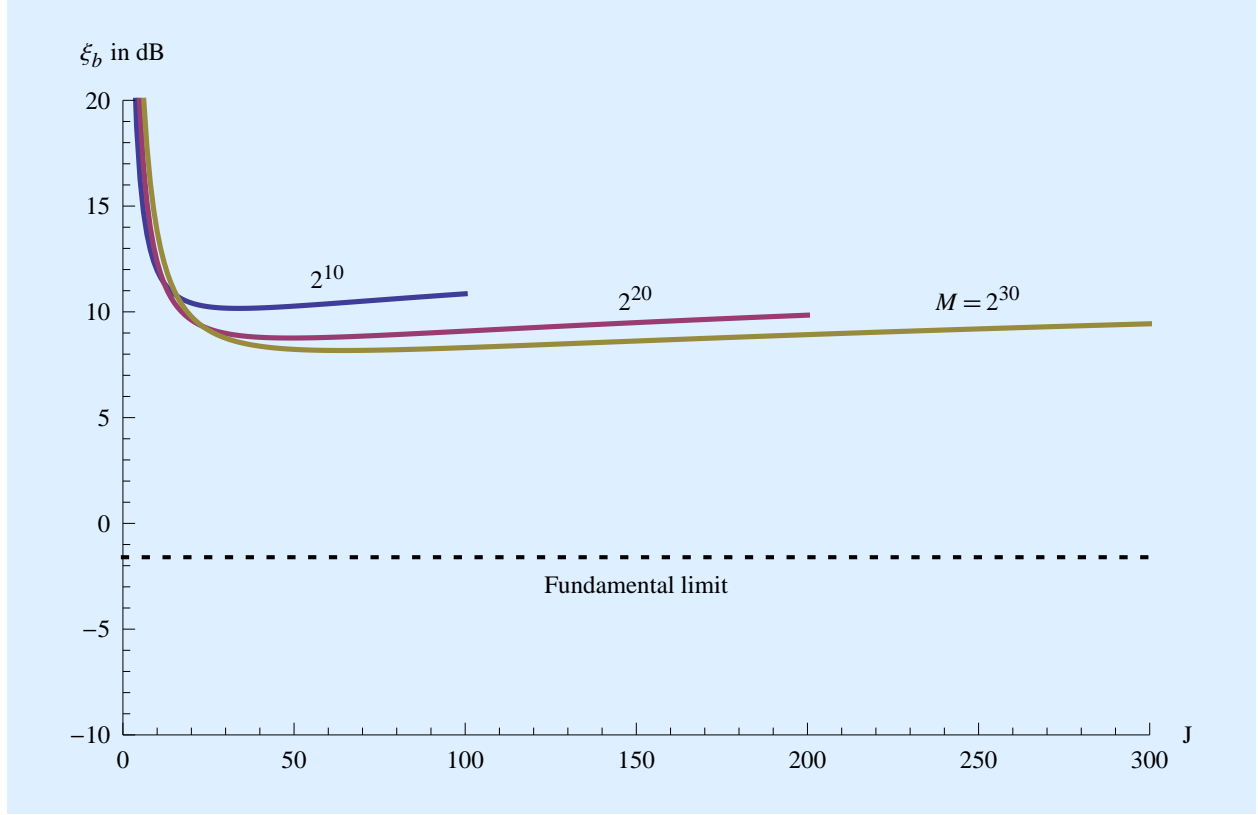


Figure 5.3: The energy contrast ratio ξ_b in dB is plotted against the degree of time diversity J for $\log_2 M = 10, 20$, and 30 . All curves correspond to information rate $\mathcal{R}T = 0.1$, or an information rate equal to 10% of an OOK signal with 100% duty factor, and an error probability $P_E = 10^{-4}$. The range of J is upper bounded by (5.1). The fundamental limit on power efficiency at $\xi_b = -1.6$ dB is shown by the dotted line.

bundle energy \mathcal{E}_h and noise power spectral density N_0 .

5.1.6 Multicarrier modulation

We have seen in Figure 5.5 that a finite-complexity channel code becomes inefficient at information rates higher than OOK with 100% duty cycle. The problem is our attempt to use a single carrier, which at higher rates does not afford sufficient time to transmit our redundant time diversification energy bundles when M is constrained to reasonable values. There is an easy way to circumvent this limitation, and that is to use multiple carriers. A sequence of codewords can be transmitted on each of L carriers, taking care to keep the information rate on each carrier sufficiently low to achieve the best power efficiency, and also taking care to space the carriers far enough apart to avoid frequency overlap. The resulting information rate is increased by a factor of L , and the average power is increased by the same factor of L , so the power efficiency is not affected. This approach is called *multicarrier modulation* MCM [25].

In 1995, S. Shostak anticipated the importance of MCM (although he didn't call it that), motivated

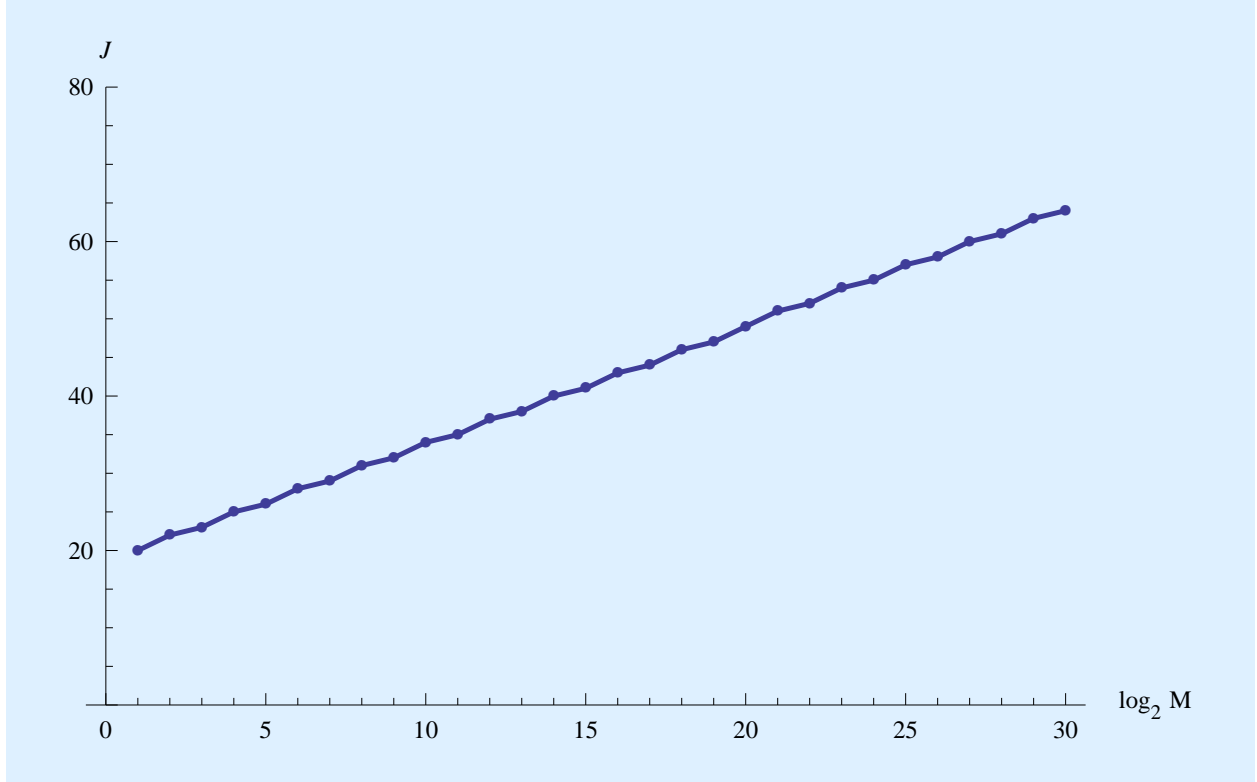


Figure 5.4: The degree of time diversity J that minimizes the energy contrast ratio per bit ξ_b (and hence maximizes the power efficiency) is plotted as a function of $\log_2 M$. The information rate is held fixed at $\mathcal{R} T = 0.1$, and the error probability is held fixed at $P_E = 10^{-4}$

(as here) by its immunity to ISM impairments [24]. Similar to M-ary FSK, MCM is a way to trade additional bandwidth and average power for higher information rate. MCM merely maintains the same power efficiency as the bandwidth expands, whereas M-ary FSK improves the power efficiency. On the other hand, MCM can achieve higher information rates for the same increase in bandwidth, so it is more spectrally efficient. MCM demonstrates one approach to trading higher spectral efficiency for poorer power efficiency. As such, it is widely used in terrestrial wireless systems, where spectral efficiency is usually a dominant consideration.

5.2 Outage strategy

Our choice of a channel code based on M-ary FSK with the addition of time diversity seeks an ambitious goal, which is to maintain consistently reliable communication in spite of scintillation. An alternative *outage strategy* relaxes this goal in the interest of simplifying the channel coding. The approach is to discard any embedded information during outage periods, defined as periods during which the average flux \mathcal{F} is low. In order to declare these outage periods, the receiver must estimate the received signal flux \mathcal{F} by monitoring the estimated energy of energy bundles. The

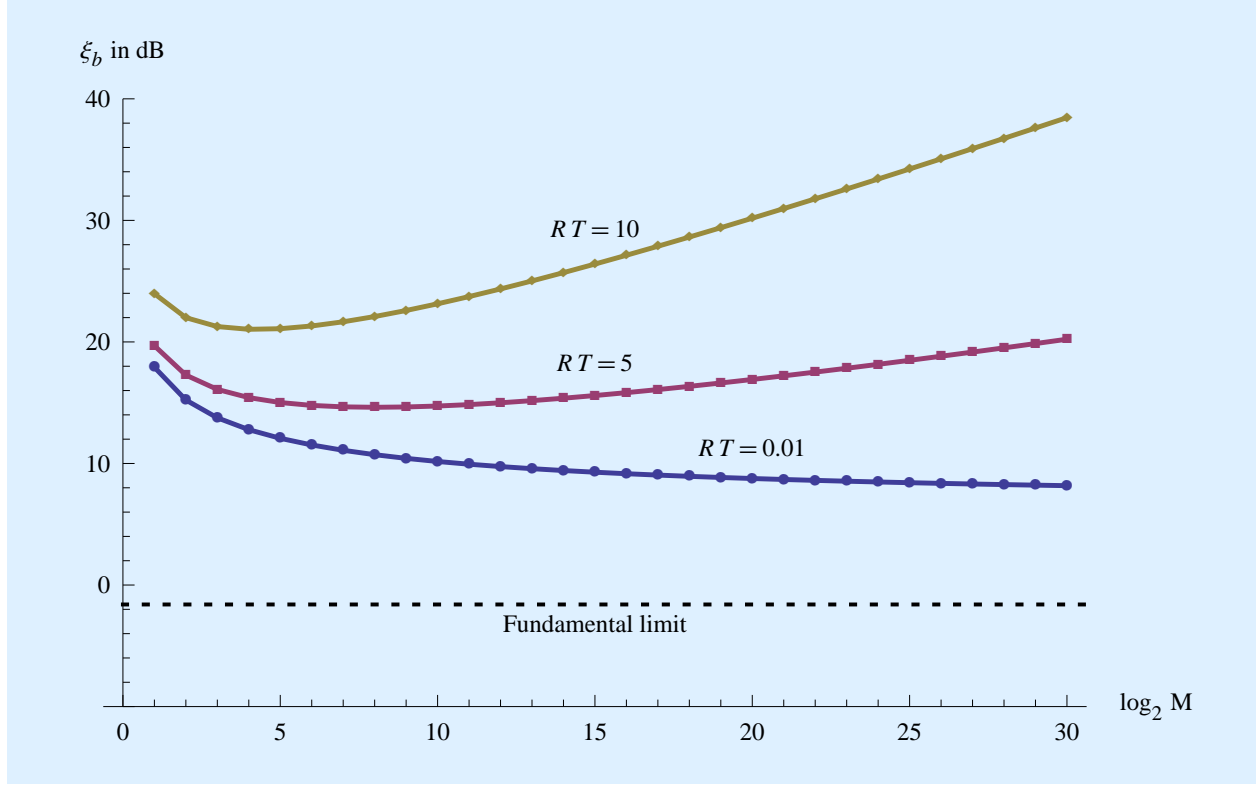


Figure 5.5: A plot of the minimum energy contrast ratio per bit ξ_b that can be achieved when the optimum value of J is used against $\log_2 M$, for three different information rates \mathcal{R} . The error probability is held fixed at $P_E = 10^{-4}$. The case $\mathcal{R}T = 0.01$ is typical of all low rates, where the achievable ξ_b does not depend on \mathcal{R} . The other two cases show that this channel code performs poorly at rates higher than OOK with 100% duty factor ($\mathcal{R}T \gg 1$), the reason being that the degree of time diversity is too constrained by (5.1) to achieve the greatest possible power efficiency for a given value of $\log_2 M$.

resulting P_E is very high averaged over all time, but desirably time is divided into outage periods when all data is lost, and non-outage periods during which $P_E \approx 0$. This provides valuable information to the reliability layer in Figure 5.1 as to what recovered information can be considered reliable what has been discarded.

This outage strategy places a burden on the reliability and message layers of Figure 5.1 to accommodate a substantial loss of information while retaining message integrity. In terrestrial systems this would be dealt with in the reliability layer by combining interleaving with another layer of redundant channel coding. In interstellar communication there is a simpler approach, because typically a message will be transmitted over and over since the transmitter has no idea when that message is being received or the current state of the scintillation. Thus a reasonable way for the receiver to deal with outages is simply to accumulate multiple received copies of the transmitter's intended message, and gradually interpolate missing information caused by random outage intervals as well as random errors occurring during non-outage periods.

Multicarrier modulation

Multicarrier modulation (MCM) is widely used because it is recognized to have a number of advantages other than immunity to dispersion and trading spectral efficiency for power efficiency. If the distinct carrier frequencies deliberately violate frequency coherence, the scintillation experienced by different carriers will be unrelated to one another (this is called *frequency-selective fading*). This observation can be used to improve the reliability for communication as well as discovery, for example by creating data redundancy across different carriers. The relative powers allocated to different carriers can be adjusted to accommodate frequency-dependent phenomena such as a planet's larger atmospheric noise due to water vapor (concentrated at $f_c \gg 15$ GHz). The power allocated to one (and only one) subcarrier can be artificially increased to make discovery easier with only a small power penalty overall. MCM also lends itself to parallelism in transmitter implementation. For example, any collection of subcarrier signals can be transmitted independently of the others using separate RF electronics and antennas, each optimized for its own carrier frequency. A transmitter designer on a limited budget can expand total information rate over time by increasing M , with a capital cost that scales no faster than \mathcal{R} . Both transmit and receive implementations lend themselves to joint subcarrier manipulation at baseband using discrete Fourier transform techniques [25].

5.2.1 Choice of an outage threshold

In an outage strategy, the receiver declares an outage whenever the received signal flux is below a threshold λ_O , or $\mathcal{F} < \lambda_O$. The question is how λ_O should be chosen. A principled way to choose λ_O is to maximize the *effective* power efficiency. Suppose the probability of an outage is P_O . Then the effective rate at which information is recovered is not the transmitted rate \mathcal{R} , but rather $(1 - P_O) \cdot \mathcal{R}$. Then a reasonable definition of effective power efficiency is

$$\mathfrak{P} = \frac{(1 - P_O) \cdot \mathcal{R}}{\mathcal{P}}. \quad (5.4)$$

The $(1 - P_O)$ factor takes into account the reduction in actual recovered information rate due to the loss of all information during outages. \mathcal{R} is the information rate embedded in the information-bearing signal, and \mathcal{P} is the average received power with or without scintillation (which are the same since $\sigma_s^2 = 1$).

For a chosen λ_O and for Rayleigh fading (scintillation due to strong scattering), the outage probability is

$$P_O = \Pr \{ \mathcal{F} < \lambda_O \} = 1 - \exp \left\{ -\frac{\lambda_O}{\sigma_s^2} \right\}. \quad (5.5)$$

During non-outages, the reliability of information recovery still varies widely depending on the actual flux \mathcal{F} . Our criterion for setting λ_O is to insure that $P_E \approx 0$ in the worst case, which is $\mathcal{F} = \lambda_O$. At all other times during non-outages the reliability is even better, and usually *much* better. It is useful to remember that when P_E is calculated for $\mathcal{F} = \lambda_O$, this is not representative of the overall average error probability during non-outages, which is much smaller, nor the overall average error rate which is strongly influenced by outages.

Zeroing in on the case $\mathcal{F} = \lambda_O$, and ignoring the actual variation in \mathcal{F} due to scintillation, the received energy per bundle is changed from \mathcal{E}_h to $\lambda_O \mathcal{E}_h$. The receiver can add a flat gain (or loss) $1/\sqrt{\lambda_O}$ without affecting the available power efficiency or the P_E that can be achieved. After this receiver adjustment, the energy per bundle becomes \mathcal{E}_h , and the additive noise power spectral density is changed from N_0 to N_0/λ_O . The resulting channel model, which applies only at the threshold of outage, is an AWGN channel with noise power spectral density equal to N_0/λ_O . The fundamental limit on power efficiency for this channel is

$$\frac{\mathcal{R}}{\mathcal{P}} < \frac{1}{(N_0/\lambda_O) \log 2} \quad (5.6)$$

and thus the fundamental limit on effective power efficiency becomes

$$\frac{(1 - P_O) \mathcal{R}}{\mathcal{P}} < \frac{\lambda_O (1 - P_O)}{N_0 \log 2}. \quad (5.7)$$

The choice of λ_O that maximizes this effective power efficiency is $\lambda_O = \sigma_s^2 = 1$, in which case $\lambda_O (1 - P_O) = 1/e$. The resulting effective power efficiency is

$$\frac{(1 - P_O) \mathcal{R}}{\mathcal{P}} < \frac{1}{N_0 e \log 2}, \quad (5.8)$$

and the resulting outage probability is $P_O = 63\%$.

At the maximum effective power efficiency, the threshold of outage is at the point where the received signal flux \mathcal{F} equals its average value $\sigma_s^2 = 1$. The resulting channel model at the threshold of outage is an AWGN channel with scintillation absent. The resulting effective power efficiency is reduced relative to that AWGN channel by a factor of $1/e = 0.368$ (or 4.3 dB) due to the deliberate loss of 63% of the embedded information during periods of outage. For any specific channel code, we can determine the penalty in power efficiency for the AWGN channel absent scintillation, and then add 4.3 dB to that penalty to find the penalty in effective power efficiency.

We will now compare OOK and M-ary FSK as two channel coding approaches that could be combined with an outage strategy.

5.2.2 Comparison of channel codes

OOK is representative of the type of signal sought by current SETI searches, so it represents a useful benchmark. M-ary FSK is known from our prior analysis to be a good channel code for maximizing power efficiency on the AWGN channel. There is no reason to include time diversity with FSK since we are using the alternative outage strategy to counter scintillation. These channel codes can be analyzed for the AWGN channel absent scintillation, which is appropriate at the optimum threshold of outage.

OOK conveys one bit of information per codeword by the presence of absence of an energy bundle with energy \mathcal{E}_h . The resulting energy per bit $\mathcal{E}_b = \mathcal{E}_h/2$ if the two choices are equally likely. The resulting P_E is determined in Appendix F.2.1.

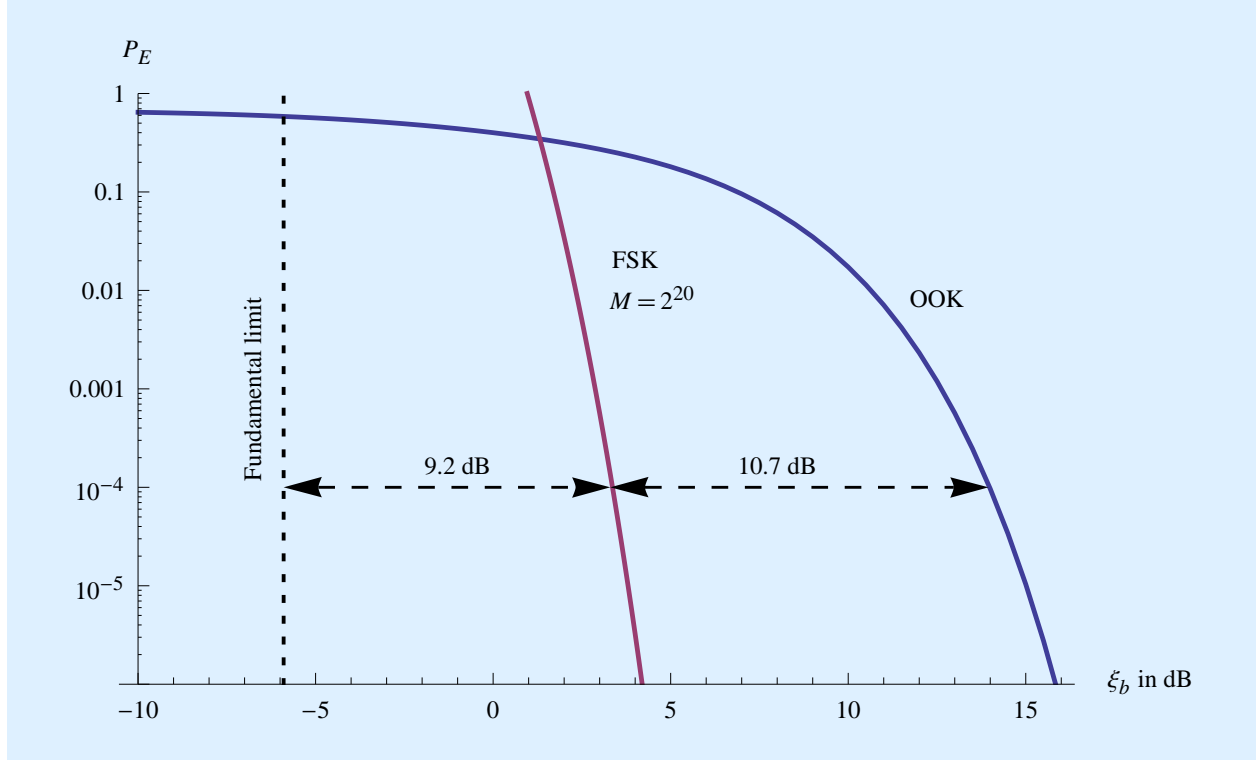


Figure 5.6: A log plot of a tight upper bound on the bit error probability P_E for both on-off keying (OOK) and M-ary frequency-shift keying (FSK) without time diversity on the AWGN channel without scintillation. This channel model applies to the outage strategy at the threshold of outage, with smaller P_E achievable whenever the received signal flux \mathcal{F} is above average. The horizontal axis is the energy contrast ratio ξ_b in dB. For M-ary FSK the value of M shown is $M = 2^{20}$. The fundamental limit on power efficiency has been moved 4.3 dB to the left to account for the loss of information during outages. At $P_E = 10^{-4}$, M-ary FSK offers a 10.7 dB advantage over OOK (a linear factor of 11.6 in average power) and FSK suffers a penalty relative to the fundamental limit of 9.2 dB (linear factor of 8.3). The OOK penalty relative to the fundamental limit is 19.8 dB (a linear factor of 96.6).

The M-ary FSK channel code is the same as studied in Section 5.1, and uses the maximum algorithm of (5.2) which (in contrast to OOK) requires no knowledge of \mathcal{E}_h or N_0 . There are two differences from Section 5.1, however. There is no time diversity needed, so $J = 1$. Also, the analysis of P_E is different from that leading to (5.3) because the channel model is absent scintillation. A tight upper bound on the bit error probability P_E is determined in Appendix F.4,

$$P_E \leq \frac{1}{4} M^{1 - \frac{\xi_b}{2 \log 2}}. \quad (5.9)$$

P_E is compared for OOK and M-ary FSK in Figure 5.6 for a typical value $M = 2^{20}$. This shows that at $P_E = 10^{-4}$ at the threshold of outage, M-ary FSK with $M = 2^{20}$ can reduce the penalty in effective power efficiency relative to the fundamental limit from a linear factor of 96.6 for OOK down to a factor of 8.3.

Recall from Figure 5.5 that M-ary FSK plus time diversity has a penalty relative to the fundamental

limit on power efficiency of a linear factor of 10.9 for the same value of $M = 2^{20}$. Thus, M-ary FSK without time diversity but employing an outage strategy is the slightly more attractive option. In view of its relative simplicity by eliminating the need for time diversity, this makes the outage strategy an attractive solution on the interstellar channel. However, it should be kept in mind that this is an “apples and oranges” comparison between two very distinctive definitions of power efficiency. The outage strategy achieves its small penalty at the expense of a deliberate 63% average loss of embedded information, and that loss can only be restored if the same message is transmitted multiple times and observed over a long period of time.

A striking property of (5.9) is that when

$$\zeta_b > 2 \log 2, \quad (5.10)$$

then $P_E \rightarrow 0$ as $M \rightarrow \infty$. This simple coding can achieve arbitrarily high reliability as $M \rightarrow \infty$ as long as (5.10) is satisfied. This lower bound on ζ_b is a factor of two larger than the fundamental limit on the AWGN channel, reflecting the loss in sensitivity due to using phase-incoherent detection. Except for this 3 dB penalty, M-ary FSK can approach the fundamental limit on power efficiency as $M \rightarrow \infty$ at the threshold of -outage. Of course we need to keep in mind that 63% of the information is totally lost to outages, which adds an additional 4.3 dB penalty in effective power efficiency. Thus, the total penalty relative to the fundamental limit on effective power efficiency approaches 7.4 dB (a linear factor of 5.4) as $M \rightarrow \infty$.

Also (5.9) can be solved for ζ_b to quantify the tradeoff between ζ_b and M at fixed P_E ,

$$\zeta_b > 2 \log 2 \cdot \left(1 - \frac{\log(4 P_E)}{\log M} \right). \quad (5.11)$$

Note that the first term equals (5.10), and the second term is the penalty relative to that limit due to using a finite M , as a function of $\{P_E, M\}$. This is plotted in Figure 5.7 and compared to the asymptote of (5.10). This illustrates that there is a slowing rate of improvement as M increases. For example, increasing M from $M = 2^{20}$ to $M = 2^{30}$ improves the effective power efficiency by only 14% (0.56 dB).

5.2.3 Adjusting information rate and average power

The previous development calculated the power efficiency for a single codeword, but the information rate \mathcal{R} is determined by how fast codewords are transmitted, and the average power \mathcal{P} is proportional to \mathcal{R} . As multiple codewords are transmitted on a single carrier at a rate F , the information rate is $\mathcal{R} = F \cdot \log_2 M$ and the average power is $\mathcal{P} = F \cdot \mathcal{E}_h$. Thus, the power efficiency remains constant, independent of F .

If the transmitter wants to reduce \mathcal{P} (at the expense of \mathcal{R}), it is advantageous to maintain $F = 1/T$, and increase T as F is decreased. This has the desirable effect of reducing the peak power as well as the average power, by spreading the codewords out over a greater time. However, there is a limit to how large T can be increased while maintaining the ICH time coherence constraint $T \leq T_c$. If further reductions in \mathcal{P} are desired, then without affecting T a duty factor $\delta < 1$ can be

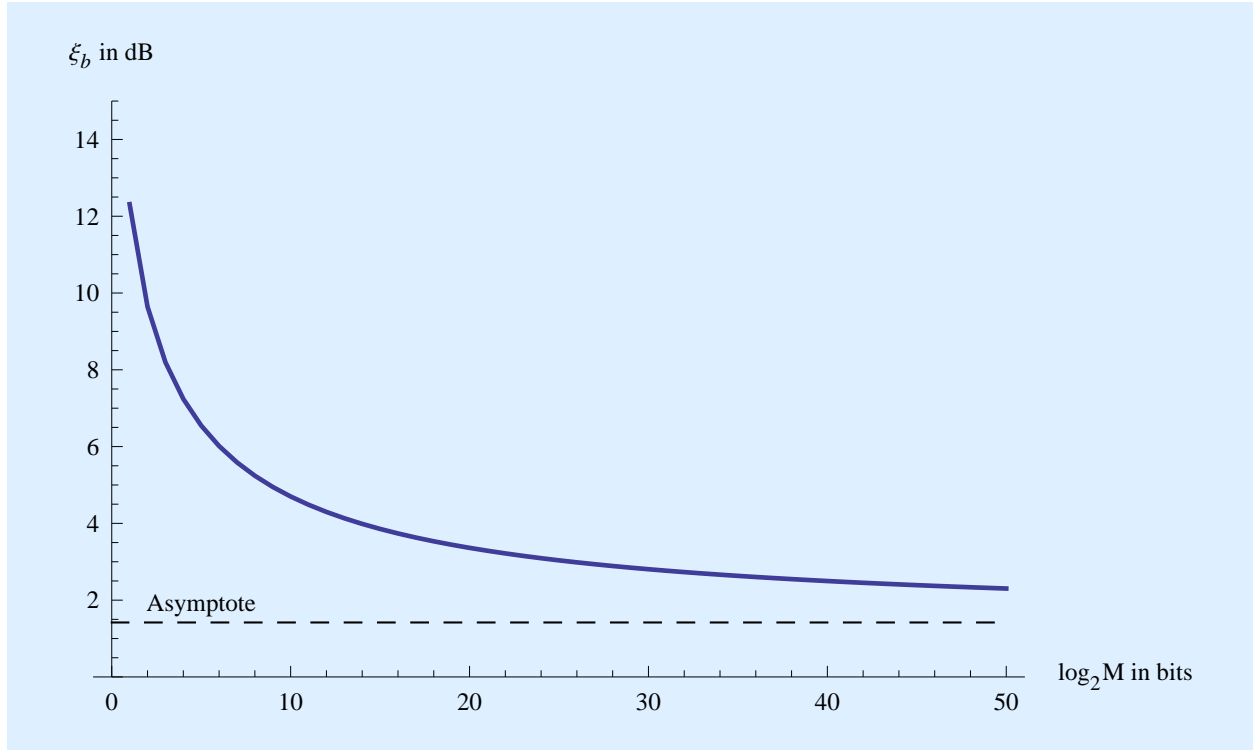


Figure 5.7: A plot of the energy contrast ratio per bit $\xi_{b,o}$ in dB required to achieve a reliability $P_E = 10^{-4}$ vs the number of bits per codeword $\log_2 M$ for M-ary FSK. As M increases the required ξ_b decreases, approaching the asymptote $2 \log 2$, shown as a dashed line.

introduced, so that the peak power becomes higher than the average power \mathcal{P} . This is illustrated in Figure 5.8.

Similarly, if an increase in \mathcal{R} is desired (at the expense of \mathcal{P}), T can be reduced while increasing F . However, a different limit is reached when it is necessary to increase bandwidth B , because eventually the ICH constraint $B \leq B_c$ will be violated. In that case, multicarrier modulation (MCM) can be used as described in Section 5.1.6 and illustrated in Figure 5.9. The desirable feature of equal peak and average powers is preserved by MCM.

5.2.4 Spectral efficiency

As M increases in M-ary FSK and \mathfrak{P} increases as a result, a decrease in spectral efficiency \mathfrak{S} is the price paid for higher power efficiency \mathfrak{P} . To characterize \mathfrak{S} , assume that a single carrier is used with a rate of transmission of energy bundles equal to F . Each codeword time (time duration of $h(t)$) is T , and the duty factor is

$$\delta = T \cdot F. \quad (5.12)$$

The bandwidth required for $h(t)$ is $B = K/T$, where K is the degrees of freedom of the signal defined in Section 3.4. To avoid overlap in the frequency domain, the minimum total bandwidth

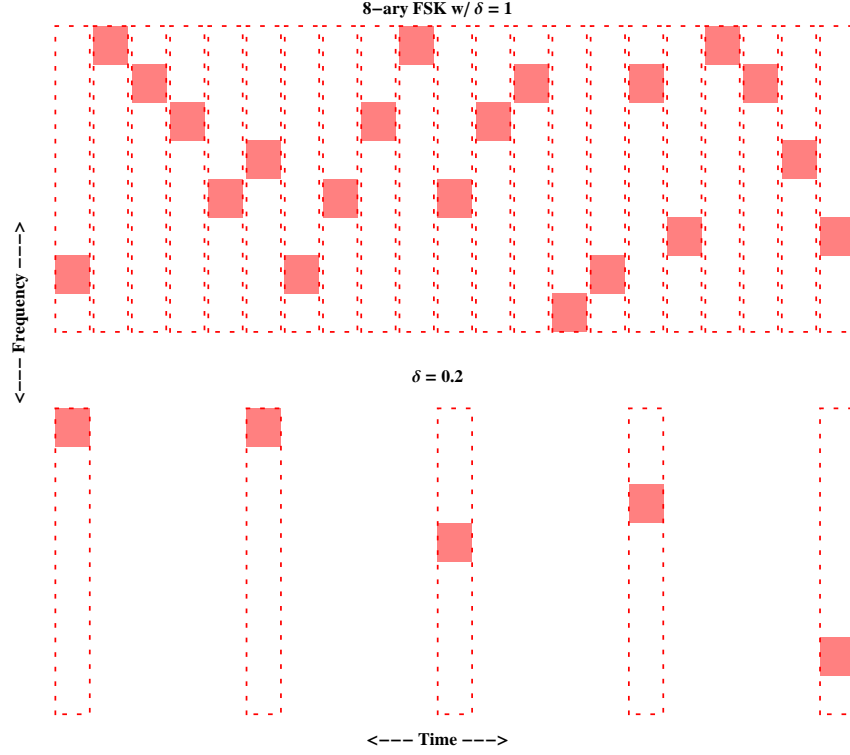


Figure 5.8: Illustration of the location of energy bundles for M-ary FSK (with $M = 8$), and how the information \mathcal{R} can be reduced by reducing the duty factor to $\delta = 0.2$ without changing T . The result is a reduction in both information rate \mathcal{R} and average power \mathcal{P} by a factor of five, while maintaining the same power efficiency.

must be

$$B_{\text{FSK}} = M \cdot B. \quad (5.13)$$

The information rate is

$$\mathcal{R} = F \cdot \log_2 M = \frac{\delta}{T} \cdot \log_2 M \quad (5.14)$$

and thus the spectral efficiency is

$$\mathfrak{S} = \frac{\mathcal{R}}{B_{\text{FSK}}} = \frac{\delta}{K} \cdot \frac{\log_2 M}{M}. \quad (5.15)$$

Thus $\mathfrak{S} \rightarrow 0$ as $M \rightarrow \infty$ as expected.

Another useful insight is that the spectral efficiency is proportional to δ . Thus, from a spectral efficiency standpoint it is desirable to run each carrier at the highest \mathcal{R} possible; that is, $\delta = 1$. If this \mathcal{R} is not large enough, multiple carriers (MCM) can be used. On the other hand, if the transmit power available to support $\delta = 1$ is not available, \mathcal{P} can be reduced by choosing a smaller δ at the expense of a smaller \mathcal{R} . Because of the fixed \mathfrak{P} , $\mathcal{P} \propto \delta$. Finally, $\mathfrak{S} \propto 1/K$, so increasing the degrees of freedom K reduces \mathfrak{S} .

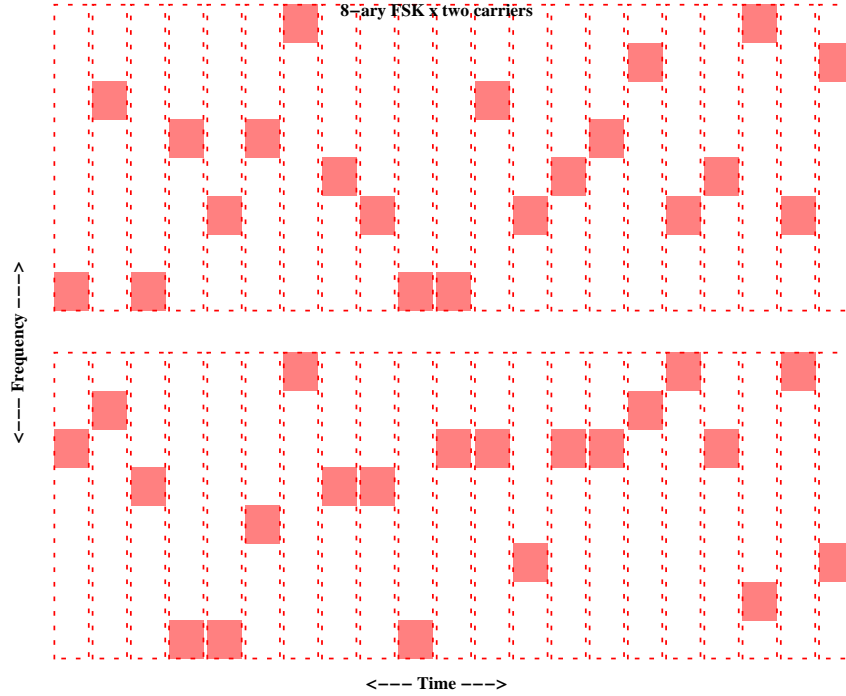


Figure 5.9: Illustration of the location of energy bundles for M -ary FSK (with $M = 8$), and how the information \mathcal{R} can be doubled by adding a second carrier. The average power \mathcal{P} is also doubled, so the power efficiency is the same. Note that this is different than doubling M to $M = 16$ (even though the diagram would look similar) which would increase \mathcal{R} by $4/3$ and \mathcal{P} not at all. The difference in the two cases is two vs. one energy bundles per codeword time duration.

5.3 Choice of $h(t)$

In the development of this chapter thus far, nothing has been said about $h(t)$ other than the assumption that it has finite bandwidth B and time duration T and unit energy. It has not been necessary to say more, because from the perspective of reliability (reflected in the bit error probability P_E) and power efficiency \mathfrak{P} the choice of the waveform $h(t)$ does not matter. Another useful (and perhaps surprising) insight is that the power efficiency \mathfrak{P} is not dependent on the parameters $\{B_c, T_c, K_c = B_c T_c\}$. Whatever these parameters may be, the transmitter can work around them while maintaining fixed power efficiency through a combination of duty factor δ and number of carriers, and achieve any desired information rate \mathcal{R} .

There are however a few practical considerations that weigh in on the choice of $h(t)$, all of them related to the detection of energy bundles during both discovery and communication. This challenge is considered in Chapter 7, where considerations in the choice of $h(t)$ will be discussed. These include the receiver designer's ability to guess $h(t)$ in order to implement a matched filter, the design of multi-channel spectral analyzers including the matched filter, and most notably immunity to radio-frequency interference (RFI).

5.4 History and further reading

Multicarrier modulation (MCM) is widely used in terrestrial wireless communications. The first commercial application (The Collins Radio Kineplex) in 1957 exploited multiple carriers to counter selective fading in military communications [48]. Because terrestrial bandwidth is a scarce resource, terrestrial applications use a clever form of MCM in which the subcarrier signals have a 50% overlap in frequency without interference (this idea was patented in 1970 [49] and gained traction in the 1990's [25]). A specific realization called orthogonal frequency-division modulation (OFDM) [50] appears in wireless communication standards such as "wireless fidelity" (WiFi), "worldwide interoperability for microwave access" (WiMAX), and the 4G digital cellular standard "long term evolution" (LTE). These standards typically combine MCM with spread spectrum [51, 52] for RFI mitigation. These numerous applications give us some additional confidence in this as an approach for interstellar communication, as well as provides relevant design experience.

5.5 Summary

The concrete design of a communication system using the five principles of power efficient design listed in Chapter 2 is undertaken, based on a finite-complexity version of the channel code of Chapter 4 as well as a simplified outage strategy. Additive white Gaussian noise (AWGN) is countered by using matched filtering in the receiver, and two methods for dealing with scintillation are compared. The simpler method declares outages and does not attempt to recover information during periods of low received signal flux due to scintillation. The more sophisticated method uses time diversity combining rather than outages to counter scintillation, and both employ M-ary FSK to counter the AWGN with high power efficiency. For interstellar communication, the outage approach appears to be the more attractive approach because there will be an opportunity to recover the lost information from multiple replicas of a message, and because the achievable effective power efficiency is actually a bit higher.

At the fundamental limit the information rate is proportional to the average received power, and this concrete design attains the same tradeoff albeit with a penalty in the achieved power efficiency relative to the fundamental limit. The size of that penalty is determined. A significant feature of the design is the way in which different rates can be achieved by a combination of the rate F at which codewords are transmitted and the choice of parameter M . After a 100% duty factor is reached ($\delta = 1$), further increases in rate can be achieved by increasing M . An alternative (which achieves lower power efficiency) is to transmit two or more carriers, which is called multicarrier modulation (MCM).

Chapter 6

Discovery

Interstellar communication cannot proceed unless and until a receiver discovers the presence of an information-bearing signal. Discovery is the grand challenge of interstellar communication because of the lack of explicit transmitter/receiver coordination and the “needle in a haystack” problem of searching for a viable signal over a large range of spacial, temporal, and frequency parameters. Even in the absence of reliable recovery of embedded information, discovery of a signal established as having a technological (as opposed to natural) origin is valuable to the receiver, because it reveals the existence and location of extraterrestrial life and a present or past intelligent civilization possessing technological capability. In this chapter the challenge of discovery of information-bearing signals designed for power efficiency is analyzed, along with beacons designed strictly for discovery without any information-bearing capability. We start with some background discussion and a basic set of assumptions that will form the basis of this analysis.

6.1 Background

Before attempting a serious attempt at discovery, some basic questions must be cleared up. What is the appropriate channel model for discovery? What kind of signals are we trying to discover? What distinguishes a “better” and “worse” design of a signal from the perspective of discovery? What are the tradeoffs that must be resolved in discovery?

6.1.1 Channel model for discovery

An interstellar channel model was developed in Chapter 3. This is the appropriate channel model for discovery as well as communication.

Coherence hole

In Chapter 4 it was established that structuring the transmit signal around the interstellar coherence hole (ICH) is necessary to approach fundamental limits on power efficiency. The ICH is even more important to discovery. There are several reasons for this. Eliminating most ISM and motion impairments as a consideration removes whole dimensions of search during discovery. For example, the computationally intensive de-dispersion algorithms used in pulsar astronomy [14] and Astropulse [32] are avoided, because unlike pulsars or transient phenomena of natural origin, interstellar communication signals should be rendered impervious to dispersion by design. Eliminating whole dimensions of search in turn reduces the false alarm rate, and thus allows discovery to operate at higher sensitivity. Finally, the ICH size can be estimated based on the observation of physical quantities, and thus it serves as a source of implicit coordination between transmitter and receiver that constrains parameters of search, principally signal bandwidth and time duration. Thus, the detection algorithms considered in this chapter assume that the transmit waveform $h(t)$ has been chosen to render impairments from the ISM and motion insignificant, save noise and scintillation.

Scintillation

During communication, the outage strategy of Chapter 5 assumed that the variation in received signal flux due to scintillation could be tracked, in which case outage periods could be declared. This is not a viable strategy for discovery, since there is no prior knowledge of a signal to observe and to track. The implication of scintillation for discovery is that there are periods during which the received signal flux is below the average, and other periods when it is above the average. The latter periods are actually quite helpful for discovery, since a receiver willing to make multiple observations will discover signals that would not be visible in the absence of scintillation.

For purposes of discovery, neglecting the unknown carrier phase a model for a single energy bundle after matched filtering and sampling is from (3.1),

$$Z = \begin{cases} \sqrt{\mathcal{E}_h} S + N, & \text{signal energy present} \\ N, & \text{noise only.} \end{cases} \quad (6.1)$$

The statistics of Z are not affected by an unknown phase. The matched filter output is zero-mean Gaussian under both conditions, the only difference being a larger variance an energy bundle is present,

$$\text{Var}[Z] = \mathbb{E}[|Z|^2] = \begin{cases} \mathcal{E}_h \sigma_s^2 + N_0, & \text{energy bundle present} \\ N_0, & \text{noise only} \end{cases}. \quad (6.2)$$

The energy contrast ratio ξ_s of (2.16) is a measure of the fractional increase in variance due to a scintillated energy bundle.

Even when an energy bundle is present, in the presence of scintillation a single observation cannot achieve reliable detection, since that observation stands a good chance of occurring during a

period of below-average received flux (when $\mathbb{E}[|S|^2] = \mathcal{F}$ is small). Thus, to take advantage of the periods of higher-than-average flux, it is necessary to make multiple observations in the same location. By "location", we mean the same line of sight and carrier frequency. In the following, it is assumed that the receiver makes L independent observations. By "independent", we mean that the observations are separated by a time interval large relative to the scintillation coherence time, so that the observations can be considered to be statistically independent. This has been pointed out previously and it was found that $L \approx 3$ suffices for high-power signals [34, 35]. Here we show that a much larger L is needed to reliably discover power-efficient signals of either the information-bearing or beacon's that conserve energy at the transmitter. This is due to the sparsity of energy bundles at low signal powers, as well as scintillation.

6.1.2 Signal structure

Past and present SETI observation programs have emphasized discovery of a beacon, rather than recovery of information. What is a beacon? Here we define a beacon as a signal that is intended to be discovered, but not empowered to convey information. This chapter analyzes the discovery of both categories of signal, in particular looking for ways to design both an information-bearing signal and a beacon that makes them "easier" to discover in terms of either complexity or reliability.

Energy bundles

This report in its totality addressed power-efficient and power-optimized design. In this context, it can be assumed that beacons are structured around the repeated transmission of energy bundles, as has been assumed for information-bearing signals designed for power-efficiency. The energy bundle is a relatively short time-duration signal that bears some amount of energy. It is based on a waveform $h(t)$ that has a bandwidth B and time duration T that falls in an interstellar coherence hole (ICH) as described further in Chapter 8.

What is the justification for this assumption? In the case of information-bearing signals structured around energy bundles it is necessary for those energy bundles to fall in an ICH to approach the fundamental limit on power efficiency as described in Chapter 4). In the case of a beacon, energy bundles confined to an interstellar coherence hole (ICH) are desirable because they can be detected without any processing related to impairments in the interstellar channel other than noise. This is significant since discovery is inherently processing-hungry due to the "needle in a haystack" challenge. Utilizing the ICH also improves the discovery reliability because the processing that is avoided would in general enhance the noise and worsen the noise immunity and increase the false alarm probability. There is no disadvantage to structuring a beacon around ICH energy bundles. Finally, basing both categories of signal on energy bundles allows the same front-end processing (matched filtering combined with multi-channel spectral analysis) to be employed in simultaneously seeking both categories of signal.

Here $h(t)$ is allowed to be any waveform that conforms to the ICH constraints for a given line

of sight and carrier frequency. Generally this class of waveform includes sinusoidal signals. In practical terms this implies an enhanced multi-channel spectral analysis that also incorporates filtering matched to non-sinusoidal signals, although certainly as a starting point it is reasonable to begin with sinusoidal signals. A search for energy bundles based on sinusoids would employ the same front end processing as is currently used following the Cyclops prescription [1]. Narrow pulses as are the target for the Astropulse search [32] have a wide bandwidth that will be impaired by the frequency incoherence of the channel, would require intensive de-dispersion processing, and are not an appropriate signal design for energy efficiency.

6.1.3 Stages of discovery

Discovery of a signal structured around energy bundles becomes a two-stage process:

Energy detection. The first stage is the detection of a single energy bundle. In making a large number of observations in different locations (with spatial, temporal, and frequency variables), a single positive detection then triggers the pattern recognition stage. With power-efficient and low-power signals a much larger number of observations with the same spatial and frequency variables is necessary to have a reasonable chance to successfully detect an energy bundle. This is because (a) energy bundles are sparse and hence most observations will not coincide with an energy bundle and (b) energy bundles are less likely to be detected during periods of low received signal flux due to scintillation.

Pattern recognition. The receiver develops more convincing statistical evidence of a discovery by detection of more than a single energy bundle along the same line of sight and at “nearby” carrier frequencies. Contrary to a Cyclops beacon, short-term persistence of the signal is not expected. That is, an energy bundle is unlikely to be followed immediately by another energy bundle, so the pattern recognition has to take account longer periods of time and different (although relatively nearby) frequencies. The pattern recognition algorithms are not looking for any prescribed deterministic pattern, since in fact the location of energy bundles is likely to vary randomly in accordance with embedded information.

In the energy-detection stage we are seeking a *signal of interest* (SoI). This SoI is distinguished by its non-natural origin, and could be either information-bearing or a beacon. At the energy-detection stage these two cases will not be distinguishable, but during the pattern recognition phase the relevant characteristics of the SoI will be estimated. At this stage an information-bearing signal can generally be statistically distinguished from a beacon by its greater randomness in the location of energy bundles.

6.1.4 Discovery reliability

In evaluating any strategy for discovery, we are primarily concerned with two probabilities,

$$P_D = \Pr \{ \text{“SoI detected”} \mid \text{“SoI is present”} \}$$

$$P_A = \Pr \{ \text{“SoI is present”} \mid \text{“SoI detected”} \} .$$

The miss probability $(1 - P_D)$ tells us how frequently, given that an SoI is present, the strategy fails to flag that signal location as worthy of further examination. Of course we desire to have $P_D \approx 1$. The accuracy probability P_A recognizes that sometimes an SoI detection is in error, by which we mean the discovery strategy flags that a SoI is present when in fact the observations consist of noise alone. Of course we desire that $P_A \approx 1$ as well, because then we can announce to the world with high confidence that an artificial signal of technological origin has been established.

In order to determine P_A , it is necessary to know two other probabilities,

$$\begin{aligned} P_{FA} &= \Pr \{ \text{"SoI detected"} \mid \text{"noise alone"} \} \\ P_B &= \Pr \{ \text{"SoI is present"} \} \end{aligned}$$

The false alarm probability P_{FA} tells us how often the discovery strategy incorrectly flags an SoI when the observations consist of noise alone. Of course we desire $P_{FA} \approx 0$. The a priori probability that an SoI is present is P_B , and this is not a characteristic of the discovery strategy but rather an assumption about the frequency with which an SoI can be expected will be present in our observations. There is no completely convincing way to justify a specific value for P_B , but surely it must be very small. Based on these probabilities, P_A can be calculated as

$$P_A = \frac{P_D \cdot P_B}{P_D \cdot P_B + P_{FA} \cdot (1 - P_B)} \approx \frac{1}{1 + \frac{P_{FA}}{P_B}} \quad (6.3)$$

When $P_B \ll P_{FA}$, most detections of an SoI are actually false alarms, and thus most of the time a detected SoI is actually noise alone and $P_A \approx 0$. The other case is $P_{FA} \ll P_B$, when $P_A \approx 1$ and a detection is much more meaningful because most of the time it flags that an SoI that is actually present. The important conclusion is that to avoid wasting a lot of effort further analyzing a signal location (or to have the confidence to announce the discovery in a public press release) P_{FA} must be mighty small, and in particular small relative to P_B .

The two most direct metrics of the reliability of any particular discovery strategy and algorithm are $\{P_{FA}, P_D\}$. The other probability of interest, P_B , is mostly a matter of judgement and not dependent on our discovery design. The analysis of $\{P_{FA}, P_D\}$ can be applied at any stage of the discovery process. In the following analysis, this analysis will first be applied to an energy bundle detection stage consisting of L independent observations. At this preliminary stage, P_{FA} is defined as the probability that one or more energy bundles are detected in the L observations in the presence of noise alone. P_D is defined as the probability that one or more energy bundles are detected when in fact a SoI overlaps the L observations. In numerical examples the values $P_{FA} = 10^{-12}$ and 10^{-8} will be chosen to get some idea of the sensitivity of the resulting $\{P_D, L\}$ to P_{FA} . These values of P_{FA} are not nearly small enough to give us confidence in the discovery of an SoI, but they may be reasonable objectives for the energy bundle detection stage because they simply capture how often the pattern recognition stage is triggered. Dramatically further reducing P_{FA} is the function of the subsequent pattern recognition stage, which observes the location and nearby locations for each discovered energy bundle over a longer period of time, looking for additional energy bundles and eventually identifying a recognizable pattern. Eventually, after a much longer period of observation we can hopefully develop sufficient confidence that our SoI

is actually an information bearing signal or beacon. This confidence requires a small enough P_{FA} relative to P_B to assert that $P_A \approx 1$.

6.1.5 Power optimization for discovery

In this report the focus is on design of a transmitted signal with the goal of minimizing the average received power that is necessary to discover that signal. However, the “minimize power” criterion of design has to be defined more carefully to distinguish discovery from communication. During communication the power efficiency criterion was adopted in Chapter 4. but this criterion has no relevance to discovery, so a different metric called *power optimization* is needed.

Unless the received power is very large and the duty factor $\delta = 1$, for the energy-detection stage to achieve simultaneously $P_{FA} \approx 0$ and $P_D \approx 1$ requires that the number of observations be large, or $L \gg 1$. An appropriate figure of merit for a signal design with respect to its discoverability is the value of L required to achieve a fixed P_{FA} and P_D . A signal design is said to be “power-optimized for discovery” when, for target values of P_{FA} and P_D and a given average power \mathcal{P} , the required L is minimized. This criterion attempts to satisfy both transmitter and receiver by jointly minimizing the discovery resources for each, the transmit power and energy consumption required of the transmitter and the processing resources and energy consumption required of the receiver, subject to a constraint on the discovery reliability.

6.1.6 Role of duty factor

In designing an information-bearing signal that achieves a high power efficiency in Chapter 5, it was found that the reliability of information extraction was dependent on the energy per bundle \mathcal{E}_h and energy per bit \mathcal{E}_b . Thus, in keeping reliability fixed, these quantities are held fixed. The way to reduce the information rate \mathcal{R} and hence average received power \mathcal{P} is to reduce the rate at which codewords are transmitted. Within the constraint of energy bundle duration T less than coherence time T_c , \mathcal{P} can be reduced by increasing T while keeping \mathcal{E}_h fixed. Larger reductions in \mathcal{P} can be achieved by reducing the duty factor δ , so that the transmission is intermittent. This raises two questions. First, is this the best way to reduce the \mathcal{P} while also doing a power optimization for discovery? Second, a beacon can be thought of as an information-bearing signal in the limit of $\mathcal{R} \rightarrow 0$. Does this imply that the design of a beacon should follow the same prescription, keeping the energy per bundle \mathcal{E}_h fixed while reducing the duty factor? It will turn out that the answer to both questions is “yes”.

This analogy to information-bearing signals suggests a *periodic beacon*. As illustrated in Figure 6.1, this beacon design consists of a periodic sequence of energy bundles. Although it bears resemblance to an information-bearing signal, it conveys no information since the location of the energy bundles is deterministic. This lack of information content is manifested by all the energy bundles being transmitted at the same carrier frequency. There is not the same motivation for a large total bandwidth B_{total} for a beacon, since the power efficiency objective is not relevant.

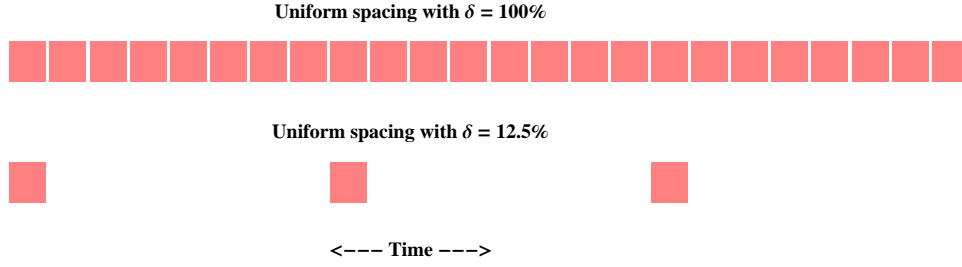


Figure 6.1: An illustration of a periodic beacon with duty factor δ for $\delta = 1$ and $\delta = 1/8$. Assuming the energy of each bundle is the same in both cases, the average power \mathcal{P} of the lower duty factor case is reduced by a factor of δ . The reliability of detection of each bundle that happens to overlap an observation is unchanged in the two cases, but a larger L is required in the second case if the duration of one observation is less than one period of the beacon, since not all observations are guaranteed to completely overlap an energy bundle. It is expected that a larger L will be required for a smaller \mathcal{P} , but the question is how much larger L needs to be and whether the resulting tradeoff between \mathcal{P} and L is the best that can be achieved.

There are two possible methods of reducing the average power \mathcal{P} for this beacon design. One is to reduce the energy per bundle, and the other is to reduce the rate at which energy bundles are transmitted. The analogy to information-bearing signals suggests that the average power \mathcal{P} should be reduced by increasing the period of the beacon, which can be done by increasing T (as long as the constraint $T \leq T_c$ is met) or reducing the duty factor δ . The duty factor approach is illustrated in Figure 6.1.

A continuously transmitted signal (equivalent to $\delta = 1$) was prescribed in the Cyclops study [1] and has been assumed in many current and past SETI searches. This beacon design is a special case of the periodic beacon, the special case with highest average power \mathcal{P} and the minimum number of observations L . There is an opportunity to reduce the average received power at the expense of increasing L by reducing the duty factor δ . This approach will reduce the average transmit power, and hence the transmitter's energy consumption, by a factor of δ .

Before concluding that reducing the duty factor is the best way to reduce power, the second approach of reducing the energy of each bundle \mathcal{E}_h must be considered and rejected. It will be established shortly that the energy per bundle does vary with \mathcal{P} for an power-optimized periodic beacon, but the variation is small because of the high sensitivity of detection probability for each energy bundle to the value of \mathcal{E}_h . Before proceeding to that argument, a subtle but important point should be highlighted. The received value of \mathcal{E}_h depends on the energy of the transmitted bundle, the propagation loss, and the transmit and receive energy gains. Thus, if a reduction in \mathcal{E}_h were feasible, that could be exploited in any of these four places, and thus could directly benefit the receiver (through a smaller collection area in the receive antenna) as well as the transmitter. In contrast, reducing \mathcal{P} only through a reduction in duty factor δ can only benefit the transmitter through lower average energy consumption. This approach also does not reduce the peak power required at the transmitter, only the average power, and it cannot be exploited by using a lower-gain transmit or receive antenna.

6.2 Periodic beacons

A periodic beacon consists of a periodic sequence of energy bundles, with an average power \mathcal{P} that is governed by the energy of each bundle \mathcal{E}_h and the rate at which bundles are transmitted F . This simple structure is a good starting point for addressing the issues surrounding power-optimization for discovery. These results are easily extended to power-efficient information-bearing signals, which add randomness to the location of the energy bundles in either time or frequency. Subsequently it will be argued that for a periodic beacon with any average power \mathcal{P} , there is an information-bearing signal with the same \mathcal{P} (and a commensurate information rate \mathcal{R}) that can be essentially as easily discovered.

6.2.1 Beacon structure and parameters

The three parameters of a periodic beacon are illustrated in Figure 6.2. Each energy bundle is assumed to have duration T , and bundles are spaced T_p apart, implying a duty factor

$$\delta_p = \frac{T}{T_p}, \quad (6.4)$$

where $0 < \delta_p < 1$. If at the receiver each energy bundle harbors the same amount of energy \mathcal{E}_h , then the average received power is

$$\mathcal{P} = \frac{\mathcal{E}_h}{T_p}. \quad (6.5)$$

Note that if \mathcal{E}_h is held fixed, \mathcal{P} decreases as the beacon period T_p is increased (the duty factor δ_p is decreased) or the energy per bundle \mathcal{E}_h is increased.

If the energy of each bundle is spread uniformly over the interval T , then the peak power is

$$\mathcal{P}_{\text{peak}} = \frac{\mathcal{E}_h}{T} = \frac{\mathcal{P}}{\delta_p}. \quad (6.6)$$

As expected the peak power $\mathcal{P}_{\text{peak}}$ remains constant if average power \mathcal{P} is reduced by reducing the duty factor δ_p . It is generally desirable in terms of the transmitter's capital costs to reduce $\mathcal{P}_{\text{peak}}$, and this can be accomplished by increasing T , with the side effect of increasing δ_p without increasing \mathcal{P} . However, this opportunity is limited by the coherence time of the channel to $T \leq T_c$.

6.2.2 Characteristics of beacon observation

Consider an observation of the received signal at a given carrier frequency and starting time. For purposes of studying the discovery probability, assume that the carrier frequency is the correct one. The parameters determined by the receiver designer are the duration of a single observation T_o and the number of independent observations L , with the total duration of the collective observations equal to $L \cdot T_o$. Each observation is assumed to begin at a random point in the beacon

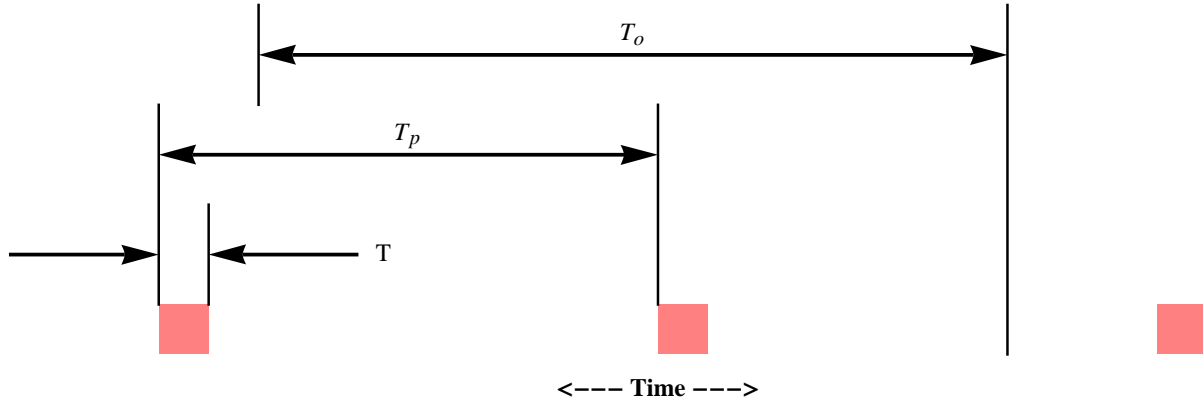


Figure 6.2: An illustration of the three parameters of a periodic beacon and its observation. The parameters determined at the transmitter are the duration of an energy bundle T and the time interval between energy bundles T_p . The parameter determined at the receiver are duration of one observation T_o and the number of independent observations L (not shown).

period, and the effect of scintillation on each observation is considered statistically independent of the others, meaning that the time interval between observations is large relative to the coherence time of the channel as modeled in Chapter 8.

An individual energy bundle is said to overlap an observation if the observation interval completely overlaps the time duration of the bundle, so that a matched filter implemented to interpret the observation captures its full energy. Then the average number of energy bundles overlapping a single observation is

$$\frac{T_o - T}{T_p} = n_o + \delta_o \quad (6.7)$$

where $0 \leq n_o$ is an integer and $0 \leq \delta_o < 1$. For example, there is always exactly one energy bundle in each observation ($n_o = 1$ and $\delta_o = 0$) when $T_o = T_p + T$. When $T_o = 2T$ the average number of energy bundles per observation is δ_p ($n_o = 0$ and $\delta_o = \delta_p$), or equivalently the probability of an energy bundle overlapping one observation is δ_p .

It is generally useful to increase the observation time, because the average number of bundles overlapping an observation also increases. However, a point of diminishing returns occurs for $T_o > T_p + T$, because for that case $1 \leq n_o$ and there can be two or more energy bundles overlapping a single observation. Two energy bundles spaced so closely in time will experience a correlated scintillation. It is overall a more efficient use of cumulative observation time to keep the observations independent, because that increases the likelihood of experiencing a large received signal flux during periods overlapping one or more of the L observations. For our examples, therefore, we assume that $T_o \leq T_p + T$, in which case $n_o = 0$ and $0 < \delta_o \leq 1$.

6.2.3 Tradeoffs in detection reliability

An analysis of the reliability of detection of a beacon is relegated to Appendix G.2. The result is expressed in a discovery relation that is fairly complicated and can only be evaluated numerically. Fortunately, some simple principles reveal much insight into the tradeoffs in power-optimized beacon design, and predict the results of the complete analysis with a fair degree of accuracy.

Opportunities for false alarms

Consider the detection of a beacon using L observations with an overall probability of false alarm (one or more energy bundles are falsely detected in noise alone) equal to P_{FA} and overall probability of detection (one or more energy bundles are detected in the presence of a periodic beacon) equal to P_{D} .

In the absence of a beacon, the observations reflect noise alone. Then P_{FA} reflects the total number of degrees of freedom N in the observations, which equals the product of the total time duration of the observations and the bandwidth of the observations,

$$N = L T_o \cdot B = L K \left(\frac{\delta_o}{\delta_p} + 1 \right). \quad (6.8)$$

For example, the continuous-time noise signal at the output of an matched filter has bandwidth no greater than B , and thus can be sampled at rate B and the number of such samples N is the total observation time $L T_o$ times B . If the noise projected into the N degrees of freedom are statistically independent (the conditions for this are considered in Appendix G.2), then P_{FA} is to good accuracy equal to N times the probability that a false alarm occurs in a single degree of freedom. Overall the detection is penalized for using a larger L and T_o by requiring a smaller false alarm probability P_{FA}/N at the level of looking for an energy bundle in a single degree of freedom.

Effect of duty factor alone

Now consider the case where a beacon is actually present at the carrier frequency and in the direction being observed. There are two ways in which L observations of duration T_o can fail to detect that signal. Either no energy bundle overlaps *any* of the L observations, or one or more bundles overlaps but they are all obscured by noise. By ignoring the second possibility, a lower bound on the miss probability follows. Ignoring the effects of noise, no bundles overlap one observation with probability $(1 - \delta_o)$ and thus no bundles overlap all L observations with probability

$$1 - P_{\text{D}} \geq (1 - \delta_o)^L \quad \text{or} \quad L \geq \frac{\log \left(\frac{1}{1 - P_{\text{D}}} \right)}{\log \left(\frac{1}{1 - \delta_o} \right)}. \quad (6.9)$$

This relation reveals how large L must be chosen to overcome just the effect of $\delta_o < 1$. Note that the larger P_{D} we require, the larger L must be. Also, larger observation duty factor δ_o is helpful in reducing the required number of observations L .

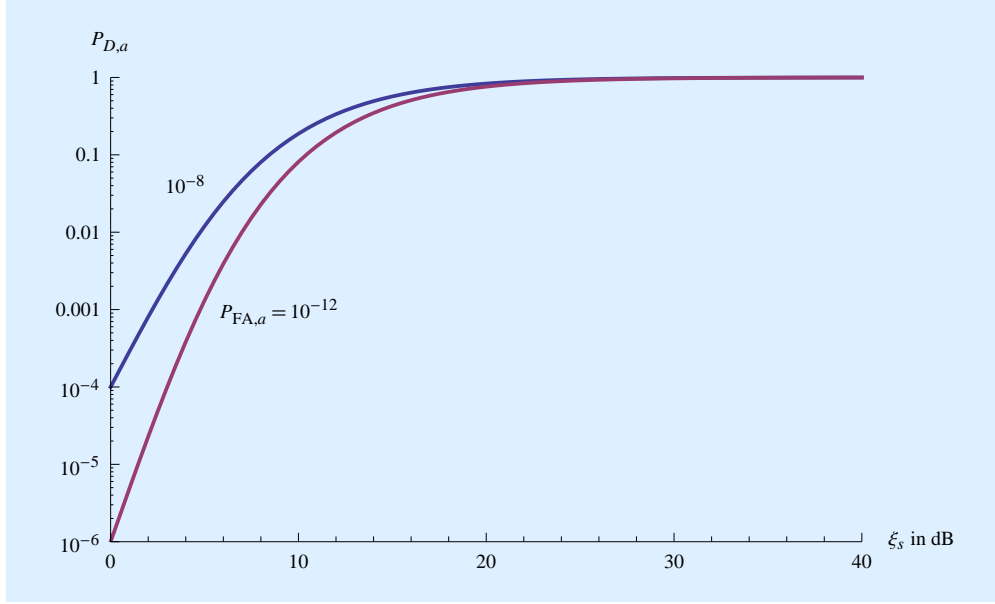


Figure 6.3: An illustration of the reliability of detection of a single energy bundle in the presence of additive Gaussian noise and scintillation. The detection probability $P_{D,a}$ is plotted vs the energy contrast ratio ξ_s in dB at the output of the matched filter. This is repeated for two different values of false alarm probability P_{FA} .

Bundle energy hypothesis

As noted earlier, the average beacon power \mathcal{P} can be reduced by a reduction in the energy \mathcal{E}_h of each bundle while keeping the duty factor δ_p fixed, or by decreasing δ_p while keeping \mathcal{E}_h fixed. If the goal is to minimize the number of observations L , then the *bundle energy hypothesis* asserts that reducing duty factor is preferable. In other words, as the average power \mathcal{P} is changed, the energy in each individual bundle \mathcal{E}_h should remain fixed.

The logic behind this hypothesis is that the probability of detection of an energy bundle that does overlap an observation is a sensitive function of \mathcal{E}_h (or equivalently the energy contrast ratio ξ_s of (2.16)). In the detection of a single energy bundle, let $P_{FA,a}$ and $P_{D,a}$ be respectively be the false alarm and detection probabilities for the matched filter detection of a single energy bundle in AWGN with power spectral density N_0 and with scintillation with average scintillation flux σ_s^2 . It is shown in Appendix G.2 that the relationship between these probabilities is

$$P_{D,a} = P_{FA,a}^{\frac{1}{1+\xi_s}} \quad (6.10)$$

and this relationship is plotted in Figure 6.3. For small ξ_s the detection probability P_D is small, so that energy bundles are rarely detected. There is a sharp threshold at about $\xi_s \approx 10$ to 15 dB where detection becomes fairly reliable. For example, at $\xi_s = 15$ dB, an energy bundle is detected 57% of the time ($P_D = 0.57$ at $P_{FA} = 10^{-12}$). Thus, assuming that \mathcal{E}_h is already about as small as possible to minimize beacon power, allowing it to decrease further as \mathcal{P} decreases would drastically reduce $P_{D,a}$, and thereby have a large impact in increasing the size of L . The alternative of reducing δ_p

also increases the required L as in (6.9), but in a less drastic way. There is thus a tradeoff, but one that strongly favors reducing δ_p rather than \mathcal{E}_h .

Maintaining fixed per-bundle energy can be accomplished by manipulating the bundle duration T and the duty factor δ_p , since from (6.5)

$$\mathcal{E}_h = \mathcal{P} \cdot T_p = \frac{\mathcal{P} T}{\delta_p}. \quad (6.11)$$

Assuming T is fixed, the bundle energy hypothesis predicts that $\delta_p \propto \mathcal{P}$, or the transmit duty factor should be reduced in proportion to the decrease in \mathcal{P} . The bundle energy hypothesis also predicts that as \mathcal{P} is decreased reducing the duty factor δ_p can be avoided by increasing T . However, the time incoherence of the channel limits this to $T \leq T_c$, so once the energy bundle duration is as large as possible (from (6.6) this is also beneficial in reducing the peak power $\mathcal{P}_{\text{peak}}$) then further reduction in \mathcal{P} requires reducing δ_p to maintain the same detection reliability.

Note that reducing δ_p also increases the needed value of L required to maintain fixed reliability, either through increasing the length of an observation T_o (increasing the false alarm probability) or reducing the observation duty factor δ_o (reducing the probability that a bundle overlaps each observation). The bundle energy hypothesis simply predicts that reducing the bundle energy \mathcal{E}_h would have a larger impact on L and is to be avoided.

It is instructive to compare a periodic beacon and an M-ary FSK signal from the limited perspective of the energy \mathcal{E}_h contained in each bundle, or equivalently the energy contrast ratio ζ_s . For purposes of this comparison, assume that the outage strategy is employed rather than time diversity. The time diversity case will be considered separately in Section 6.4.2. For the beacon, ζ_s is determined by the requirement on reliability of detection of the bundle in the presence of noise and scintillation. For the FSK signal, ζ_s is determined by the requirement on probability of error P_E in the presence of noise and at a scintillation flux chosen to be at the threshold of outage. This comparison is germane to the question of how hard it is to discover an information-bearing signal at an average power \mathcal{P} sufficiently high to reliably recover information at the threshold of outage. Rewriting the upper bound on P_E of (5.9) in terms of ζ_s rather than the energy contrast ratio per bit ζ_b ,

$$P_E \leq \frac{M}{4} e^{-\zeta_s/2}. \quad (6.12)$$

This bound is plotted in Figure 6.4, where we see that an FSK signal requires an $\zeta_s \approx 13$ to 16 dB to achieve reliable information extraction, depending on the value of M and the desired P_E . This is very similar to the $\zeta_s \approx 14$ to 15 that was required for reliable detection of a beacon. The similarity of these contrast ratios is not surprising, since in both cases an energy bundle is being detected. In the case of the FSK signal at the threshold of outage, the scintillation is assumed to equal its average value, whereas for the beacon the scintillation is random, sometimes attenuating and sometimes amplifying the bundle energy. This result anticipates the later argument that a beacon offers no advantage over an information-bearing signal for ease of discovery.

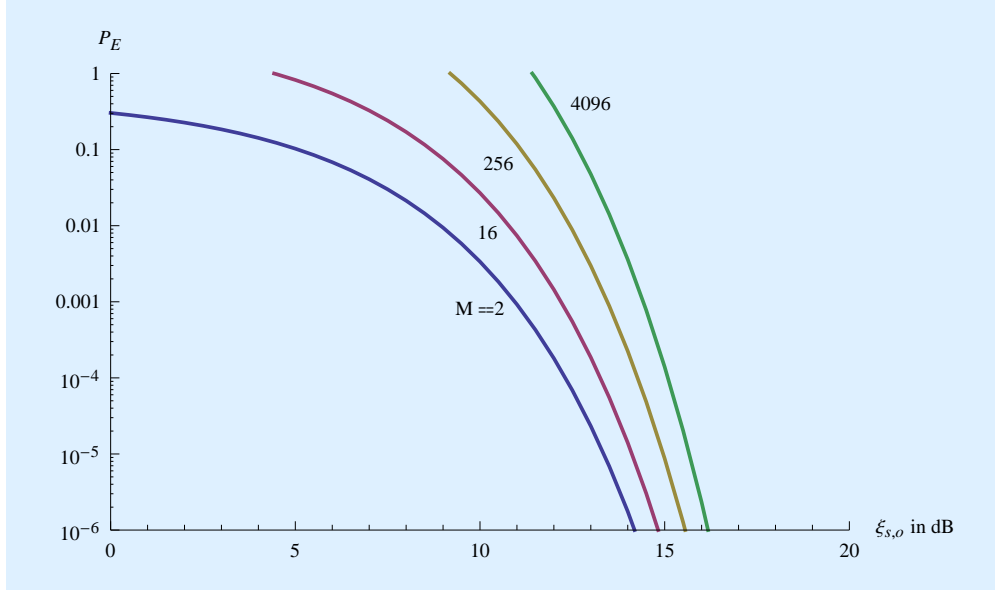


Figure 6.4: A log plot of an upper bound on the error probability for M-ary FSK vs. the energy contrast ratio ξ_s for an individual energy bundle making up that signal. This is plotted for $M = 2^n$ and $n = 1, 4, 8$ and 12 . At fixed ξ_s the P_E bound increases with M because there are $(M - 1)$ opportunities for a noise sample to be greater than the energy bundle sample at the output of a bank of M matched filters. P_E is greater than unity for smaller ξ_s because it is an upper bound that is accurate only for small P_E .

Total effective energy hypothesis

The bundle energy hypothesis offers insight into the appropriate choice of duty factor δ_p for a given beacon average power \mathcal{P} , namely the δ_p required to achieve that power without reducing \mathcal{E}_h . On the other hand, it offers no insight into the values of $\{L, T_o\}$ required to achieve a certain overall level of reliability $\{P_D, P_{FA}\}$ in detection of the beacon. This is the role of the *total effective energy hypothesis*. The total effective energy \mathcal{E}_{eff} is the total energy of all the bundles overlapping the L observations, each observation of duration T_o . The total effective energy hypothesis states that \mathcal{E}_{eff} should be held approximately fixed as $\{\mathcal{P}, L, T_o\}$ are varied. The logic behind this hypothesis follows from an analogy to information-bearing signals, where the reliability of information extraction is determined by \mathfrak{E}_b , the received energy per bit. A beacon is designed to convey a single bit of information, namely whether "beacon is present" or "beacon is not present". Thus, it is reasonable to assume that the total received energy overlapping L observations is germane to the reliability with which that one bit of information embedded in the beacon can be extracted.

To apply this hypothesis, the average number of bundles that are overlapping the collective observations is $L \cdot \delta_o$, the energy per bundle is \mathcal{E}_h , and thus

$$\mathcal{E}_{\text{eff}} = L \delta_o \mathcal{E}_h. \quad (6.13)$$

Note that \mathcal{E}_{eff} is merely an average, since the actual number of overlapping bundles is random. It

is also useful to define an energy contrast ratio ζ_{eff} expressed in terms of \mathcal{E}_{eff} ,

$$\zeta_{\text{eff}} = \frac{\mathcal{E}_{\text{eff}} \sigma_s^2}{N_0} = L \delta_o \zeta_s. \quad (6.14)$$

The analogy to information-bearing signals suggests that it is ζ_{eff} rather than \mathcal{E}_{eff} alone that determines the required value of L , or rather what matters is the ratio of total effective energy to noise power spectral density.

If \mathcal{E}_h (and hence ζ_s) is held fixed in accordance with the bundle energy hypothesis, then a couple of notable observations can be made. First, $L \propto 1/\delta_o$, or there is a direct tradeoff between observation time T_o and the number of observations L . In particular the relation

$$\delta_o = \left(\frac{T_o}{T} - 1 \right) \cdot \delta_p. \quad (6.15)$$

illustrates the possible tradeoffs as the average beacon power \mathcal{P} is reduced, and this is accompanied by a reduction in transmit duty factor δ_p in order to keep \mathcal{E}_h fixed. One option is to keep the observation time T_o fixed, in which case $\delta_o \propto \delta_p$, and thus $L \propto 1/\delta_p$. Another option is to keep δ_o (and hence L) fixed by some combination of reducing T and increasing T_o . However the assumption that $T_o \leq T_p + T$ puts a cap on this opportunity, and ultimately it will be necessary to start reducing δ_o (and thus increasing L) to achieve a further reduction in \mathcal{P} .

The second observation is that ζ_{eff} can be made as large as desired simply by increasing L , suggesting (correctly as it turns out) that there is no lower limit to the average power \mathcal{P} of a beacon that can be reliably detected if we are willing to make a sufficiently large number of observations. This is due to the presumed long-term presence of the beacon, so that a larger L is always able to capture a larger total effective energy. It is also due to the assumption that the energy per bundle should not be reduced as the \mathcal{P} is reduced, so that observations overlapping an energy bundle are just as likely to detect it.

How to reduce average beacon power

The two hypotheses guide the reduction in beacon average power without affecting detection reliability, namely $\delta_p \propto \mathcal{P}$ and (oversimplifying a bit) $L \propto 1/\mathcal{P}$. Achieving very low \mathcal{P} requires action on the part of both the transmitter and receiver designers. The transmitter has to reduce the duty factor, and the receiver has to increase the number of observations it makes at each frequency and line of sight. Fortunately these actions need not be coordinated. The transmitter can reduce its average transmit power as long as it also reduces δ_p in proportion, keeping \mathcal{E}_h fixed. This preserves the receivers chance at detecting the beacon, although only those receivers that choose a sufficiently large L or sufficiently large observation time T_o to compensate the smaller δ_p will reliably detect the beacon. From the receiver perspective, the antenna collection area must be large enough to preserve an acceptable value for \mathcal{E}_h , and T_o (up to a limit) or L have to be sufficiently large to allow beacons with a smaller \mathcal{P} to be detected.

6.2.4 Detection reliability for a periodic beacon

The intuitive logic of the last section helps with understanding the tradeoffs, but fails to take account of the quantitative tradeoff between the number of energy bundles that overlap observations and the relationship between \mathcal{E}_h and detection reliability. Thus, these hypotheses give no hint as to the actual value of L that may be necessary, and also yields only qualitative and approximate results. A complete analysis is given in Appendix G.2. The detection reliability is characterized by $\{P_{\text{FA}}, P_{\text{D}}\}$, where P_{FA} is the probability of one or more detected energy bundles out of L observations in the presence of noise alone, and P_{D} is the same probability in the presence of a beacon. It is then shown that the relationship between P_{FA} and P_{D} is

$$P_{\text{D}}[P_{\text{FA}}, \xi_s, \delta_o, L] \approx 1 - \left[1 - \delta_o \left(\frac{P_{\text{FA}}}{N} \right)^{\frac{1}{1+\xi_s}} \right]^L, \quad (6.16)$$

where N is the degrees of freedom in all observations given by (6.8). P_{D} is monotonically increasing with L , and thus the receiver always improves reliability by implementing a larger L . For any $P_{\text{FA}} > 0$, $\xi_s > 0$, $0 < \delta_p \leq 1$, and $K \geq 1$

$$P_{\text{D}} \xrightarrow{L \rightarrow \infty} 1. \quad (6.17)$$

Thus, as suggested by the total effective energy hypothesis, $P_{\text{D}} \approx 1$ can always be achieved if L is sufficiently large. Another consequence of this principle is that for any reliability $\{P_{\text{FA}}, P_{\text{D}}\}$ we can safely ask what L is required to achieve that reliability without worrying about the feasibility of achieving that reliability.

This property is a happy outcome of scintillation, since periods of large flux reliably coincide with an energy bundle in at least one observation if L is sufficiently large. In this sense, scintillation is the savior of discovery, since it permits discovery under the most adverse conditions. However, in practical terms the size of L could easily be too large. For example, if L is so large that it requires observations over a period of time large relative to the existence (or for that matter patience) of a civilization, in practical terms the beacon is non-discoverable. The transmitter designer must be aware of this and insure that the received signal flux at the destination is sufficient for discovery with parameters (antenna collection area, observation time, and number of observations) that it considers practical.

6.2.5 Reducing average power by manipulating the energy per bundle

As a reference point for considering variations in the parameters δ_p and δ_o , consider the *Cyclops beacon* of the type prescribed by the Cyclops report [1]. The primary characteristic that makes this beacon inefficient at low powers is its 100% duty factor at all power levels. The average power \mathcal{P} of a Cyclops beacon can be reduced by increasing T as the bundle energy \mathcal{E}_h is held fixed. However, when T reaches the limit of time coherence $T \leq T_c$, the only way to reduce \mathcal{P} further is to reduce \mathcal{E}_h . This runs counter to the bundle energy hypothesis, and as we will see results in a dramatic inflation in the number of observations L .

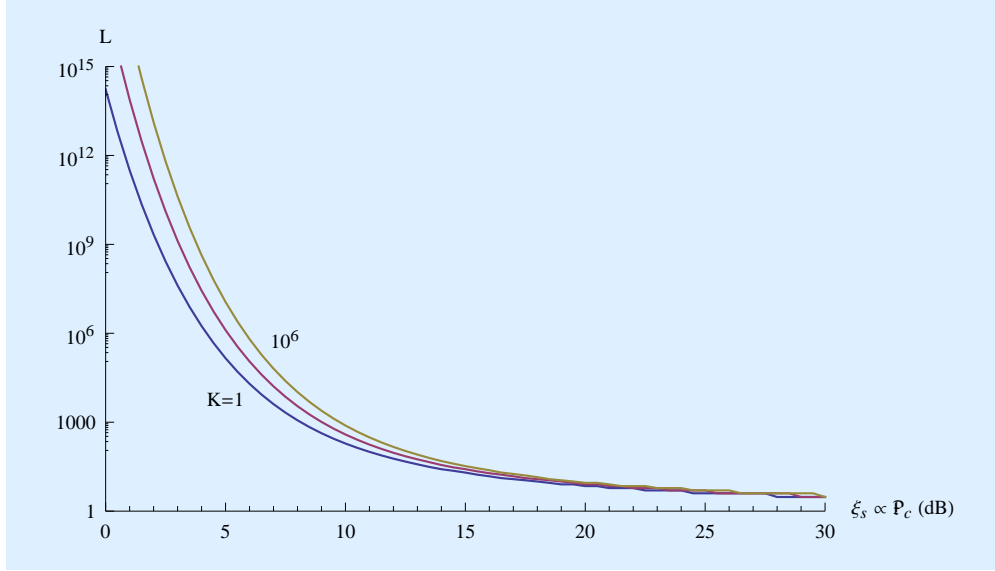


Figure 6.5: For a Cyclops beacon with fixed 100% duty factor ($\delta_p = 1$), a log plot of the required number of observations L vs the energy contrast ratio $\xi_s \propto \mathcal{P}_s$ in dB for each energy bundle. The assumed detection reliability is $P_{FA} = 10^{-12}$ and $P_D = 10^{-4}$. Three values of degrees of freedom are plotted, $K = 1, 10^3$, and 10^6 .

The parameters for a Cyclops beacon with average power \mathcal{P} are

$$\delta_p = 1 \quad (6.18)$$

$$\mathcal{P} = \frac{\mathcal{E}_h}{T} \quad \text{or} \quad \xi_s = \frac{\mathcal{P} T}{N_0} \quad (6.19)$$

$$T_o = 2 T \quad \text{or} \quad \delta_o = 1 \quad (6.20)$$

$$N = 2 L K. \quad (6.21)$$

The required L as a function of $\xi_s \propto \mathcal{P}_s$ is illustrated in Figure 6.5, where we see a very large L is required to achieve low powers. Recall from Figure 6.3 that the turning point where the detection probability for a single energy bundle approaches unity is $\xi_s \approx 12$ to 15 , and the same effect can be seen in Figure 6.5. At $\xi_s = 15$ dB the required number of observations is $L = 19$ for $K = 1$ ($L = 33$ for $K = 10^6$). At lower powers than this L increases very dramatically and the degrees of freedom K starts to have a larger effect. At larger average powers, on the other hand, L is reduced, reaching $L = 3$ at $\xi_s = 30$ dB. Thus, even for the inefficient Cyclops beacon design, an increase in the number of observations from $L = 3$ to $L = 19$ allows a reduction in the average beacon power by 15 dB, or a linear factor of 31.6. Larger reductions in power this way become very costly in terms of L because of the rapidly increasing miss probability in the detection of individual energy bundles shown in Figure 6.3.

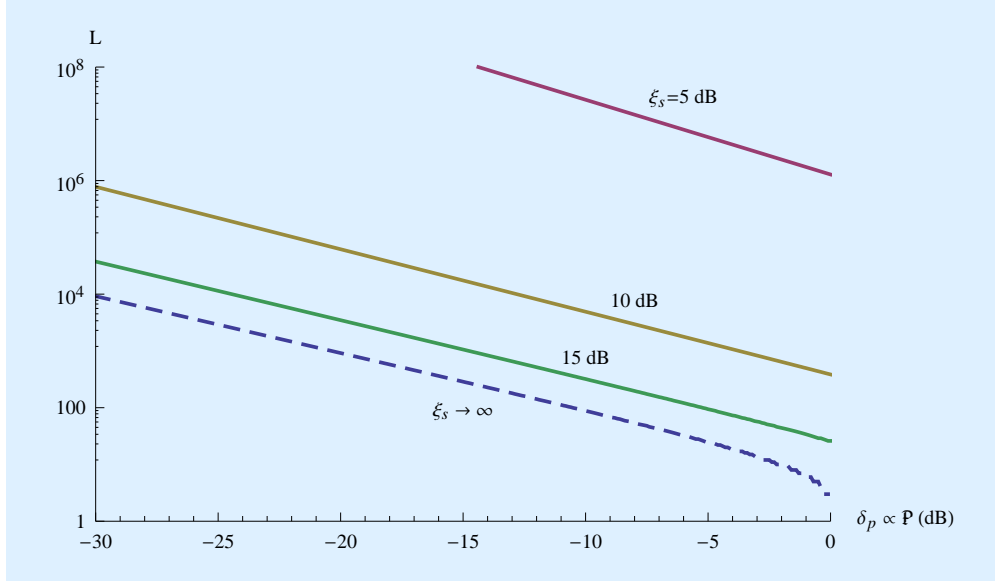


Figure 6.6: To illustrate the reduction in average power \mathcal{P} by reducing the transmit duty factor δ_p , a log plot of the required number of observations L vs the δ_p in dB is shown. The assumed detection reliability is $P_{\text{FA}} = 10^{-12}$ and $P_{\text{D}} = 10^{-4}$. A single values for the degrees of freedom $K = 10^3$ is shown. The different curves show different values for the energy contrast ratio ξ_s , where the power \mathcal{P} is also proportional to ξ_s . The dashed line is the lower bound on L imposed by δ_p alone (ignoring the effects of noise) given by (6.9).

6.2.6 Reducing average power by manipulating the duty factor

The average power \mathcal{P} can be reduced by reducing the energy contrast ratio ξ_s while keeping the transmit duty factor δ_p fixed (as just seen) or by reducing δ_p while keeping ξ_s fixed. The latter approach follows from the bundle energy hypothesis, so our intuition suggests that this is a more efficient way to reduce power. There are two diametrically opposed strategies to detecting such a beacon at the receiver. The first is to use the minimum observation interval $T_o = 2T$, which will maximize the number of observations L required to achieve the desired detection reliability. The parameters for a beacon with average power \mathcal{P} are

$$\mathcal{P} = \frac{\mathcal{E}_h}{T_p} \quad \text{or} \quad \delta_p = \frac{\mathcal{P} T}{\xi_s N_0} \quad (6.22)$$

$$\delta_o = \delta_p \quad (6.23)$$

$$N = 2 L K. \quad (6.24)$$

The transmit duty factor δ_p is proportional to the average power \mathcal{P} . The required L for this approach as a function of $\delta_p \propto \mathcal{P}$ is illustrated in Figure 6.6. The reduction in L is dramatic when compared with Figure 6.5. Consistent with Figure 6.5, the reduction in L is also dramatic as ξ_s decreases, at least up to $\xi_s \approx 15$ dB, after which comes a point of diminishing returns where L is close to its duty factor lower bound of (6.9). For example, at \mathcal{E}_s

As an example of the dramatic reduction in L from manipulating δ_p rather than \mathcal{E}_s , take as a baseline case a Cyclops beacon with $\xi_s = 30$ dB. This beacon may actually be detected in current

searches, since it requires only $L = 3$. Now suppose the average power is reduced by 30 dB, or a linear factor of 1000. Achieving that by reducing the bundle energy while retaining 100% duty factor requires $L \approx 10^{16}$ from Figure 6.5. This Cyclops design approach is clearly impractical. However, achieving this by reducing δ_p alone requires $\xi_s = 30$ dB and $\delta_p = -30$ dB (a duty factor of 0.1%). This large an ξ_s achieves close to the lower bound in Figure 6.6 (the dashed line) and thus requires $L \approx 10^4$. This is still inefficient because the value $\xi_s = 30$ dB is considerably past the point of diminishing returns. A more efficient approach would be to use a combination of a 15 dB reduction in ξ_s (or equivalently a 15 dB reduction in energy per bundle \mathcal{E}_h) and a 15 dB reduction in δ_p . That approach requires $L \approx 10^3$, or a further order of magnitude reduction relative to using duty factor alone. The total reduction in the number of observations required by the receiver is always a factor of about 10^{13} . The 15 dB reduction in duty factor (to 3.2%) can only be implemented in the transmitter, and the transmitter realizes as a result a 15 dB reduction in average transmit power (but no reduction in peak transmit power). As far as the 15 dB reduction in energy per bundle, this could be implemented at either the transmitter (by reducing the peak and average power by 15 dB) or alternatively at the receiver (by reducing the receive antenna collection area by 15 dB or a linear factor of 31.6).

The diametrically opposite strategy at the receiver is to use the maximum observation interval $T_o = T_p + T$ ($\delta_o = 1$), which will minimize the number of observations L required to achieve the desired detection reliability at the expense of greater observation time. The parameters for a beacon with average power \mathcal{P} are

$$\mathcal{P} = \frac{\mathcal{E}_h}{T_p} \quad \text{or} \quad \delta_p = \frac{\mathcal{P} T}{\xi_s N_0} \quad (6.25)$$

$$\delta_o = 1 \quad (6.26)$$

$$N = L K \left(\frac{1}{\delta_p} + 1 \right). \quad (6.27)$$

Note that \mathcal{P} is proportional to δ_p . The required L for this observational strategy as a function of $\delta_p \propto \mathcal{P}$ is illustrated in Figure 6.7. As expected, choosing a long duration for each observation eliminates the duty factor effect in L and results in an L that is both much smaller ($L = 28$ for $\xi_s = 15$ dB and $\delta_p = -15$ dB) and does not increase much as \mathcal{P} is reduced as long as \mathcal{E}_s is large enough to reliably detect individual energy bundles. When ξ_s is too small, the result is a much larger L for all duty factors and an L that increases substantially as \mathcal{P} is reduced reflecting the poor reliability in detecting individual energy bundles.

6.2.7 Optimization of energy contrast ratio and duty factor

Two diametrically opposed ways to reduce average power \mathcal{P} have been considered. The first is the Cyclops beacon, where \mathcal{P} is reduced by a reduction in the energy per bundle \mathcal{E}_h (and hence ξ_s) while keeping 100% duty factor. The second reduces the duty factor δ_p while keeping ξ_s fixed. In our earlier examples, reducing ξ_s proved effective at higher powers until $\xi_s \approx 15$ dB was reached, but after that further reductions resulted in a dramatic increase in the number of observations L . Reducing δ_p was much more effective at limiting the size of L at low powers. The size of L can be

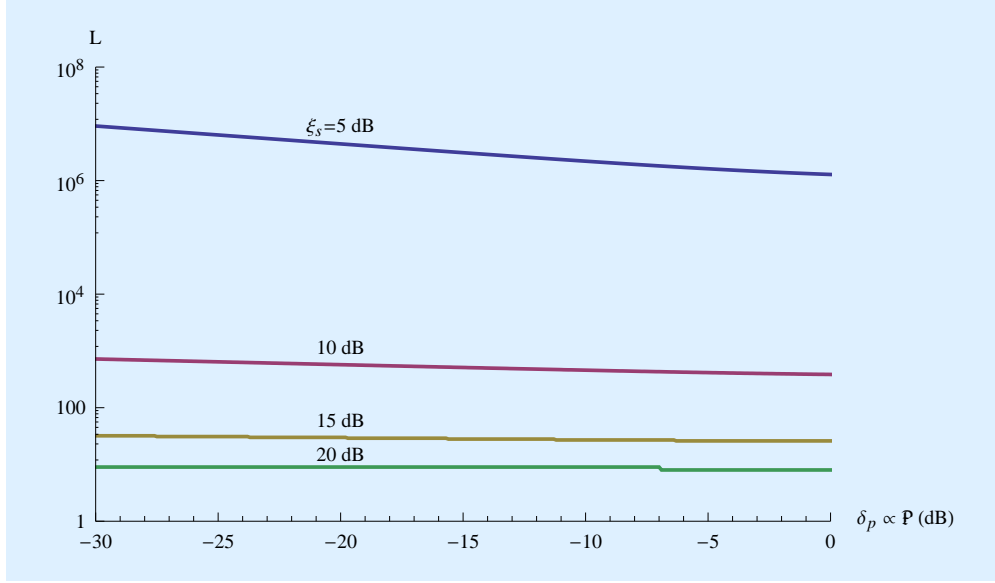


Figure 6.7: Figure 6.6 is repeated, except that each observation is over a full period of the periodic beacon ($T_o = T_p + T$, or $\delta_o = 1$). A longer observation interval has been exchanged for a smaller number of observations L .

kept very modest ($L \approx 30$ or so) at low powers by extending the duration of each observation to equal the period of a incoming periodic beacon.

In summary, reducing ξ_s was more effective at higher powers, and reducing δ_p was more effective at lower powers. To truly capture the design tradeoffs, particularly in the transition region, we must minimize L by the *joint* choice of ξ_s and δ_p . This is easily accomplished by considering a beacon with fixed average power \mathcal{P} and varying both the energy contrast ratio for each energy bundle ξ_s and the duty factor δ_p to maintain that fixed \mathcal{P} . The parameters of this fixed-average-power periodic beacon are

$$\xi_s = \frac{\xi_0}{\delta_p} \quad \text{where} \quad \xi_0 = \frac{\mathcal{P} T}{N_0} \quad (6.28)$$

$$N = L K \left(\frac{\delta_o}{\delta_p} + 1 \right). \quad (6.29)$$

The parameter ξ_0 is the per-bundle energy contrast ratio for the Cyclops beacon at 100% duty factor. Two choices for the receiver's observation strategy bracket the observation times of interest, the minimum per-observation duration ($\delta_o = \delta_p$) and the maximum duration ($\delta_o = 1$).

The resulting L is plotted in Figure 6.8, where each curve corresponds to a fixed power \mathcal{P} . For each curve, as δ_p is decreased, the energy contrast ratio ξ_s is increased to maintain a fixed \mathcal{P} . For lower power beacons, there is an optimum $\delta_p < 1$ for which L is minimum, and that δ_p decreases as \mathcal{P} decreases. A beacon with this duty factor is power-optimum, in that it minimizes the number of observations L required to achieve the target detection reliability. For larger \mathcal{P} the Cyclops beacon ($\delta_p = 1$) is power-optimum. The lowest-power Cyclops beacon that is power-optimum has an

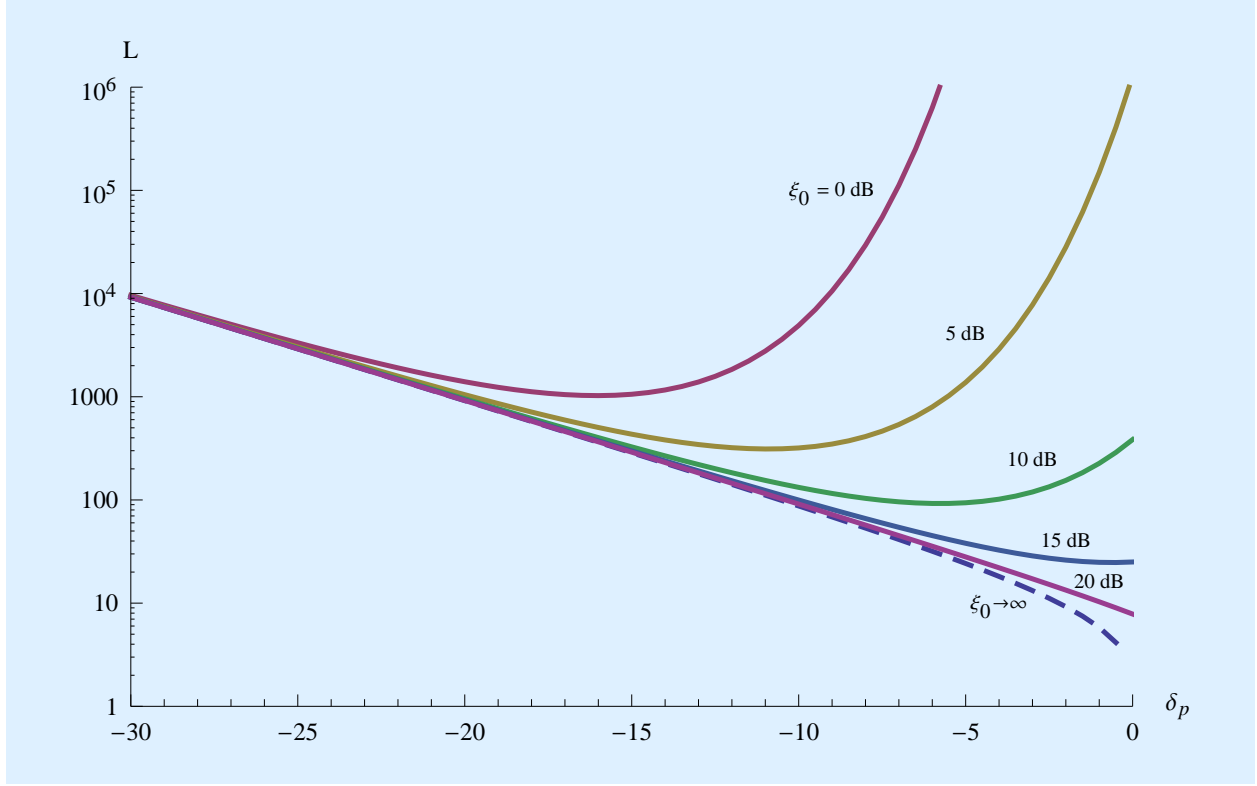


Figure 6.8: For the minimum per-observation window, a log plot of the number of observations L vs the transmit duty factor δ_p in dB. The right endpoint is the Cyclops beacon with 100% duty factor ($\delta_p = 0$ dB). For each curve, the average power \mathcal{P} is kept fixed as δ_p is reduced. For all the plots, the reliability is fixed at $P_{FA} = 10^{-12}$ and $1 - P_D = 10^{-4}$. The different curves correspond to different values of \mathcal{P} (represented by energy contrast ratio ξ_0 in dB at $\delta_p = 1$). The dashed curve is the lower bound on L from (6.9) that captures only misses attributable to $\delta_p < 1$. The duration of each observation is $T_o = 2T$ ($\delta_o = \delta_p$).

energy contrast ratio of approximately $\xi_s = 14$ dB for each energy bundle.

The bundle energy hypothesis predicts that $\delta_p \propto \xi_0$, of course with the constraint that $\delta_p \leq 1$. The optimum value of δ_p (the minimum of the curves in Figure 6.8) as a function of ξ_0 is shown in Figure 6.9, where we see that it closely adheres to this hypothesis. As one anchor, the optimum duty factor is $\delta_p = 3.0\%$ at $\xi_s = 0$ dB.

The bundle energy hypothesis is verified in a more direct way in Figure 6.10. When energy contrast ratio ξ_s is plotted, in the low-power regime it is approximately constant at $\xi_s \approx 15$ dB. In view of Figure 6.3 this is not surprising, since an ξ_s on this order is required to obtain even a 50% detection probability P_D . This is due to the scintillation, which adds another source of randomness that adds to the randomness of the noise. The small variation that does exist is in the opposite direction than we might expect, toward higher ξ_s as δ_p (and hence \mathcal{P}) decreases. Of course $\xi_s \propto \xi_0$ in the high-power region since $\delta_p = 1$ is fixed.

The effect of reducing the duty factor on the number of observations L is illustrated in Figure 6.11. In the low-power regime, the effect of using a low transmit duty factor is quite dramatic. For

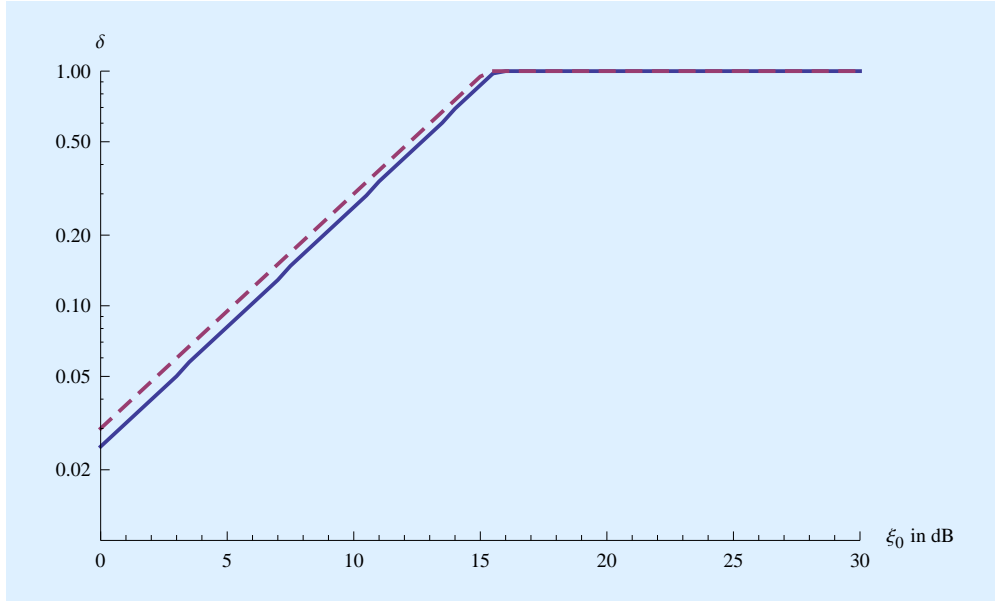


Figure 6.9: A log plot of the optimum duty factor δ_p as a function of the beacon average power (represented by ξ_0 in dB) for the same conditions as in Figure 6.8. At $\xi_0 = 0$ dB, the optimum value is $\delta_p = 0.030$ (3%). The value of δ_p predicted by the bundle energy hypothesis ($\delta_p \propto \xi_0$) is shown as the dashed line.

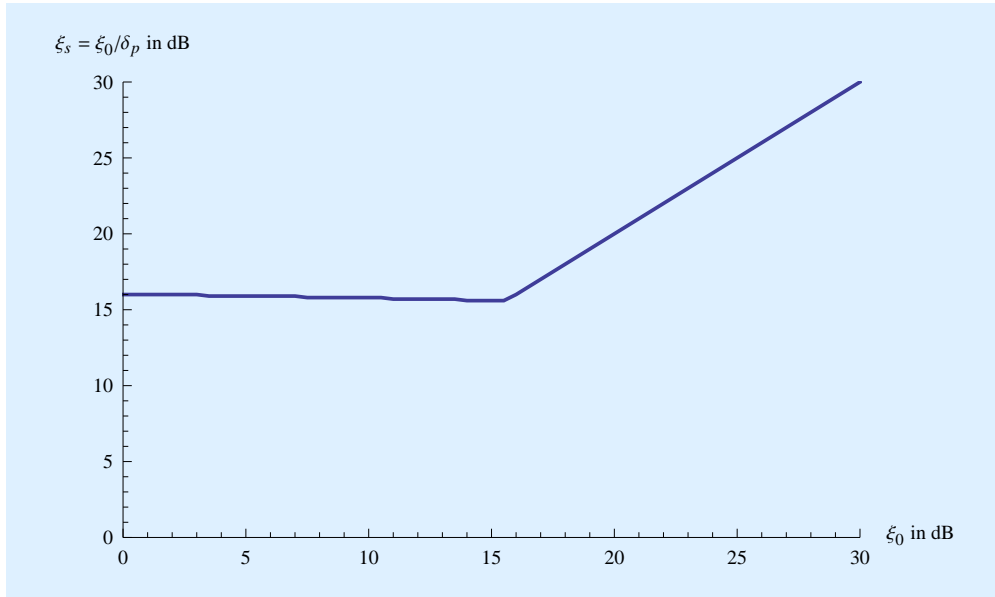


Figure 6.10: For a beacon power-optimized for detection, the energy contrast ratio $\xi_s = \xi/\delta$ in dB is plotted against ξ_0 in dB (which represents the beacon average power \mathcal{P}). This is a repeat of Figure 6.9, except it plots ξ_s rather than δ_p . At lower powers, where $\delta_p < 1$, ξ_s is approximately constant as predicted by the bundle energy hypothesis. For larger powers, where the duty factor saturates at $\delta_p = 1$, the only way to increase the average power \mathcal{P} is to increase \mathcal{E}_s .

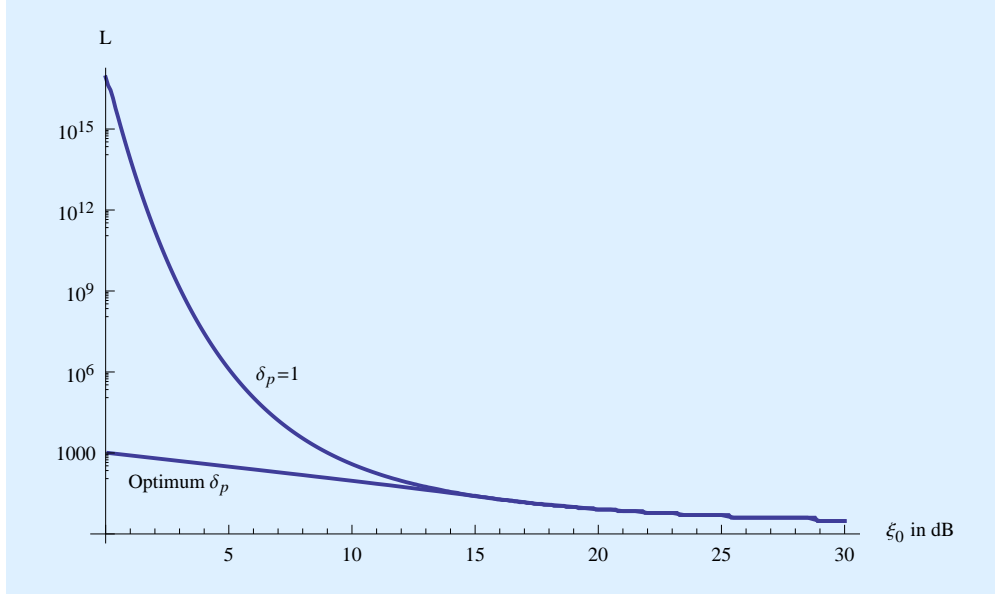


Figure 6.11: A log plot of the number of observations L required to achieve the same performance parameters as Figure 6.8 vs the average beacon power (represented by ξ_0 , which is the energy contrast ratio for a Cyclops beacon with the same average power). This is shown for both a Cyclops beacon with 100% duty factor ($\delta_p = 1$) and for the optimum duty factor δ_p .

example, at $\xi_0 = 0$ dB, the value of L is reduced by about 12 orders of magnitude (to $L = 848$) by reducing the duty factor from $\delta_p = 1$ to $\delta_p = 0.03$ (3%). Clearly it is not practical to discover a Cyclops beacon at this low power, but reducing the duty factor to 3% saves the day as long as the receiver is willing to implement hundreds of independent observations. An alternative way to quantify the effect of duty factor is to measure horizontally rather than vertically. The reduction in signal power that is possible for a fixed $L = 848$ observations attributable to reducing the duty factor is 8.3 dB, or an 85% reduction in average beacon power.

The level of reliability that is demanded in the detection of a beacon has an impact on the required L as illustrated in Figure 6.12. If a lower reliability is demanded (larger P_{FA} and smaller P_D), this naturally reduces the required L . The prediction of the total effective energy hypothesis that $L \propto 1/\xi_0$ (modified slightly so that $L \rightarrow 1$ as $\xi_0 \rightarrow \infty$) is shown by the dashed line. Notably, however, the total effective energy hypothesis is only valid if δ_p is chosen optimally, or in other words the bundle energy hypothesis is applied simultaneously.

The overall conclusion is that imposing a multiple-observation requirement on the receiver can have a dramatic impact in reducing the required transmit power. For the detection reliability parameters $\{P_{FA}, P_D\}$ chosen in Figure 6.8, increasing the number of observations from $L = 10$ to $L = 831$ reduced the required average transmit power by 17 dB, or a linear factor of about 50. The transmitter designer may view this imposition on the receiver as relatively modest in light of its 50 \times reduction in average transmitted power, especially since it is the receiver that derives all the value from successful beacon discovery. A second conclusion is that a low duty factor δ_p is required in the transmitter if L is to be kept to a reasonable level in the low-power regime. Of

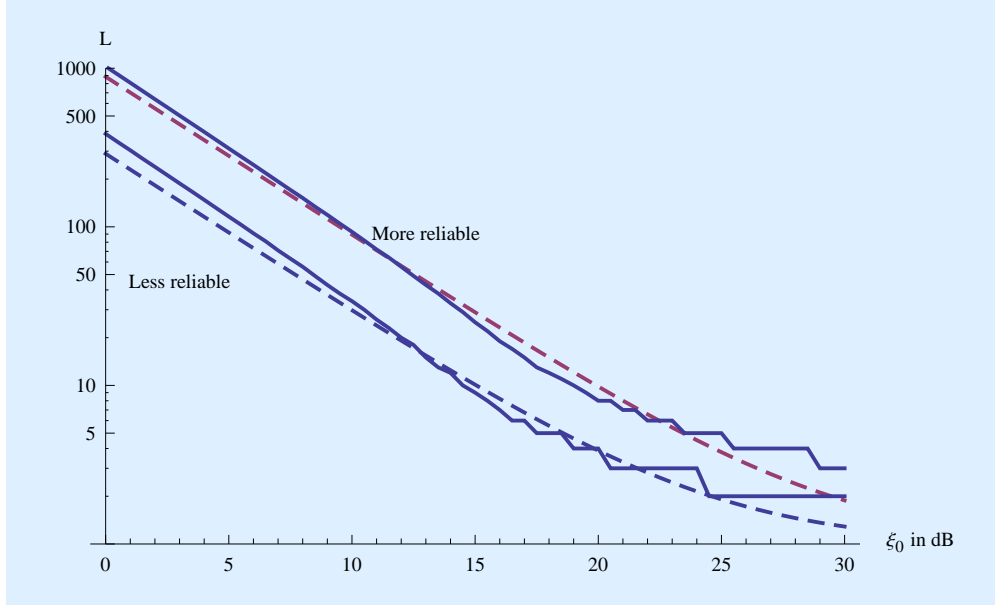


Figure 6.12: Figure 6.11 is repeated showing only the number of observations required when the transmit duty factor δ_p is optimized to minimize L . Two levels of reliability are shown: "More reliable" is $P_{FA} = 10^{-12}$ and $P_D = 0.9999$ (the same as in Figure 6.8) and "Less reliable" is $P_{FA} = 10^{-8}$ and $P_D = .99$. Smaller L results in reduced reliability. The dashed lines illustrate the prediction of the total effective energy hypothesis that $L \propto 1/\xi_0$.

course small δ_p in itself implies a relatively large L , so there is no avoiding a relatively large L for low-power beacons. Indeed, past and present SETI searches would have a negligible hope of success in discovering a beacon power-optimized for discovery in the low-power regime.

Long duration per observation

The preceding results assumed the shortest possible duration of interest for a single observation, $T_o = 2T$. The number of observations L can be dramatically reduced by extending the duration of each individual observation as shown in Figure 6.13. In this case, where $T_o = T_p + T$, L decreases monotonically as the transmit duty factor δ_p decreases. This suggests that if the receiver is going to make long individual observations, the transmitter should choose the smallest duty factor possible. However, this is misleading because in this case the total observation time may be a better indicator of the processing resources required by the receiver than the number of observations. When the total observation time is plotted in Figure 6.14, the result is very similar to the short individual observation in that the optimum duty factor δ_p is about the same. The conclusion is that the transmitter designer can safely choose its duty factor according to the average power and energy consumption objective without consideration of the receiver's strategy of using a small T_o with large L vs large T_o with small L .

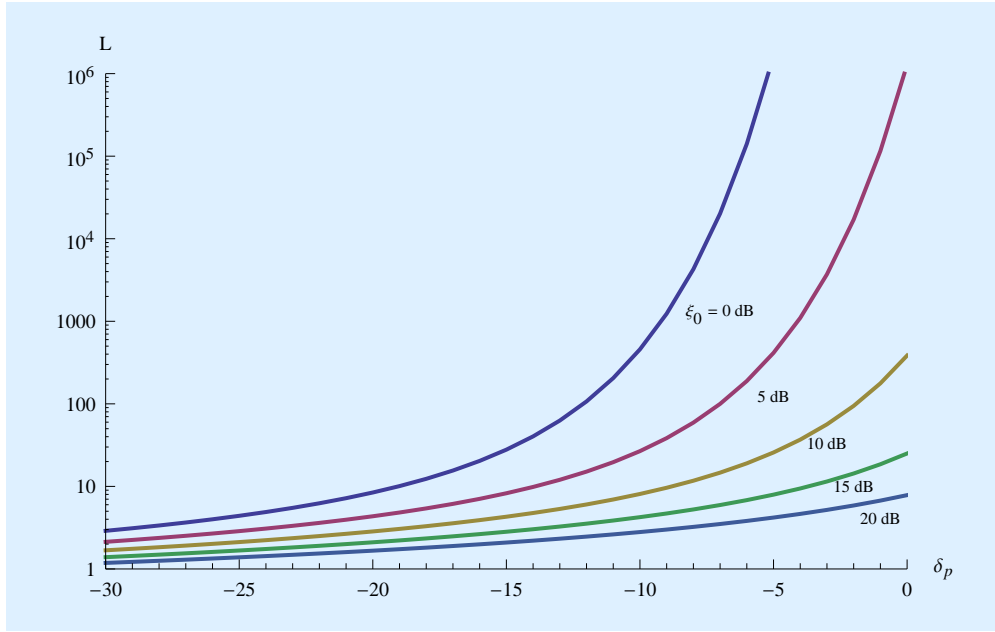


Figure 6.13: Figure 6.8 is repeated for the longest duration of each individual observation of interest, $T_o = T_p + T$ ($\delta_o = 1$). The number of observations L is dramatically reduced for small δ_p because the duty-factor effect on L is eliminated.

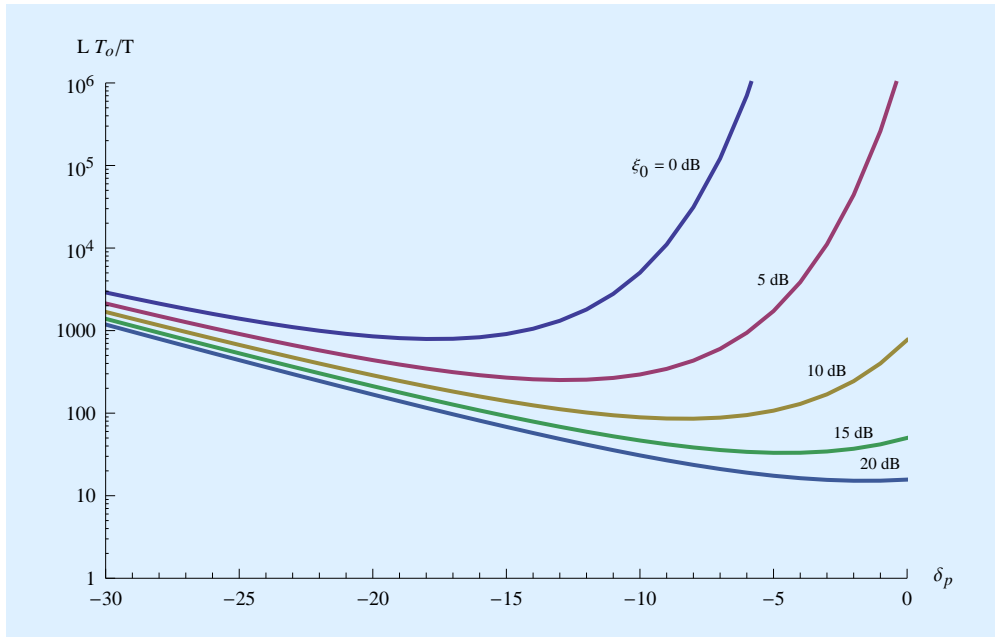


Figure 6.14: Figure 6.13 is repeated, except that the vertical axes is not L , but rather the total observation time $L T_o$ normalized by the duration of one energy bundle T . With respect to minimization of the total observation time, the optimum value of δ_p is about the same as in Figure 6.8.

6.2.8 Uncoordinated periodic beacon design

The previous comparisons have assumed the joint optimization of the beacon parameters. In practice, the responsibility for choice of parameters is divided between transmitter and receiver without coordination. It is the transmitter that determines the parameters $\{T, T_p\}$, and it is the receiver that chooses the parameters $\{T_o, L\}$. Both the transmitter and receiver designers have influence over the energy contrast ratio ξ_s of each energy bundle, the transmitter through choice of the transmit energy per bundle (which is related to the peak transmitted power $\mathcal{P}_{\text{peak}}$) and transmit antenna gain, and the receiver through choice of the receive antenna collection area. Thus neither transmitter nor receiver has unilateral control over the reliability with which individual energy bundles can be detected.

The partitioning of decision making can be characterized as follows:

Common knowledge. The one parameter the transmitter and receiver can agree on (with some remaining degree of uncertainty) in the duration T of an energy bundle. The receiver designer can reasonably assume that the transmitter wishes to minimize the peak transmitted power, and will thus choose $T = T_c$, the coherence time of the interstellar channel. Since T_c is based on observable physical parameters, we can expect some consistency between the transmitter's and receiver's assumptions as to T_c .

Transmitter designer's assumptions. The transmitter must make assumptions about the *minimum* resources devoted by the receiver. In particular, a combination of (a) the propagation loss (based on knowledge of the distance), (b) the minimum assumed receive antenna collection area, and (c) an assumption as to the maximum noise power spectral density N_0 at the receiver together determine the required transmitted energy per bundle. In particular, the bundle energy hypothesis determines that these parameters collectively must yield an energy contrast ratio ξ_s at the receiver of about $\xi_s \approx 14$ dB or higher.

The transmitter also controls the average transmitted power through a choice of beacon period T_p . The transmitter can make this power as small as it wishes, but must recognize that while a larger T_p beneficially decreases the transmit power, it also imposes a requirement that the receiver devote a longer total observation time $L \cdot T_o$ commensurate with that lower power. Thus, in making a choice as to transmitted power, an assumption is being made about the minimum observation time devoted by the receiver.

Consequences of receiver designer's choices. In general if the receiver makes resource decisions that exceed the minimum assumptions of the transmitter, the beacon will be detected with high reliability. Otherwise, the beacon is unlikely to be detected. First, the receiver must choose a large enough receive antenna collection area to achieve a sufficiently large energy contrast ratio ξ_s for each energy bundle. Second, the receiver must choose the duration T_o that is compatible with the transmitter's choice of T . Generally this will be the easiest choice the receiver has to make, since $T_o = 2 T_c$ will work well for all transmitter choices of T_p without affecting the total observation time. Third, the receiver must also choose a sufficiently large number of observations L to accommodate the observation duty factor δ_o , which is determined by $\{T, T_p, T_o\}$. Otherwise, again, the beacon is unlikely to be detected.

This is a worst-case design methodology used to overcome the lack of explicit coordination. The receiver makes an assumption about the minimum receive signal flux of the beacon, and how that flux is partitioned between energy per bundle \mathcal{E}_h and bundle repetition period T_p . The receiver will be successful at detecting the beacon if these assumptions are met or exceeded, and is unlikely to be successful otherwise. Figure 2.12 ($K = 1000$ was assumed) illustrated the tradeoff between transmit resources (average power) and receive resources (processing, but not antenna capture area), making the unrealistic assumption that the transmitter and receiver designs are coordinated. A more realistic scenario is presented in Figure 6.15 with the assumption that the beacon and observation parameters are given by

$$\mathcal{P} = \frac{\mathcal{E}_h}{T_p} \quad \text{or} \quad \zeta_s = \frac{\zeta_0}{\delta_p} \quad \text{for} \quad \zeta_0 = \frac{\mathcal{P} T}{N_0} \quad (6.30)$$

$$T_o = 2 T \quad \text{or} \quad \delta_o = \delta_p \quad (6.31)$$

$$N = 2 L K. \quad (6.32)$$

This assumes the minimum duration of each observation, thus relying on a larger number of observations L rather than a longer observation time T_o to compensate for a lower beacon power. The energy contrast ratio ζ_0 corresponds to a Cyclops beacon with 100% duty factor ($\delta_p = 1$) with the same¹ \mathcal{P} .

In Figure 6.15 it is assumed that the transmitter has reduced the transmit signal power by 15.2 dB (97%) relative to the Cyclops beacon design by choosing a 3% duty factor ($\delta_p = 0.03$). The receiver is not cognizant of this choice, but is using an antenna with sufficiently large capture area to achieve the optimum received energy contrast ratio ζ_s . We then examine the consequences of using different values of L . This illustrates that the receiver gets what it pays for, with increased detection reliability when it devotes more processing resources to a larger number of observations L . The transmitter design envisioned that $L = 1000$ could achieve a miss probability of 10^{-4} at $\zeta_0 = 0$ dB. In fact, as long as $L \geq 305$, the receiver can achieve that same miss probability, but it does require a larger ζ_0 and hence a larger receive antenna collection area. In this case, the receiver can trade off less processing overhead for a larger antenna, or vice versa. On the other hand, if the receiver implements $L = 3$ (as if this was a high-power 100% duty factor Cyclops beacon) it has virtually no chance of detection even at considerably higher power levels than required for a 100% duty factor Cyclops beacon (which corresponds to $\zeta_0 \approx 15$ dB). This is because so few observations fail to compensate for the low 3% duty factor, no matter how large the receive antenna collection area.

Overall the conclusion is that the transmitter has two ways to reduce its average transmit power, each imposing an additional resource burden on the receiver. First, average power can be reduced significantly (with no reduction in peak power) by reducing the duty factor δ_p , if the receiver compensates for this by a commensurate increase in its total observation time (as represented by L in case of the minimum duration of each observation). Second, both average and peak transmit power can be reduced by decreasing the energy per bundle \mathcal{E}_h , if the receiver compensates by increasing its antenna collection area.

¹ The horizontal axis of Figure 2.12 was also ζ_0 , although it wasn't necessary to mention that level of detail in Chapter 2 where only a relative comparison was being made.

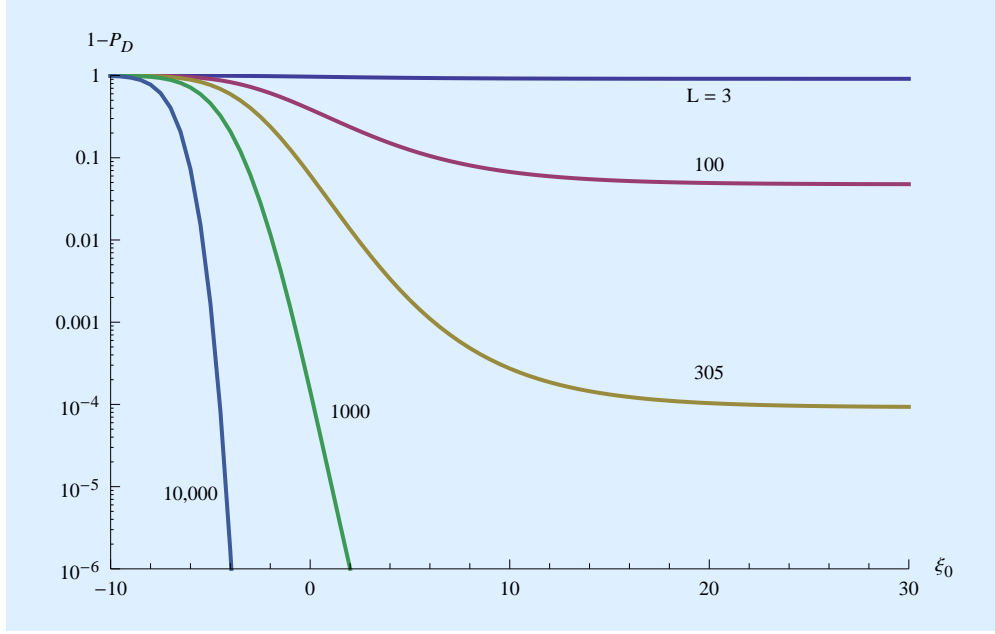


Figure 6.15: A log plot of the miss probability ($1 - P_D$) vs the energy contrast ratio ξ_0 of a Cyclops beacon with 100% duty factor at the same average power. Each curve thus represents how the reliability in detection of the beacon varies with the average received power \mathcal{P} . It is assumed that the transmitter has chosen a 3% duty factor of ($\delta_p = 0.03$) and the receiver has chosen the minimum duration for each observation ($T_o = 2T$, which results in $\delta_o = 0.03$). The different curves represent different numbers of observations L . $L = 1000$ is more than sufficient to achieve a $1 - P_D = 10^{-4}$ at $\xi_0 = 0$ dB. The lower bound of (6.9) predicts that the same reliability can be achieved for large ξ_0 with $L = 305$. The remaining choices of L illustrate that detection reliability is improved with larger L and deteriorates if L is chosen to be too small.

6.3 Discovery of information-bearing signals

The previous section simplified the problem of discovery by specializing to a beacon consisting of a periodic sequence of energy bundles, and then power-optimizing that beacon by adjustment of the duty factor and energy per bundle. This does not address directly the question of discovery of information-bearing signals. However, information-bearing signals of the type considered in Chapter 5 have a similar structure. They consist of a sequence of codewords, each of which conveys $\log_2 M$ bits of information by transmitting an energy bundle in one of M locations in time or frequency. By adjusting the rate at which these codewords are transmitted, the total information rate \mathcal{R} and average power \mathcal{P} can be adjusted in direct proportion to one another.

Note the parallel to adjusting the duty factor of a beacon. Each codeword consumes the same energy (adhering to a bundle energy hypothesis), but the power is adjusted by choosing a rate at which to transmit a codeword (equivalent to an adjustment in duty factor) as described in Section 5.2.3. Thus, it is no surprise that discovery of power-efficient information-bearing signals of the type considered in Chapter 5 is essentially the same challenge as the discovery of beacons that are power-optimized for discovery. The same tradeoff exists between transmitter and receiver resource allocation. The average transmit power \mathcal{P} can be reduced by a commensurate reduction

in information \mathcal{R} , and the most efficient possible way of doing this is to reduce the rate at which codewords are transmitted, which is equivalent to reducing the duty factor. The average and peak transmitted power $\mathcal{P}_{\text{peak}}$ can both be reduced by reducing the transmitted energy per bundle, but a certain level of energy per bit \mathfrak{E}_b and hence energy per bundle must be maintained in the receiver to achieve reliable extraction of information from the signal, and the receive antenna collection area has to be large enough to achieve this.

In contrast to a beacon, the objective is not only to discover the signal but also to extract information from it during the communication phase. These two challenges are considerably different, but normally the average received power \mathcal{P} will be the same, unless the receive antenna is changed out in the transition from discovery to communication. There are two very different interpretations of this common value of \mathcal{P} . The difference can be summarized as follows:

Discovery. \mathcal{P} relates to the number of independent observations L required to detect a signal of interest. The smaller \mathcal{P} , the larger the required L , and at all but very high average powers L must be relatively large (tens to hundreds). This large L is required for two reasons. First, the receiver has no idea where an energy bundle may occur, so much of the time it is observing during blank periods in the duty factor when there is no energy bundle present. Second, the receiver has no idea as to the current state of scintillation, so much of the time it is observing during periods of low received flux due to scintillation.

Communication. During communication the receiver has two major advantages. First, it is aware of the structure of the signal, and will observe only at times when codewords are present. The presence or absence of energy bundles at these times is determined by the random information bits being communicated. Second, it can form an estimate of the current level of received flux, and observe only during periods of non-outage (if an outage strategy is in use). Thus, it is not disadvantaged by the periods of low received flux in the same way as discovery. The value of \mathcal{P} is thus determined by the reliability with which the presence or absence of an energy bundle can be detected by a *single* observation at the threshold of outage. That outage threshold corresponds to a receive flux equaling its average value, which is the same value as it would have in the absence of scattering and scintillation.

From this comparison, it is not clear whether a larger \mathcal{P} is required during discovery or during communication. There are arguments in favor of both outcomes. During discovery, detection is based on multiple observations, and during communication it is restricted to a single observation. This favors discovery, as the receiver can always increase the observation time $L \cdot T_o$ to reduce the required \mathcal{P} . During communication, the receiver may discard periods when the received flux is below average as outages, and thus scintillation is aided by consistent amplification of the received flux during periods of non-outage.

These competing factors can only be resolved by a quantitative comparison of the two cases. An M-ary FSK signal is essentially identical to a periodic beacon with the same duty factor, in that energy bundles occur in a regular periodic factor with a duty factor δ determined by the information rate \mathcal{R} , which is also proportional to the average power \mathcal{P} . The one difference between a periodic beacon and an FSK signal is that these periodic energy bundles will be positioned at one of M frequencies, and that frequency will vary randomly (in accordance with the embedded

information) from one codeword to the next. A discovery search algorithm that examines only one carrier frequency at a time will thus see energy bundles that are not uniformly spaced, but rather occur randomly at those uniformly spaced positions but with a density that is a factor of M lower. This would have a substantial effect on detection, according to the total effective energy hypothesis increasing the number of observations L by a factor of M to maintain the same detection reliability (since the energy per bundle does not change with M). In practice, however, a discovery search will typically be conducted by a multi-channel spectral analysis combined with matched filtering to $h(t)$. Thus discovery can proceed in essentially the same manner as for a periodic beacon, with one modification. Rather than defining a detection at one frequency, it can be defined as a detection at any frequency within a range of M frequencies. This will affect the reliability parameters $\{P_{FA}, P_D\}$, because the receiver is observing in more places. The effect is fairly minor, however.

For purposes of discovery, a power-efficient information-bearing M -ary FSK or PPM signal possesses three parameters $\{\xi_s, M, \delta_p\}$ that together determine the tradeoff between detection reliability P_D and the observation time $L \cdot T_o$ for a given false alarm probability P_{FA} . On the other hand, the reliability of information extraction at the threshold of outage is measured by the error probability P_E , and in Chapter 5 this is shown to be determined by $\{\xi_b, M\}$ in (5.11), where ξ_b is the energy contrast ratio per bit ξ_b measured at the threshold of outage. The duty factor δ has no relation to the reliability of information recovery, but it does determine the information rate \mathcal{R} as described in Section 5.2.4. As shown in Chapter 5, the flux at the outage threshold is equal to the average flux, and thus $\xi_b = \xi_s = \xi_s / \log_2 M$. Thus, from (5.11) the parameters of the FSK signal for purposes of discovery are

$$\xi_s = 2 \log_e \left(\frac{M}{4 P_E} \right) \quad (6.33)$$

$$N = 2 L K M. \quad (6.34)$$

The most important characteristic of an information-bearing signal for discovery is ξ_s , because it determines the probability of detection of an individual energy bundle, as was illustrated in Figure 6.3. The bundle energy hypothesis predicts that ξ_s should remain fixed as duty factor δ_p is varied, and later numerical results (for a particular target P_{FA} and P_D) confirm this hypothesis and indicates that $\xi_s \approx 14$ to 15 dB offers the best tradeoff between misses due energy bundles that go undetected and observations that do not overlap an energy bundle. Any smaller value causes an undue increase in L due to misses, and any larger value wastes energy on each bundle. As an alternative way to view this tradeoff from Figure 6.3, ξ_s is plotted for different values of M and P_E in Figure 6.16. As expected, ξ_s increases with M and as higher reliability in information extraction (measured by P_E) is required. Figure 6.16 reveals that for most cases, there is a pretty close alignment between the energy per bundle (as reflected in the energy contrast ratio ξ_s) desired for discovery and for information recovery. This is not a surprising result, since both functions require the detection of an individual energy bundle, and (for the chosen reliability parameters) a detection reliability that is comparable.

Another difference between a periodic beacon and an FSK signal is the number of locations where energy bundles may occur. In the case of an M -ary FSK signal, that number of locations is M times

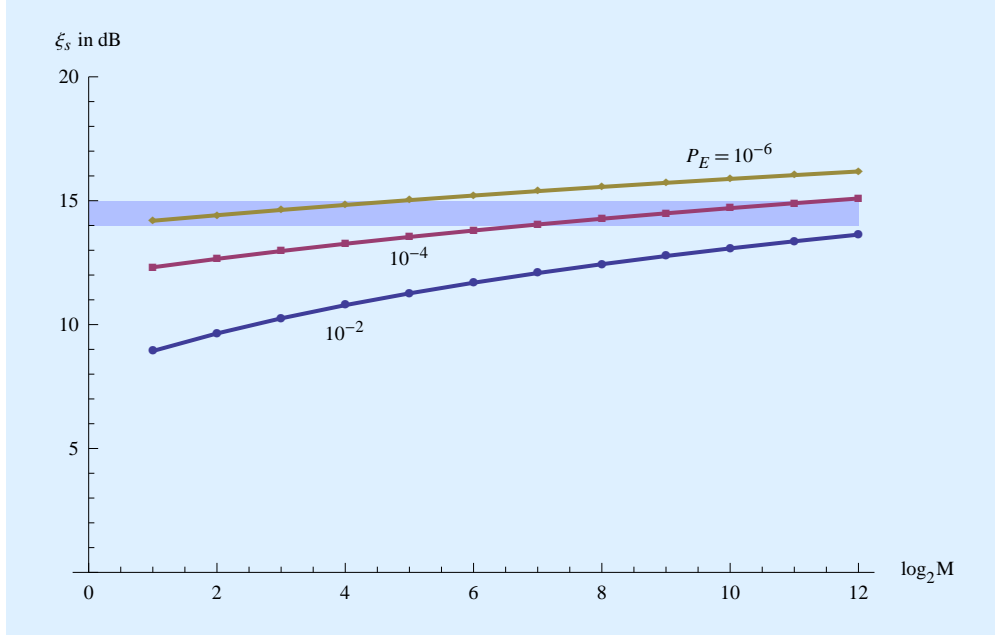


Figure 6.16: For an M-ary FSK signal, a plot of the energy contrast ratio ξ_s for each energy bundle vs. M . Several values of probability of error P_E are plotted. The shaded rectangle corresponds to $\xi_s = 14$ to 15 dB, which is an ideal value to minimize the signal average power \mathcal{P} . Any higher value of ξ_s makes inefficient use of bundle energy from a discovery standpoint, and any lower ξ_s requires a substantial increase in the number of observations L .

larger, and this will increase the false alarm probability P_{FA} relative to a beacon. In particular, this increases the value of N , and a larger N will increase somewhat the number of observations L required to achieve a given $\{P_{FA}, P_D\}$. Thus discovery of an M-ary FSK signal needs to be examined more fully than simply comparing the detection reliability for a single energy bundle. The first question is how many observations are required to reliably detect the FSK signal with an average power \mathcal{P} that is sufficiently high to reliably extract information from that signal after it is discovered. Since $\mathcal{P} \propto \mathcal{R}$, signals with a larger information rate \mathcal{R} will be easier to discover (in the sense of requiring a smaller L). Figure 6.17 shows how L is related to the miss probability $(1 - P_D)$ for a single-carrier signal with the highest possible \mathcal{R} ($\delta = 1$) for a single carrier. For example, on the order of $L = 50$ suffices for $M = 2^8$. This is a much smaller L than often required to discover a power-optimized beacon in general (see Figure 6.12), because this large- \mathcal{R} signal has relatively high average power \mathcal{P} and, commensurate with that, a $\delta = 100\%$ duty factor.

The dependence on M in Figure 6.17 predicts that signals become easier to discover as M increases. This reflects a tradeoff between larger energy per bundle \mathcal{E}_h (to maintain a fixed energy per bit) as M increases, against a larger $N \propto M$ to account for the larger number of locations to look for energy bundles. This tradeoff is explored in more detail in Figure 6.18. Increasing M can decrease the miss probability over a range of one to two orders of magnitude. The net effect of increasing M is favorable for discovery as well as for power efficiency, but of course also increases average power $\mathcal{P} \propto \log_2 M$.

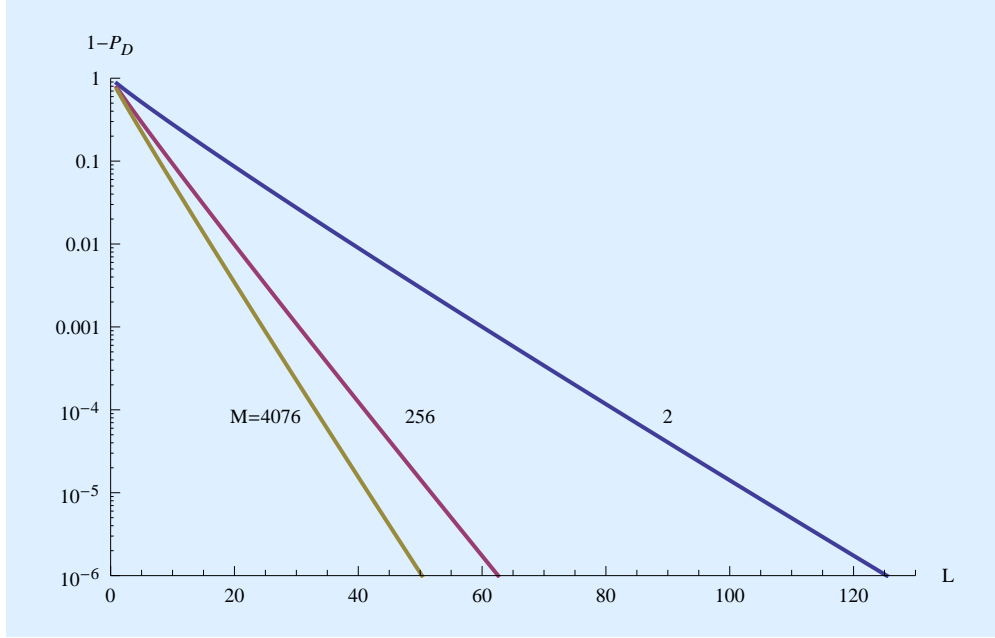


Figure 6.17: For an information-bearing M-ary FSK or PPM signal, a log plot of the detection miss probability ($1 - P_D$) vs the number of observations L for $M = 2, 2^8$, and 2^{12} . The highest power \mathcal{P} and rate \mathcal{R} for a single carrier is assumed ($\delta_p = 1$), an observation duration of $T_o = 2T$ ($\delta_o = 1$), a false alarm probability of $P_{FA} = 10^{-12}$, and a degrees of freedom $K = 1000$. The average power \mathcal{P} is chosen to be sufficiently high to extract information from the signal at the threshold of outage with error probability $P_E = 10^{-4}$.

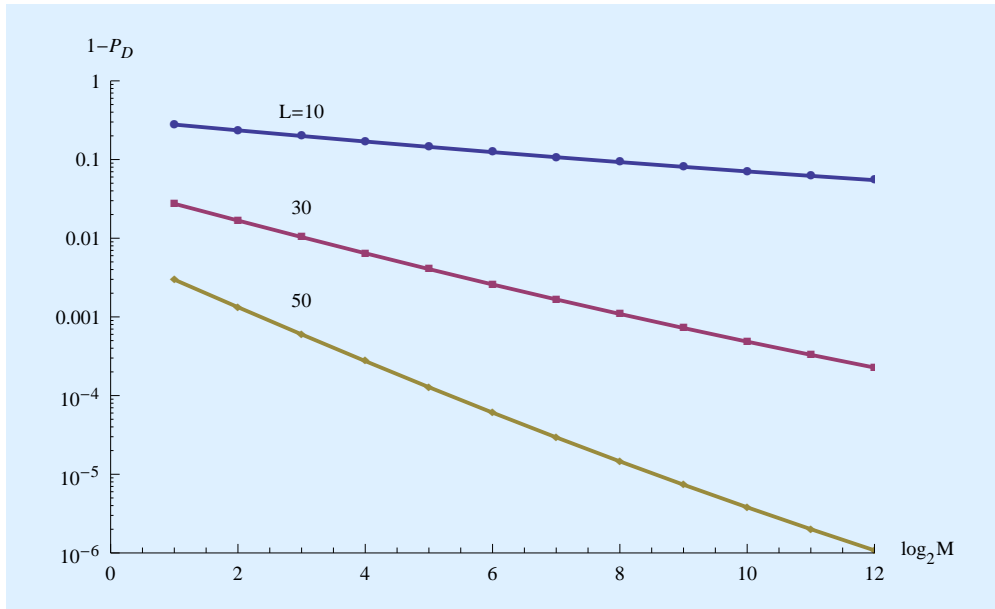


Figure 6.18: A log plot of the miss probability ($1 - P_D$) vs the number of bits per codeword $\log_2 M$ for several values of L . The other conditions are the same as in Figure 6.17.

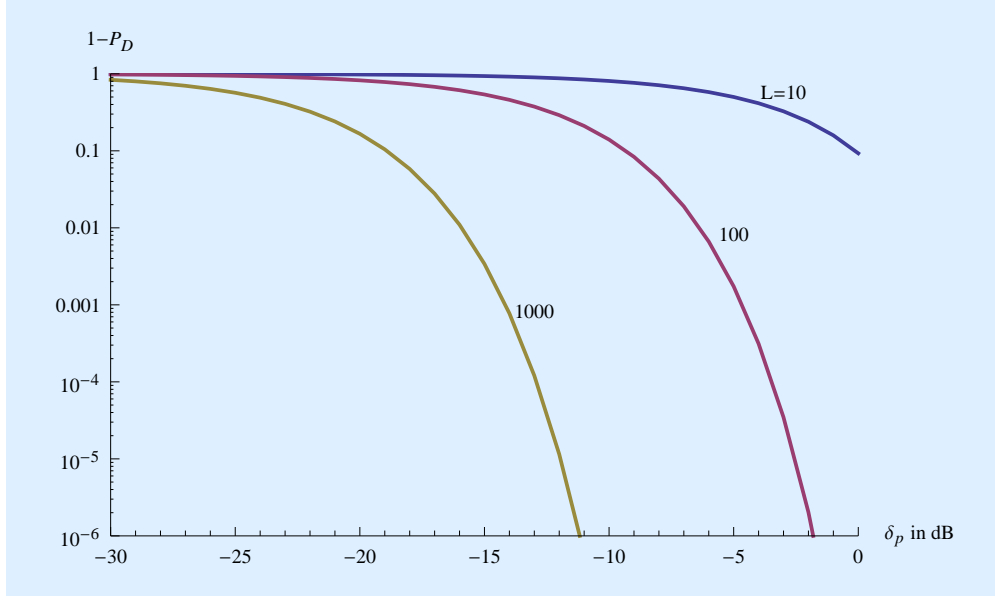


Figure 6.19: A log plot of the miss probability ($1 - P_D$) vs the duty factor δ_p in dB for several values of $L = 80$. As δ_p is reduced, the information rate also decreases as $\mathcal{R} \propto \delta_p$. Thus, a 10 dB reduction in δ_p reduces \mathcal{R} by one order of magnitude. It is assumed that $M = 2^8$, and the remaining conditions are the same as in Figure 6.17. Smaller δ corresponds to smaller average signal power $\mathcal{P} \propto \delta_p$.

The preceding applies to an information rate \mathcal{R} (and hence power \mathcal{P}) that is the highest possible for a single carrier. The impact of reducing \mathcal{R} is shown in Figure 6.19. Reducing the rate by reducing δ_p renders discovery less reliable, which is not surprising since the average signal power \mathcal{P} is being reduced in proportion to \mathcal{R} and δ_p . This illustrates how the transmitter can reduce its average transmitted power \mathcal{P} , paying two prices for this reduction. First, there is a proportional reduction in information rate \mathcal{R} , since at constant power efficiency $\mathcal{P} \propto \mathcal{R}$. Second, there is an increase in the number of observations L necessary in the receiver that is inversely proportional to the power, since by the total effective energy hypothesis $L \propto 1/\mathcal{P}$. Ordinarily one would think that reducing \mathcal{R} would reduce the required resources. That is a valid assertion for the transmitter, but with regard to the discovery phase and resources required in the receiver the effect is just the opposite.

Another tradeoff that should be kept in mind is between the transmitted energy per bundle and the receive antenna collection area in order to maintain a large enough \mathcal{E}_h in the receiver for reliable discovery and communication. What we have found is that the required \mathcal{E}_h is comparable for reliable discovery and for reliable communication, and thus it is appropriate to use approximately the same receive antenna collection area at both stages. Relatively modest adjustments may be appropriate, depending on the specific objectives for reliability. In particular, increasing the antenna size in moving from discovery to communication can dramatically reduce the probability of error P_E , which in turn makes the underlying message semantics easier to interpret. It may be relatively easy for the receiver designer to acquire additional resources at this stage, since the existence of a information-bearing signal of interstellar origin has been established.

6.4 Power-optimizing information-bearing signals for discovery

The discovery of periodic beacons and information-bearing signals have been considered separately, but with different emphasis. Beacons were examined from the perspective of achieving the lowest receive power \mathcal{P} consistent with a fixed number of observations L . Since a beacon has no purpose other than to be discovered, the sole design criterion is to minimize its power \mathcal{P} for a fixed L or equivalently minimize L for a fixed \mathcal{P} . Information-bearing signals have the additional objective of reliably conveying information, and a higher information rate \mathcal{R} is generally desirable if the resulting \mathcal{P} is affordable. Thus, aside from discovery there are two other criteria to consider, the achievable information rate \mathcal{R} and an energy per bit \mathcal{E}_b that is sufficient for reliable recovery of the information bits according to some error probability objective P_E . For any achievable power efficiency \mathfrak{P} , we know that $\mathcal{P} \propto \mathcal{R}$ and there is no lower limit on either \mathcal{P} or \mathcal{R} . Thus, at any target \mathcal{P} , there is both a beacon and an information-bearing signal with that average receive power. At a small \mathcal{P} , the information-bearing signal will have a commensurately low \mathcal{R} . The only remaining question is whether the information-bearing signal is as discoverable as the beacon, and in particular whether it requires the same or nearly the same L .

The manner in which we achieve a low $\mathcal{P} \propto \mathcal{R}$ as described in Section 5.2.3 is compatible with efficient discovery. Just as with the periodic beacon, $\mathcal{P} \propto \mathcal{R}$ is reduced by reducing the rate at which codewords are transmitted or equivalently reducing the duty factor δ . Consistent with the bundle energy hypothesis for a beacon, in order to preserve low P_E the energy per bit and hence the energy per bundle \mathcal{E}_h is kept fixed as the duty factor is reduced. As shown in Figure 6.16, that \mathcal{E}_h is comparable to a beacon, depending on M and the objective for P_E .

Starting with a periodic beacon, turning it into an information-bearing signal requires the fairly minor step of randomizing somewhat the location of energy bundles in either time or frequency. That randomization is keyed to the information being conveyed. This randomization need not affect the discovery of the signal much, since that discovery focuses on detecting energy bundles at random observation times, so some randomness in the time or frequency of the bundles added to the randomness of the observation times has little added impact. The randomness will inevitably increase the number of potential locations in time and/or frequency where an energy bundle can occur, but in the context of a multichannel spectral analysis this should not affect the false alarm probability.

6.4.1 M-ary FSK

The results of Chapter 5 can be reexamined from a discovery perspective. Suppose that an M-ary FSK signal is constrained to have an energy contrast ratio of $\zeta_s = 15$ dB, which is a good choice for discovery, and suppose that the outage strategy is used to deal with scintillation. What is the reliability of information extraction from such a signal, as measured by probability of error P_E ? For M-ary FSK the energy contrast ratio ζ_b required to achieve reliable information extraction is given by (5.11) and plotted in Figure 5.7. However, $\zeta_b = \zeta_s / \log_2 M$ is expressed in terms of the bundle energy per bit in an M-bit codeword. Expressing it instead in terms of the energy contrast

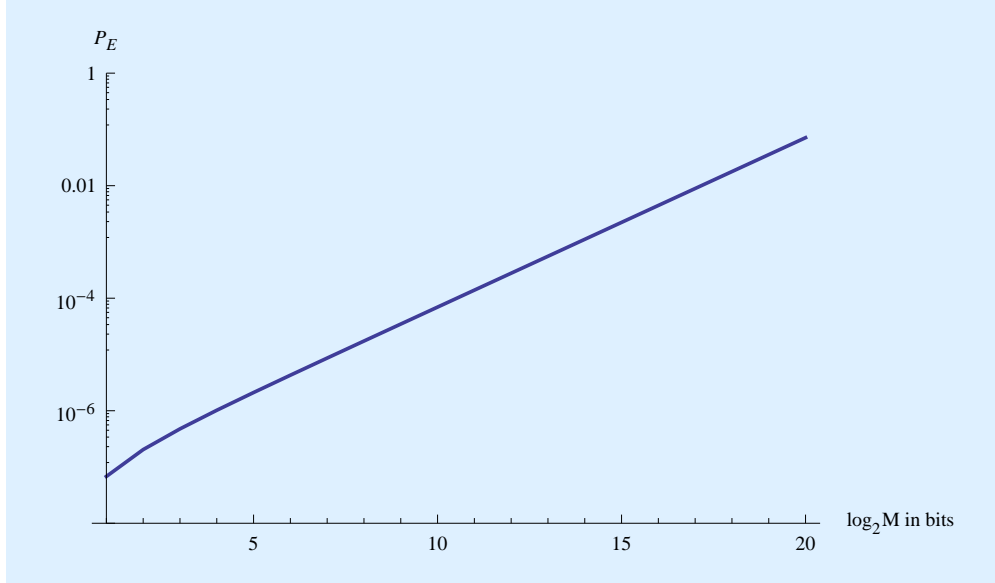


Figure 6.20: A log plot of the probability of bit error P_E vs the number of bits per codeword $\log_2 M$ between one and 20 for an energy contrast ratio $\zeta_s = 15$ dB. This applies to an M-ary FSK information-bearing signal that has been power-optimized for discovery for low-power case where the duty factor $\delta < 1$. The assumption $\zeta_s = 15$ dB applies approximately independently of the average power \mathcal{P} . At higher powers, P_E will decrease rapidly with average power \mathcal{P} for any value of M .

ratio ζ_s for the constituent energy bundles,

$$\log_2 P_E \leq \log_2 M - \frac{\zeta_s}{2 \log_e 2} - 2. \quad (6.35)$$

Thus $\log P_E$ is a linear function of $\log_2 M$, the number of bits per codeword.² The error probability is plotted in Figure 6.20. The error probability increases as M increases because the energy contrast ratio per bit ζ_b grows smaller. A physical explanation for this behavior is that as M increases there are more opportunities for noise in one or more of the $(M - 1)$ locations that lack energy bundles to mimic an energy bundle. The primary conclusion from Figure 6.20 is that information can be extracted with high reliability from an M-ary FSK signal that has been power-optimized for discovery. This is especially true in the regime $\log_2 M \leq 10$. For larger M , the required value of ζ_s grows larger, and this makes discovery more reliable, but it also becomes somewhat inefficient for discovery since smaller values of ζ_s would suffice.

In conclusion, in the context of power-efficient design, there is little reason to consider transmitting a beacon, since an information-bearing signal at the same power can be discovered as effectively at the receiver. However, if we want to match the low power that we might seek in a beacon, that information-bearing signal will have a low information rate commensurate with that low power. Further, a low information-rate \mathcal{R} signal will require a commensurately larger number

² Note that $P_E > 1$ for sufficiently large M . This is possible because this is merely an upper bound on P_E , and the bound is tight only when $P_E \ll 1$.

of observations. Low \mathcal{R} information-bearing signals are more difficult to discover than high \mathcal{R} , because they have lower average power \mathcal{P} .

6.4.2 M-ary FSK with time diversity

The bundle energy hypothesis tells us that efficient discovery occurs when the energy contrast ratio ξ_s of individual bundles is sufficiently large to enable their individual detection with a reasonably high probability P_D . In the absence of time diversity, using an outage strategy an M-ary FSK information-bearing signal with sufficient average power to reliably extract its information consists of individual energy bundles that meet this criterion. There is an issue, however, when time diversity is added to the mix. A variation of the total energy hypothesis confirmed in Section 5.1.2 predicts that the required energy of each bundle decreases as the number of time diversity copies of that bundle is increased, or $\mathcal{E}_h \propto 1/J$. This is because the diversity combining in the receiver “gathers up” all this energy in J copies, maintaining detection reliability.

This allowed reduction in \mathcal{E}_h creates a challenge for discovery. To fully benefit from this energy in J copies, the discovery strategy would have to include diversity combining, which would introduce a whole new dimension to the discovery search. This added dimension would substantially increase the processing requirements, and more importantly increases the false alarm probability. Is there an alternative? Yes, there is. Although it entails a penalty in average power, the transmitter can deliberately use a larger energy than necessary (from an information extraction perspective) for one or more of the energy bundle copies, choosing that energy to be sufficiently large for those individual high-energy bundles to be efficiently detected. While this higher energy actually aids information extraction as well as discovery, this is inefficient because the higher-energy bundles overlap periods of lower received signal flux due to scintillation. The result is that this approach will increase the penalty in average power relative to the fundamental limit.

To quantify this effect, assume that the total degree of time diversity is $J = J_0 + J_1$, where J_0 is the number of replicas of the FSK energy bundle with energy contrast ratio $\xi_{s,0}$, and J_1 is the number with ratio $\xi_{s,1}$. Assume that $\xi_{s,0} > \xi_{s,1}$ because $\xi_{s,0}$ is chosen to enable efficient discovery of those J_0 energy bundles, while $\xi_{s,1}$ is chosen so that the total energy is sufficient to insure subsequent reliable extraction of information from the signal using time diversity combining. It follows that the energy contrast ratio per bit ξ_b is

$$\xi_b = \frac{J_0 \xi_{s,0} + J_1 \xi_{s,1}}{\log_2 M}. \quad (6.36)$$

An upper bound on the bit error probability P_E is determined in Appendix F.3, and plotted in Figure 6.21 for one typical value of M and J . Choosing one energy bundle (out of J) to have sufficiently large energy to permit reliable discovery creates a fraction of a dB penalty in average power. This penalty is multiplied as a larger number of energy bundles are chosen to have the larger power, thereby reducing the number of observations necessary in the receiver for reliable detection.

The penalty relative to the fundamental limit is fairly modest. If time diversity is employed to counter scintillation while minimizing average power, there is little alternative to this approach.

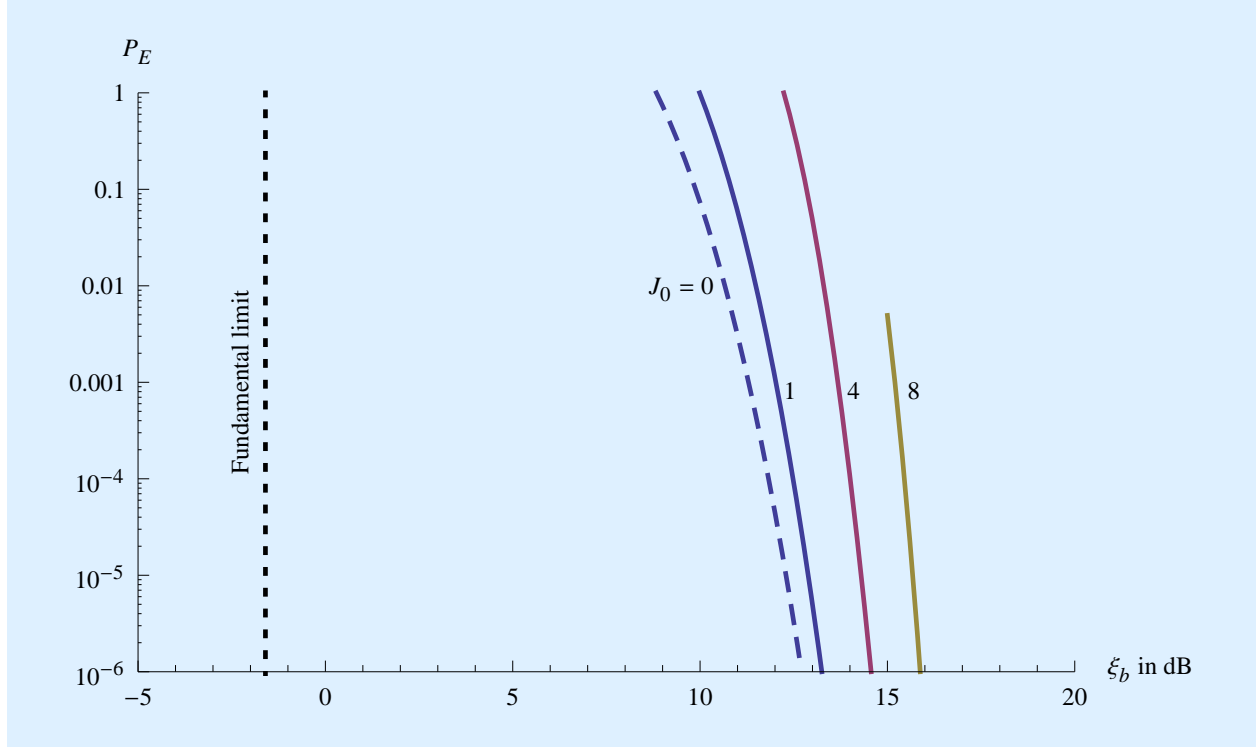


Figure 6.21: A comparison of an upper bound on the bit error probability P_E for M -ary FSK with time diversity, not optimized for discovery (dashed curve) and optimized for discovery (solid curves) with some penalty in average power relative to the fundamental limit. In all cases $M = 2^8$ and $J = 2^7$, and P_E is shown as a function of the energy contrast ratio per bit ξ_b . The dashed curve assumes all energy bundles have identical energy contrast ratio ξ_s , or $J_0 = 0$ and $J_1 = J$. The solid curves show the penalty in ξ_b for making $J_0 = 1, 4$ and 8 , where J_0 is the number of energy packets out of $J = 2^7$ that have sufficiently large energy ($\xi_{s,0} = 15$ db) to be more easily discovered. The value of $\xi_{s,1}$ is inferred from the values of $\{\xi_b, J_0, J_1, \xi_{s,0}\}$.

It can be thought of as embedding a beacon within an information-bearing signal, although this perspective is not strictly valid since the large-energy bundles participate fully in conveying information as well as attracting the attention of the receiver. These high-energy bundles also occur at data-dependent random frequencies, rather than a fixed frequency as in the periodic beacon.

6.5 Discovery search strategies

General strategies for discovery of power-efficient information-bearing signals are now discussed. These strategies apply with little modification to beacons that have been power-optimized for discovery.

Some lessons for SETI programs

A question faced by SETI observation programs is whether to search for beacons, which are information-free but serve to attract attention to the transmitting civilization, or an information bearing signal. Existing SETI programs have been influenced by terrestrial communications, where power efficiency is sacrificed in favor of spectral efficiency. In that domain, the classic argument that a beacon is worthwhile because it is "obvious" or "easier to discover" has some merit, because generally achieving spectral efficiency requires complicated techniques that may generally interfere with discovery and are likely to be very difficult to reverse engineer after discovery.

The power-efficient regime has several conditions favorable to interstellar communication. One is that power-efficient signals are structured around on-off signals, where detecting the presence of absence of an energy bundle is the underlying receiver functionality. This functionality is extremely simple, and the same signal processing techniques apply to beacons and information-bearing signals. As a result, it is simple to seek both types of signals simultaneously. There is no "simplicity" argument in favor of a beacon. A beacon has no advantage over a low information rate signal in terms of the receiver resources required to discover a signal at a given average receive power. It is desirable to always embed information in a signal at no extra cost to transmitter or receiver. Our main issue would be whether to choose a very low information rate necessary to achieve the lowest receive power, which also requires a larger number of observations to discover, or a higher information rate associated with a higher power that requires less resources to discover.

Current and past SETI searches for the Cyclops beacon will only be successful if the transmitter designer has freely expended energy consumption. There is an argument to be made for this, for example if that designer has available inexpensive or free energy resources. However, it seems unlikely that such a designer would fail to embed information, since similar energy expenditure can achieve high information rates at no cost to discovery. The intermittency created by embedded information would, however, also compromise current and past discovery.

In searching for more complex and wider-bandwidth signals, a big concern expressed by researchers has been the interstellar impairments and the receiver processing required to deal with those impairments. In power-efficient design this is not a concern, because a basic principle is to choose a transmit signal that avoids these impairments altogether. There is a resulting penalty in bandwidth, so using more bandwidth results in less impairment due to the interstellar medium, the opposite of a common assumption among SETI researchers. During discovery, no processing associated with interstellar impairments other than noise is required. On the other hand, in the power-efficient regime the receiver does have to deploy the processing necessary to perform multiple independent observations at the same location and at or near the same carrier frequency, as well as pattern recognition algorithms to interpret the results.

6.5.1 Energy detection in discovery

During the energy detection phase, energy bundles that may be present are detected using a multichannel spectral estimation combined with filtering matched to $h(t)$. In the degenerate case of single-frequency energy bundles, where $h(t)$ is a constant, the matched filtering comes for free as an outgrowth of spectral estimation. In all cases, the phase of the matched filter output is ignored, and the magnitude-squared of the output is used as an estimate of the energy of the bundle. If the noise energy is known this value can be applied to a threshold, or if there is some uncertainty in the noise level the output can be normalized by the total energy within the bandwidth and time duration of $h(t)$, yielding an estimate of the energy contrast ratio rather than energy. This detection algorithm is described and analyzed in Chapter 7.

In contrast to current SETI searches, to have hope of detecting power-efficient signals it is necessary to revisit the same location (line of sight and frequency) numerous times. If after L such observations no energy bundles have been detected, this location can be permanently abandoned. The larger L , the lower the average signal power \mathcal{P} that will be reliably detected. Thus, as a given location is revisited, in effect the sensitivity of the detection (as measured by \mathcal{P}) improves. If current technology does not permit a very large L , that is perfectly acceptable because further observations in that location can be performed at some future time. The key requirement is to maintain a database of locations, and for each location the cumulative number of observations that have been performed, as well as relevant details of those observations such as observation times and candidate choices of $h(t)$ including T and B . That database will serve as guidance to future searches as to the least explored regions. The transmitter should maintain the same carrier frequency, so that the receiver maintains the greatest flexibility in conducting multiple observations over the long term.

If it is assumed that the transmitter designer is motivated to minimize its energy consumption through the use of low duty factor, the resulting signals are unlikely to be detected in existing SETI searches. These existing searches do not realize the tens, hundreds, or thousands of independent observations necessary to achieve a reasonable detection probability for a power-efficient information-bearing signal or beacon that has been power-optimized for discovery. In addition, these existing searches typically assume short-term persistence of the signal in an attempt to identify "waterfall" patterns (a carrier frequency changing linearly with time) and to help rule out false alarms. This existing approach is ineffective for intermittent power-efficient signals of the type we have considered here. It is possible that past SETI searches have in fact detected legitimate signals of interest but incorrectly categorized them as false alarms because they did not take account of the relatively low probability of detection of a single energy bundle nor the possible intermittent nature of the signal. These existing searches can, however, benefit future searches for power-efficient signals by maintaining a location database which captures for future analysis all detected energy bundles that have been classified (perhaps incorrectly) as false alarm events. These locations are promising starting locations for any future pattern-recognition analysis while searching for power-efficient signals.

6.5.2 Pattern recognition in discovery

The previous analysis has presumed that detection of a beacon or an information-bearing signal requires only the presence of a single energy bundle in L observations of duration T_o . In the numerical examples the false alarm probability was set fairly low, at $P_{FA} = 10^{-12}$ or 10^{-8} . Nevertheless, this form of detection will never suffice to declare the discovery of a signal. As discussed in Section 6.1.4, these values of P_{FA} are presumably still much larger than the a priori probability of a signal being present, and thus false alarms will dominate these detections leading to a low confidence in an actual discovery.

Once an energy bundle is discovered, it is appropriate to continue observing in that same location (line of sight and frequency) to see if other energy bundles are detected. In essence, conditional on a successful detection the number of observations L can be increased. In view of the possibility of a time-varying frequency shift due to uncompensated acceleration and due to information-bearing signals that utilize more than one frequency (such as the M-ary FSK used in our examples), these observations should be conducted over a range of frequencies in the vicinity of detected energy bundles.

Should these continued observations detect more energy bundles, the receiver can extend the observations at that location, and switch to a pattern recognition mode in which discernible patterns of energy are sought. A recognizable and repeatable pattern presents even more significant evidence of the presence of a signal. The confidence in this evidence can be quantified by calculating the probability that a given pattern represents a false alarm. The location database should capture and document all observations that have been made in the promising location and nearby frequencies, as well as all detected energy bundles.

A multichannel spectral analysis may cover a much wider range of frequencies than what would be expected for a single information-bearing signal, or especially for a beacon which may well be narrowband. Thus, the most efficient way to follow up on detected energy bundles may be to pass observations to a separate processing that analyzes promising locations over a narrower range of frequencies.

The location database can be analyzed separately, and repeatedly. Statistical (rather than deterministic) pattern recognition is required since at low average power levels the probability of detection of an individual energy bundle is expected to be small (on the order of $P_D \approx 0.5$ at the limits of average power), and also because the location of bundles is likely to be associated with a random stream of information bits. Ideally a single database will be shared by all SETI observers worldwide, so that the database represents the worldwide cumulative observations. The database offers an attractive target for future research and statistical analysis. The literature and algorithms for statistical pattern recognition appropriate for discovery of power-efficient signals is also an interesting topic for future research, and this research can benefit future analysis of the database.

6.6 Summary

The general issue of the discovery of artificial signals of interstellar origin has been addressed from the perspective of minimizing energy consumption in transmitter and receiver, and tradeoffs between resource allocation in the transmitter and receiver. It is argued that a signal structured around the repeated transmission of energy bundles, as has been proven to achieve the fundamental limit on power efficiency in information transfer, is also meritorious for discovery. Beacons, which transmit deterministic patterns of energy bundles, and information-bearing signals, which transmit random patterns, have been studied. Some general hypotheses about the amount of energy in the bundles and the amount of energy overlapping the receiver's observation time have been proposed and verified through more detailed statistical modeling.

Our conclusion is that for any average received power, there is an information-bearing signal that is as easy to discover as a beacon at that power. A beacon is neither easier to discover nor does it offer any other advantage such as lower average power for a given reliability of discovery. Beacons with a small average power are particularly compelling because they demand lower energy resources at the transmitter. Since average power is proportional to information rate for a power-efficient information-bearing signal, an information-bearing signal with the same average power as such a beacon has a low information rate. An information-bearing signal with low information rate is more difficult to discover than one with a higher information rate, because its average power is lower. Any civilization seeking low energy consumption is likely to transmit an information-bearing signal with a low information rate rather than a beacon with the same average power.

In contrast to present and past SETI observation programs, it has been concluded that multiple observations are needed to reliably discover signals designed according to power-efficient principles. Information-bearing signals at the highest rate for single carrier and with sufficiently high power to extract information reliably require on the order of tens of observations in the initial energy bundle detection phase. As the power (and hence rate) of the information-bearing signal is decreased, the number of required observations increases. The regime of up to 1000 observations has been explored, but there is no lower limit on the rate and power that can be discovered, and thus no limit on the number of observations that is required. The observation program at each carrier frequency should be viewed as a long-term endeavor, with additional observations as permitted by advancing technology and budgetary resources.

While existing SETI searches will fail to discover signals designed according to energy-conserving principles, these searches can be extended to this class of signals with fairly straightforward modifications. Aside from multiple observations, strategies for separating true energy bundles from false alarms in the pattern recognition phase have been discussed. This is an area deserving of additional research.

An important conclusion is that a single worldwide database capturing the location of all observations and all detection events as well as their characteristics should be maintained. Detection events in current searches that are characterized as false alarms may in rare cases in fact represent actual low-average-power beacons or information-bearing signals, but this can only be ascer-

tained by analyzing a longer-term set of observations in the same and nearby locations.

Chapter 7

Detection

Detection of the location of energy bundles is the first step in the recovery of information from a power-efficient information-bearing signal and detection of the presence or absence of an energy bundle is the first stage of discovery. There are clear distinctions between these two types of detection. During communication, for assumed channel coding (based on M-ary FSK), it is known that an energy bundle is present, but the only question is its location from among M possibilities. During discovery, the role of detection is to determine whether an energy bundle is present or not, absent any prior knowledge. In both cases, the energy in a bundle is affected in an unknown way by scintillation, although in the case of communication it will be possible to track the state of scintillation with some degree of accuracy.

For both discovery and communication the best pre-processing for the detection algorithm is a matched filter. This is the best way to counter the AWGN, regardless of whether scintillation is a factor or not. In this chapter, the argument that the matched filter is the best pre-processing will be made for the discovery case. In that case, the appropriate metric of reliability of detection is the false alarm probability P_{FA} and the detection probability P_D . In this chapter those two probabilities are calculated for a single matched filter output applied to a threshold in the presence of scintillation. Only the strong scattering case will be considered, for which the scintillation follows Rayleigh (rather than Rician) statistics. The argument that the matched filter is also the best front end for communication follows similar lines and is omitted.

Another possible source of uncertainty is the noise power spectral density N_0 . For our assumed channel coding (based on M-ary FSK), this is not an issue since the maximum likelihood algorithm of (5.2) automatically adjusts to changing conditions on both \mathcal{E}_h and N_0 , taking advantage of the prior knowledge that exactly one energy bundle is present. For discovery, on the other hand, knowledge of N_0 is important in the interpretation of the energy estimate at the matched filter output. In response to this challenge, we will show how the detection can be modified (from the simple matched filter followed by threshold) to be sensitive to only the relative size of the signal level and the noise level. We will also show how choosing a larger number of degrees of freedom $K = BT$ for $h(t)$ is helpful in this, giving an opportunity to implicitly and more accurately estimate the signal and noise levels in the course of deciding whether signal is present or not.

7.1 Matched filter

The use of a matched filter as the basis for detection of a single energy bundle will now be justified.

7.1.1 Continuous-time channel model

To justify the use of a matched filter, a continuous-time model for the interstellar channel at the baseband input to the receiver is needed. Assuming that the carrier waveform $h(t)$ falls in an interstellar coherence hole (ICH), the only impairments are AWGN and scintillation. Neglecting any impairments other than these, the reception is

$$R(t) = \begin{cases} \sqrt{\mathcal{E}_h} S h(t) + N(t) & \text{energy bundle present} \\ N(t) & \text{noise only} \end{cases} \quad (7.1)$$

The random process $N(t)$ is AWGN with power spectral density N_0 and S is a zero-mean complex-valued Gaussian scintillation random variable with variance $\mathbb{E}[|S|^2] = \sigma_s^2 = 1$. The real- and imaginary parts of S are identically distributed and statistically independent, or equivalently $\mathbb{E}[S^2] = 0$. The magnitude-squared of the scintillation is the received flux $\mathcal{F} = |S|^2$.

The matched filter followed by a sampler reduces the continuous-time signal in (7.1) to a single complex-valued random variable Z , given in the cross-correlation formulation by

$$Z = \int_0^T R(t) h^*(t) dt. \quad (7.2)$$

Notice that the correlation interval is the same as the assumed duration $t \in [0, T]$ of $h(t)$. We also assume that $h(t)$ is bandlimited to the frequency interval $f \in [0, B]$, in which case (7.2) implicitly incorporates an ideal lowpass filter that rejects all "out of band" noise.

The optimality of the matched filter as a pre-processing to reduce the continuous-time reception of (7.1) to a single random variable for decision making will now be made. This optimality can be approached with varying degrees of sophistication, but all roads lead to the same conclusion. We follow two of these, motivated by the significant insight they provide into the detection problem, and especially the way to deal with not only an unknown signal magnitude (due to scintillation) but also an unknown noise power N_0 . The following development is more intuitive than mathematical, so as to place understanding ahead of rigor.

7.1.2 Sufficient statistic formulation

The most powerful argument for using an matched filter as the pre-decision processing is that the matched filter output of (7.2) is a *sufficient statistic* for reception (7.1). Roughly this argument says that the matched filter throws away much information, but none of that discarded information is statistically relevant to the subsequent decision as to the presence or absence of an energy bundle.

It is simple to argue that the out of band noise is irrelevant, because it is (a) not changed in any way if an energy bundle is present or absent and (b) it is statistically independent of the in-band noise (because the noise is assumed to be white) and thus offers no information about the in-band noise that could aid the detection.

Most of the remaining in-band noise is also irrelevant, namely that which is not correlated with $h(t)$, although it is more work to formulate this argument. As discussed in Section 3.4, $h(t)$ has degrees of freedom $K = BT$. Similarly, both the noise $N(t)$ and reception $R(t)$, following ideal bandlimiting to $f \in [0, T]$ and over time interval $t \in [0, T]$, have K degrees of freedom. The mathematical interpretation of this is that there exists a set of K orthonormal basis functions $\{g_k(t), 1 \leq k \leq K\}$, the weighted summation of which can represent either $h(t)$ or, after bandlimiting and time-limiting, $N(t)$ and $R(t)$. By orthonormal, we mean

$$\int_0^T g_m(t) g_n^*(t) dt = \delta_{m-n}. \quad (7.3)$$

It doesn't matter what $\{g_k(t), 1 \leq k \leq K\}$ are chosen, so for convenience choose as the first basis function $g_1(t) = h(t)$, and the remaining basis functions arbitrarily to fill out a complete orthonormal basis. Then the reception $R(t)$ (restricted to bandwidth B and time duration T) can be represented by a set of K coefficients w.r.t. this basis,

$$R_k = \int_0^T R(t) g_k^*(t) dt = \begin{cases} \sqrt{\mathcal{E}_h} S + M_1, & k = 1 \\ M_k, & 2 \leq k \leq K. \end{cases} \quad (7.4)$$

Note that $R_1 = Z$, the output of a filter matched to $h(t)$ sampled at time $t = 0$, and the remaining coordinates are noise-only. The noise components $\{M_k, 1 \leq k \leq K\}$ are readily shown to be statistically independent, and thus the $\{R_k, 2 \leq k \leq K\}$ offers no information as to either \mathcal{E}_h or M_1 and can be ignored just like the out of band noise.

What is notable about (7.4) is the concentration of signal energy in only one out of the total of K coordinates. This concentration is the signature of the presence of signal $h(t)$ within the bandwidth B and time duration T , and will be evident as long as $\mathcal{E}_h |S|^2 \gg N_0$ no matter what the specific values of \mathcal{E}_h and N_0 . This concentration can be observed without the need to explicitly compute the $\{R_k, 2 \leq k \leq K\}$. Define the total in-band energy of the reception as \mathcal{E}_r , then

$$\mathcal{E}_r = \sum_{k=1}^K |R_k|^2 = \int_0^T R(t) g(-t) dt \quad (7.5)$$

where $g(t)$ is the impulse response of an ideal lowpass filter that rejects all out of band noise energy. Then a decision variable Q that measures the concentration of energy would normalize the matched filter output by the total energy,

$$Q = \frac{|R_1|^2}{\mathcal{E}_r}. \quad (7.6)$$

The value of Q is constrained to fall in $0 \leq Q \leq 1$, with larger values of Q signaling a concentration of energy in the first coordinate, and a value on the order of $Q \approx 1/K$ signaling a uniform

distribution of energy across all the coordinates. Q is a desirable decision variable when the size of N_0 is unknown or uncertain. Q can serve as the basis of a decision as to whether $h(t)$ is present or absent by comparing it to a threshold $0 < \lambda < 1$, where $Q > \lambda$ results in the decision that a signal is present.

7.1.3 Least-squares formulation

A least-squares formulation gives another perspective on the Q of (7.6) as a decision variable, and also shows that $Q > \lambda$ is a reasonable criterion to decide the presence of an energy bundle even when the AWGN assumption is not valid. An example of when it is clearly not valid is the presence of radio-frequency interference (RFI).

Suppose the received signal with a known unit-energy waveform $\{h(t), 0 \leq t \leq T\}$ is expected but in the reception $r(t)$ it is delayed by some unknown τ , multiplied by some unknown complex-valued factor z representing an unknown magnitude and phase, and corrupted by noise, interference, etc,

$$r(t) = z \cdot h(t - \tau) + \text{noise} + \text{interference} + \dots \quad (7.7)$$

The least squares solution seeks to produce an estimate \hat{z} of the complex-valued amplitude z and an estimate $\hat{\tau}$ of time offset τ by minimizing a distance metric between $r(t)$ and $\hat{z} \cdot h(t - \hat{\tau})$. The metric we chose in the least squares criterion is the energy in the error,

$$\varepsilon(z, \tau) = \int_{\tau}^{\tau+T} |r(t) - z \cdot h(t - \tau)|^2 dt. \quad (7.8)$$

Our strategy is to determine, for each τ , the value $z = \hat{z}$ that minimizes $\varepsilon(z, \tau)$. This eliminates one of the unknowns, leaving a resulting least squares error $\varepsilon_{\min}(\tau) = \varepsilon(\hat{z}, \tau)$ that depends only on τ .

It is shown in Appendix B.2 that the resulting estimate and residual error are

$$\hat{z}(\tau) = \int_{\tau}^{\tau+T} r(t) h^*(t - \tau) dt = r(\tau) \otimes h^*(-\tau) \quad (7.9)$$

$$\varepsilon_{\min}(\tau) = \varepsilon(0, \tau) - |\hat{z}(\tau)|^2 \geq 0 \quad (7.10)$$

where \otimes is the convolution operator. The estimate $\hat{z}(\tau)$ as a function of time can be generated by a filter with impulse response $h^*(-t)$, which is by definition a filter matched to $h(t)$. The size of $0 \leq \varepsilon_{\min}(\tau) \leq \varepsilon(0, \tau)$ is a direct indication of the goodness of the fit between $h(t)$ and $r(t)$. For example, if $\varepsilon_{\min}(\tau) \approx 0$, or equivalently $|\hat{z}(\tau)|^2 \approx \varepsilon(0, \tau)$, it follows that $r(t) \approx \hat{z}h(t - \tau)$.

A convenient way to measure the goodness of the fit is to calculate the decision variable

$$Q = \frac{|\hat{z}(\tau)|^2}{\varepsilon(0, \tau)}. \quad (7.11)$$

Then Q is normalized to range $0 \leq Q \leq 1$, where the value $Q = 1$ indicates that $r(t)$ is totally aligned with $h(t)$ and $Q = 0$ indicates that $r(t)$ is orthogonal to $h(t)$. Although the notation is different, (7.11) and (7.6) are mathematically identical definitions of Q at $\tau = 0$.

7.1.4 Detection performance

A detector based on applying Q to a threshold $0 < \lambda < 1$ does not need knowledge of either \mathcal{E}_h or N_0 or the energy contrast ratio ξ_s , which was defined in (2.16). We will now show that it does the reasonable thing, which is respond to the size of ξ_s (rather than \mathcal{E}_h or N_0 individually), or in other words it is sensitive to the energy contrast ratio but not the absolute level of the energy of a bundle or the energy of the noise. Depending on threshold λ , it will declare signal when ξ_s is larger (bundle energy is larger than noise energy) and will declare noise only when ξ_s is smaller (bundle energy is smaller than noise energy) or zero (there is no energy bundle).

The analysis proceeds by determining P_{FA} and P_{D} parameterized by λ , and then eliminating λ to find the direct relationship between P_{FA} and P_{D} . This analysis is performed in Appendix G for strong scattering,¹ finding that

$$P_{\text{D}} = \left(\frac{\xi_s + 1}{\xi_s + P_{\text{FA}}^{\frac{1}{1-K}}} \right)^{K-1}. \quad (7.12)$$

Note that \mathcal{E}_h and N_0 enter only through their ratio in ξ_s , so the detection algorithm automatically adjusts to unknown values for \mathcal{E}_h and N_0 , responding only to their ratio. The detection algorithm implicitly estimates N_0 by examining the noise within the ICH that falls in the $K - 1$ coordinates that are absent signal, and comparing the matched filter output (which is the first coordinate) to that noise estimate. The detection probability is plotted for a fixed P_{FA} in Figure 7.1 as a function of K and ξ_s . The increasing P_{D} with K is because the estimate of N_0 built into (7.11) has increasing accuracy in estimating N_0 as there are more coordinates available to form the estimate. The higher the actual energy contrast ratio ξ_s , the more likely the energy bundle is to be detected. In Chapter 6 it was found that $\xi_s \approx 15$ dB is the goal for the power optimization of discovery, and at that level $K = 20$ is about the point of diminishing returns, in the sense that further increases in P_{D} are small.

For any ξ_s , P_{D} increases monotonically with K , approaching an asymptote of

$$P_{\text{D}} \xrightarrow{K \rightarrow \infty} P_{\text{FA}}^{\frac{1}{1+\xi_s}} < 1. \quad (7.13)$$

Even $K \rightarrow \infty$ cannot achieve $P_{\text{D}} \approx 1$, except in the case where $\xi_s \rightarrow \infty$ or $P_{\text{FA}} \approx 1$. This is the reason that multiple observations were found necessary in Chapter 6 to approach reliable detection. This can be blamed on scintillation, which sometimes results in periods with a low signal strength, and during such "outage" periods the detector invariably declares "noise", thereby failing to declare "signal". Figure 7.2 illustrates how P_{D} is monotonically increasing in P_{FA} for this $K \rightarrow \infty$ asymptote.

¹ For weak scattering such simple results as (7.12) are unattainable, but it can be confirmed that discovery becomes easier (see Appendix G.1.2) due to the presence of a specular component of flux.

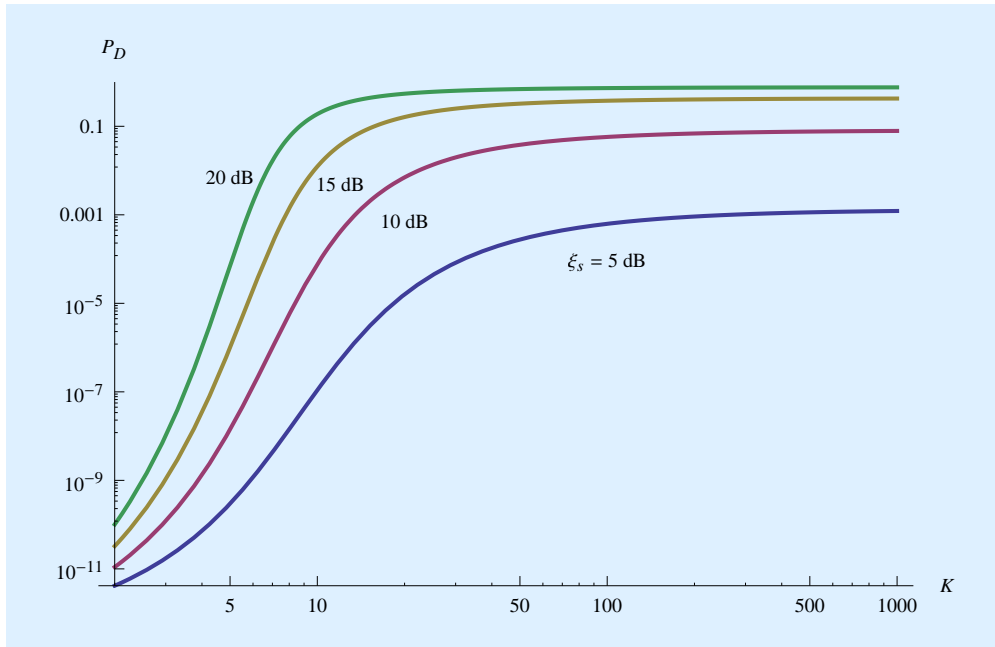


Figure 7.1: A log-log plot of detection probability P_D for an actual energy contrast ratio of $\xi_s = 5, 10, 15$, and 20 dB. The horizontal axis is the degrees of freedom K for a fixed $P_{FA} = 10^{-12}$.

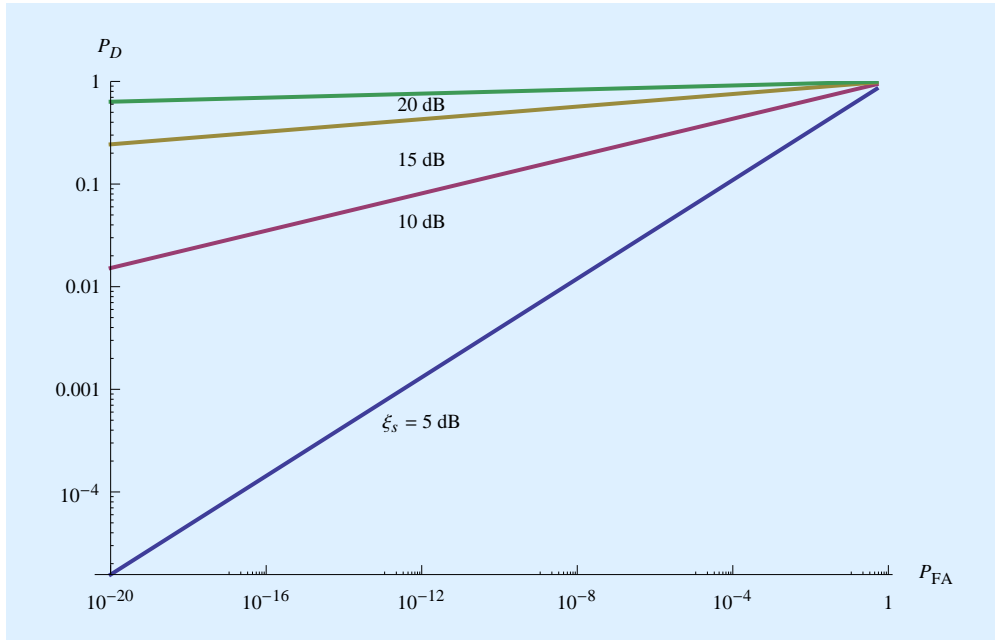


Figure 7.2: A log-log plot of detection probability P_D at the asymptote $K \rightarrow \infty$ for an actual energy contrast ratio of $\xi_s = 5, 10, 15$, and 20 dB. The horizontal axis is the false alarm probability P_{FA} .

Do sinusoidal signals get too much respect?

In the presence of AWGN, it has been shown that the tradeoff between P_{FA} and P_{D} does not depend on the waveform of $h(t)$, nor on any of its parameters like B and T . This includes a continuous-wave signal like $h(t) = \sqrt{2/T} \cdot \sin(2\pi ft)$, which has a small $BT \approx 1$, or a noise-like spread-spectrum signal with a large BT .

It is sometimes asserted that sinusoidal waveforms are “special” in that they cannot be generated by natural processes, and thus are in some sense easier to distinguish from natural sources of noise. If the noise in question is of thermal origin, this is not true. *Any* deterministic waveform $h(t)$ with unit energy is distinguishable from AWGN to the same degree. This is even true of an $h(t)$ that is noise-like, as in spread spectrum. The noise-like character is not relevant to discovery, as the receiver is applying a filter matched to a very specific deterministic waveform $h(t)$, rather than basing detection of an estimate of the statistics of $h(t)$. As an aid to intuition on this significant point, Appendix E describes an analogy to noise generated by random coin tosses, which is easier to understand but displays the same characteristics.

The sinusoidal signal does have one advantage, which is that signals with $BT \approx 1$ require one fewer dimension of search. When $BT \gg 1$ a discovery search is forced to search over different values of B or different values of T (fortunately not both) with a fine granularity [11]. Our suggestion here is to narrow the range of this search substantially based on physical parameters observable by both transmitter and receiver and the resulting coherence time and coherence bandwidth. A natural choice is the coherence time T_c , since regardless of the choice of B a transmitter designer wishing to minimize peak transmitted power will choose the largest T possible consistent with $T \leq T_c$.

7.1.5 Known noise power spectral density

If the noise power spectral density N_0 is known, then decision variable (7.6) can be replaced by $Q = |R_1|^2$. Because N_0 is known, the threshold λ can be chosen to control P_{FA} based on that knowledge, and the resulting P_{D} is determined unambiguously. Not surprisingly, the relationship for P_{D} vs P_{FA} becomes (Appendix G) the same as the $K \rightarrow \infty$ asymptotic result of (7.13). This is because the implicit estimate of N_0 built into (7.6) becomes increasingly accurate (by the law of large numbers) as $K \rightarrow \infty$.

The lesson to take away from Figure 7.1 is not that small K precludes reliable detection. Rather, the conclusion is that if K is small then the receiver needs to know N_0 in order to properly set the threshold λ , or if prior knowledge is absent the receiver must estimate N_0 by some other means.

7.2 Search for an energy bundle

The basic building block for discovery is the filter matched (matched filter) to waveform $h(t)$ defined in (B.3). To achieve high discovery sensitivity, the receiver must guess the waveform $h(t)$ in use, or it may be able to search for a set of possible $h(t)$ waveforms as long as the number of distinct possibilities is relatively small. However, even making this guess successfully, there are

several degrees of uncertainty. The actual waveform as observed at the receiver will be of the form $h(\beta(t - \tau))e^{i2\pi f_1 t}$, where the three uncertain parameters are $\{\beta, \tau, f_1\}$. The parameter β is the *time dilation*, τ is the *starting time*, and f_1 is the *carrier frequency offset*. The receiver must search over some range of these parameters, because there is no possible way to infer them precisely.

The time dilation parameter β reflects uncertainty in the time scaling of the signal. Aligning the signal with an ICH can reduce (although not eliminate) this uncertainty. For a reception $r(t)$, during discovery (7.2) is replaced by

$$Z(\tau, \beta, f_1) = \int R(t) h^*(\beta(t - \tau)) e^{-i2\pi f_1 t} dt, \quad (7.14)$$

which calculates the matched filter for different values of τ . During the search the integral representing the matched filter must be repeated for different values of β and f_1 . The baseband processing will typically operate with a signal of bandwidth JB for some large value of J , and use the fast Fourier transform to simultaneously calculate a bank of matched filter outputs (representing different f_1) over time (representing different τ).

One question is what granularity is necessary in searching these three parameters, this relating directly to the needed processing resources. The granularity of τ is, by the sampling theorem, $1/B$. As discussed in Appendix J, the required granularity of β is on the order of $1/K$, and the granularity of f_1 is on the order of $1/T$. Thus, increasing either K (to counter RFI, for example) or T (to reduce peak transmitted power) results in a finer granularity of search and increases the required processing resources.

7.3 Choice of $h(t)$

Any discussion of how to choose $h(t)$ has been deliberately deferred to last to emphasize that with respect to all the concerns addressed thus far, including discovery and communication in the presence of interstellar impairments, the only properties of $h(t)$ that matter are its energy (assumed to be unity), bandwidth B , and time duration T . In particular, the waveform representing $h(t)$ does not matter. Our design is tailored to a specific line of sight and f_c , which in turn influences the size of the ICH. This places a restriction on $B \leq B_c$ and $T \leq T_c$, and $K = BT$ for the chosen waveform $h(t)$, but within these constraints any B and T can be chosen. All of our results depend on using the matched filter (matched filter) for detection, and thus it is important to choose an $h(t)$ that is relatively easy for the receiver to guess.

7.3.1 Radio-frequency interference

A consideration that has not been discussed thus far is radio-frequency interference (RFI), which is a serious and growing problem for terrestrially based radio telescopes. The choice of $h(t)$ does have a substantial effect on RFI immunity, in the sense that the response of the matched filter to

the RFI affects the detection reliability. If after bandlimiting to B the RFI waveform is $r(t)$, then the response of the matched filter is

$$\int_0^T r(t) h^*(t) dt. \quad (7.15)$$

This value, which represents an unwanted bias in signal before application to the detection threshold, depends on both $r(t)$ and $h(t)$. Analysis of this undesired interaction was covered in a previous paper [11]. As is well known in terrestrial communications, the choice of an $h(t)$ with some properties known as *spread spectrum* result in a much more robust matched filter response to the RFI, in the sense that the probability of a large response is greatly diminished and the response is much more uniform over a wide range of interferers. These properties are (a) a larger value for the degrees of freedom K , and (b) a choice of $h(t)$ that spreads the energy uniformly over the full time duration T and bandwidth B . Such a waveform has characteristics that mimic bandlimited and time-limited white noise. As an aid to intuition on this point, in Appendix E the analogy to a discrete-time version of $h(t)$ generated by a pseudo-random coin toss generator is discussed.

For an $h(t)$ that falls in the ICH for a given line of sight and carrier frequency, there is a limit to how large K can be. The maximum K was plotted in Figure 3.6 for a typical set of physical parameters of the ICH, and over a range of carrier frequencies. Fortunately the available K is typically large, on the order of 10^3 to 10^5 , which offers considerable opportunity for RFI immunity. If the strategy is to maximize K in the interest of achieving greater immunity to RFI in the receiver. then it is favorable to choose $B = B_c$ and $T = T_c$. Given the inevitable uncertainty in estimating B_c and T_c , the smallest credible values of B_c and T_c should be used.

7.3.2 Implicit coordination

In the context of interstellar communication, there is another argument for using a spread-spectrum signal of this type, one that may be stronger than its advantages for RFI immunity [11]. Due to the lack of coordination between the transmitter and receiver designs it is important to have fundamental principles to guide the design, principles that address concerns likely to be shared by both designers and concerns that easily yield an optimal mathematical solution that can be arrived at by both designers. In Chapter 2 the five principles of power-efficient design were cited for exactly this reason. They all address aspects of a set of shared concerns, namely a desire for a low received average power \mathcal{P} in relation to the information rate \mathcal{R} and a relatively few independent observations required for reliable discovery of the signal. These principles led directly to conclusions as to the likely choice of channel coding (M-ary FSK or M-ary PSK) and power reduction through reduced duty cycle, but unfortunately only offer insight into the bandwidth and time duration of $h(t)$ but not any other aspect of its waveform. Since RFI immunity speaks directly to the choice of waveform, it can act as an implicit form of coordination between transmitter and receiver that complements the power-efficiency principles.

Simple optimization principles for RFI immunity lead to the conclusion that $h(t)$ should statistically resemble white Gaussian noise, appropriately bandlimited and time-limited. Further infor-

mation about appropriate choices of $h(t)$ follow from pragmatic considerations [11]. These include the feasibility of guessing $h(t)$ at the receiver (dictating algorithmically-generated pseudo-random waveforms), and Occam's razor (a four-level QPSK signal is the minimum-complexity signal that meets the randomness requirements). In the interest of minimizing the search space during the discovery process, a critical requirement is embedding, in which a shorter-length pseudo-random sequence must be the precursor to a longer sequence, eliminating one entire dimension of discovery search for the receiver. Either a search over B is required (using a fixed K and hence a variable $T = K/B$), or a search over T is required (using a fixed K and hence a variable $B = K/T$). In both cases, detection sensitivity is improved if some different values of K are tried, but a relatively coarse granularity is sufficient. The choice between these two options might be governed by the estimated uncertainty in B_c vs that in T_c .

7.3.3 Example

The desired statistical properties of $h(t)$ for RFI immunity can be achieved using a pseudorandom sequence generator, so that the receiver need only guess the *algorithm* employed by the transmitter. The statistical characteristics dictated by RFI immunity can be met, in the simplest way, by a binary sequence that replicates the statistics of a sequence of independent coin tosses, but which also has a well-defined starting state. Fortunately such signals are mathematically easy to generate, for example by the binary expansion of an irrational number. In particular, a readily guessable choice is based on a pseudorandom sequence generated by the binary expansion of e , π , or $\sqrt{2}$ [11].

Consider, for example, an $h(t)$ design based on the binary expansion of π . As described in [11], $h(t)$ is generated as a quadrature phase-shift keying (QPSK) signal (the lowest complexity meeting the requirement for statistical independence of the real- and imaginary parts), two successive bits from a binary expansion π can be mapped onto a complex amplitude chosen from four QPSK points at rate B_c . The resulting waveform $h(t)$ takes the concrete form

$$h(t) = \frac{1}{\sqrt{K}} \sum_{k=0}^{K_c-1} c_k g(t - k/B_c), \quad (7.16)$$

where each $c_k = (2b_k - 1) + i(2b_{k+1} - 1)$ is chosen using two successive bits $\{b_k, b_{k+1}\}$ from the binary expansion of π . For example, the first 30 digits of π equal

$$\{b_k, 1 \leq k \leq 30\} = \{1, 1, 0, 0, 1, 0, 0, 1, 0, 0, 0, 0, 1, 1, 1, 1, 1, 0, 1, 1, 0, 1, 0, 1, 0, 0, 0\}, \quad (7.17)$$

resulting in

$$\{c_k, 1 \leq k \leq 15\} = \{1 + i, 0, 1, i, 0, 0, 1 + i, 1 + i, 1 + i, i, 1, 1, 1, 1, 0\}. \quad (7.18)$$

The *chip waveform* $g(t)$ is a sampling interpolation function (and thus $g(0) = 1$) for sampling rate B , and the match between transmitter and receiver in the choice of $g(t)$ is non-critical. Due to the embedded properties of the $\{b_k\}$ sequence, the receiver is permitted to use a different $K = K_r$ from the transmitter with some loss of signal energy if $K_r < K_c$, or some unnecessary noise if $K_r > K_c$.

As an alternative, the simple sine wave or pulse could be used. A sinusoid is especially attractive if the receiver designers are expected to be astronomers or experimental physicists rather than communication engineers, as spectral analysis is a familiar form of scientific inquiry in many sub-disciplines of astronomy, physics, and chemistry. The use of a short pulse as described in [22] is not attractive in our power-efficient design because it is extremely broadband and will thus violate the bandwidth coherency requirement for power-efficient design. It also requires very high peak power transmission.

7.4 Summary

The detection of a single energy bundle in the presence of additive white Gaussian noise (AWGN) has been considered. Using two different criteria of optimality, the matched filter is shown to be the best receiver processing. When there is uncertainty about the power spectral density of the AWGN, it is shown that a simple normalization of the matched filter output results in a detector that automatically responds to the ratio of signal energy to noise energy, rather than either signal energy or noise energy alone. The detection performance does not depend on any property of the waveform carrying the energy bundle except its total energy. However, that waveform does strongly influence the immunity to interference. The design of a waveform chosen to maximize that immunity is illustrated.

Chapter 8

Sources of incoherence

In Chapter 3 the impairments introduced in the ISM and due to source/observer motion were divided into those that can be circumvented by reducing the time duration and bandwidth of the waveform $h(t)$ serving as the carrier for an energy bundle, and those that can't. The impairments that remain are a fundamental impediment to interstellar communication, and those were modeled in more detail in Chapter 3. The present chapter will model the remaining impairments, those that are circumvented by restricting duration and bandwidth. The goal is twofold. First, these impairments are modeled with a sufficient detail to establish that they can be circumvented. This does not require a detail or sophistication of modeling typical of the astrophysics literature, since the goal is much more modest. Second, the typical size of the coherence time T_c and coherence bandwidth B_c of the interstellar coherence hole (ICH) is estimated. Of particular interest is establishing that the resulting degrees of freedom satisfies $K_c = B_c T_c \gg 1$, which is a necessary condition for stable interstellar communication utilizing the power-efficient design methodologies covered earlier in this report.

8.1 Types of incoherence

When the impairments are considered individually, two distinctive forms of incoherence are encountered:

Frequency incoherence. In the presence of the impairment, if the overall effect is linear and time-invariant, it can be equivalently modeled in the frequency domain. In this case, if there is a frequency-dependent change in amplitude or phase that causes a distortion of the signal, this is called frequency incoherence. This effect can usually be mitigated by reducing the bandwidth of the signal until the frequency response is approximately constant over the signal bandwidth and this source of signal distortion becomes insignificant.

Time incoherence. If in the presence of the impairment, the effect varies with time, then frequency-domain modeling is not useful. This time dependence is called time incoherence. This effect

can usually be mitigated by reducing the time duration of the signal until the this source of distortion is rendered insignificant.

Most of the impairments encountered in interstellar communication cause either a frequency-dependent or time-dependent phase shift. They are lossless, and thus do not cause a magnitude shift in either time or frequency. Our general criterion for coherence is when the magnitude of the phase change is less than $\alpha\pi$ for a parameter $0 \leq \alpha \leq 1$. Choosing α smaller makes the criterion more strict. At the limits of incoherence, there is generally both time and frequency incoherence with additive phases, so the maximum value $\alpha = 0.5$ insures that the total phase shift is at most π . The appropriate value of α depends on the use to which the ICH is put, and the impact of incoherence on that use. In all numerical examples, the conservative choice of $\alpha = 0.1$ is assumed, except in a couple cases where the uncertainty is greater and we assume a smaller value $\alpha = 0.01$. The coherence bandwidth B_c and coherence time T_c are determined by the most stringent of the conditions that arise across all the impairments.

8.2 Plasma dispersion

Although it approaches an ideal vacuum, the ISM contains an extremely low-density plasma consisting of hydrogen ions and free electrons arising from the presence of hydrogen gas and ionizing radiation from the stars [53]. The charged particles create a conductive medium that influences radio waves propagating over long distances. This results in plasma dispersion, a frequency-dependent group delay due to the free electrons' lossless absorption and wavelength-dependent delayed emission of photons.

Plasma dispersion causes a frequency-dependent group delay $\tau(f)$. Let the transfer function at passband be

$$G(f) = e^{i2\pi\phi(f)} \quad (8.1)$$

so that there is a phase shift $\phi(f)$ with no effect on signal magnitude. The group delay $\tau(f)$ and $\phi(f)$ are related by

$$\tau(f) = -\frac{1}{2\pi} \cdot \frac{\partial\phi(f)}{\partial f}. \quad (8.2)$$

The standard model for this group delay used in pulsar astronomy is [14]

$$\tau(f) = \frac{\mathcal{D} \text{DM}}{f^2} \quad (8.3)$$

As illustrated in Figure 8.1, $\tau(f)$ decreases monotonically (and approximately linearly) with f . While *dispersion constant* $\mathcal{D} \approx 4.15 \times 10^{15}$ depends only on known physical constants (and has units of $\text{Hz}^2 \text{pc}^{-1} \text{cm}^3 \text{s}$), the *dispersion measure* DM summarizes all that needs to be known about the current interstellar "weather" in order to predict the group delay profile for a given direction of arrival (and has units of $\text{cm}^{-3} \text{pc}$). Typically DM ranges over about two orders of magnitude, from about 10 to about 1000, depending on the columnar electron density along the line of sight.

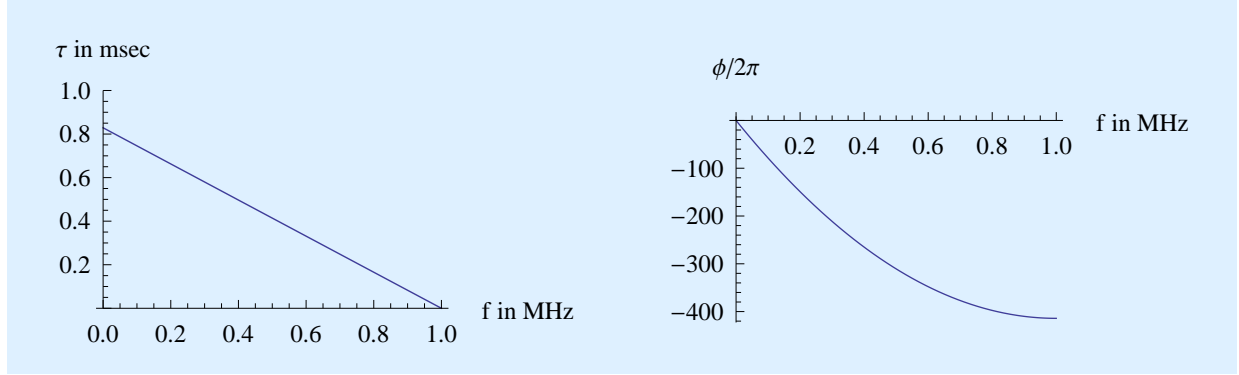


Figure 8.1: The dispersive group delay $\tau(f)$ in msec (with τ_0 chosen so that $\tau(B) = 0$) and resulting unwrapped phase $\phi(f)/2\pi$ (with $\phi(f)$ in radians and $\phi_0 = 0$) plotted against baseband frequency f for $f_c = 1$ GHz, $B = 1$ MHz, and $DM = 100 \text{ cm}^{-3} \text{ pc}$. The phase experiences more than 400 rotations across the bandwidth, and this phase variation will increase with $DM \uparrow$, $B \uparrow$, or $f_c \downarrow$.

The ICH test is shown in Figure 8.3. Over the frequency range $f \in [f_c, f_c + B]$, if B is kept small enough $\phi(f)$ can be modeled by a linear dependence on f ,

$$\phi(f) \approx \phi(f_c) - \tau(f_c) \cdot f \quad (8.4)$$

which corresponds to an unknown phase $\phi(f_c)$ plus a fixed (not frequency-dependent) group delay $\tau(f_c)$. If the deviation of the actual $\phi(f)$ from (8.4) is less than $\alpha \pi$ radians over the entire range $f \in [f_c, f_c + B]$ then the distortion of $h(t)$ due to nonlinear phase can be neglected.

It is shown in Appendix H.1 that approximation (8.4) is accurate within $\alpha \pi$ radians when

$$B < B_0 = \rho f_c^{3/2} \quad \text{for} \quad \rho = \sqrt{\frac{\alpha}{2 \mathcal{D} DM}}. \quad (8.5)$$

As illustrated in Figure 8.2, B_0 decreases (dispersion becomes more severe) as DM increases or f_c decreases. The value of B_0 varies over about four orders of magnitude for the parameters shown. The line of sight "interstellar weather conditions" also influence B_0 through the $\sqrt{1/DM}$ term in ρ .

The baseband model for dispersion when (8.5) is satisfied is illustrated in Figure 8.3. The result is the phase shift $\phi(f_0)$ which is unknown and added to unknown carrier phase θ together with a baseband delay equal to the plasma dispersion delay at the carrier frequency $\tau(f_c)$. In the time domain, this model becomes

$$|z(t)| \approx |R_h(t - \tau(f_c))|. \quad (8.6)$$

The phase shift does not affect $|z(t)|$, and flat delay $\tau(f_c)$ can be neglected since it is added to an already-large and unknown propagation delay. When $B > B_0$, however, the MF output becomes smeared over time and, as a result reduced in amplitude. This is illustrated in Figure 8.4, where the effect of dispersion on $R_h(t)$ as in Figure 8.3 is illustrated for different values of B . Violating (8.5) reduces the sensitivity of a detector that depends on the statistic $|z(0)|$.

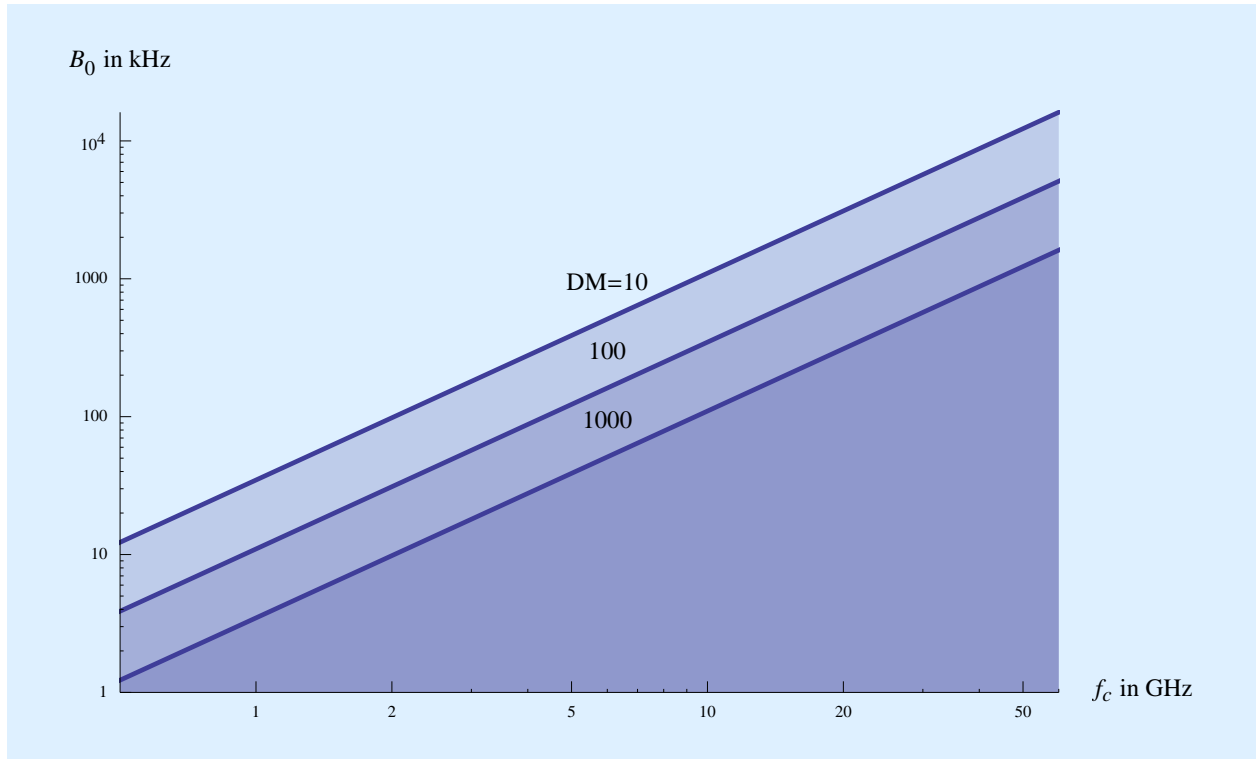


Figure 8.2: A log-log plot of the coherence bandwidth B_0 of (8.5) in kHz vs carrier frequency f_c in GHz for low, moderate, and severe dispersion. A $\alpha = 0.1$ criterion for coherence is used.

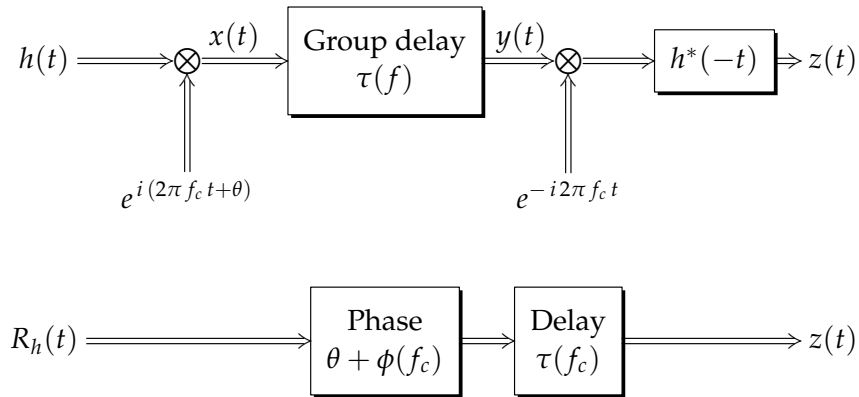


Figure 8.3: A model for plasma dispersion within an ICH. At passband (top diagram) the effect is a frequency-dependent group delay $\tau(f)$. The bottom baseband model results when approximation (8.4) is applied, the resulting passband filter is referred to baseband, and then the order of the dispersion and matched filters is reversed.

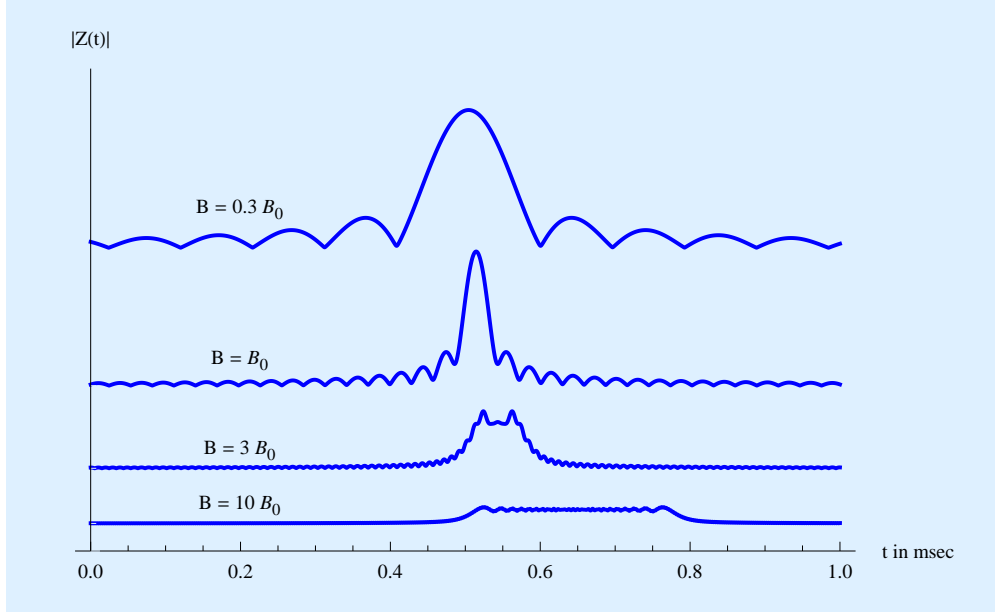


Figure 8.4: The response $z(t)$ to input $R_h(t)$ in Figure 8.3 shown for difference values of B . The parameters are the same as Figure 8.1 except the bandwidth is much smaller (B satisfying (8.5) is 34.7 kHz). Plotted is magnitude $|f(t) \otimes R_h(t)|$ (but not phase) for different values of B ranging from $B = 0.3 B_0$ to $B = 10 B_0$. For $B < B_0$ the pulse broadens due to reduced bandwidth rather than dispersion. For $B > B_0$ the pulse is smeared out in time and reduced in magnitude. The effect of dispersion at $B = B_0$ in terms of smearing and magnitude reduction is visible but has no material effect on $|z(0)|$.

There is an alternative interpretation of (8.5) that lends additional insight, and follows the convention in wireless communications [16] of focusing on group delay rather than phase. The effect of $B \gg B_0$ can be observed in the impulse response of the dispersion, which is illustrated in Figure 8.5 for the same parameters as Figure 8.1. After removing the smallest fixed band-edge group delay $\tau(f_c + B)$, the remaining group delay is approximately distributed uniformly through $[0, \tau_s]$. Thus the magnitude of the impulse response is approximately spread uniformly over time $[0, \tau_s]$, where τ_s is called the *delay spread*, defined as the range of group delays across the bandwidth

$$\tau_s = \tau(f_c) - \tau(f_c + B). \quad (8.7)$$

The phase, however, is chaotic and very sensitive to DM. Delay spread τ_s is a measure of how much the dispersion increases the time duration of a signal. It is easily shown that

$$B \tau_s = \left(\frac{B}{B_0} \right)^2 \quad \text{for } \alpha = 1. \quad (8.8)$$

This is strikingly similar to (3.8) because $B_0 \tau_s = 1$. A coherence bandwidth defined as the inverse of the delay spread is a fundamental characteristic of wireless propagation [16].

There are two related issues related to transmitter/receiver coordination that are addressed in Appendix H.2. First, based on pulsar observations both the transmitter and receiver can estimate DM along the line-of-sight. However, both estimates have some uncertainty, both individually

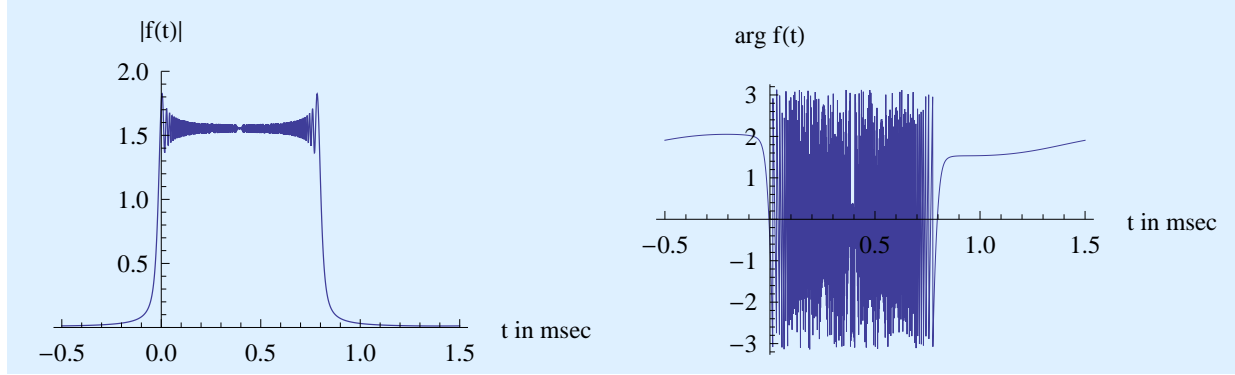


Figure 8.5: The magnitude and phase of the dispersive impulse response $f(t)$ for the $F(f)$ illustrated in Figure 8.1 after bandlimiting to $f \in [0, B]$. The magnitude is roughly uniformly spread between 0 and 0.83 msec, corresponding to a delay spread $\tau_s = 0.83$ from (8.7). The oscillations and non-causality in $|f(t)|$ are caused by ideal band limiting of the impulse response rather than dispersion, whereas the rapidly varying phase (reflecting the 1 MHz bandwidth) is due primarily to dispersion.

and jointly. Second, it is possible for either the transmitter or the receiver to equalize the dispersion, presumably for the lowest DM estimate. Either may do this because they are motivated to increase the worst-case coherence bandwidth B_0 , which is dominated by the highest DM estimate (possibly reduced by the equalization of the lowest DM estimate). This has implications for the receiver strategy in estimating a value for B_0 to inform its search strategy.

8.3 Source/observer motion

Source-observer motion is potentially an important source of impairment in the form of Doppler shifts in frequency, time dilation, and fading. Although elementary physics texts describe motion effects in terms of a shift in frequency, this is a monochromatic approximation and the effect on nonzero-bandwidth signals is more complicated. This effect is now modeled, making the approximation that the velocities are small relative to the speed of light so that relativistic effects can be neglected.

8.3.1 Effect of time-varying distance and passband signals

Assume that the component of distance between source and observer in the direction of the line of sight is a function of time $d_{\parallel}(t)$. This time-varying distance results in a time-varying group delay $d_{\parallel}(t)/c$, where c is the free-space speed of light. The effect of this delay on a passband signal of the form of (B.1) is

$$y(t) = \Re \left\{ \exp \left\{ i 2\pi f_c \left(t - \frac{d_{\parallel}(t)}{c} \right) \right\} \cdot h \left(t - \frac{d_{\parallel}(t)}{c} \right) \right\} \quad (8.9)$$

Thus, the equivalent complex-valued baseband signal is

$$\exp\left(-i2\pi\frac{d_{\parallel}(t)}{\lambda_c}\right) \cdot h\left(t - \frac{d_{\parallel}(t)}{c}\right). \quad (8.10)$$

There are two distinct effects to consider:

Time incoherence. A time-varying phase shift due to the effect of velocity on the carrier is negligible if T is sufficiently small. The total change in phase will be less than $\alpha\pi$ if T satisfies

$$\frac{d_{\parallel}(t+T) - d_{\parallel}(t)}{\lambda_c} \ll \frac{\alpha}{2}. \quad (8.11)$$

Frequency incoherence. There is a time-varying group delay experienced by the baseband waveform $h(t)$, which is potentially a source of frequency incoherence. However, when T satisfies (8.11), this effect is negligible because the corresponding delay spread affecting $h(t)$ is

$$\tau_s = \frac{d_{\parallel}(t+T) - d_{\parallel}(t)}{c} \ll \frac{\alpha}{2f_c}. \quad (8.12)$$

Since it will always be true that $B \ll f_c$, it follows that $2B\tau_s \ll \alpha B/f_c \ll 1$ and thus by the criterion of (3.8) this delay spread can be neglected.

The condition on coherence time (8.11) will now be investigated for typical motion scenarios.

8.3.2 Constant velocity

Any constant delay term in $d_{\parallel}(t)$ can be ignored as a fixed phase shift. It is also possible to neglect any constant velocity term in $d_{\parallel}(t)$ within a given ICH, but not necessarily for different ICH's. To see why, assume that $d_{\parallel}(t)$ represents a fixed velocity, or $d_{\parallel}(t) = v_{\parallel}t$, over the time interval $[0, T]$ corresponding to a single ICH. Then the baseband signal over that interval is

$$\exp\left(-i2\pi\frac{v_{\parallel}}{\lambda_c}t\right) \cdot h\left(t\left(1 - \frac{v_{\parallel}}{c}\right)\right) \quad (8.13)$$

The effect is a frequency shift of v_{\parallel}/λ_c and a time dilation of $h(\cdot)$. Neither effect is significant because the receiver has no absolute reference for either the carrier frequency or the time dilation, as both these parameters can be freely chosen by the transmitter.

On the other hand, suppose that two ICH's experience different velocities, v_1 and v_2 . Then the frequency offsets and time dilations are different for the two ICH's. Clearly this cannot be ignored when a receiver is, for example, doing pattern matching on energy bundles across time. These different velocities signal the presence of acceleration, which will be caused by the solar system dynamics, as modeled shortly.

The foregoing applies to the component of velocity parallel to the line of sight v_{\parallel} . In contrast, the velocity transverse to the line of sight v_{\perp} is the direct cause of fading, which is the time variation component of scintillation. This effect is considered in Section 8.5.

8.3.3 Diurnal rotation and orbital motion

While two solar systems may have a substantial relative velocity, we have seen that this results in a carrier frequency offset and time dilation of $h(t)$ that cannot be distinguished from parameter choices made by the transmitter. Generally the only germane origin of *variation* in velocity is the diurnal rotation of a planet about its axis and its orbital motion about its host star. Of course both the transmitter and receiver will typically contribute to these effects, unless either locates its equipment on a spacecraft that is not subject to rotation and orbital motion.

To qualitatively understand the effect this has on the baseband signal, the effects due to rotation and orbital motion at transmitter and at receiver will be considered separately. Also make the simplification that the resulting motion is circular and the worst-case assumption that it falls in a plane containing the line of sight. Of course this analysis can be made more accurate with a more complete model of the dynamics, but this doesn't introduce much additional insight. The time-variation of distance for a simple circular motion is

$$d_{\parallel}(t) = R \cdot \sin\left(2\pi \frac{t}{P}\right) \quad (8.14)$$

where R is the radius of the circular motion and P is the period. Approximate values for these parameters for Earth are give in Table 8.1.

Consider one ICH extending over time interval $t \in [t_1, t_1 + T]$. Assuming the distance change is small over this time interval, a Taylor series expansion of the distance about $t = t_1$ yields

$$d_{\parallel}(t) = R \sin\left(\frac{2\pi t_1}{P}\right) + \frac{2\pi R (t - t_1) \cos\left(\frac{2\pi t_1}{P}\right)}{P} - \frac{2\pi^2 R (t - t_1)^2 \sin\left(\frac{2\pi t_1}{P}\right)}{P^2} \quad (8.15)$$

$$- \frac{4\pi^3 R (t - t_1)^3 \cos\left(\frac{2\pi t_1}{P}\right)}{3 P^3} + \dots + . \quad (8.16)$$

The first term can be neglected since there are other sources of unknown fixed phase, including carrier phase and scintillation. The next term is a constant velocity, which can be neglected within a single ICH. However, it will cause a differential shift in frequency across different ICH's, with a frequency shift as large as

$$|\Delta f| \leq \frac{4\pi R}{\lambda_c P} . \quad (8.17)$$

From Table 8.1, $|\Delta f|$ is larger for orbital motion, and increases in proportion to f_c . However, the frequency shift will be much smaller over time scales short relative to P (one day or one year).

Within an ICH, the most significant source of impairment is the acceleration term $(t - t_0)^2$. This is potentially a significant source of time incoherence, but one that can be rendered negligible by choosing T sufficiently small. A maximum phase shift less than $\alpha\pi$ determines the maximum T as

$$\frac{2\pi^2 R T^2}{\lambda_c P^2} \ll \frac{\alpha}{2} \quad \text{or} \quad T \ll \frac{P}{2\pi} \cdot \sqrt{\frac{\alpha \lambda_c}{R}} \quad (8.18)$$

Table 8.1: The approximate radius R and period P for Earth and the resulting coherence time T_c and frequency shift Δf_c , where f_{GHz} is the carrier frequency in GHz. Since many planets or moons in the Milky Way may have a smaller radius or shorter period, a safety factor of $\alpha = 0.01$ on the maximum phase shift is assumed in calculating T .

Case	Parameter	Coherence time	Frequency shift
Diurnal rotation	$R = 6.39 \times 10^6 \text{ m}$	$T \text{ sec} = 3 f_{\text{GHz}}^{-1/2}$	$ \Delta f \text{ kHz} = 3 f_{\text{GHz}}$
	$P = 8.6 \times 10^4 \text{ sec}$		
Orbital motion	$R = 1.5 \times 10^{11} \text{ m}$	$T \text{ sec} = 7 f_{\text{GHz}}^{-1/2}$	$ \Delta f \text{ kHz} = 200 f_{\text{GHz}}$
	$P = 3.15 \times 10^7 \text{ sec}$		

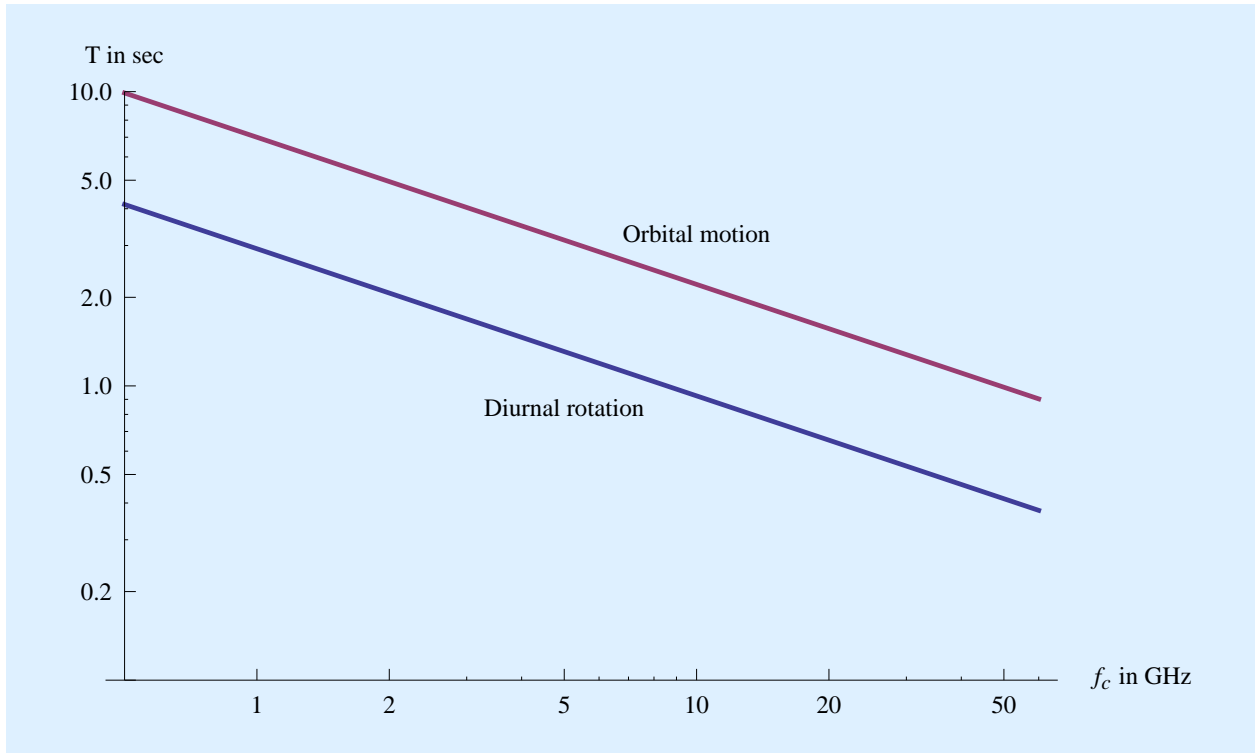


Figure 8.6: A log plot of the coherence time T vs. the carrier frequency f_c . The dynamics of Earth are assumed with an additional safety factor of $\alpha = 0.01$ using the formulas from Table 8.1.

From Table 8.1, the coherence time T of the ICH decreases as $f_c^{-1/2}$, and acceleration becomes an increasingly significant phenomenon for larger f_c . The resulting coherence times are plotted as a function of f_c in Figure 8.6.

8.3.4 Motion compensation

While the relative velocity of two stars may not be known accurately, the dynamics of each solar system is well known to the local inhabitants. For example, on Earth the HORIZONS System from

the Jet Propulsion Laboratory provides real-time data on the current status of the solar system [54]. There is an opportunity for the transmitter and the receiver to compensate for this known dynamics. The full correction within an ICH and among ICH's can be performed at baseband by multiplying by the conjugate of the time-varying phase factor of (8.10),

$$\exp \left(i 2\pi \frac{d_{\parallel}(t)}{\lambda_c} \right). \quad (8.19)$$

If the transmitter and receiver both do this independently, it will eliminate the component of motion aligned with the line of sight (at least that source due to solar system dynamics) as a source of incoherence and relax the constraint on T due to this physical phenomenon. A simpler compensation would be to adjust for the frequency offset among different ICH's without compensating for the time-varying phase shift within an ICH. The remaining time incoherence within an ICH can be rendered negligible by choosing T in accordance with (8.18).

8.4 Scattering

Interstellar scattering has been investigated by a variety of techniques, including relatively simple geometric optics [55, 56, 57] and numerical evaluation of turbulent gas models [58], always evaluating the models by comparison to empirical observations of pulsar signals. Here we employ the simplest possible methodology, geometrical optics and ray tracing assuming a one-dimensional scattering screen. A recommended tutorial on scattering that assumes a two-dimensional screen is [18]. Of course reality is much more complicated, as the scattering medium is dispersed through three-dimensional space, but three-dimensional modeling is necessarily based on computational approaches, which are less useful as a source of intuition, and while this can improve the accuracy of numerical results it does not introduce any major new issues or insights.

Our motivation in using a deliberately simple model is threefold. First, the goal is to convey the mechanisms of scattering in the simplest fashion, to emphasize intuition over accuracy. Second, the limited objective is to convince the reader of the existence of the ICH and convey an appreciation of the physical mechanisms that determine its size. Third, the needs of interstellar communication are much different from astrophysics. Astrophysics must work backwards to estimate the characteristics of a natural source after propagation through the interstellar medium, whereas communication seeks to design an artificial signal that circumvents the impairments introduced in that propagation. If this design is successful, the detailed modeling of those impairments is unnecessary because they can be neglected. Having said this, a serious effort at quantifying the size of the ICH in the context of an interstellar communication system design will want to draw upon the full suite of modeling and observations represented in the astrophysics literature, rather than relying on the simple model illustrated here, in order to obtain the most numerically accurate results.

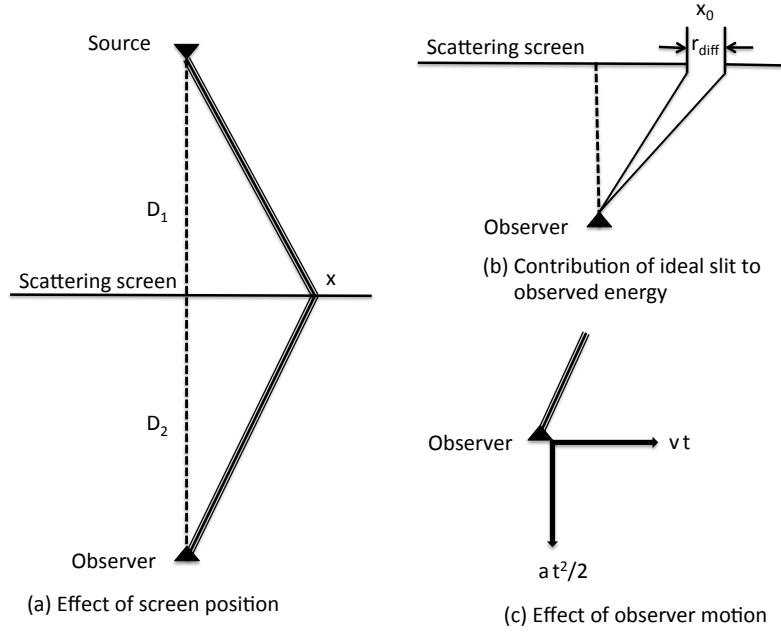


Figure 8.7: Illustration of the geometry of scattering using a simplified one-dimensional scattering screen. (a) Rays passing through the screen at different lateral distances x encounter different group delays and phase shifts due to small variations in electron density. The total distance from source to observer is $(D_1 + D_2)$, divided between D_1 from source to screen and D_2 from screen to observer. (b) An ideal slit is opaque to all rays except over the range $[x_0 - r_{\text{diff}}/2, x_0 + r_{\text{diff}}/2]$. (c) Motion of the observer in the direction of the line of sight with acceleration a and transverse to the line of sight with velocity v .

8.4.1 Geometry of scattering

For the interstellar medium, where scales are vastly larger than one wavelength, scattering can be qualitatively explained in terms of the simple ray model of Figure 8.7, where a thin one-dimensional scattering screen is assumed [18]. The actual ISM has variations in electron density, which manifest themselves as spatial variations in the plasma dispersion effects. In the thin screen model, these variations are represented by a variation in group delay and phase shift with lateral distance x . The variations in electron density are typically quite small, and thus have little effect on the group delay of propagation through the screen, but do cause a substantial variation in phase shift. Phase is very sensitive to small perturbations in electron density.

A slightly refined model to Figure 3.2 is shown in Figure 8.7a. It is still one dimensional and assumes a thin screen, but it captures the distance from source to screen and screen to observer. Consider a single ray passing through point x on the screen as shown in Figure 8.7a. Define the excess distance travelled along the ray (relative to $x = 0$) as $d(x)$, and that $|x| \ll D_1$ and $|x| \ll D_2$.

The Fresnel approximation assumes that third and higher powers of x can be neglected,

$$d(x) = \sqrt{D_1^2 + x^2} + \sqrt{D_2^2 + x^2} - (D_1 + D_2) \approx \frac{x^2}{2D} \quad \text{for } |x| \ll D \quad (8.20)$$

where D is defined by

$$\frac{1}{D} = \frac{1}{D_1} + \frac{1}{D_2}. \quad (8.21)$$

Thus, after the Fresnel approximation, the simpler model of Figure 3.2 still applies, with D defined by (8.21).

The excess propagation delay associated with a ray passing through point x on the screen is thus approximately $d(x)/c$. This delay has frequency transfer function

$$\exp \left\{ -i 2\pi f \frac{d(x)}{c} \right\} \approx \exp \left\{ -i \pi \frac{f x^2}{c D} \right\} = \exp \left\{ -i \pi \frac{x^2}{r_F^2} \right\}. \quad (8.22)$$

The Fresnel scale r_F was defined in (3.5). It is interpreted as the scale $0 \leq x \leq r_F$ over which there is a π radian phase shift in the transfer function. Notably $r_F(f)$ is a function of frequency f , but this dependency has been suppressed in (8.22) because the variation is negligibly small over the band $f \in [f_c, f_c + B]$. To see this, expand in a Taylor series,

$$\frac{r_F(f_c + \Delta f)}{r_F(f_c)} = 1 - \frac{\Delta f}{2 f_c} - \dots, \quad (8.23)$$

so that $r_F(f_c + \Delta f) \approx r_F(f_c)$ for $\Delta f \leq B \ll f_c$.

When the screen itself introduces an extra phase shift $\phi(f, x)$, the transfer function of (8.22) should be multiplied by $\exp \{ i 2\pi \phi(f, x) \}$. This phase can be a function of both x (because of inhomogeneities in the turbulent clouds of ionized gasses) and f (because of plasma dispersion).

The idea behind ray tracing in geometric optics is that the total response at the observer is the superposition of the responses due to individual rays corresponding to different values of x . The total response is given by the Fresnel-Kirchoff integral, which integrates the transfer function of screen plus delay over all values of x ,

$$\psi(f) = \frac{e^{-i\pi/4}}{r_F} \int_{-\infty}^{\infty} \exp \left\{ i \phi(x, f) - i \pi \frac{x^2}{r_F^2} \right\} dx. \quad (8.24)$$

Due to the identity

$$\int_{-\infty}^{\infty} \exp \left\{ -i \pi \frac{x^2}{r_F^2} \right\} dx = r_F e^{i\pi/4}, \quad (8.25)$$

the normalization constant in (8.24) results in $\psi(f) \equiv 1$ (no attenuation or phase shift) for the special case $\phi(x, f) \equiv 0$ (no scattering). In particular this normalization renders the attenuation to be frequency-independent, in agreement with the plane wave solution of Maxwell's equations for freespace propagation. It does, however, ignore the propagation loss (which increases as the square of distance). Thus, (8.24) isolates the effects of the scattering screen while omitting propagation loss.

8.4.2 Scattering within a coherence hole

The scattering model of (8.24) can be simplified considerably within an ICH. Although scattering may place more restrictive conditions, the bandwidth B of the signal at minimum satisfies (8.5), and the resulting model for $\phi(f, x)$ simplifies to that of Figure 8.3. Namely, the phase through the scattering screen consists of a fixed phase $\theta + \phi(f_c, x)$ together with a group delay $\tau(f_c, x)$ that depends on carrier frequency but is otherwise frequency-independent. In addition, within the turbulent ionized gasses, the inhomogeneity in electron density over the scales of interest is quite small, so that the group delay $\tau(f_c, x)$ can be considered to be independent¹ of x , and further can be neglected because it is added to the very large propagation delay. The net effect of these assumptions is that we substitute a phase that is frequency-independent, or $\phi(f, x) \approx \phi(x)$. The fixed unknown carrier phase θ can also be neglected, since $\phi(x)$ is also unknown.

In view of these approximations, any waveform distortion of signal $h(t) e^{i2\pi f_c t}$ passing through the screen on a ray through point x can be neglected, but rather $h(t)$ is merely delayed by $d(x)/c$ and shifted in phase by $\phi(x)$. The resulting observed signal is

$$e^{i\phi(x)} h(t - d(x)/c) \exp\{i2\pi f_c (t - d(x)/c)\}, \quad (8.26)$$

with corresponding baseband signal (after substituting for $d(x)$)

$$h(t - d(x)/c) \cdot \exp\{i\phi(x) - i2\pi x^2/r_F^2\}. \quad (8.27)$$

Within an ICH, the bandwidth of $h(t)$ is small enough that the delay can be neglected. In that event, the total observation is the superposition of this signal over all x , or $\sqrt{\mathcal{F}} \cdot h(t)$ for scintillation flux

$$\mathcal{F} = \left| \frac{1}{r_F} \int_{-\infty}^{\infty} \exp\left\{i\phi(x) - i\pi \frac{x^2}{r_F^2}\right\} dx \right|^2. \quad (8.28)$$

Again, (8.28) has been normalized so that $\mathcal{F} = 1$ when $\phi(x) \equiv 0$. Also note the parallel between this model and the simplified modeling of Section 3.2.1, with the replacement of a sum by the Fresnel-Kirchoff integral.

8.4.3 Coherent patches on the scattering screen

The size of integral (8.28) depends on the spatial coherency of the phase. In regions of x for which that phase is changing rapidly, the contribution to the integral will be small, while the most significant contributions to \mathcal{F} come from areas of slow phase variation. There are two contributors to phase variation, the random phase due to inhomogeneities in electron density $\phi(x)$, and the geometric variation due to path length changes that is proportional to x^2 . The latter increases in importance with large x , and its greater rate of variation with increasing x effectively limits the scale over which a significant contribution to \mathcal{F} can occur.

¹ Even if there were a variation of $\tau(f_c, x)$ with x , the resulting effect would be negligible within an ICH if $2B\tau_s \ll 1$ for a total delay spread τ_s .

Statistically $\phi(x)$ displays “coherence patches” over distances in x over which the variation in $\phi(x)$ is small roughly equal to its diffraction scale r_{diff} [18]. It is these coherent patches that contribute most of the energy in \mathcal{F} . As illustrated in Figure 8.7b, the effect can be captured qualitatively by modeling a single coherent patch located at $x = x_0$ as an ideal slit $[x_0 - r_{\text{diff}}/2, x_0 + r_{\text{diff}}/2]$, within which the phase shift introduced by the screen is a constant $\phi(f_c, x) = \phi_0$. The contribution of such a slit to \mathcal{F} is

$$\mathcal{F} = \left| \frac{1}{r_F} \int_{-r_{\text{diff}}/2}^{r_{\text{diff}}/2} \exp \left\{ -i \pi \frac{(x_0 + u)^2}{r_F^2} \right\} du \right|^2. \quad (8.29)$$

When modeling a small scale patch on the screen, the Fraunhofer approximation can simplify the integration by eliminating the x^2 term. This approximation notes that

$$(x_0 + u)^2 = x_0^2 + 2x_0 u + u^2 \quad (8.30)$$

and the first term introduces a constant phase that can be neglected, while the u^2 term can be neglected when $r_{\text{diff}} \ll x_0$. Thus, the Fraunhofer approximation to the magnitude of (8.29), is

$$\mathcal{F} \approx \left| \frac{1}{r_F} \int_{-r_{\text{diff}}/2}^{r_{\text{diff}}/2} \exp \left\{ -i 2\pi x_0 u / r_F^2 \right\} du \right|^2 = \left| \frac{r_{\text{diff}}}{r_F} \cdot \text{sinc} \left(\frac{\pi r_{\text{diff}} x_0}{r_F^2} \right) \right|^2. \quad (8.31)$$

This spells out how, as the location $x = x_0$ of an ideal slit (with scale r_{diff}) is changed, the magnitude of the contribution of that slit to \mathcal{F} changes. This is a “reverse” diffraction pattern, capturing the effect of a variation in slit location to the energy arriving at a single point of observation. This pattern defines the new refraction scale $r_{\text{ref}} = r_F^2 / r_{\text{diff}}$, and written in terms of r_{diff} (8.31) becomes

$$\mathcal{F} \approx \left| \frac{r_{\text{diff}}}{r_F} \cdot \text{sinc} \left(\frac{\pi x_0}{r_{\text{ref}}} \right) \right|^2. \quad (8.32)$$

The scale r_{ref} equals half the width of the main lobe in the pattern, and thus $|x| \leq r_{\text{ref}}$ is the primary source of energy arriving at the observer (that is why it is called the refraction scale). Of course, some energy originates from outside the screen’s refraction scale, but it is smaller. The energy \mathcal{F} in (8.32) is plotted in Figure 8.8 for two strong scattering scenarios. From (8.32) the energy arriving at the observer for $x_0 = 0$ is greater for a wider slit (larger r_{diff}) because a wider slit allows more total energy to pass the screen. The nulls occur at multiples of r_{ref} , so these nulls are closer together for a wider slit (larger r_{diff}).

8.4.4 Focusing by the scattering screen

Coherent patches cannot explain the behavior $\mathcal{F} > 1$, since in the limit of dense coherent patches with the same constant phase, $\mathcal{F} \approx 1$ (this becomes equivalent to freespace propagation). Focusing by the screen offers a physical explanation for $\mathcal{F} > 1$. In (8.28) the contribution to \mathcal{F} from a given region can be large, even for very large x_0 , if the screen-induced phase approximately cancels out

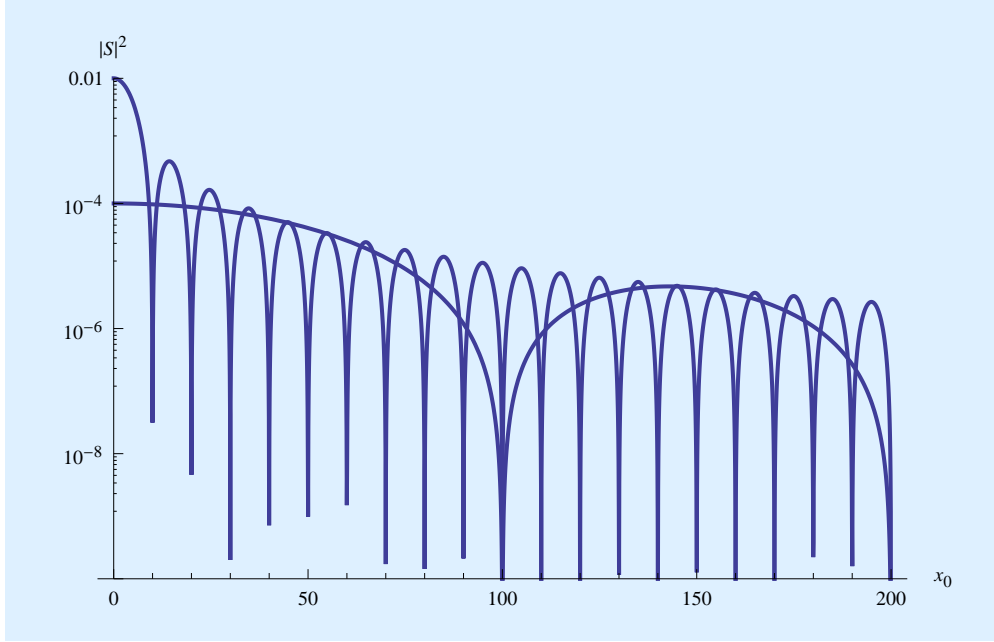


Figure 8.8: A log plot of the energy $|S|^2$ arriving at the observer and emanating from an ideal slit of width r_{diff} located at point x_0 on the screen. It is assumed that $r_F = 1$, so in effect the abscissa has units of one Fresnel scale. Two values of r_{ref} are shown: $r_{\text{diff}} = 0.1$ (or $r_{\text{ref}} = 10$) has its first null at $x_0 = 10$, and $r_{\text{diff}} = 0.01$ (or $r_{\text{ref}} = 100$) has its first null at $x_0 = 100$. The amplitude at $x_0 = 0$ is higher for the wider slit ($r_{\text{diff}} = 0.1$) because more incident energy is able to pass through.

the pathlength-induced phase, or²

$$\phi(f_c, x) \approx \pi \frac{x^2}{r_F^2} \quad \text{or} \quad \frac{\partial \phi(f_c, x)}{\partial x} \approx 2\pi \frac{x}{r_F^2}. \quad (8.33)$$

This is, of course, the definition of a lens that focuses the energy on the observer's reference point. While (8.33) is unlikely to be satisfied over significantly large scales, it is certainly possible within the diffraction scale r_{diff} . Note that over the range $[x_0 - r_{\text{diff}}/2, x_0 + r_{\text{diff}}/2]$, $\phi(f_c, x)$ must vary over the range of $2\pi x_0/r_{\text{ref}}$ to satisfy (8.33). Outside the refraction scale $|x_0| > r_{\text{ref}}$ this variation must be larger than 2π , which makes it statistically unlikely. When lensing does occur, its contribution to $|S|$ is the same as the ideal slit with the same aperture located at $x_0 = 0$, regardless of whether the lensing occurs inside or outside the refraction scale.

8.4.5 Frequency coherence of scattering

Approximation (8.28) assumes that the effect of delay on $h(t)$ in (8.27) can be neglected, and this in turn limits the acceptable B . The criterion for this is $2B\tau_s < \alpha$, where τ_s is the delay spread or

² If (8.33) were valid for all x then $\mathcal{F} \rightarrow \infty$, which indicates a problem with the model. This non-physical behavior is because the Fresnel approximation is not valid for large $|x|$. This is not of concern because (8.33) is unlikely to be satisfied for any range of x much larger than r_{diff} .

equivalently the excess delay of components for the largest $|x|$ that contributes significant scattering energy.

Consider first the strong scattering case. The main lobe of the interference pattern at the observer corresponds to $|x| \leq r_{\text{ref}}$. If we include the energy from a scale n times larger than this to be conservative, the delay spread becomes

$$\tau_s = \frac{d(n r_{\text{diff}})}{c} \approx \frac{n^2}{2 f_c} \cdot \left(\frac{r_F}{r_{\text{diff}}} \right)^2. \quad (8.34)$$

Thus frequency coherence is achieved when

$$B < \frac{\alpha}{n^2} \cdot f_c \left(\frac{r_{\text{diff}}}{r_F} \right)^2. \quad (8.35)$$

Taking into account the frequency dependence of r_{diff} and r_F , the B in (8.35) increases as $f_c^{4.4}$, which is much more rapidly than the coherence bandwidth for plasma dispersion. Thus, the relative importance of plasma dispersion increases with f_c .

For weak scattering, most of the scattered energy arrives from the first Fresnel zone $|x| \leq r_F$, and again to be conservative by including n times this scale,

$$\tau_s \leq \tau_s = \frac{d(n r_F)}{c} \approx \frac{n^2}{2 f_c}. \quad (8.36)$$

The criterion for frequency coherence is then

$$B < \frac{\alpha}{n^2} \cdot f_c. \quad (8.37)$$

Thus, once we move into the weak scattering regime, the coherence bandwidth increases more slowly with f_c . However, the coherence bandwidth is so large in this regime that frequency incoherence is unlikely to be a significant impairment.

Arriving at a more accurate estimate for the B that guarantees frequency coherence depends on the detailed statistics of $\phi(x)$ and the resulting distribution of the energy arriving as a function of delay. For energy arriving within a scale $|x| \leq r$, the scattering amplitude seen at the MF output is given by (8.7),

$$\mathcal{F} = \left| \frac{1}{r_F} \cdot \int_{-r}^r \exp \left\{ i \phi(x) - i \pi \frac{x^2}{r_F^2} \right\} dx \right|^2. \quad (8.38)$$

This model is a considerable improvement to the ideal slit in that it captures the effects of coherent patches and lensing as well as other detailed effects. A methodology used in the astrophysics literature is to generate a large set of sample functions of phase $\phi(x)$ based on models of wavenumber spectrum, and perform a Monte Carlo simulation of the resulting flux \mathcal{F} .

8.5 Fading and the time coherence of scintillation

In a static model of scattering of Section 8.4, time coherence is not an issue because the model for S is not time-dependent. In reality, there are two sources of nonstationarity. One is changes in $\phi(x)$ with time due to the turbulence of the interstellar clouds. This is a phenomenon that plays out over days or weeks, and thus is not a factor in defining the size of an ICH. Over shorter time scales, the dominant source of non-stationarity is the interaction of source/observer motion with scattering. As T is decreased the total degree of variation decreases and eventually becomes insignificant.

Within an ICH, fading is a velocity rather than acceleration phenomenon. In Figure 8.7c, the velocity of the receiver causes a carrier frequency offset that was neglected in Section 8.3. However in the presence of scattering, velocity cannot be neglected because the component of receiver motion in the direction of each incoming ray from the scattering screen varies slightly with x . This results in a small relative frequency offset among the rays, and that in turn causes the constructive and destructive interference mechanism of refraction to vary with time and this in turn causes a variation in scintillation amplitude. This effect cannot be compensated at the receiver as argued in Section 8.3 by a simple carrier-frequency offset. The superposition of the Doppler-shifted rays occurs *before* to the receiver's observation, and thus there is no single correction that can simultaneously take care of all the Doppler frequency shifts for all the rays.

The effect of observer motion can be modeled by assuming two components of velocity, v_{\parallel} parallel to the line of sight and v_{\perp} transverse to the line of sight. As pictured in Figure 8.7c, only v_{\perp} is a significant source of fading. The variation in velocity for $t \in [0, T]$ due to acceleration is very small and can be neglected. The total excess length of a ray through point x on the screen then becomes, as a function of time,

$$\sqrt{D_1^2 + x^2} + \sqrt{(D_2 + v_{\parallel}t)^2 + (x - v_{\perp}t)^2} - (D_1 + D_2) \approx d(x) + v(x) \cdot t. \quad (8.39)$$

In Appendix I a Fresnel approximation is applied to (8.39), and it is shown that the resulting effect at baseband is a time varying phase that depends on x . If T is kept sufficiently small, the total phase change can be kept small. This phase variation is less than $\alpha \pi$ radians when

$$\left| \frac{f_c v_{\perp} x T}{c D_2} \right| < \alpha \quad (8.40)$$

for all values of x . In particular (8.40) must be satisfied for the largest x that is a significant contributor to energy arriving at the observer.

Consider first the strong scattering regime. Following Section 8.4.5, suppose that only $|x| \leq n r_{\text{ref}}$ is a significant source of energy, in which case the most stringent condition on T for (8.40) becomes

$$T \ll \frac{\alpha c D_2}{f_c |v_{\perp}| n r_{\text{ref}}}. \quad (8.41)$$

Since $D \leq D_2$, a slightly more stringent version of (8.41) is

$$T < \frac{\alpha c D}{f_c |v_{\perp}| n r_{\text{ref}}} = \frac{\alpha r_{\text{diff}}}{n |v_{\perp}|}. \quad (8.42)$$

Thus, significant time variations in scintillation amplitude occur on spatial scales of observer motion that are greater than a multiple of the diffraction scale $n r_{\text{diff}}$. Since whatever happens at the plane of motion of the observer is a mirror of the scattering screen (with appropriate geometric corrections), this significant change over a scale that mirrors significant phase change at the screen is not surprising. Since $r_{\text{diff}} \propto f_c^{6/5}$, this coherence time increases (albeit relatively slowly) with f_c .

For the weak scattering regime, the significant range is $|x| \leq n r_F$. The coherence time becomes (8.42) with r_{diff} replaced by r_F , or

$$T < \frac{\alpha r_F}{n |v_{\perp}|}. \quad (8.43)$$

This case (which for a given D corresponds to larger f_c) sees a decreasing T with increasing f_c .

8.6 Numerical example

While some impairments have been deemed to be insignificant, the operative sources of incoherence are summarized in Table 8.2. A safety factor of $\alpha \leq 1$ permits an adjustment of the stringency of the criterion. There are two primary contributions to frequency incoherence, both resulting from a spreading of the arriving energy over time. One is the frequency-dependence of group delay that is characteristic of plasma dispersion, and the other is the spatial-dependence of group delay due to scattering. Two primary contributors to time incoherence have been identified, both due to time-varying phase shift caused by relative source/observer motion. One is the component of acceleration of source and observer along the line of sight, and the other is the interaction between the velocity of the observer transverse to the line of sight and the spatial distribution of angle of arrival due to scattering. Rendering all these effects insignificant within an ICH determines the coherence time T_c and coherence bandwidth B_c of the ICH, and thus the degrees of freedom K_c . The most important physical determinants are the distribution of electron density in the ISM along the line of sight and the relative motion of source and observer. There is also a strong dependence on the carrier frequency f_c .

The coherence bandwidth and coherence time are plotted in Figure 8.9 for the numerical values given in Table 3.2. A value $\alpha = 0.1$ is used, except for acceleration where a more conservative factor $\alpha = 0.01$ is used to account for the strong possibility that another planet or moon may experience a stronger acceleration than Earth, and also to account for the possible accumulation of accelerations due to transmitter and receiver. Over the entire range of carrier frequencies, one impairment is more constraining than the other. In the case of frequency coherence, plasma dispersion determines the ICH coherence bandwidth B_c . For time coherence, acceleration dominates the coherence time T_c . The resulting B_c increases with f_c , and T_c decreases with f_c . As shown in Figure 3.6, the net effect is a $K_c = B_c T_c$ that starts at $K_c \gg 1$ and increases monotonically with f_c .

Any receiver designer should be cognizant of two possible corrections that may be performed in the transmitter. In the interest of increasing the coherence bandwidth B_c , the transmitter may

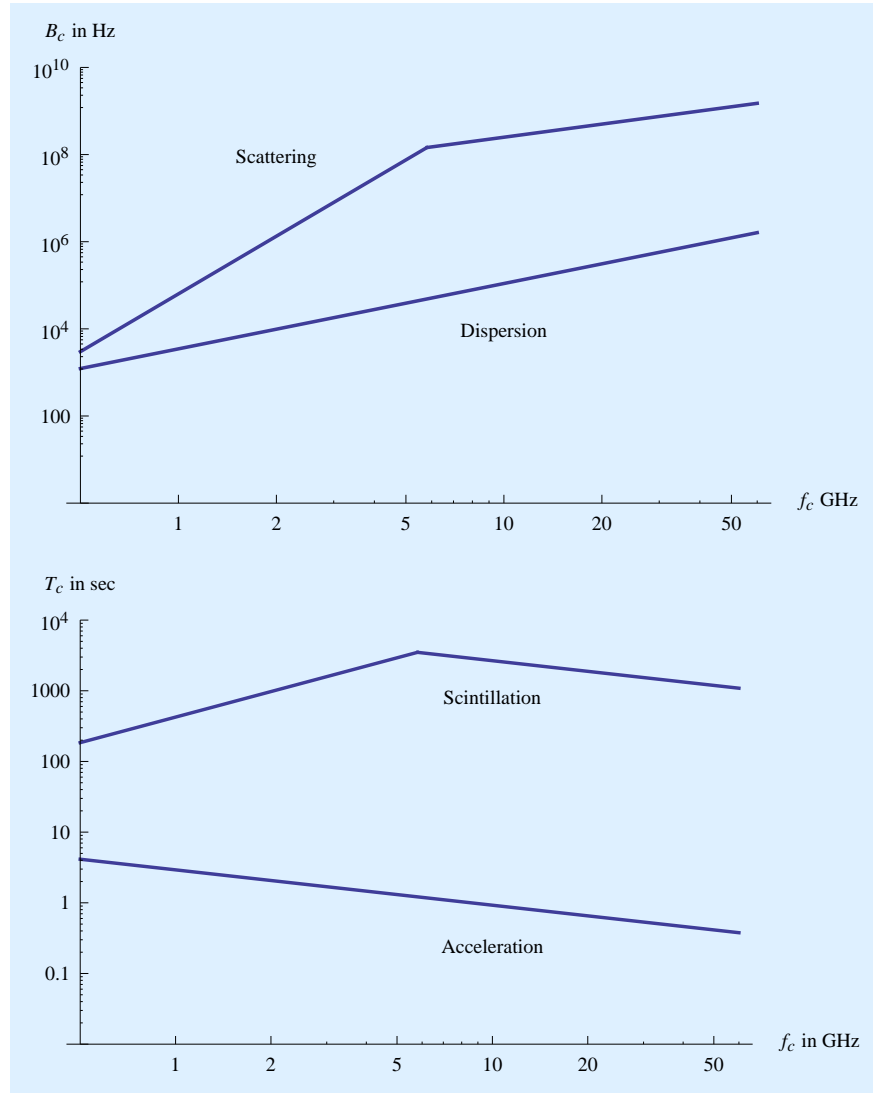


Figure 8.9: Log-log plots of coherence bandwidth B_c above and coherence time T_c below, plotted against carrier frequency f_c for the assumed physical parameters of Table 3.2. In all cases, it is assumed that $\alpha = 0.1$ and $n = 2$. For scattering phenomena, the break in the slope corresponds to the transition from strong scattering (at lower f_c) to weak scattering (at higher f_c). In each case there are two impairments that limit the size of an ICH, but one always is dominant

Table 8.2: The significant sources of time and frequency incoherence in interstellar communication, distinguishing between the strong and weak scattering regimes.

Type	Source	Strong	Weak
Frequency	Plasma dispersion	$B < \rho f_c^{3/2}$	Same
	Scattering delay spread	$B < \frac{\alpha}{n^2} \cdot f_c \left(\frac{r_{\text{diff}}}{r_F} \right)^2$	$B < \frac{\alpha}{n^2} \cdot f_c$
Time	Acceleration	$T < \frac{P}{2\pi} \cdot \sqrt{\frac{\alpha \lambda_c}{R}}$	Same
	Scintillation	$T < \frac{\alpha r_{\text{diff}}}{n v_{\perp} }$	$T < \frac{\alpha r_F}{n v_{\perp} }$

perform partial equalization for the minimum dispersion. In the interest of increasing the coherence time T_c , the transmitter may correct for the component of acceleration along the line of sight. Interestingly, these are the very same impairments that dominate B_c and T_c , and thus there is motivation to make these corrections if there is a desire to increase K_c , for example to obtain greater immunity to RFI.

8.7 Summary

The sources of time and frequency incoherence have been modeled in sufficient detail to be convincing that they can be circumvented in the interstellar coherence hole (ICH) by restricting the time duration and bandwidth of a waveform used for an individual energy bundle. Included in the analysis have been plasma dispersion and scattering due to clouds of interstellar gasses within the interstellar medium, as well as relative motion of transmitter and receiver due to solar system dynamics. The resulting coherence time and bandwidth have been estimated for typical values of governing physical parameters. The results show that the available degrees of freedom are much larger than unity, providing assurance that the coherence of the interstellar channel is sufficient to support power-efficient communication. This also opens up the possibility of choosing noise-like waveforms in an energy bundle, for example as a means to gaining immunity to interference. If the transmitter and receiver both compensate for their respective contribution to acceleration, the coherence time and degrees of freedom can be substantially increased.

Chapter 9

Conclusions

This report has addressed the end-to-end design of an interstellar communication system taking account of all known impairments from the interstellar medium and induced by the motion of source and observer. Both discovery of the signal and post-discovery communication have been addressed. It has been assumed that the transmitter and receiver designers wish to jointly minimize the cost, and in that context we have considered tradeoffs between resources devoted in the transmitter vs. the receiver. The resources considered in minimizing cost are principally energy consumption for transmitting the radio signal and energy consumption for signal processing in a discovery search.

Thus study is applicable to communication with interstellar spacecraft (sometimes called "starships") in the future, although it will probably be quite some time before these spacecraft wander far enough to invoke many of the impairments considered here. In the present and nearer term this study is relevant to communication with other civilizations. In the case of communication with other civilizations, we of course will be designing either a transmitter, or a receiver, which in either case has to be interoperable with a similar design by the other civilization. In either case, it is very helpful to consider the end-to-end design and resource tradeoffs, as we have attempted here. In our view, a major shortcoming of existing SETI observation programs (which requires the design of a receiver for discovery) is the lack of sufficient attention to the issues faced by the transmitter in overcoming the large distances and the impairments introduced in interstellar space.

One profound conclusion of this study is that if we assume that the transmitter seeks to minimize its energy consumption, which is related to average transmit power, then the communication design becomes relatively simple. The fundamental limit on power efficiency in interstellar communication has been determined, that limit applying not only to us but to any civilization no matter how advanced. Drawing upon the early literature in power-efficient communication design, five simple but compelling design principles have been identified. Following these principles has been shown to permit designs that approach the fundamental limit. Although the same fundamental limit does not apply to the discovery process, we have defined an alternative resource-constrained design approach that minimizes processing resources for a given power level, or power level for

a given processing resource. Again, application of a subset of the five principles leads to a design that can achieve dramatic reductions in the transmitter's energy consumption relative to the type of Cyclops beacons that have been a common target of SETI observation programs, at the expense of a more modest increase in the receiver's energy consumption through an increased observation time in each location.

If we assume that a transmitter designer considers energy to be a scarce resource, and bandwidth to be a relatively ample resource, then the type of signals the transmitter will be deemed to be false alarm events in current and past SETI observation programs, and will likely be dismissed. Fortunately, however, fairly straightforward modifications to these search strategies can open up the possibility of detection of such signals. These modifications include a substantial increase in the number of observations conducted on each line of sight and carrier frequency, and a more sophisticated statistical pattern recognition algorithm.

The results here has direct bearing on a topic of relatively recent interest, the so-called broadband SETI. As we have shown by invoking the fundamental limits, information-bearing signals designed for power efficiency are intrinsically and inevitably inefficient in their use of bandwidth. A concern in broadband SETI has been the dispersive impairments of the interstellar medium, which tend to be invoked with increasing bandwidth. We have shown that in spite of their higher-bandwidth requirement, information-bearing signals designed according to power-efficiency principles need *not* invoke greater impairments. In fact, they *must* not invoke greater impairments. To that end have identified and quantified the interstellar coherence hole (ICH), which allows the building blocks of a transmit signal (the energy bundles) to be designed to have wider bandwidth and still not be subject to any interstellar impairments other than noise and scintillation. By transmitting patterns of these energy bundles in time and frequency, the broadband requirement for power-efficient designs to approach the fundamental limit can be satisfied without invoking interstellar impairments other than noise and scintillation. No processing in either transmitter nor receiver related to other impairments is necessary, save the relatively minor burden of compensating for acceleration. Adhering to the constraints of the ICH in the transmit design is one of the five principles of power-efficient design. A commonly stated disadvantage of broadband SETI is the receiver processing requirements associated with overcoming interstellar impairments. We have shown that these impairments can instead be circumvented at the transmitter through the judicious choice of signal waveform and without processing overhead. On the other hand, the discovery of power-efficient signals at the receiver does require processing resources devoted to multiple observations, and the sensitivity of the discovery to low-power signals is directly related to the processing resources devoted to these observations.

Finally, it has been shown that in the power-efficient regime information-free beacons offer essentially no advantage over information-bearing signals with respect to the average power and energy consumption or the difficulty of discovery. Searches targeted at information-bearing signals can readily discover beacons, although the reverse is not true. Thus it makes sense to design our discovery searches that seek out power-efficient and power-optimized signals to simultaneously seek both types of signals.

Acknowledgements

This research was supported in part by a grant from the National Aeronautics and Space Administration to the SETI Institute. The author is indebted to the following individuals for generously sharing their time for discussion and comments: James Benford, Samantha Blair, Gerry Harp, Andrew Siemion, Jill Tarter, David Tse, and Dan Werthimer. Ian Morrison has been particularly helpful in maintaining an ongoing dialog on these issues and reading and commenting on drafts of this work.

Appendix A

Interstellar link budget

In an interstellar communication link, the required average transmit power can be determined by first establishing the receive power \mathcal{P}_R necessary for a desired reliability, and then referring that power to the transmitter and determining the corresponding average transmit power \mathcal{P}_T . In both cases the power is proportional to the information rate \mathcal{R} , with a constant of proportionality equal to the energy per bit \mathfrak{E}_b .

A.0.1 Required average receive power

The fundamental limit for the interstellar channel, taking into account noise and scintillation, is given by (4.1). This places a lower bound on the energy per bit measured at baseband in the receiver,

$$\mathfrak{E}_b > N_0 \log 2 \text{ joules.} \quad (\text{A.1})$$

The value of the noise power spectral density introduced in the receiver circuitry is $N_0 = k T_n$, where k is Boltzmann's constant (numerically equal to $k = 1.38 \times 10^{-23}$ joules per degree kelvin) and T_n degrees kelvin is the equivalent noise temperature. White noise is a good approximation at radio frequencies, where sources of thermal noise can be considered white and quantum effects can be ignored.

The state of the art in receiver design on Earth can achieve a receiver internal noise temperature of 5 degrees kelvin. This would be a representative value that a transmitter would have to assume in order to communicate reliably with us. If we were to construct our own transmitter, it might be reasonable to assume a lower value. Added to this is cosmic background radiation at 3 degrees kelvin, applicable to more advanced civilizations as well as ourselves, giving a total noise temperature of $T = 8$ degrees kelvin. This is the most optimistic case, since it does not take into account star noise. Based on an assumption of 8 degrees kelvin, the fundamental limit for received energy per bit is

$$\mathfrak{E}_b > k T_n \log 2 = 7.66 \times 10^{-23} \text{ joules.} \quad (\text{A.2})$$

For example, at a bit rate equal to $R = 1$ bit per second, the corresponding average power is

$$\mathcal{P}_R = 7.66 \times 10^{-23} \text{ watts } (-221.2 \text{ dBW}). \quad (\text{A.3})$$

A.0.2 Required average transmit power

A power link budget for a typical interstellar communication system can be developed. Assume that the transmitter and receiver are separated by a distance D , with average power \mathcal{P}_T transmitted and \mathcal{P}_R received. Then for an ideal receive aperture antenna with area A_R , the power loss is given by

$$\frac{\mathcal{P}_R}{\mathcal{P}_T} = G_T \cdot \frac{A_R}{4\pi D^2}, \quad (\text{A.4})$$

where G_T is the gain of the transmit antenna. For the isotropic case (where $G_T = 1$) the fraction of the transmit power that is captured is the ratio of A_R to the area of a sphere with radius D . If the transmit antenna is also an aperture antenna with area A_T , the maximum gain is

$$G_T = \frac{4\pi A_T}{\lambda_c^2} \quad (\text{A.5})$$

where λ_c is the wavelength at carrier frequency f_c . Defining a similar gain G_R for the receive antenna (with area A_R substituted for A_T), the Friis transmission equation is

$$\frac{\mathcal{P}_R}{\mathcal{P}_T} = G_T G_R \left(\frac{\lambda_c}{4\pi D} \right)^2. \quad (\text{A.6})$$

While G_T and G_R are geometrical parameters of the antenna designs, the term in parenthesis captures the effect of propagation. For a given average received power \mathcal{P}_R , the average transmit power \mathcal{P}_T scales as $\mathcal{P}_T \propto D^2$, and (taking into account the wavelength dependence of the antenna gains) $\mathcal{P}_R \propto f_c^{-2}$.

For a numerical example, assume that $D = 500$ light years and $f_c = 5$ GHz ($\lambda_c = 6$ centimeters). For both transmit and receive antennas, use our own Arecibo antenna as a prototype, with a 305 meter diameter and assume that inefficiency reduces the effective antenna area by 50% at both transmitter and receiver. For these parameters, the antenna gains are $G_T = G_R = 81.1$ dB, and the path loss is 419.9 dB. At the fundamental limit, the transmit power is

$$\mathcal{P}_T = 4623 \text{ watts } (36.3 \text{ dBW}). \quad (\text{A.7})$$

Appendix B

Matched filtering

This appendix provides an analysis and justification of the matched filter as the optimum receiver processing in the presence of AWGN alone.

B.1 Modulation and demodulation

To prepare this signal for radio transmission, it is multiplied by $\sqrt{\mathcal{E}_h}$ to give it total energy \mathcal{E}_h , and then modulated by carrier frequency f_c before taking twice the real part $\Re\{\cdot\}$. The modulating carrier has a phase θ that is unknown to the receiver. The resulting real-valued signal

$$2 \Re \left\{ \sqrt{\mathcal{E}_h} h(t) e^{i\theta} e^{i2\pi f_c t} \right\} \quad (\text{B.1})$$

is suitable for transmission by electromagnetic means through the interstellar medium (ISM), and is confined to frequency range $|f| \in [f_c, f_c + B]$.

For purposes of defining the ICH, the front-end of a receiver is optimized for AWGN while pretending that there are no other ISM impairments. The first step is to demodulate the received signal to baseband, and in the absence of any impairments from the ISM this yields

$$r(t) = \text{LPF} \left\{ 2 \Re \left[\sqrt{\mathcal{E}_h} h(t) e^{i\theta} e^{i2\pi f_c t} \right] e^{-i2\pi f_c t} \right\} = \sqrt{\mathcal{E}_h} h(t) e^{i\theta}, \quad (\text{B.2})$$

where the low pass filter (LPF) eliminates frequency components in the vicinity of $2f_c$ and eliminates all noise outside the bandwidth of $h(t)$.

The optimum baseband receiver processing to counter AWGN is the matched filter (see Section 7.1 for a derivation of this). As illustrated in Figure 3.1 a filter matched to $h(t)$ has impulse response $h^*(-t)$, yielding output signal $z(t)$, where

$$z(t) = \int_{-\infty}^{\infty} r(\tau) h^*(\tau - t) d\tau. \quad (\text{B.3})$$

In particular

$$z(0) = \sqrt{\mathcal{E}_h} e^{i\theta} + \text{noise} . \quad (\text{B.4})$$

Although θ is unknown to the receiver, its effect can be eliminated by the energy estimate

$$|z(0)|^2 = \mathcal{E}_h + \text{noise} , \quad (\text{B.5})$$

yielding an estimate of the received energy \mathcal{E}_h .

B.2 The LS solution

Minimizing (7.8) can be accomplished by differentiation with respect to z . However, (7.8) is not an analytic function of z because it includes both z and z^* . Written in the following form, ε is a real-valued analytic function of z and z^* considered as independent variables.

$$\varepsilon(z, z^*, \tau) = \int_{\tau}^{\tau+T} (r(t) - z \cdot h(t - \tau)) (r^*(t) - z^* \cdot h^*(t - \tau)) dt . \quad (\text{B.6})$$

As shown in [59], a stationary point can be determined by setting

$$0 = \frac{\partial}{\partial z^*} \varepsilon(z, z^*, \tau) = - \int_{\tau}^{\tau+T} (r(t) - z \cdot h(t - \tau)) h^*(t - \tau) dt . \quad (\text{B.7})$$

Solving for z yields (7.9), and substituting \hat{z} into (B.6) yields (7.9).

Appendix C

Statistical model for a coherence hole

C.1 Scintillation without modulation

The statistical properties of the model for an ICH given in (3.1) will now be established. Define the random variable S as

$$S = \sum_{n=1}^N r_n e^{i(\Phi_n)} \quad (\text{C.1})$$

where the $\{r_n\}$ are fixed but unknown quantities and the $\{\Phi_n\}$ are independent and uniformly distributed. By the Central Limit Theorem we can approximate S as Gaussian for reasonably large N . It follows from independence and $\mathbb{E}[e^{i\Phi_m}] = 0$ that $\mathbb{E}[S] = 0$ and

$$\mathbb{E}[S^2] = \mathbb{E}\left[\sum_{n=1}^N \sum_{m=1}^N r_n r_m e^{i(\Phi_m + \Phi_n)}\right] = \sum_{n=1}^N r_n^2 \mathbb{E}[e^{i2\Phi_m}] = 0. \quad (\text{C.2})$$

This establishes that the $\Re\{S\}$ and $\Im\{S\}$ have equal variance and are uncorrelated and hence independent. The variance of S is

$$\mathbb{E}[|S|^2] = \mathbb{E}\left[\sum_{n=1}^N \sum_{m=1}^N r_n r_m e^{i(\Phi_m - \Phi_n)}\right] = \sum_{n=1}^N r_n^2. \quad (\text{C.3})$$

For the $n \neq m$ terms, the expected values are zero due to independence, leaving only the $n = m$ terms.

From (3.17), that $E|M|^2 = N_0$ is easily established. More interesting is the conclusion that $\Re\{M\}$ and $\Im\{M\}$ have equal variance and are uncorrelated and hence independent. This follows from

$$\mathbb{E}[M^2] = N_0 \int_0^T e^{-i4\pi f_c t} (h^*(t))^2 dt = 0, \quad (\text{C.4})$$

where $(h^*(t))^2$ has bandwidth $2B$, and after modulation with carrier frequency $2f_c$ its spectrum is guaranteed not to overlap $f = 0$ and thus the integrand averages to zero.

C.2 Scintillation and amplitude modulation

Suppose $h(t)$ is amplitude modulated by A , where the flux for weak scattering given by (3.14) is assumed. Then the MF output is

$$Z = \sqrt{\mathcal{E}_h} \cdot \left(\sqrt{\gamma} e^{i\Psi} \sigma_s + \sqrt{1-\gamma} S \right) A + M, \quad (\text{C.5})$$

where $0 \leq \gamma \leq 1$ is the fraction of signal that arrives in the specular path. Conditioned on a particular specular phase $\Psi = \psi$, and writing the data symbol in polar coordinates $A = a e^{i\theta}$, Z becomes Gaussian with independent real- and imaginary parts, and with first and second order statistics

$$\mathbb{E} [\Re\{Z\}] = \sqrt{\mathcal{E}_h \gamma} a \sigma_s \cos(\psi + \theta) \quad \text{and} \quad \mathbb{E} [\Im\{Z\}] = \sqrt{\mathcal{E}_h \gamma} a \sigma_s \sin(\psi + \theta) \quad (\text{C.6})$$

$$\text{Var} [\Re\{Z\}] = \text{Var} [\Im\{Z\}] = \frac{\mathcal{E}_h a^2 (1-\gamma) \sigma_s^2 + N_0}{2}. \quad (\text{C.7})$$

Observe that only $\mathbb{E} [Z]$ (and not $\text{Var} [Z]$) is dependent on θ . When ψ is unknown and uniformly distributed, $\mathbb{E} [Z]$ yields no information on the value of θ . The conclusion is that any phase component in A is rendered unobservable by scintillation for any κ and γ . On the other hand $Q = |Z|^2$ makes a good real-valued decision variable since its mean value includes a component of a^2 for any $0 \leq \gamma \leq 1$ (and in particular for strong scattering where $\gamma = 0$) and any ψ , since

$$\mathbb{E} [|Z|^2] = \mathcal{E}_h a^2 \sigma_s^2 + N_0. \quad (\text{C.8})$$

Particularly notable is the lack of dependence on γ , or in other words the strength of the scattering.

Appendix D

Derivation of fundamental limits

We begin by reviewing a couple of bounding techniques that will prove indispensable, and then proceed to proving some results on the fundamental limits on power efficiency.

D.1 Probabilistic bounds

D.1.1 Union bound

A simple bound that often proves useful in bounding an event of the form of "A or B or C or ..." is the *union bound*. Mathematically, the term "or" turns into "union". For any set of events $\{A_i, 1 \leq i \leq N\}$,

$$\Pr \left\{ \bigcup_{i=1}^N A_i \right\} \leq \sum_{i=1}^N \Pr \{A_i\} \quad (\text{D.1})$$

with equality if and only if the events are disjoint ($A_i \cap A_j = \emptyset$ for all $i \neq j$).

D.1.2 Weak law of large numbers

Let X be a random variable with average value $\mathbb{E}[X] = \mu$. Suppose that $\{X_1, X_2, \dots, X_J\}$ is a set of J identically distributed independent random variables with the same distribution as X . The weak law of large numbers asserts that for any $\epsilon > 0$

$$\Pr \left\{ \left| \frac{1}{J} \sum_{k=1}^J X_k - \mu \right| > \epsilon \right\} \rightarrow 0 \quad \text{as } J \rightarrow \infty. \quad (\text{D.2})$$

Thus, as J increases the probability distribution of the sum becomes increasingly concentrated about μ .

D.1.3 Chernoff bound

The *Chernoff bound* is one of the favorite tools of communications engineering, because it yields exponentially tight bounds on the tail probability for a sum of independent random variables. Let $u(x)$ be the unit step function, and note that $u(x) \leq e^{\rho x}$ for all x and any $\rho \geq 0$. Then for any random variable X , threshold λ , and $\rho \geq 0$,

$$\Pr \{X \geq \lambda\} = \mathbb{E} [u(X - \lambda)] \leq \mathbb{E} [e^{\rho(X - \lambda)}] = e^{-\rho \lambda} \mathbb{E} [e^{\rho X}] = e^{-\rho \lambda} \mathbb{M}_X [\rho] \quad (\text{D.3})$$

$$\Pr \{X < \lambda\} \leq e^{\rho \lambda} \mathbb{M}_X [-\rho] , \quad (\text{D.4})$$

where $\mathbb{M}_X [t]$ is the moment generating function of X . The bound can be minimized by the choice of $\rho \geq 0$.

Suppose that $\{X_1, X_2, \dots, X_J\}$ is a set of J identically distributed independent random variables with the same distribution as X . The Chernoff bound is particularly convenient for bounding the tail probability for the sum of independent random variables, because the moment generating function is readily shown to be

$$\mathbb{E} \left[\exp \left\{ \sum_{k=1}^J X_k \right\} \right] = \mathbb{M}_X [\rho]^J . \quad (\text{D.5})$$

D.2 Channel code based on M-ary FSK and time diversity

The result stated in (4.3) will now be shown to be a consequence of the strong law of large numbers applied to the decision variable Q_m defined in (4.8). This proof follows [47, Section II] closely, except for the added assumption that energy bundles conform to the constraints of the ICH. We also show that this result applies whether or not scintillation is present; that is, for AWGN alone as well as the AWGN with scintillation. The scintillation is assumed to be the result of strong scattering, so it is governed by Rayleigh statistics.

Without loss of generality, assume that the actual energy bundle falls in decision variable Q_M , while $\{Q_m, 1 \leq m < M\}$ consist of noise only. For a given threshold λ there are two types of error that can occur in the detection of the location of the energy bundle. The first is a miss in the case of $m = M$, and the other is a false alarm in the case of $1 \leq m < M$. Assuming a threshold λ , the probabilities of these two types of error are

$$1 - P_D = \Pr \{Q_M < \lambda\} \quad (\text{D.6})$$

$$P_{\text{FA}} = \Pr \{Q_m \geq \lambda\} , \quad (\text{D.7})$$

where P_D is the probability of detection. Since the $\{Q_m, 1 \leq m \leq M\}$ are statistically independent, the probability of a symbol error is

$$P_S = 1 - P_D \cdot (1 - P_{\text{FA}})^{M-1} . \quad (\text{D.8})$$

A symbol error is defined as either a choosing the wrong location for the energy bundle or an ambiguous outcome (an energy bundle is detected at two or more frequencies). We will establish conditions under which $P_S \rightarrow 0$, which implies that the probability of bit error $P_E \rightarrow 0$. The union bound of Appendix D.1.1 yields a simpler expression,

$$P_S \leq 1 - P_D + (M - 1) P_{FA} < 1 - P_D + M P_{FA}. \quad (D.9)$$

To show that $P_S \rightarrow 0$, it is only necessary to show that $P_D \rightarrow 1$ and $M P_{FA} \rightarrow 0$.

Address first $m = M$, where we are interested in showing that $P_D \rightarrow 1$. The expected value of Q_M is

$$\mathbb{E}[Q_M] = \begin{cases} \mathcal{E}_h \sigma_s^2 + N_0, & \text{AWGN + scintillation} \\ \mathcal{E}_h + N_0, & \text{AWGN alone.} \end{cases} \quad (D.10)$$

Assuming that $\sigma_s^2 = 1$, which is true for interstellar scattering, the value of $\mathbb{E}[Q_M]$ is identical with and without scintillation. The weak law of large numbers of Appendix D.1.2 insures that $P_D \rightarrow 1$ as $J \rightarrow \infty$ as long as the threshold is chosen to be less than the mean, or in particular the value

$$\lambda = N_0 + (1 - \epsilon) \mathcal{E}_h \quad (D.11)$$

for any value $0 < \epsilon < 1$ will suffice. If we were to remove time diversity and let $J = 1$, then $P_D < 1$. Even in the absence of scintillation this is true, and thus time diversity is necessary ($J \rightarrow \infty$) for the results that follow, even in the absence of scintillation.¹

Address next the case $1 \leq m < M$, where the Q_m consist of noise alone and our interest is in demonstrating conditions under which $M P_{FA} \rightarrow 0$. For this purpose, since Q_m is the sum of J independent random variables the Chernoff bound of Appendix D.1.3 is useful. The moment generating function of $|Z|^2$ where Z is a zero-mean complex-valued Gaussian random variable with independent real and imaginary parts and $\mathbb{E}[|Z|^2] = \sigma^2$,

$$\mathbb{M}_{|Z|^2}[\rho] = \frac{1}{1 - \sigma^2 \rho} \quad \text{for } \rho < \frac{1}{\sigma^2}. \quad (D.12)$$

In the case of $\{Q_m, 1 \leq m < M\}$, $\sigma^2 = N_0$. Thus the Chernoff bound (after choosing the optimum ρ) is

$$P_{FA} \leq \left(\frac{\lambda e^{1 - \frac{\lambda}{N_0}}}{N_0} \right)^J. \quad (D.13)$$

Substituting for threshold λ ,

$$M P_{FA} < M \left(e^{-\xi_s (1 - \epsilon)} (1 + \xi_s (1 - \epsilon)) \right)^J, \quad (D.14)$$

¹ An upper bound on the error probability P_E for M-ary FSK on an AWGN channel without scintillation is determined in Appendix F.4. The conclusion is that as long as the energy contrast ratio per bit $\xi_b > 2 \log 2$ then $P_E \rightarrow 0$ as $M \rightarrow \infty$. Thus, in the absence of scintillation there is a 3 dB penalty in power efficiency for setting $J = 1$, attributable to the phase-incoherent detection. Time diversity in conjunction with low duty cycle are necessary to avoid this 3 dB penalty even in the absence of scintillation.

where ζ_s is the energy contrast ratio defined by (2.16). Substituting for M from (4.4) and \mathcal{E}_h from (4.5),

$$M P_{\text{FA}} < \left(2^{\frac{\mathcal{R}T}{\delta}} e^{-\frac{\mathcal{P}T\sigma_s^2(1-\epsilon)}{N_0\delta}} \left(1 + \frac{\mathcal{P}T(1-\epsilon)}{\delta N_0} \right) \right)^J. \quad (\text{D.15})$$

Thus, when the condition

$$\mathcal{R} \log 2 < \frac{\mathcal{P}(1-\epsilon)}{N_0} - \frac{\delta}{T} \log \left(1 + \frac{\mathcal{P}(1-\epsilon)}{N_0\delta} \right) \quad (\text{D.16})$$

is satisfied, $M P_{\text{FA}} \rightarrow 0$ as $J \rightarrow \infty$. The term containing δ is positive and monotonically approaches 0 as $\delta \rightarrow 0$. Thus as long as

$$\frac{\mathcal{R}}{\mathcal{P}} < \frac{\log_2 e}{N_0}, \quad (\text{D.17})$$

then (D.16) is satisfied for sufficiently small values of ϵ and δ .

That $\epsilon \rightarrow 0$ is necessary for $P_s \rightarrow 0$ shows that approaching the fundamental limit requires precise knowledge of \mathcal{E}_h and N_0 in order to establish the threshold. That $\delta \rightarrow 0$ implies that it is necessary for $\mathcal{E}_h \rightarrow \infty$. This latter fact explains why phase-incoherence detection is not an obstacle to approaching the fundamental limit, even on the AWGN channel where phase-coherent detection would be possible. As the signal energy grows without bound the noise is swamped out so the distinction between coherent and incoherent disappears.

Appendix E

Coin tossing analogy

Although it doesn't apply directly to interstellar communication, the analogy between the discovery of a continuous-time signal $h(t)$ in AWGN and the discovery of a specific binary sequence in the presence of noise created by random coin tosses may be helpful to intuition. This analogy explains in a simple and less-mathematical way why the shape of $h(t)$ *doesn't* matter for detection in noise, and also why the shape of $h(t)$ *does* matter with respect to interference immunity.

E.1 Discrete matched filter

Consider a reception which consists of a sequence of K elements, where each element is either a HEAD or a TAIL,

$$r_k = \begin{cases} h_k, & \text{signal} \\ n_k, & \text{noise.} \end{cases} \quad (\text{E.1})$$

We know that n_k is generated randomly by nature, and can be modeled as a sequence of statistically independent fair coin tosses. Thus, each possible sequence $\{n_k, 1 \leq k \leq K\}$ is equally likely with probability 2^{-K} . In the other case, signal $\{h_k, 1 \leq k \leq K\}$ is presumed to have been generated by some technological means, rather than a natural process. Our goal is to observe $\{r_k, 1 \leq k \leq K\}$ and make a decision between signal and noise. One might surmise that one distinguishing characteristic of a technologically-generated signal is that it was generated by an algorithm, or sequence of steps that could be executed by a software program or generated by a piece of Boolean hardware.

Unfortunately there is no practical way to identify whether $\{r_k\}$ was generated by an algorithm, without making much stronger assumptions about the characteristics of that algorithm. For example, if the Boolean hardware consisted of a memory storing a sequence $\{h_k\}$, then that hardware could generate literally any sequence $\{r_k\}$. If no assumptions are made, any $\{r_k\}$ could have been generated by noise with probability 2^{-K} .

If on the other hand, if it is known that the signal is a single unique sequence (or this is correctly guessed), then the detection algorithm can simply compare $\{r_k\}$ to that $\{h_k\}$ and declare signal if there is agreement in all K positions of the sequence. In that case, the probability of detection is $P_D = 1$. On the other hand, the detector will incorrectly declare signal if $\{n_k\}$ happens to replicate $\{r_k\}$ precisely, which occurs with probability 2^{-K} . Thus, the false alarm probability is $P_{FA} = 2^{-K}$. The important point is that this detector performance does not depend on the signal sequence $\{h_k\}$, because the noise $\{n_k\}$ is completely random and it can replicate any $\{h_k\}$ with the same probability. This is analogous to our result that the waveform $h(t)$ does not matter in the presence of AWGN (which is also completely random).

Suppose due to our uncertainty about $\{h_k\}$, we allow the signal to be any one of $N > 1$ specific sequences (or corresponding algorithms). In this case it remains that $P_D = 1$ if one of those sequences is valid. However, P_{FA} increases with N , since $\{n_k\}$ can more easily replicate one of N sequences. In the limit as $N \rightarrow 2^K$, $P_{FA} \rightarrow 1$. This illustrates why the detector must keep N small to keep P_{FA} under control.

E.2 Immunity to discrete interference

Consider now a very different challenge,

$$r_k = \begin{cases} h_k, & \text{signal} \\ i_k, & \text{interference,} \end{cases} \quad (\text{E.2})$$

where the noise sequence has been replaced by $\{i_k, 1 \leq k \leq K\}$, an unknown interference. (Interference, when present, is likely to be much larger than the noise, and thus it is not unreasonable to assume that the receiver has to deal with interference, or noise, but not both at the same time.) The question is how we can choose signal $\{h_k\}$ to make it unlikely to be replicated by $\{i_k\}$, but without knowledge of $\{i_k\}$. The transmitter designers have no knowledge of the origin of $\{i_k\}$, and thus are unwilling to even make any assumptions about its statistics. We define the transmitter's challenge as somehow choosing $\{h_k\}$ so that the false alarm probability $P_{FA} = 2^{-K}$ is a constant, independent of $\{i_k\}$ and with the same P_{FA} as we saw with noise. As just seen, the choice of $\{h_k\}$ doesn't matter when it comes to noise, so the transmitter is free to choose $\{h_k\}$ any way we choose.

The following way of choosing $\{h_k\}$ satisfies our goals. Choose $\{h_k\}$ randomly by performing K independent fair coin tosses. Having determined $\{h_k\}$ in this manner, the choice of $\{h_k\}$ can be shared with the receiver. (In practice $\{h_k\}$ would be generated by a pseudo-random coin toss generator, and the receiver would have to guess or infer that algorithm and generate the same sequence $\{h_k\}$ itself.) where it is compared with $\{r_k\}$, our discrete MF algorithm. Now P_{FA} is the probability that K coin tosses exactly match $\{i_k\}$, which is $P_{FA} = 2^{-K}$, the same for any $\{i_k\}$. Thus, the detector performance is identically the same for noise and interference, regardless of the interference. If $\{h_k\}$ were chosen in any other way, such as another random ensemble with different statistics, then some interferers $\{i_k\}$ would be replicated by $\{h_k\}$ with higher probability than others.

Appendix F

Communication reliability

Throughout a random variable V will be a normalized complex-valued Gaussian random variable with

$$\mathbb{E}[V] = \mathbb{E}[V^2] = 0 \quad \text{and} \quad \mathbb{E}[|V|^2] = 2. \quad (\text{F.1})$$

Then the random variable

$$X = \left| \sqrt{\xi} + V \right|^2 \quad (\text{F.2})$$

is a non-central χ^2 random variable with non-centrality parameter ξ and two degrees of freedom. (For $\xi = 0$ it is a central χ^2 random variable with two degrees of freedom.) Write this as $X \sim \chi^2(\xi)$, and let the probability density and cumulative distribution functions be $f(\xi, x)$ and $F(\xi, x)$. The moment generating function is

$$\mathcal{M}(\xi, t) = \mathbb{E}[e^{tX}] = \frac{e^{\frac{\xi t}{1-2t}}}{1-2t} \quad \text{for } 2t < 1. \quad (\text{F.3})$$

F.1 Multilevel on-off keying (OOK)

It is easy to see that multilevel modulation is less power efficient than two-level OOK. Consider a more data symbol constellation $A_k \in \{n, 0 \leq n \leq N-1\}$, where $N = 2$ corresponds to OOK, and the spacing between levels is kept constant to keep the noise immunity fixed. If each point in the constellation is equally likely, then the average energy in each symbol is

$$\mathcal{E}_h \cdot \mathbb{E}[A^2] = \mathcal{E}_h \cdot \frac{(2N-1)(N-1)}{6} \quad (\text{F.4})$$

and the information embedded in each symbol is $\log_2 N$. The power efficiency is the ratio the latter to the former, and it is maximized by $N = 2$. For example, choosing $N = 4$ (two bits per symbol) reduces the power efficiency relative to $N = 2$ by a factor of 3.5 (5.4 dB).

F.2 Probability of error for OOK

On-off keying (OOK) provides a baseline case similar to the types of signals often assumed in the SETI literature. They therefore provide a baseline against which to compare channel codes that seek the greatest power efficiency. The bit error probability will now be determined in the presence of AWGN, with and without Rayleigh fading (which models scintillation in the presence of strong scattering).

F.2.1 Additive white Gaussian noise (AWGN)

In the absence of fading, the decision variable is $Q = |\sqrt{\mathcal{E}_h} + N|^2$, where $\mathcal{E}_h = 0$ for a zero bit and $\mathcal{E}_h > 0$ for a one bit. In contrast to FSK, we do not know that there is an energy bundle present, so there is no way to avoid the need for knowledge of N_0 . Assume that Q is applied to a threshold λ , it is natural to choose $\lambda = \mathcal{E}_h + N_0$, which is halfway between the two mean values. The probability of a false alarm (energy bundle detected when there is none present) is

$$P_{\text{FA}} = \Pr \{ |N|^2 > \lambda \} = e^{-1 - \xi_s}. \quad (\text{F.5})$$

The probability of a miss (energy bundle not detected when there is one present) is

$$1 - P_{\text{D}} = \Pr \{ |\sqrt{\mathcal{E}_h} + N|^2 < \lambda \}.$$

There is no closed-form expression for P_{D} , but the Chernoff bound of Appendix D.1.3 gives us an exponentially tight bound,

$$\begin{aligned} 1 - P_{\text{D}} &\leq \mathbb{E} \left[\exp \left\{ -\rho \left(|\sqrt{\mathcal{E}_h} + N|^2 - \lambda \right) \right\} \right] = e^{\rho \lambda} \mathbb{M}_{|\sqrt{\mathcal{E}_h} + N|^2} [-\rho] \\ &= \frac{\exp \left\{ \rho \left(-\frac{2\mathcal{E}_h}{N_0\rho+1} + \mathcal{E}_h + N_0 \right) \right\}}{N_0\rho + 1} \end{aligned}$$

for any $\rho > 0$. Choosing ρ to minimize the right side,

$$1 - P_{\text{D}} \leq \frac{2(\xi_s + 1) \exp \left(\frac{\xi_s (-3\sqrt{8\xi_s^2 + 8\xi_s + 1} + 8\xi_s + 5)}{\sqrt{8\xi_s^2 + 8\xi_s + 1} + 1} \right)}{\sqrt{8\xi_s^2 + 8\xi_s + 1} + 1}$$

Assuming that the two cases are equally likely, P_{E} is half the sum of (F.5) and (F.2.1). This result is plotted in Figure 2.8.

F.2.2 AWGN and scintillation

The decision variable is $Q = |\sqrt{\mathcal{E}_h} S + N|^2$, where $\mathcal{E}_h = 0$ for a zero bit. This case is easier because the statistics are χ^2 rather than noncentral χ^2 , and closed form results are easy to obtain. Apply Q

to a threshold $\lambda = N_0 + a$ for some value of $a > 0$. Then assuming the two cases are equally likely, the error probability is

$$P_E = \frac{1}{2} (1 - P_D + P_{FA}) = \frac{1}{2} \left(1 - e^{-\frac{a+N_0}{\mathcal{E}_h+N_0}} + e^{-\frac{a+N_0}{N_0}} \right). \quad (\text{F.6})$$

Choosing a to minimize P_E , this becomes

$$P_E = \frac{1}{2} (\xi_s + 1)^{-\frac{\xi_s+1}{\xi_s}} \left((\xi_s + 1)^{\frac{1}{\xi_s}} + \xi_s \left((\xi_s + 1)^{\frac{1}{\xi_s}} - 1 \right) \right). \quad (\text{F.7})$$

This relation is plotted in Figure 2.8.

F.3 Error probability for M-ary FSK and time diversity

The probability of bit error P_E will now be upper bounded for the combination of M-ary FSK with time diversity using the maximum algorithm of (5.2). This differs from a similar development in Appendix D.2, where a threshold algorithm is used instead. While the threshold algorithm is necessary to asymptotically approach the fundamental limit, the maximum algorithm has greater practical appeal for finite M and J because the detection algorithm requires no knowledge of the signal parameters $\{\mathcal{E}_h, N_0, \xi_s\}$. A bound is determined because calculation of the exact error probability requires messy numerical integrations. The Chernoff bounding technique of Appendix D.1.3 is employed because it gives exponentially tight bounds for small P_E .

The more general formulation of Section 6.4.2 is used, since the simpler case of Section 5.1 is simply a special case for $J_0 = 0$ and $J_1 = J$. Let P_S be the symbol error probability, or in other words the probability that the maximum detection algorithm chooses the wrong location. Since P_S does not depend on the actual location, assume the actual energy bundle is located at $m = M$. Then

$$P_S = \Pr \left\{ \left(\max_{1 \leq m \leq M-1} Q_m \right) > Q_M \right\} = \Pr \left\{ \bigcup_{m=1}^{M-1} (Q_m > Q_M) \right\}. \quad (\text{F.8})$$

The union bound of Appendix D.1.1 replaces the union by a sum,

$$P_S \leq \sum_{m=1}^{M-1} \Pr \{Q_m > Q_M\} = (M-1) \cdot \Pr \{Q_1 > Q_M\}, \quad (\text{F.9})$$

since all the $\{Q_m, 1 \leq m < M\}$ are identically distributed.

Each term can be upper bounded using the Chernoff bound. For any $\rho > 0$,

$$\Pr \{Q_1 > Q_M\} = \Pr \{Q_1 - Q_M > 0\} \leq \mathbb{E} [\exp\{-\rho (Q_1 - Q_M)\}] = \mathbb{M}_{Q_1} [-\rho] \cdot \mathbb{M}_{Q_M} [\rho]. \quad (\text{F.10})$$

The moment generating function $\mathbb{M}_{|Z|^2} [\rho]$ where Z is complex-Gaussian with variance σ^2 is given by (D.12). Each random variable $\{Q_m, 1 \leq m \leq M\}$ is the sum of $(J_0 + J_1)$ independent random

variables, so the moment generation functions are

$$\mathbb{M}_{Q_1}[\rho] = \left(\frac{1}{1 - \rho N_0} \right)^{J_0 + J_1}$$

$$\mathbb{M}_{Q_M}[\rho] = \left(\frac{1}{1 - \rho (\mathcal{E}_{h,0} \sigma_s^2 + N_0)} \right)^{J_0} \cdot \left(\frac{1}{1 - \rho (\mathcal{E}_{h,1} \sigma_s^2 + N_0)} \right)^{J_1}$$

for $\rho < 1/(\mathcal{E}_{h,0} \sigma_s^2 + N_0)$. The final bound on P_S is determined by minimizing over $\rho < 1/(\mathcal{E}_{h,0} \sigma_s^2 + N_0)$. We omit the final result, which is complicated.

Now let's relate P_S to P_E . Consider the set of M possible symbols. To calculate the bit error probability, assume there has been a random symbol error. For any particular bit position in the symbol, $M/2$ of the symbols disagree and $M/2$ symbols (including the correct one) agree. Assuming that all $M - 1$ incorrect symbols are equally likely, the conditional probability of bit error is $M/2$ divided by $M - 1$, and

$$P_E = \frac{M/2}{M-1} \cdot P_S. \quad (\text{F.11})$$

Specializing to $J_0 = 0$ results in the simple expression of (5.3).

F.4 Error probability for M-ary FSK

The analysis of Appendix F.3 can be repeated for the outage strategy. One difference is the absence of time diversity ($J_0 = 0$ and $J_1 = 1$), which allows us to avoid bounding in favor of a closed form result. The second difference is non-central χ^2 statistics for Q_M .

For the normalized MF outputs the symbol error probability P_S equals the probability that one or more of the first $(M - 1)$ matched filter outputs is larger in magnitude than the M -th output,

$$P_S = \Pr \left\{ \left(\max_{1 \leq m \leq M-1} |V_m|^2 \right) > \left| \sqrt{2 \log_2 M} \cdot \xi_{b,o} + V_M \right|^2 \right\} \quad (\text{F.12})$$

$$= \Pr \left\{ \bigcup_{m=1}^{M-1} \left(|V_m|^2 > \left| \sqrt{2 \log_2 M} \xi_{b,o} + V_M \right|^2 \right) \right\} \quad (\text{F.13})$$

$$= \int_0^\infty \Pr \left\{ \bigcup_{m=1}^{M-1} (|V_m|^2 > x) \right\} f(2 \log_2 M \xi_{b,o}, x) dx. \quad (\text{F.14})$$

The union bound replaces the union by a sum,

$$\begin{aligned} P_S &\leq \sum_{m=1}^{M-1} \int_0^\infty \Pr \{ |V_m|^2 > x \} f(2 \log_2 M \xi_{b,o}, x) dx \\ &= (M-1) \cdot \int_0^\infty (1 - F(0, x)) \cdot f(2 \log_2 M \xi_{b,o}, x) dx \\ &= (M-1) \cdot \mathcal{M}(2 \log_2 M \xi_{b,o}, -1/2) \\ &= \frac{1}{2} (M-1) M^{-\frac{\xi_{b,o}}{2 \log_2}}. \end{aligned} \quad (\text{F.15})$$

Combining (F.15) and (F.11) the result is (5.9).

F.4.1 Error Probability for (M,N)-ary FSK

After normalization, each of the M matched filter outputs takes the form

$$\left| \sqrt{\frac{2\mathcal{E}_h}{N_0}} + V \right|^2 = \left| \sqrt{2\xi} + V \right|^2$$

$$\xi = \frac{\mathfrak{E}_b \log_2 \binom{M}{L}}{L N_0}.$$

For $(M - L)$ of the M outputs, $\mathcal{E}_h = 0$. The probability of a single noise-only estimate being larger than a single signal-plus-noise estimate is $e^{-\xi/2}/2$. There are $L(M - L)$ different ways this type of error can occur, so by the union bound of Appendix D.1.1 the probability of symbol error is bounded by

$$P_S \leq L(M - L) e^{-\xi/2}/2 \quad (\text{F.16})$$

and the bit error probability $P_E \approx P_S/2$. Thus we get that for a given value of P_E

$$\xi_b = \frac{\mathfrak{E}_b}{N_0} \geq \frac{2L \log \left(\frac{L(M-L)}{4P_E} \right)}{\log_2 \binom{M}{L}} \quad (\text{F.17})$$

The maximum spectral efficiency \mathfrak{S} occurs when the duty factor $\delta = 1$, in which case

$$\mathfrak{S} = \frac{\log_2 \binom{M}{L} / T}{M B} = \frac{\log_2 \binom{M}{L}}{M}, \quad (\text{F.18})$$

where the choice $BT = 1$ also maximizes \mathfrak{S} .

Appendix G

Discovery reliability

G.1 Detection probability for single observation

Consider the decision variable Q is given by (7.6). An equivalent condition to $Q > \lambda$ is

$$(1 - \lambda) \cdot \left| \sqrt{\mathcal{E}_h} \left(\sqrt{\gamma} \sigma_s e^{i\psi} + \sqrt{1 - \gamma} S \right) + M_1 \right|^2 > \lambda \cdot \sum_{k=2}^K |M_k|^2. \quad (\text{G.1})$$

Specular phase ψ does not affect the statistics, so set $\psi = 0$. Define a normalized noise $V_k = M_k / \sqrt{N_0/2}$ with unit-variance real and imaginary parts. Then (G.1) becomes

$$\frac{1 - \lambda}{\lambda} \cdot V > W \quad (\text{G.2})$$

where

$$V = \left| \sqrt{\frac{2 \mathcal{E}_h}{N_0}} \left(\sqrt{\gamma} \sigma_s + \sqrt{1 - \gamma} S \right) + V_1 \right|^2 \quad (\text{G.3})$$

$$W = \sum_{k=2}^K |V_k|^2 \quad (\text{G.4})$$

The distribution W is χ^2 with $(2K - 1)$ degrees of freedom, and only the statistics of V depend on the parameters of the model. Since the statistics of W are divorced from all the parameters, this relation demonstrates how Q is sensitive to the signal-to-noise ratio ξ_s rather than signal and noise energies individually.

G.1.1 Rayleigh fading

For $\gamma = 0$, closed-form results for false alarm probability P_{FA} and detection probability P_{D} can be obtained. The simplification for this case is that $(\sqrt{2 \mathcal{E}_h / N_0} S + V_1)$ is a zero-mean Gaussian

random variable with variance $2(1 + \xi_s)$. Hence (G.2) can be rewritten as

$$\alpha \cdot |U_1|^2 > W \quad \text{for} \quad \alpha = \frac{1 - \lambda}{\lambda} \cdot (1 + \xi_s) \quad (\text{G.5})$$

where U_1 is also a Gaussian random variable with unit-variance real- and imaginary parts. In (G.5) $|U_1|^2$ is χ^2 with two degrees of freedom and W is χ^2 with $(2K - 2)$ degrees of freedom. The probability of event (G.5) is readily determined,

$$P_D = \int F\left(\frac{w}{\alpha}, 2\right) f(w, 2K - 2) dw = \left(\frac{\alpha}{1 + \alpha}\right)^{K-1}, \quad (\text{G.6})$$

where $F(x, n)$ and $f(x, n)$ are the cumulative distribution and probability density functions for a χ^2 distribution with n degrees of freedom. Then P_{FA} equals (G.6) for $\xi_s = 0$, and eliminating λ from these two relations yields (7.12).

When N_0 is known, the probability of $Q = |R_1|^2 > \lambda$ is

$$P_D = F\left(\frac{2\lambda}{\mathcal{E}_h \sigma_s^2 + N_0}, 2\right) = \exp\left\{-\frac{\lambda}{\mathcal{E}_h \sigma_s^2 + N_0}\right\}. \quad (\text{G.7})$$

P_{FA} is obtained by setting $\mathcal{E}_h = 0$. Eliminating λ to solve for P_D in terms of P_{FA} yields

$$P_D = P_{FA}^{\frac{1}{1+\xi_s}}, \quad (\text{G.8})$$

which is repeated as (7.13).

G.1.2 Rician fading

When $\gamma > 0$, V in (G.2) is non-central χ^2 with two degrees of freedom. There is no easy closed-form expression for P_D as in the Rayleigh fading case. Our intuition that Rayleigh fading is "worst case" in the sense of being more difficult case to discover (because of the absence of a specular component) can be confirmed by calculating a signal-to-noise ratio. The first and second moments of V are

$$\mathbb{E}[V] = 2(1 + \xi_s) \quad (\text{G.9})$$

$$\text{Var}[V] = 4(1 + 2\xi_s + (1 - \gamma^2)\xi_s^2). \quad (\text{G.10})$$

A larger P_D and smaller P_{FA} are associated with a bigger difference between mean values (signal plus noise vs noise alone) and a smaller standard deviation. These effects can be captured in a signal-to-noise ratio measure

$$\text{SNR}_{\text{Rice}} = \frac{(\mathbb{E}[V] - \mathbb{E}[V]_{\mathcal{E}_h=0})^2}{\text{Var}[V]} = \frac{\xi_s^2}{1 + 2\xi_s + (1 - \gamma^2)\xi_s^2}. \quad (\text{G.11})$$

SNR_{Rice} is plotted in Figure G.1 for different values of γ . It is notable how small SNR_{Rice} is for small values of γ . This is the influence of the increasing prominence of outages when the Rayleigh case is approached. However, SNR_{Rice} improves as γ gets larger, reflecting the increasing discovery reliability, particularly for larger ξ_s .

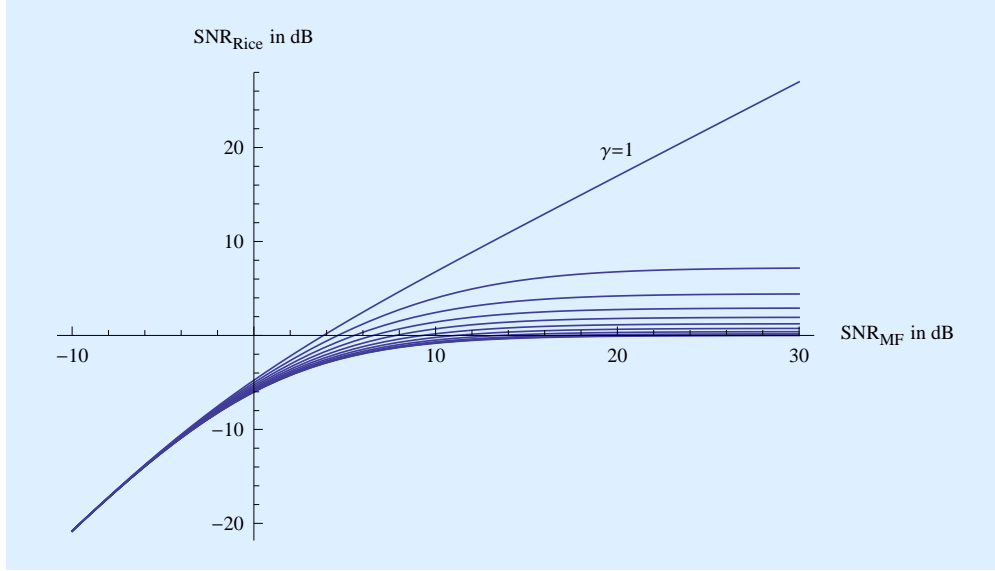


Figure G.1: A plot of SNR_{Rice} in dB vs ξ_s in dB for $\gamma = 0$ to 1 in steps of 0.1. For a larger specular component (γ larger) SNR_{Rice} gets larger, reflecting the increasing reliability in signal flux due to the increasing proportion of flux arriving in the specular component.

G.2 Detection probability for multiple independent observations

The discovery relation of (6.16) will now be derived. Consider three granularities of observation: (a) individual energy bundle, (b) one contiguous observation window, and (c) the collection of L observations. It is assumed that the received flux remains constant over a contiguous observation window, but is statistically independent from one observation window to the next. Let the probabilities at granularity (a) be $\{P_{\text{FA},a}, P_{\text{D},a}\}$ and at granularity (c) $\{P_{\text{FA}}, P_{\text{D}}\}$. Thus, $\{P_{\text{FA}}, P_{\text{D}}\}$ reflect the overall sensitivity of the L -observation detector, where a "detection" is defined as one or more detected energy bundles (at the level of (a)) in the L observations. We limit our analysis to the simpler Rayleigh fading case, where closed-form results are obtainable.

G.2.1 False alarm probability

Suppose there is no beacon present. If $h(t)$ has bandwidth B , then the output of an MF also has bandwidth B and can be sampled at a rate B without losing information. Then the total number of samples in L observations, each of duration T_o , is

$$N = L T_o B = L K \left(\frac{\delta_o}{\delta_p} + 1 \right). \quad (\text{G.12})$$

N is the collective degrees of freedom in all the observations. The false alarm probability in one of these samples is $P_{\text{FA},a}$, and if they are statistically independent then the false alarm probability at granularity (c) is

$$1 - P_{\text{FA}} = (1 - P_{\text{FA},a})^N \quad \text{or} \quad P_{\text{FA}} \approx N \cdot P_{\text{FA},a}. \quad (\text{G.13})$$

Typically $P_{\text{FA},a}$ is very small, so the approximation is very accurate.

The independence of these samples depends on $h(t)$. Let $h(t)$ have Fourier transform $H(f)$, and let the autocorrelation function of $h(t)$ be $R_h(t)$, which is the inverse Fourier transform of $|H(f)|^2$. Then the noise at the output of the MF has a power spectral density $|H(f)|^2$ and autocorrelation function $R_h(t)$. The samples of noise at the MF output are Gaussian and independent if and only if $R_h(k/B) = \delta_k$, or equivalently

$$\sum_m \left| H \left(f - \frac{m}{B} \right) \right|^2 = \frac{1}{B}, \quad 0 \leq f < B. \quad (\text{G.14})$$

For example, if $h(t)$ is ideally band limited to $f \in [0, B]$, then this condition becomes

$$|H(f)| = \begin{cases} \frac{1}{\sqrt{B}}, & 0 \leq f < B \\ 0, & \text{otherwise.} \end{cases} \quad (\text{G.15})$$

Thus, we can say that the samples at the output of the MF are statistically independent ((G.12) is valid) if, roughly, the energy of $h(t)$ is uniformly spread over the range of frequencies $f \in [0, B]$. Equivalently the magnitude of $H(f)$ is an ideal lowpass filter with an arbitrary phase response.

G.2.2 Detection probability

Suppose now that a periodic beacon with period T_p is present. The relationship between $P_{\text{FA},a}$ and $P_{\text{D},a}$ for a filter matched to an individual energy bundle is given by (G.8),

$$P_{\text{D},a} = P_{\text{FA},a}^{\frac{1}{1+\xi_s}}. \quad (\text{G.16})$$

Now consider a single observation of duration T_o . If the observation time is limited to $T_o \leq T_p + T$, then there is either zero (probability $1 - \delta_o$) or one (probability δ_o) energy bundle overlapping this observation.

There are two cases to consider. If there is an energy bundle overlapping this observation, out of the $B T_o$ samples at the output of a MF, we can assume that all but one harbor noise only. (Again this is for the case $R_h(k/B) = \delta_k$.) Strictly speaking a detection can occur due to (a) a detection with probability $P_{\text{D},a}$ for the one sample containing signal or (b) a false alarm with probability $P_{\text{FA},a}$ in any of the other samples. In practice $P_{\text{FA},a} \approx 0$ is very small relative to $P_{\text{D},a} \approx 1$, so we can ignore those false alarms and accurately approximate the detection probability for a single observation overlapping an energy bundle by $P_{\text{D},a}$. For the case where there is no energy bundle overlapping the observation, we can accurately approximate the detection probability as 0. Thus, the probability of detection in one observation is

$$\Pr \{ \text{energy packet detected} \} \approx P_{\text{D},a} \cdot \delta_o + 0 \cdot (1 - \delta_o) = \delta_o P_{\text{D},a}. \quad (\text{G.17})$$

Finally, consider the aggregate of L observations. Assuming those observation times are random relative to the period of the beacon, the L binary variables representing "detection" or "no detection" in each of the L observations are statistically independent. With that assumption, the number of "detections" has a binomial distribution. A "miss" occurs only in the case where all L observations yield "no detection", which occurs with probability

$$1 - P_D = (1 - \delta_o P_{D,a})^L . \quad (\text{G.18})$$

Combining (G.13), (G.16), and (G.18), (6.16) follows.

Appendix H

Plasma dispersion

H.1 Coherence bandwidth

Integrating both sides of (8.2), the phase in (8.1) is

$$\phi(f) = \phi(f_c) - 2\pi \int_{f_c}^f \tau(u) du = \phi(f_c) - 2\pi \mathcal{D} \text{DM} \left(\frac{1}{f_c} - \frac{1}{f} \right) \quad (\text{H.1})$$

Expanding $\phi(f)$ in a Taylor series about $f = f_c$,

$$\phi(f) = \phi(f_c) - 2\pi \mathcal{D} \text{DM} \left(\frac{f - f_c}{f_c^2} - \frac{(f - f_c)^2}{f_c^3} + \frac{(f - f_c)^3}{f_c^4} - \dots \right). \quad (\text{H.2})$$

The linear term is benign because it corresponds to a fixed group delay, so the actual distortion is caused by the second-order and higher terms. The second-order term (and hence the higher-order terms) have variation less than $\alpha\pi$ for $f \in [f_c, f_c + B]$ if

$$2\pi \mathcal{D} \text{DM} \frac{B^2}{f_c^3} \ll \alpha\pi \quad (\text{H.3})$$

which yields (8.5). In that case, (H.2) becomes for $f \in [f_c, f_c + B]$

$$\phi(f) \approx \phi(f_c) - 2\pi \tau(f_c) \cdot (f - f_c). \quad (\text{H.4})$$

Thus, (8.1) becomes

$$G(f) \approx e^{i\phi(f_c)} \cdot e^{-i2\pi(f-f_c)\tau(f_c)}. \quad (\text{H.5})$$

The equivalent baseband transfer function is $G(f + f_c)$, and this too is illustrated in Figure 8.3.

H.2 Partial equalization

Even though DM refers to a measurable physical property pertaining to the line of sight between transmitter and receiver, the state of knowledge of DM may be different at the transmitter and

the receiver. Astronomical observations provide a priori knowledge about DM [53] in the form of upper and lower bounds $DM_L \leq DM \leq DM_U$. The resulting uncertainty is captured by $DM_\Delta = (DM_U - DM_L)$. A more advanced civilization may possess tighter bounds and a smaller DM_Δ , but can probably never reduce the uncertainty entirely.

There is the possibility of equalization for any specific value of DM by introducing by adding an artificial group delay such that the artificial group delay plus the group delay corresponding to DM is constant over $f \in [0, B]$. This can be done in either transmitter or receiver, and the combined effect is indistinguishable from a benign fixed delay which adds to the very large propagation delay. Specifically a causal allpass filter with response $F_{eq}(f) = \exp\{i 2\pi \phi_{eq}(f)\}$, where

$$\tau_{eq}(f) = \mathcal{D} \cdot DM \cdot \left(\frac{1}{f_c^2} - \frac{1}{(f + f_c)^2} \right) \quad \text{and} \quad \frac{\phi_{eq}(f)}{2\pi} = -\mathcal{D} \cdot DM \cdot \frac{f^2}{f_c^2 (f + f_c)} \quad (\text{H.6})$$

placed before or after the dispersion results overall in a constant group delay $\mathcal{D} \cdot DM / f_c^2$. Done in the transmitter, this pre-equalization has no effect on the noise. Done in the receiver, this post-equalization does change the noise *waveform* but has no effect on the noise *statistics* since $F_{eq}(f)$ is an all pass (phase-only) filter [45, Chap. 8].

An issue for the receiver to consider is whether or not the transmitter has performed pre-equalization DM_L , after which $0 \leq DM \leq DM_\Delta$. Since $DM_\Delta < DM_U$, this would increase the dispersion coherence bandwidth B_0 . Thus, a receiver estimating a range of B_0 for a given line of sight prior to discovery may wish to consider two cases: with and without pre-equalization.

Appendix I

Coherence time with fading

The Fresnel approximation expands the left side of (8.39) in a Taylor series and retains terms up to x^2 and t^2 . The constant term is a flat delay and is discarded. The result is the right side of (8.39)

$$v(x) = v_{\parallel} - \frac{v_{\perp}x}{D_2} - \frac{v_{\parallel}x^2}{2D_2^2} \approx v_{\parallel} - \frac{v_{\perp}x}{D_2}. \quad (\text{I.1})$$

The fact that the net velocity $v(x)$ depends on x limits the time coherence, because different rays have slightly different Doppler shifts which causes their superposition to change with time.

Within an ICH, where the distortion of $h(t)$ by plasma dispersion can be neglected, the observer sees, associated with a ray through point x , the passband response

$$\Re \left\{ h \left(t - \frac{d(x) - v(x)t}{c} \right) \exp \left\{ i 2\pi f_c \left(t - \frac{d(x) - v(x)t}{c} \right) \right\} \right\}. \quad (\text{I.2})$$

Within an ICH, the effect of delay on $h(t)$ can be neglected, and thus the equivalent complex baseband signal is

$$h(t) \exp\{-i 2\pi f_c d(x)/c\} \exp\{i 2\pi f_c v(x)t/c\}. \quad (\text{I.3})$$

The first two terms in (I.3) are familiar, but the third is the interesting one,

$$\exp\{i 2\pi f_c v(x)t/c\} = \exp\{i 2\pi f_c v_{\parallel}t/c\} \exp\{-i 2\pi f_c v_{\perp}xt/cD_2\}. \quad (\text{I.4})$$

The effect of v_{\parallel} can be compensated by a simple carrier frequency offset as described in Section 8.3. That v_{\parallel} can be rendered impotent in this manner is not surprising, since this component of velocity aligned with the light of sight affects all rays in the same way. The second term is a time-varying phase at baseband which affects the time coherence unless the total phase shift it causes over $t \in [0, T]$, which is condition (8.40).

Appendix J

Search granularity in dilation and frequency

Any mismatch between the time dilation parameter β used in the implementation of the MF and the actual value of β results in incoherence. The same is true for any mismatch between the carrier frequency f_1 and reality. These sources of incoherence are totally under the control of the receiver in its choice of a granularity in a search over these parameters. Hence we don't put them in the same category as natural sources of incoherence.

J.1 Time dilation error

Since a search over β will generally need a small range, write it as $\beta = 1 + \delta$, and ask how $\delta \neq 0$ affects coherence. This can be studied by assuming that $r(t) = h(t)$ but the MF used is $h^*(-(1 + \Delta\delta)t)$. The largest acceptable value of $|\Delta\delta|$ depends to some extent on $h(t)$. We now show that for a signal $h(t)$ with a flat magnitude spectrum over bandwidth $0 \leq f \leq B$, the MF output is affected very little when $|\Delta\delta| \ll 1/\pi K$. Thus the fractional dilation offset is on the order of $1/\pi K$, which implies that an $h(t)$ with larger K requires a finer-grain search over the dilation parameter. Time dilation error is a factor in both time and frequency coherence, since a given error $\Delta\delta$ places an error on the product $K = BT$.

The Fourier transform of $h((1 + \Delta\delta)t)$ is $H(f/(1 + \Delta\delta))$. Assume that $\Delta\delta > 0$ (the final result is the same for $\Delta\delta < 0$). Then the MF output is

$$Z = \int_0^{B/(1+\Delta\delta)} H(f) H^*\left(\frac{f}{1+\Delta\delta}\right) df = \frac{1}{B} \int_0^{B/(1+\Delta\delta)} \exp\{i\left(\phi(f) - \phi\left(\frac{f}{1+\Delta\delta}\right)\right)\} df \quad (\text{J.1})$$

The group delay $\tau(f)$ is defined by (8.2). Since $h(t)$ is confined to $t \in [0, T]$, it follows that $0 \leq \tau(f) \leq T$. The sensitivity of Z to $\Delta\delta$ can be gauged by the derivative

$$v = \left. \frac{\partial Z}{\partial \Delta\delta} \right|_{\Delta\delta=0} = \frac{i}{B} \int_0^B f \frac{\partial \phi(f)}{\partial f} df - 1 = \frac{-i 2\pi}{B} \int_0^B f \tau(f) df - 1 \quad (\text{J.2})$$

where

$$0 \leq \int_0^B f \tau(f) df \leq \frac{B^2 T}{2} \quad \text{or} \quad 1 \leq |v|^2 \leq 1 + \pi^2 K^2. \quad (\text{J.3})$$

Thus, $|Z|$ is relatively little affected if $\Delta\delta|v| \ll 1$ or $\Delta\delta \ll 1/\pi K$.

J.2 Carrier frequency offset

As with delay and dilation, the receiver will calculate the MF output for discrete values of carrier frequency. There may be a mismatch $\Delta\zeta_b$ between reality and the receiver's assumption. In this case, the MF output becomes

$$Z = \int_0^T |h(t)|^2 e^{-i2\pi\Delta\zeta_b f_c t} dt. \quad (\text{J.4})$$

The offset will have an insignificant effect of Z if the total phase shift is much less than π , or $|\Delta\zeta_b| \ll 1/2f_c T$. Time coherence is maintained if the absolute carrier frequency spacing is small relative to $1/T$.

Bibliography

- [1] "Project Cyclops: A design study of a system for detecting extraterrestrial intelligent life," Stanford/NASA/Ames Research Center Summer Faculty Program in Engineering Systems Design, Tech. Rep., 1971.
- [2] R. G. Gallager, *Information theory and reliable communication*. New York: Wiley, 1968.
- [3] D. G. Messerschmitt and I. S. Morrison, "Design of interstellar digital communication links: Some insights from communication engineering," *Acta Astronautica*, vol. 78, p. 80, Sept-Oct 2012.
- [4] P. A. Fridman, "SETI: The transmission rate of radio communication and the signal's detection," *Acta Astronautica*, vol. 69, p. 777, Nov-Dec 2011 2011. [Online]. Available: <http://arxiv.org/abs/1102.3332v2>
- [5] M. Horvat, A. Nakć, and I. Otočan, "Impact of technological synchronicity on prospects for SETI," *International Journal of Astrobiology*, vol. 11, no. 1, p. 51, 2012.
- [6] H. W. Jones, "Optimum signal modulation for interstellar communication," in *Astronomical Society of the Pacific Conference Series*, G. S. Shostak, Ed., vol. 74, 1995, p. 369, accessed at <http://www.aspbooks.org/a/volumes> on 18 Feb. 2010.
- [7] J. Benford, D. Benford, and G. Benford, *Building and searching for cost-optimized interstellar beacons*, ser. Communication with Extraterrestrial Intelligence. SUNY Press, 2011, p. 279.
- [8] C. E. Shannon, "A mathematical theory of communication," *Bell System Technical Journal*, vol. 27, no. 3, p. 379, 1948.
- [9] A. L. Zaitsev, "The first musical interstellar radio message," *Journal of Communications Technology and Electronics*, vol. 53, no. 9, pp. 1107–1113, 2008.
- [10] J. R. Ehman, "Wow!"-A Tantalizing Candidate, ser. Searching for Extraterrestrial Intelligence. Springer, 2011, pp. 47–63.
- [11] D. G. Messerschmitt, "Interstellar communication: The case for spread spectrum," *Acta Astronautica*, vol. 81, p. 227, 2012.
- [12] A. Siemion, J. V. Korff, P. McMahon, E. Korpela, D. Werthimer, D. Anderson, G. Bower, J. Cobb, G. Foster, and M. Lebofsky, "New seti sky surveys for radio pulses," *Acta Astronautica*, vol. 67, no. 11, pp. 1342–1349, 2010.
- [13] I. Crawford, "Interstellar travel: a review for astronomers," *Quarterly Journal of the Royal Astronomical Society*, vol. 31, pp. 377–400, 1990.
- [14] D. R. Lorimer and M. Kramer, *Handbook of pulsar astronomy*. Cambridge Univ Pr, 2005.
- [15] J. Cordes and B. Rickett, "Diffractive interstellar scintillation timescales and velocities," *The Astrophysical Journal*, vol. 507, no. 2, pp. 846–860, 1998.

- [16] D. Tse and P. Viswanath, *Fundamentals of wireless communication*. Cambridge Univ Pr, 2005.
- [17] M. Lampton, "Optical SETI: the next search frontier," in *Bioastronomy 99*, vol. 213, 2000, p. 565.
- [18] R. Narayan, "The physics of pulsar scintillation," *Philosophical Transactions of the Royal Society of London. Series A: Physical and Engineering Sciences*, vol. 341, no. 1660, p. 151, 1992.
- [19] R. S. Kennedy, *Fading dispersive communication channels*. Wiley-Interscience, 1969.
- [20] C. Berrou, A. Glavieux, and P. Thitimajshima, "Near Shannon limit error-correcting coding and decoding: Turbo-codes. 1," in *Communications, 1993. ICC 93. Geneva. Technical Program, Conference Record, IEEE International Conference on*, vol. 2. IEEE, 1993, pp. 1064–1070 vol. 2.
- [21] D. J. MacKay and R. M. Neal, "Near shannon limit performance of low density parity check codes," *Electronics Letters*, vol. 32, no. 18, p. 1645, 1996.
- [22] P. F. Clancy, "Some advantages of wide over narrow band signals in the search for extraterrestrial intelligence (SETI)," *Journal of the British Interplanetary Society*, vol. 33, pp. 391–395, 1980.
- [23] J. Cordes and W. Sullivan, "Astrophysical coding: New approach to SETI signals. I. signal design and wave propagation," G. S. Shostak, Ed., 1995, accessed at <http://www.aspbooks.org/a/volumes> on 18 Feb. 2010.
- [24] G. S. Shostak, "SETI at wider bandwidths?" *Progress in the Search for Extraterrestrial Life*, ed. G. Seth Shostak, *ASP Conference Series*, vol. 74, 1995.
- [25] J. A. C. Bingham, "Multicarrier modulation for data transmission: An idea whose time has come," *Communications Magazine, IEEE*, vol. 28, no. 5, pp. 5–14, 1990.
- [26] G. R. Harp, R. F. Ackermann, S. K. Blair, J. Arbunich, P. R. Backus, and J. Tarter, *A new class of SETI beacons that contain information*, ser. Communication with Extraterrestrial Intelligence. State University of New York Press, 2011.
- [27] I. S. Morrison, "Detection of antipodal signalling and its application to wideband SETI," *Acta Astronautica*, vol. 78, p. 90, Sept-Oct 2012 2011.
- [28] N. Cohen and D. Charlton, "Polychromatic SETI," *Astronomical Society of the Pacific Conference Series*, 1995.
- [29] J. Benford, G. Benford, and D. Benford, "Messaging with cost-optimized interstellar beacons," *Astrobiology*, vol. 10, no. 5, pp. 475–490, 2010.
- [30] G. Benford, J. Benford, and D. Benford, "Searching for cost-optimized interstellar beacons," *Astrobiology*, vol. 10, no. 5, pp. 491–498, 2010.
- [31] A. L. Zaitsev, "Sending and searching for interstellar messages," *Acta Astronautica*, vol. 63, no. 5-6, pp. 614–617, 2008.
- [32] J. V. Korff, P. Demorest, E. Heien, E. Korpela, D. Werthimer, J. Cobb, M. Lebofsky, D. Anderson, B. Bankay, and A. Siemion, "Astropulse: A search for microsecond transient radio signals using distributed computing. i. methodology," *submitted to Astrophys.J.*, 2011.
- [33] P. Lafrance, *Fundamental concepts in communication*. Prentice-Hall, Inc., 1990.
- [34] J. Cordes and J. Lazio, "Interstellar scintillation and SETI," *Third Decennial US-USSR Conference on SETI*, vol. 47, 1993.
- [35] J. M. Cordes, J. W. Lazio, and C. Sagan, "Scintillation-induced intermittency in SETI," *The Astrophysical Journal*, vol. 487, no. 2, pp. 782–808, 1997.

- [36] R. Fano, *Transmission of information: A statistical theory of communication*. The MIT Press, 1961.
- [37] I. Garrett, "Pulse-position modulation for transmission over optical fibers with direct or heterodyne detection," *Communications, IEEE Transactions on*, vol. 31, no. 4, pp. 518–527, 1983.
- [38] S. Shostak, "Limits on interstellar messages," *Acta Astronautica*, vol. 68, no. 3-4, pp. 366–371, 2011.
- [39] C. E. Jones, K. M. Sivalingam, P. Agrawal, and J. C. Chen, "A survey of energy efficient network protocols for wireless networks," *wireless networks*, vol. 7, no. 4, pp. 343–358, 2001.
- [40] H. Pollak and D. Slepian, "Prolate spheroidal wave functions, Fourier analysis and uncertainty." *Bell Syst.Tech.Journal*, vol. 40, p. 43, 1961.
- [41] H. J. Landau and H. O. Pollak, "Prolate spheroidal wave functions, fourier analysis and uncertainty ii," *Bell Syst.Tech.J*, vol. 40, no. 1, pp. 65–84, 1961.
- [42] J. M. Cordes and T. J. W. Lazio, "Ne2001. II. using radio propagation data to construct a model for the galactic distribution of free electrons," *ArXiv preprint astro-ph/0301598*, 2003, draft version Feb. 2, 2008.
- [43] T. Cover and J. Thomas, *Elements of Information Theory*. New York: John Wiley and Sons, 1991.
- [44] D. G. Messerschmitt, "Some digital communication fundamentals for physicists and others," EECS Department, University of California, Berkeley, Tech. Rep. UCB/EECS-2008-78, Jun 2008, accessed at <http://www.eecs.berkeley.edu/Pubs/TechRpts/2008/EECS-2008-78.html> on 18 Feb. 2010.
- [45] J. R. Barry, E. A. Lee, and D. G. Messerschmitt, *Digital communication*, 3rd ed. Boston: Kluwer Academic Publishers, 2004.
- [46] E. Biglieri, J. Proakis, and S. Shamai, "Fading channels: Information-theoretic and communications aspects," *Information Theory, IEEE Transactions on*, vol. 44, no. 6, pp. 2619–2692, 1998.
- [47] I. E. Telatar and D. N. C. Tse, "Capacity and mutual information of wideband multipath fading channels," *Information Theory, IEEE Transactions on*, vol. 46, no. 4, pp. 1384–1400, 2000.
- [48] N. LaSorte, W. J. Barnes, and H. H. Refai, "The history of orthogonal frequency division multiplexing," in *Global Telecommunications Conference, 2008. IEEE GLOBECOM 2008. IEEE*. IEEE, 2008, pp. 1–5.
- [49] R. W. Chang, "Orthogonal frequency multiplex data transmission system," U.S. Patent 3,488,445, Jan. 6, 1970.
- [50] A. R. S. Bahai, B. R. Saltzberg, and M. Ergen, *Multi-carrier digital communications: theory and applications of OFDM*. Springer Verlag, 2004.
- [51] S. Hara and R. Prasad, "Overview of multicarrier CDMA," *Communications Magazine, IEEE*, vol. 35, no. 12, pp. 126–133, 1997.
- [52] K. Fazel, S. Kaiser, and J. Wiley, *Multi-carrier and spread spectrum systems*. Wiley Online Library, 2003.
- [53] J. M. Cordes and T. J. W. Lazio, "Ne2001. I. a new model for the galactic distribution of free electrons and its fluctuations," *ArXiv preprint astro-ph/0207156*, 2002, draft version Feb. 1, 2008.
- [54] J. P. Laboratory, "Horizons system," Oct. 31, 2012. [Online]. Available: <http://ssd.jpl.nasa.gov/?horizons>
- [55] I. P. Williamson, "Pulse broadening due to multiple scattering in the interstellarmedium," *Monthly Notices of the Royal Astronomical Society*, vol. 157, p. 55, 1972.
- [56] I. Williamson, "Pulse broadening due to multiple scattering in the interstellarmedium-ii," *Monthly Notices of the Royal Astronomical Society*, vol. 163, p. 345, 1973.

- [57] —, “Pulse broadening due to multiple scattering in the interstellar medium-ii,” *Monthly Notices of the Royal Astronomical Society*, vol. 163, p. 345, 1973.
- [58] H. Lambert and B. Rickett, “On the theory of pulse propagation and two-frequency field statistics in irregular interstellar plasmas,” *The Astrophysical Journal*, vol. 517, p. 299, 1999.
- [59] D. G. Messerschmitt, “Stationary points of a real-valued function of a complex variable,” EECS Department, University of California, Berkeley, Tech. Rep. UCB/EECS-2006-93, June 2006 2006.

AUTHOR

David G. Messerschmitt is the Roger A. Strauch Professor Emeritus of Electrical Engineering and Computer Sciences (EECS) at the University of California at Berkeley. At Berkeley he has previously served as the Chair of EECS and the Interim Dean of the School of Information. He is the co-author of five books, including *Digital Communication* (Kluwer Academic Publishers, Third Edition, 2004). He served on the NSF Blue Ribbon Panel on Cyberinfrastructure and co-chaired a National Research Council (NRC) study on the future of information technology research. His doctorate in Computer, Information, and Control Engineering is from the University of Michigan, and he is a Fellow of the IEEE, a Member of the National Academy of Engineering, and a recipient of the IEEE Alexander Graham Bell Medal recognizing “exceptional contributions to the advancement of communication sciences and engineering”.